International Symposium

TOPICAL PROBLEMS OF NONLINEAR WAVE PHYSICS (NWP-2017)

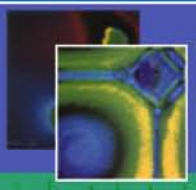

22 - 28 July 2017
Moscow - St.-Petersburg, Russia

2017 NWP

Nonlinear Dynamics and Complexity (NWP-1)

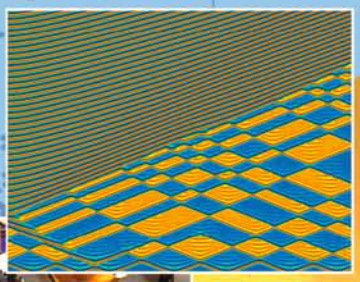

Lasers with High Peak and High Average Power (NWP-2)

Nonlinear Phenomena in the Atmosphere and Ocean (NWP-3)

Workshop Magnetic Fields in Laboratory High Energy Density Plasmas (LaB)

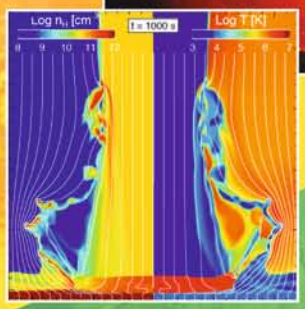

Cremlin workshop Key technological issues in construction and exploitation of 100 PW class lasers

Cremlin Connecting Russian and European Measures for Large-scale Research Infrastructures

PROCEEDINGS

Russian Academy of Sciences
Institute of Applied Physics

International Symposium

TOPICAL PROBLEMS OF NONLINEAR WAVE PHYSICS

22 – 28 July, 2017

Moscow – St. Petersburg, Russia

P R O C E E D I N G S

Nizhny Novgorod, 2017

NWP-1: Nonlinear Dynamics and Complexity

NWP-2: Lasers with High Peak and High Average Power

NWP-3: Nonlinear Phenomena in the Atmosphere and Ocean

***WORKSHOP*: Magnetic Fields in Laboratory High Energy Density Plasmas (LaB)**

***CREMLIN WORKSHOP*: Key Technological Issues in Construction and Exploitation of 100 Pw Lass Lasers**

Board of Chairs

Organized by

Institute of Applied Physics
of the Russian Academy of Sciences
www.iapras.ru

GYCOM Ltd
www.gycom.ru

International Center for Advanced Studies
in Nizhny Novgorod (INCAS)
www.incas.iapras.ru

Supported by

www.avesta.ru

www.lasercomponents.ru

www.coherent.com

www.lasertrack.ru

www.thalesgroup.com

www.standa.lt

www.phcloud.ru

www.epj.org

The electron version of the NWP-2017 Symposium materials was prepared
at the Institute of Applied Physics of the Russian Academy of Sciences,
46 Ulyanov Str., 603950 Nizhny Novgorod, Russia

CONTENTS

PLENARY TALKS

NWP 1:
NONLINEAR DYNAMICS AND COMPLEXITY

NWP 2:

LASERS WITH HIGH PEAK AND HIGH AVERAGE POWER

CREMLIN WORKSHOP: KEY TECHNOLOGICAL ISSUES IN CONSTRUCTION AND EXPLOITATION OF 100 PW LASS LASERS

NWP 3:

NONLINEAR PHENOMENA IN THE ATMOSPHERE AND OCEAN

WORKSHOP:

MAGNETIC FIELDS IN LABORATORY HIGH ENERGY DENSITY PLASMAS (LAB)

International Symposium

TOPICAL PROBLEMS OF NONLINEAR WAVE PHYSICS

Plenary Talks

XCAN, ECOLE POLYTECHNIQUE-THALES COHERENT BEAM COMBINATION JOINT LASER PROGRAM

J.-C. Chanteloup[1], A. Heilmann[1], J. Le Dortz[2], M. Antier[3], S. Bellanger[1], J. Bourderionnet[2], A. Brignon[2], L. Daniault[1], I. Fsaifes[1], E. Lallier[2], C. Larat[2], and C. Simon-Boisson[3]

[1] Ecole Polytechnique, Université Paris-Saclay, F-91128 Palaiseau cedex, France
[2] Thales Research & Technology, 1 avenue Augustin Fresnel, 91767 Palaiseau Cedex, France
[3] Thales Optronique SAS, 2 avenue Gay Lussac, 78995 Elancourt cedex, France

The XCAN project carried out by *Thales* and *Ecole Polytechnique* is a laser system relying on the Coherent Addition of laser beams produced through a Network (CAN) of Large Mode Area (LMA) Yb doped amplifying optical fibers. This technique known as Coherent Beam Combination (CBC) offers an attractive approach to simultaneously achieve the high peak and high average powers required for various scientific, industrial, and societal applications. The coherent addition of 61 individual beams should allow us to obtain a single beam carrying a 3 mJ/300 fs/200 kHz pulse train; i.e. about half a kW average power.

Interferometric phase measurement has proven to be particularly well suited for CBC of a very large number of fiber amplifiers in continuous regime operation [1]. By using this technique, we have demonstrated the coherent combination of 19 femtosecond pulses in passive (i.e. non-amplifying) fiber architecture [2] and the phase locking of seven fiber amplifiers with nonlinearities.

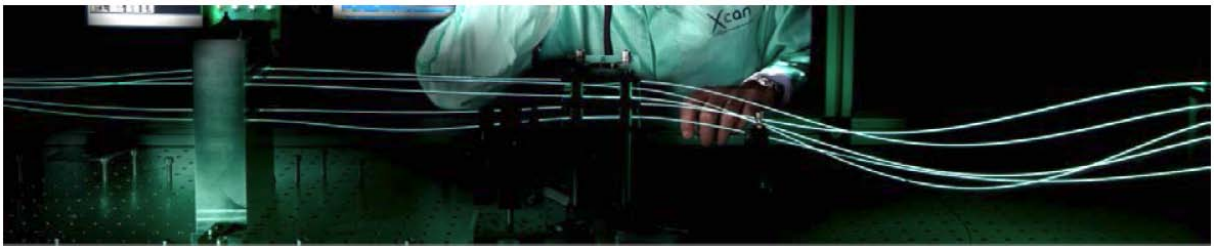

Fig. 1. Pictures of XCAN fluorescing Yb doped amplifying fiber

Acknowledgements

This project has received funding from the French Ministry of Defense (Direction Générale de l'Armement) and the European Union's Horizon 2020 research and innovation programme under grant agreement no 654148 Laserlab-Europe.

References

1. J. Bourderionnet, C. Bellanger, J. Primot, and A. Brignon, "Collective coherent phase combining of 64 fibers", *Opt. Express*, 2011, **19**(18), 17053–17058.
2. J. Le Dortz, A. Heilmann, M. Antier, J. Bourderionnet, C. Larat, I. Fsaifes, L. Daniault, S. Bellanger, C. Simon Boisson, J.-C. Chanteloup, E. Lallier, and A. Brignon, "Highly scalable femtosecond coherent beam combining demonstrated with 19 fibers", *Optics Letters*, 2017, **42**(10), 1887–1890, May 15.

ON THE INITIATION OF LIGHTNING IN THUNDERCLOUDS

A. Chilingarian

Yerevan Physics Institute, Yerevan, Armenia, chili@aragats.am
National Research Nuclear University MEPhI, Moscow, Russia
Space Research Institute of RAS, Moscow, Russia

Abstract. The relationship of lightning and elementary particle fluxes in the thunderclouds is not fully understood to date. Using the particle beams (the so-called Thunderstorm Ground Enhancements – TGE) as a probe we investigate the characteristics of the interrelated atmospheric processes. The well-known effect of the TGE dynamics is the abrupt termination of the particle flux by the lightning flash. With new precise electronics, we can see that particle flux decline occurred simultaneously with the rearranging of the charge centers in the cloud. The analysis of the TGE energy spectra before and after the lightning demonstrates that intense high-energy part of the TGE energy spectra disappeared just after the lightning. The decline of particle flux coincides on a millisecond time scale with first atmospheric discharges and we can conclude that Runaway *Breakdown* (*RB*) in the thundercloud assist initiation of the negative cloud to ground lightning.

Thunderstorm Ground Enhancements (TGEs) and Runway Breakdown (RB) process

We analyzed largest TGE events [1] of spring – summer 2016 abruptly terminated by the lightning discharge (TGE data are available from the site http://www.crd.yerphi.am/adei/). Particle flux increased when the electrostatic field droped in the deep negative domain; after reaching a maximum (or on the declining phase) a lightning flash abruptly terminated the particle flux. In 2016 several severe storms were accompanied with intense particle fluxes observed by facilities of the Aragats Space Environmental Center (ASEC). By examining these events we see that before the lightning the intensity of the TGE reaches a maximal value and maximal energy of avalanche particles reach 40 MeV and more. After lightning, we detect an abrupt decrease of particle flux caused by the removal of high-energy particles. All these processes occurred within a few hundreds of millisecond. All observed TGE-terminating lightning flashes lowered negative charge overhead. Therefore, we can connect by causal relation the RB process and the lightning initiation, i.e. RB process in the thundercloud serves as a trigger to the negative lightning. The group from the Langmuir Laboratory in central New Mexico during balloon flights on 3 July 1999 measured the maximal field of 1.86 kV/cm (130% of the threshold for a runaway process) at 5.77 km altitude just before nearby lightning flashes [2]. The authors conclude that RB avalanches have limited the magnitude of the electric field inside storms and initiated lightning flashes. Thus, both our measurements based on the detection of TGEs terminated by a lightning flash and published by other research groups *in situ* measurements of an intracloud electric field following by lightning flashes, prove that RB is an obvious mechanism for the initiation of the negative lightning flashes.

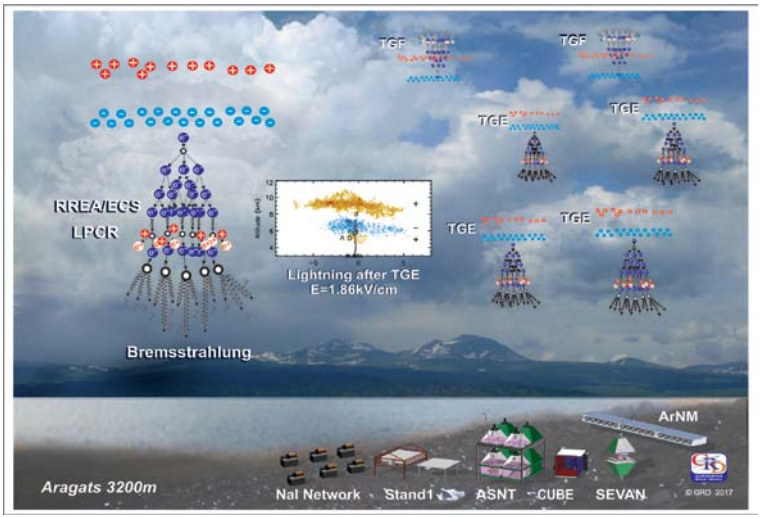

Fig. 1. TGE and TGF initiation above Aragats Mountain

References

1. A. Chilingarian, A. Daryan, K. Arakelyan, *et al*., *Phys. Rev. D*, 2010, **82,** 043009.
2. T.C. Marshall, M. Stolzenburg, C.R. Maggio, *et al*., *Geophys. Res. Let.*, 2005, **L03813**.

NONLINEAR DYNAMICS IN MULTIPLEX NETWORKS

A. Diaz-Guilera[1,2]

[1] Departament de Física de la Matèria Condensada, Universitat de Barcelona, Barcelona, Spain
albert.diaz@ub.edu
[2] Universitat de Barcelona Institute of Complex Systems (UBICS), Universitat de Barcelona, Barcelona, Spain

Abstract. Complex networks have been investigated for two decades as a paradigm for the interaction pattern behind many complex systems. Nowadays, these networks are not complex enough and the interactions in complex systems are given by even more complex structures: multilayers, interdependent networks, time dependent networks, …. We show here the analysis of some nonlinear phenomena on this new class of networks.

We will show some of the recent result in our group concerning dynamics in multiplex networks. On the one hand, we consider multiplex networks as a set of nodes in different layers. At each layer the set of nodes is the same but the connections among the nodes can be different in the layers. Furthermore, the connections among the layers are described by a "network of layers". We have studied different processes across the layers (diffusion) and between the layers (reaction) [1]. In this case Turing patterns appear as an effect of different average connectivities in different layers [2]. We also show that a multiplex construction where the layers correspond to contexts in which agents make different sets of connections can make a model of opinion formation to show stationary states of coexistence that are not observed in simple layers [3]. Finally, as a particular case of multiplex network, one can also analyze networks that change in time, since in this case each layer of the multiplex corresponds to a snapshot of the interaction pattern. For this situation, we have shown that there are different mechanisms that dominate the diffusion of information in the system depending on the relative effect of mobility and diffusion among the nodes [4, 5].

References

1. R.J. Requejo and A. Diaz-Guilera, "Replicator dynamics with diffusion on multiplex networks", *Physical Review E*, 2016, **94**, 022301.
2. N.E. Kouvaris, S. Hata, and A. Diaz-Guilera, "Pattern formation in multiplex networks", *Scientific Reports*, 2015, **5**, 10840.
3. R. Amato, N.E. Kouvaris, M. San Miguel, and A. Díaz-Guilera, "Agreement and disagreement on multiplex networks", in preparation.
4. L. Prignano, O. Sagarra, and A. Díaz-Guilera, "Tuning Synchronization of Integrate-and-Fire Oscillators through Mobility", *Phys. Rev. Lett*., 2013, **110**, 114101.
5. D. Levis, I. Pagonabarraga, and A. Diaz-Guilera, "Synchronization in dynamical networks of locally coupled self-propelled oscillators", *Phys Rev X* (in press).

THE PHYSICS OF EL NIÑO

H.A. Dijkstra

Institute for Marine and Atmospheric research Utrecht, Department of Physics and Astronomy,
Utrecht University, Utrecht, the Netherlands,
h.a.dijkstra@uu.nl

The El Niño variability in the equatorial Tropical Pacific is characterized by sea surface temperature anomalies and associated changes in the atmospheric circulation. Through an enormous observational effort over the last decades, the relevant time scales and spatial patterns of El Niño are now well-documented. In the meantime, a hierarchy of models has been developed to understand the physics of this phenomenon and to make predictions of future events. In this presentation, an overview will be given of

(i) the robust and relevant details of the observations,
(ii) the current state of the theory of the El Niño phenomenon and
(iii) the forecast skill of models as evaluated after recent El Niño events.

WAKEFIELD ACCELERATION IN RELATIVISTIC SHOCKS: ORIGIN OF ULTRA-HIGH-ENERGY COSMIC RAYS

M. Hoshino[1], M. Iwamoto[1], T. Amano[1], and **Y. Matsumoto[2]**

[1] University of Tokyo, Tokyo, Japan, hoshino@eps.s.u-tokyo.ac.jp
[2] Chiba University, Chiba, Japan

Abstract. We investigate particle acceleration by using a newly developed PIC code in a relativistic shock by paying a special attention to large amplitude electromagnetic precursor waves generated in shock upstream, and discuss that the scheme of the wakefield acceleration, which is proposed in an ultra-intense laser pulse by Tajima and Dawson (197), can be applied for the origin of ultra-high-energy cosmic rays in the universe.

Background. Large amplitude waves are known to be generated in both upstream and downstream at high Mach number collisionless shocks, and in the case of relativistic shocks large amplitude electromagnetic waves (i.e., free radiation mode), which are generated at the shock front by synchrotron maser instability, can propagate into shock upstream (Hoshino et al., 1992). Since the wave intensity of the precursor electromagnetic waves is very strong, the ponderomotive force of the precursor waves is suggested to be subject to the particle acceleration by the wakefield acceleration, and then energetic particle generation has been demonstrated by using one-dimensional PIC simulation (e.g., Lyubarsky, ApJ 2006; Hoshino, ApJ 2008).

Open question. However, it remains an open question whether or not the coherent electromagnetic wave can be excited in multi-dimensional systems. In a multi-dimensional system, in addition to the synchrotron maser instability whose wave vector is perpendicular to the shock front, other plasma instabilities whose wave vectors are parallel to the shock front may be excited, and the shock front structure may become more turbulent. The candidate of the plasma instability is the Weibel instability due to temperature anisotropy. The competing process between the synchrotron maser instability and the Weibel instability may destroy the emission of the large amplitude precursor waves. Furthermore, the superposition of many precursor waves propagating from the different locations of the shock front region may destroy the wave coherency, and then the ponderomotive force may diminish with the superposition of waves.

Result and conclusion. In order to answer the above question, we extended the previous study of the wakefield acceleration of one-dimensional PIC simulation to the two-dimensional system with a newly developed PIC code (Ikeya and Matsumoto, PASJ 2015). In my talk, I will show that the large amplitude and coherent electromagnetic waves can survive in two-dimensional relativistic shocks, even though the shock front region becomes turbulent with the excitation of Weibel instability. As a result, we observe the strong particle acceleration due to the wakefield acceleration as seen in the previous one-dimensional simulation. We will assume that the large amplitude precursor waves in relativistic shocks can contribute to the origin of the ultra-high-energy cosmic rays in plasma universe.

References

1. M. Hoshino, J. Arons, Y.A. Gallant, & A.B. Langdon, *ApJ*, 1992, **390**, 454–479.
2. M. Hoshino, *ApJ*, 2008, **672**, 940–956.
3. N. Ikeya and M. Matsumoto, *PASJ*, 2015, **67**, 64.
4. Y.E. Lyubarsky, *ApJ*, 2006, **652**, 1297–1305.
5. T. Tajima and J.M. Dawson, *Phys. Rev. Lett.*, 1979, **43**, 267–270.

HIGH PEAK POWER LASERS AT INRS AND APPLICATIONS OF LASER-WAKEFIELD-BASED X-RAY SOURCES: FROM BIO-MEDICAL TO GLOBAL FOOD SECURITY

J.C. Kieffer[1*], S. Fourmaux[1], and **E. Hallin[2]**

[1] INRS-EMT, Varennes, Québec, Canada, kieffer@emt.inrs.ca
[2] Global Institute on Food Security, U. of Saskatchewan, Saskatoon, Canada

We upgraded over the past two years the INRS high peak power laser facility from 200 TW (5 J, 25 fs) to 600 TW (11 J, 18 fs). The experimental programs have been restarted at the beginning of 2017 in the continuity of our previous scientific directions, i.e. high intensity laser-matter interaction and ultrafast X-ray sources. In this talk we will present and discuss the first experiments realized with our new laser facility, with a particular emphasis on the generation of ultrafast bright hard X-rays.

We discussed previously [1, 2] the potential impact of ultrafast laser-based X-ray sources. We will present here the generation of high throughput hard X-ray radiation by Laser Wakefield Acceleration (LWFA) process [3], which could allow a paradigm shift in a wide range of applications [4]. Ultrafast laser wakefield accelerated electrons perform wiggler-like oscillations creating a very bright micrometer-sized highly directional emission x-ray source. Such a laser-based betatron x-ray source is very attractive due to its ultrahigh brilliance, microscopic effective size, and cone beam geometry offering a large field of view for imaging.

We demonstrated in 2011 at INRS [5], and simultaneously similar results were obtained at U. of Michigan [6], that one phase contrast hard x-ray image could be produced in one X-ray pulse with a reasonable signal to noise ratio. This is opening a new route for fast 3D imaging of various objects [7]. These X-ray sources have also a unique duration characteristics, since they are as short as the optical driving laser pulses, offering extraordinary potential for femtosecond molecular imaging and Warm Dense Matter probing [8].

We will present the characterization of our upgraded LWFA betatron beam line coupled to our new laser system. X-ray source parameters are around 10^9 photons/0:1% bandwidth/sr/shot at 40 keV, a critical energy between 40 and 70 keV, an effective X-ray source size of 1 µm, a divergence between 10 and 50 mrads (FWHM), an X-ray beam pointing stability and an X-ray energy stability in the 2% rms range.

We will describe our funded program in developing high throughput phase contrast screening system based on LWFA X-ray sources for plant imaging through an initiative led by the Global Institute on Food Security (GIFS) at the U of Saskatchewan that aims to elucidate that part of the functional that maps specific environmental inputs onto specific plant phenotypes. X-ray images realized with the betatron source will be compared to thermal neutron images of same plants realized at the Canadian Nuclear Laboratory N5 Beam line. This program is the first of this kind in the world and we will show the very promising advantages of LWFA based betatron X-ray sources for the Agriculture sector and for the Global Food Security challenge.

References

1. J.C. Kieffer *et al*., *Appl. Phys. B*, 2002, **74**, S75.
2. J.C. Kieffer *et al*., 19th International Conference and School on Quantum Electronics: Laser Physics and Applications, edited by Tanja Dreischuh, Sanka Gateva, Albena Daskalova, Alexandros Serafetinides, *Proc. of SPIE*, 2017, **10226**, 1022612.
3. S. Corde *et al., Rev. Mod. Phys*., 2013, **85**, 1.
4. J.C. Kieffer *et al., SPIE Newsroom*, 2016, 10.1117/2.1201610.006713.
5. S. Fourmaux *et al., Opt. Lett*., 2011, **36**, 2426.
6. S. Kneip *et al., Appl. Phys. Lett*., 2011, **99**, 093701.
7. J. Wenz *et al*., *Nature Communications*, 2015, 6:7568 doi: 10.1038/ncomms8568.
8. M. Mo *et al*., *Rev. Sci. Instrum*., 2013, **84**, 123106.

ASTROPHYSICALLY RELEVANT, MAGNETIZED HIGH-ENERGY-DENSITY PHYSICS EXPERIMENTS AT THE UNIVERSITY OF MICHIGAN

C.C. Kuranz[1], R.P. Young[1], M.J.-E. Manuel[2], A.M. Rasmus[1,3], J. Levesque[1], G. Fiksel[1], S.R. Klein[1], M.R. Trantham1, P. Hartigan[4], A. Liao[4], C.K. Li[5], H.W. Sio[5], and **J.M. Foster[6]**

[1] University of Michigan, Ann Arbor, MI, USA, ckuranz@umich.edu
[2] General Atomics, San Diego, CA, USA
[3] Los Alamos National Laboratory, Los Alamos, New Mexico, USA
[4] Rice University, Houston, TX, USA
[5] Massachusetts Institute of Technology, Cambridge, MA, USA
[6] AWE Aldermaston, Reading, United Kingdom

Abstract. We summarize experiments performed by or in collaboration with, the University of Michigan regarding astrophysically relevant, magnetized high-energy-density (HED) plasmas. Magnetized plasmas are ubiquitous throughout our universe, but the study of these systems relies heavily on numerical simulations in limited parameter regimes and has had little guidance from controlled laboratory experiments to test underlying principles. Using high-energy lasers, we aim to create plasma conditions similar to those found in astrophysical systems.

We seek to create supersonic plasma flows by irradiating a thin (10 s of μm), solid material with a high-energy laser pulse in an externally seeded magnetic field. To study astrophysically relevant systems we require the thermal and magnetic pressures to balance ($\beta \sim 1$) and the magnetic field to advect with the plasma ($Re_M << 1$. This regime allows us to study the structure of accretion shocks and how they are affected by magnetic fields, which will aid in understanding the spatial structure of hotspots on the surface of a young star [1]. We can also experimentally create conditions where a plasma flow encounters a magnetic obstacle, which is similar to a planet's magnetosphere interacting with the stellar wind [2]. Finally, we can examine the effects of magnetic fields on collimated outflows, which are observed in young stellar objects [3]. These experiments are performed at various high-energy laser facilities and use optical diagnostics (e.g. optical pyrometry, gated optical imaging, interferometry) and proton radiography to study these systems.

Acknowledgements

This work is funded by the U.S. Department of Energy, through the NNSA-DS and SC-OFES Joint Proggram in High-Energy-Density Laboratory Plasmas, grant number DE-NA0002956, and the National Laser User Facility Program, grant number DE-NA0002719, and through the Laboratory for Laser Energetics, University of Rochester by the NNSA/OICF under Cooperative Agreement No. DE-NA0001944.

References

1. R.P. Young, C.C. Kuranz, R.P. Drake, and P. Hartigan "Accretion shocks in the laboratory: Design of an experiment to study star formation," *High Energy Density Physics,* in press.
2. A.S. Liao, S.L. Shule, P. Hartigan, P. Graham, G. Fiksel, A. Frank, J. Foster, and C. Kuranz, "Numerical simulation of an experimental analogue of a planetary magnetosphere," *High Energy Density Physics*, 2015, **17**, 38–41.
3. M. J-E. Manuel, C.C. Kuranz, A.M. Rasmus, S. Klein, M.J. Macdonald, M.R. Trantham, J.R. Fein, P.X. Belancourt, R.P. Young, P.A. Keiter, R.P. Drake, B.B. Pollack, J. Park, A.U. Hazi, G.J. Williams, and H. Chen, "Experimental results from magnetized-jet experiments at the Jupiter Laser Facility," *High Energy Density Physics*, 2015, **17** , 52–62.

PREDICTABILITY OF EXTREME CLIMATE EVENTS VIA A COMPLEX NETWORK APPROACH

Ju. Kurths

Potsdam Institute for Climate Impact Research, Humboldt University, Germany
Institute of Applied Physics RAS
Juergen.Kurths@pik-potsdam.de

Abstract. We analyse climate dynamics from a complex network approach. This leads to an inverse problem: Is there a backbone-like structure underlying the climate system? For this we propose a method to reconstruct and analyze a complex network from data generated by a spatio-temporal dynamical system. This approach enables us to uncover relations to global circulation patterns in oceans and atmosphere.

We analyse climate dynamics from a complex network approach. This leads to an inverse problem: Is there a backbone-like structure underlying the climate system? For this we propose a method to reconstruct and analyze a complex network from data generated by a spatio-temporal dynamical system. This approach enables us to uncover relations to global circulation patterns in oceans and atmosphere.

This concept is then applied to Monsoon data; in particular, we develop a general framework to predict extreme events by combining a non-linear synchronization technique with complex networks. Applying this method, we uncover a new mechanism of extreme floods in the eastern Central Andes which could be used for operational forecasts. Moreover, we analyze the Indian Summer Monsoon (ISM) and identify two regions of high importance. By estimating an underlying critical point, this leads to an improved prediction of the onset of the ISM.

References

1. J. Runge, J. Heitzig, V. Petoukhov, and J. Kurths, *Phys. Rev. Lett.*, 2012, **108**, 258701.
2. N. Boers, B. Bookhagen, N. Marwan, J. Kurths, and J. Marengo, *Geophys. Res. Lett.*, 2013, **40**, 4386.
3. N. Boers, B. Bookhagen, H.M.J. Barbosa, N. Marwan, J. Kurths, and J.A. Marengo, *Nature Communications*, 2014, **5**, 5199.
4. N. Boers, R. Donner, B. Bookhagen, and J. Kurths, *Climate Dynamics*, 2015, **45**, 619.
5. J. Runge *et al.*, *Nature Communications*, 2015, **6**, 8502.
6. V. Stolbova, E. Surovyatkina, B. Bookhagen, and J. Kurths, *Geophys. Res. Lett.*, 2016.

CHARACTERIZATION OF COLLECTIVE CHAOS IN MEAN-FIELD MODELS

A. Politi

Department of Physics, University of Aberdeen, Aberdeen, UK
a.politi@abdn.ac.uk

Abstract. Networks of dynamical systems are often characterized by a collective (macroscopic) irregular behavior. Mean-field (globally coupled) models provide the simplest setup where this regime can be accurately investigated. This is the case of unidimensional maps, but also of Stuart-Landau and phase oscillators. The connection between microscopic and macroscopic dynamics is discussed by making use of various indicators such as standard (microscopic) Lyapunov exponents, collective Lyapunov exponents, and monitoring the evolution of perturbations of finite amplitude. Robustness and generality of collective chaos will be also discussed, exploring the behavior of sparse networks, as well as one-dimensional systems with long-range interactions.

High-dimensional nonlinear dynamical systems are often characterized by a chaotic behavior, whose complexity can be quantified in terms of, e.g., fractal dimension and Kolmogorov-Sinai entropy. Both observables can be determined from the standard Lyapunov spectra, i.e. from the (in)stability along the various directions in phase space. The Lyapunov exponents in fact provide a very detailed characterization of a dynamical system.

In several physical (typically network-like) setups, an additional layer of complexity emerges and manifests itself as a fluctuating behavior of macroscopic variables such as the average of some local observable. This behavior is highly nontrivial in that it proves the existence of subtle correlations among the various units in spite of them behaving chaotically. Rigorously speaking, the collective dynamics is mathematically well defined in the so-called thermodynamic limit, i.e. for an infinite number of dynamical units. In such a limit, the natural object of study is a suitable probability distribution whose dynamics is ruled by Liouville-type or Perron-Frobenius-type equations. As it was already realized more than a century ago, while moving from the microscopic Newtonian laws towards a general theory of statistical mechanics, microscopic and macroscopic dynamics deal with different entities. Nevertheless, collective chaos can be effectively studied in large but finite ensembles.

It is therefore natural to ask whether the stability properties of the macroscopic dynamics can be inferred from the knowledge of the usual microscopic Lyapunov exponents, which proved so powerful in characterizing the microscopic dynamics. I discuss this problem in the simplest possible setup: a mean-field model of one-dimensional units (such as logistic maps). I show that the two worlds can be compared in a meaningful way by using the microscopic variables to reconstruct a probability-like representation. As a result, I find that small macroscopic perturbations of the probability density cannot be typically represented as small perturbations of the variables of the single units [1].

Models with a diversity among the single units are also discussed [2] as an example where collective chaos emerge even in phase oscillators, where the single-unit dynamics cannot per se be chaotic at all.

Finally, I will explore the robustness of this regime, by discussing its emergence in models with a few mutual connections (sparse networks) [3] and even more traditional setups such as one-dimensional lattices with long-range interactions [4], where the coupling strength decays as a power law.

References

1. A. Politi, A. Pikovsky, and E. Ullner, "Chaotic macroscopic phases in one-dimensional oscillators", preprint 2017.
2. E. Ullner and A. Politi, *Phys. Rev. X*, 2016, **6,** 011015.
3. S. Luccioli, S. Olmi, A. Politi, and A. Torcini, *Phys. Rev. Lett*., 2012, **109**, 138103.
4. G. Robb and A. Politi, "Collective dynamics out of thermodynamic equilibrium", preprint 2016.

COHERENCE RESONANCE CHIMERAS IN DYNAMICAL NETWORKS

E. Schöll

Institut für Theoretische Physik,
Technische Universität Berlin, Hardenbergstraße 36, 10623 Berlin, Germany
schoell@physik.tu-berlin.de

We show that chimera patterns can be induced by noise in nonlocally coupled neural networks in the excitable regime [1, 2]. In contrast to classical chimeras, occurring in noise-free oscillatory networks, they have features of two phenomena: coherence resonance and chimera states. Therefore, we call them coherence-resonance chimeras. These patterns demonstrate the constructive role of noise and appear for intermediate values of noise intensity, which is a characteristic feature of coherence resonance. In the coherence-resonance chimera state a neural network of identical elements splits into two coexisting domains with different behavior: spatially coherent and spatially incoherent, a typical property of chimera states. Moreover, these noise-induced chimera states are characterized by alternating behavior: coherent and incoherent domains switch their location periodically. We show that this alternating switching can be explained by analyzing the coupling functions.

Joint work together with Anna Zakharova, Nadya Semenova, and Vadim Anishchenko.

References

1. N. Semenova, A. Zakharova, V. Anishchenko, and E. Schöll, "Coherence-resonance chimeras in a network of excitable elements", *Phys. Rev. Lett.*, 2016, **117**, 014102.
2. A. Zakharova, N. Semenova, V. Anishchenko, and E. Schöll, "Noise-induced chimerastates in a neural network", *Springer Proceedings in Mathematics Statistics*, 2017, arXiv:1611.03432.

THERMAL-LENS-FREE HEAT CAPACITIVE ACTIVE MIRROR

K. Ueda[1,2,3,4,5]

[1] Institute for Laser Science, Univ. of Electro-Communications, Chofu, Tokyo 182-8585, Japan
[2] Institute of Laser Engineering, Osaka University, Osaka, Japan
[3] Hamamatsu Photonics K.K., Hamamatsu, Japan
[4] JST, PRESTO, Tokyo, Japan
[5] Institute of Applied Physics, RAS, Nizhny Novgorod, Russia
* e-mail: ueda@ils.uec.ac.jp

Abstract. A new concept for thermal-lens-free solid state lasers, Heat Capacitive Active Mirror (HCAM), is proposed according to the systematic calculation of temperature profile and thermal-induced phase shift on 0.25–5 mm thick active mirrors of 10-mm diameter with 5-mm area pumping. Three orders of magnitude of thermal-lens reduction under the efficient cooling condition is possible. This is the first proposal for the paradigm shifting technology of thermal-lens-free active mirror available for coherent beam combination.

How to generate super-high power by the solid state lasers? Power scaling law of a laser is changing from the aperture scaling to the beam number scaling. Coherent beam combining has been a dream of the laser technology since 1960. Thermal-lens is a difficult problem to solve for solid state laser technology for a long time. There are two kinds of solution. One is the development of thermal laser ceramics using mixed solid solution to tune the optical parameter. And another is the thermal-lens compensation inside the laser material.

We propose a simple and efficient idea of Heat Capacitive Active Mirror (HCAM) capable of reducing the thermal-lens-effect by three orders with respect to 100% bottom cooled case.

HCAM in thermal equilibrium condition is shown in Fig. 1. The bottom cooling area is tuned to the pumping volume, typically 50% radius pumping and 50% bottom cooled (B-cool). Top to the bottom heat flow in the pumping volume gives us an efficient cooling almost equivalent to the 100 B-cool case. Most important point is the constant temperature halo area in the unpumped outer edge. This is a heat capacitive volume because there is no heat generation and heat sink. Thermal insulation on the heat capacitive volume reduces the non-flat wave component less than 1/50 over a wide range of disk thickness as shown in Fig. 2. When we tune the bottom surface temperature of heat capacitive volume to be constant to the average temperature of pumping volume, the thermal-shift decreases less than 1/1000 for thin disk (t = 0.25 mm) to thick disk (1 mm < t < 5 mm) range. Even a thick active mirror shows the order of magnitude smaller thermal shift than a typical thin disk. HCAM design relaxes the requirement on the doping concentration and pumping optics significantly. This is a simple solution toward thermal-lens-free solid state lasers for the coherent beam combining under CW and high rep. rate operation. The detailed properties of HCAM will be discussed in the presentation.

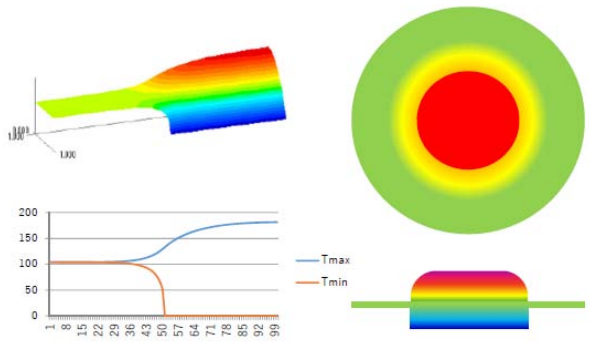

Fig. 1. Temperature profile of a HCAM laser

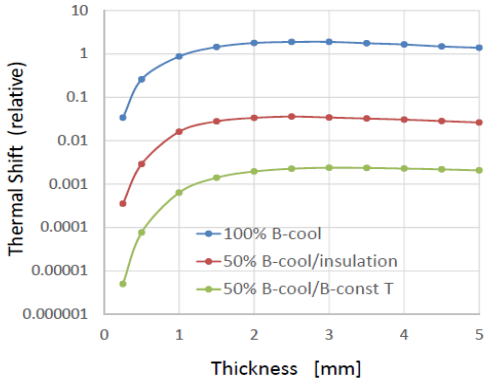

Fig. 2. Thermal-lens reduction curve

Acknowledgements

This work is partially supported by Toyota Physical and Chemical Research Institute and Mega Grant Program of Russian Federation No. 14.B25.31.0024.

International Symposium

TOPICAL PROBLEMS OF NONLINEAR WAVE PHYSICS

Nonlinear Dynamics and Complexity

Chairs

Albert Luo, Southern Illinois University, USA
Vladimir Nekorkin, Institute of Applied Physics RAS, Russia

Program Committee

Valentin Afraimovich,	Autonomous University of San Luis Potosí, Mexico
Marat Akhmet,	Middle East Technical University, Turkey
José María Amigó García,	Miguel Hernández University of Elche, Spain
Vadim Anishchenko,	Saratov State University, Russia
Jean-Marie Bilbault,	University of Burgundy, France
Maurice Courbage,	Paris Diderot University, France
Alexander Dmitriev,	Moscow Institute of Physics and Technology, Russia
Michal Feckan,	Comenius University, Slovakia
Maria Luz Gandarias,	University of Cádiz, Spain
Tassilo Küpper,	University of Cologne, Germany
Carlo Laing,	Massey University, New Zealand
Xavier Leoncini,	Aix-Marseille University, France
Elbert Macau,	National Institute for Space Research, Brasil
Miguel A. F. Sanjuán,	King Juan Carlos University, Spain
Eckehard Schöll,	Technical University of Berlin, Germany
J. A. Tenreiro Machado,	Polytechnic Institute of Porto, Portugal
Dmitry Trubetskov,	Saratov State University, Russia
Serhiy Yanchuk,	Technical University of Berlin, Germany
Jiazhong Zhang,	Xi'an Jiaotong University, China

Invited

DYNAMICAL AND STATISTICAL CHARACTERISTICS OF DIFFERENT CHIMERA STRUCTURES IN NETWORKS OF NONLOCALLY COUPLED OSCILLATORS

V.S. Anishchenko, N.I. Semenova, and **G.I. Strelkova**

Saratov National Research State University, Saratov, Russia
wadim@info.sgu.ru

Abstract. We explore the bifurcation transition from coherence to incoherence in ensembles of nonlocally coupled chaotic systems. It is firstly shown that two types of chimera states, namely, amplitude and phase chimeras, can be found in a network of coupled logistic maps. We reveal a bifurcation mechanism by analyzing the evolution of space-time profiles and the coupling function with varying coupling coefficient and formulate the necessary and sufficient conditions for realizing the chimera states in the ensemble. The regularities are established for the evolution of cross-correlations of oscillations in the network elements at the bifurcations related to the coupling strength variation. We reveal the distinctive features of cross-correlations for phase and amplitude chimera states.

We study the dynamics of the ensemble of coupled maps [1, 2]:

$$x_i^{t+1} = f(x_i^t) + \frac{\sigma}{2P} \sum_{j=i-P}^{i+P} \left[f(x_j^t) - f(x_i^t) \right], \qquad (1)$$

where x_i are real dynamical variables, $i = 1, 2, \ldots, N$ is the serial number of partial oscillators closed in the ring, t denotes the discrete time, σ is the coupling strength, P defines the number of neighbors on the left and right of the i-th element, $r = P/N$ is the coupling radius, and the logistic map $f(x_i) = ax_i(1 - x_i)$ describes the i-th oscillator. System (1) is analyzed with the parameter $a = 3.8$, which corresponds to the chaotic regime, for $N = 1000$ elements in the ring and with initial conditions randomly distributed in the unit interval [0, 1]. We fix the coupling radius as $r = 0.32$.

The second term in (1) describes the overall effect of neighbors on the particular i-th element of the ensemble (1) and we call it as the coupling function. We explore numerically the behavior of the coupling function and the dynamics of the network (1) with the parameter values given above. We plot snapshots and space-time profiles and study their evolution when the coupling strength is varied. We have found two different types of chimera states, namely, phase and amplitude chimeras [3].

The transition from coherence to incoherence and chimera states are analyzed quantitatively by calculating the cross-correlation coefficient [4]. We reveal that this characteristic is principally different for various chimera states found in the considered network.

Acknowledgements

This research is supported by the Russian Science Foundation (grant No. 16-12-10175) and the Russian Ministry of Education and Science (project code 3.8616.2017).

References

1. I. Omelchenko, Y. Maistrenko, P. Hövel, and E. Schöll, *Phys. Rev. Lett.*, 2011, **106**, 234102.
2. I. Omelchenko, B. Riemenschneider, P. Hövel, Y. Maistrenko, and E. Schöll, *Phys. Rev. E*, 2012, **85**, 026212.
3. S.A. Bogomolov, A.V. Slepnev, G.I. Strelkova, E. Schöll, and V.S. Anishchenko, *Commun. Nonlinear Sci. Numer. Simulat.*, 2017, **43**, 25–36.
4. T.E. Vadivasova, G.I. Strelkova, S.A. Bogomolov, and V.S. Anishchenko, *Chaos*, 2016, **26**, 093108.

Invited

IMPACT OF PERTURBATIONS ON NEURON RESPONSE

S. Morfu, M. Bordet, M. Rossé, and **J.M. Bilbault**

Laboratoire Le2i FRE2005, CNRS, Arts et Métiers, Univ. Bourgogne Franche-Comté, F21000 Dijon, France,
smorfu@u-bourgogne.fr, maxime.bordet@gmail.com, matthieu.rosse@u-bourgogne.fr, bilbault@u-bourgogne.fr

Abstract. We propose an overview of the effects of deterministic and stochastic perturbations on the response of a neuron. Our study is based on numerical simulations and experiments with an elementary neural circuit. We use different excitations to highlight various phenomena such as Mode locking, Vibrational Resonance, Ghost Stochastic Resonance... We close the study with a lattice of coupled circuit.

Summary

The understanding of the information encoding by neural system undoubtedly constitutes a fascinating challenge to overcome. Indeed, a great interest has been devoted to the response of neuronal models to various stimuli. Sinusoidal driving has been considered to demonstrate that the emergence of phase-locking modes in the spike triggering depends on both the amplitude and the frequency of the stimulation [1]. More complex excitations have also been considered by including the contribution of random fluctuations. For instance, Stochastic Resonance has been established in neuronal systems to show that noise can enhance the detection of subthreshold stimuli [2, 3]. Moreover, the electrical activity of neurons in the absence of deterministic excitation has been explained by the presence of noise which can induce a maximum of regularity in the spiking dynamics [4, 5]. On the other hand, bichromatic excitations, which consist in a low frequency sine component perturbed by an additive high frequency sine wave, have attracted a considerable interest in reaction-diffusion media [6]. Two main nonlinear signatures with relevant implication in neuro-context have been highlighted depending on whether the low and high frequencies are close or not [7]. Indeed, considering two close frequencies has allowed to explain how a ghost frequency, which is lower than the two frequencies of the input bichromatic excitation, can be perceived by sensory neurons of the auditory system [8, 9]. The role of noise in the detection of this ghost frequency has been highlighted in various reaction-diffusion media [10, 11], including the FitzHugh-Nagumo system [12]. Moreover, the influence of noise features has been also addressed to better understand the underlying mechanisms leading to pitch perception [13, 14]. Lastly, bichromatic excitations with distant frequencies have also attracted a considerable attention with the highlight of Vibrational Resonance (VR) [7, 15-18]. VR expresses the property of a nonlinear system to use a high frequency perturbation to enhance its response to a low frequency sine excitation. It is the aim of this communication to presents all these effects of resonance in an elementary neural circuit. We conclude with information propagation assisted by a high frequency perturbation in a lattice of coupled elementary circuits [19].

References

1. S.G. Lee and S. Kim, *Phys Rev E*, 2006, **73**, 041924.
2. L. Gammaitoni, P. Hänggi, P. Jung, and F. Marcesoni, *Rev Mod Phys*,1998, **70**,223–287.
3. J. Douglass, L. E. P. Wilkens, and F. Moss, *Nature, London* , 1993, **365**, 337–340.
4. A.S. Pikovsky, and J. Kurths, *Phys Rev Lett*, 1997, **78**, 775–778.
5. G. Lassere, S. Morfu and P. Marquié, *Electron. Lett.*, 2009, **45** (13), 669–670.
6. S. Rajamani, S. Rajasekar, and M.A.F. Sanjuan, *Commun Nonlinear Sci.*, 2014, **19** (11), 4003–4012 .
7. S. Rajasekar and M.A.F. Sanjuan, *Nonlinear Resonances. Springer Series in Synergetics* 2016.
8. D.R. Chialvo, *Chaos*, 2013, **13**, 1226–1230.
9. S. Martignoli and R. Stoop, *Phys Rev Lett*, 2010, **105**, 048101.
10. P. Balenzuela and J. Garcia-Ojalvo, *Chaos*, 2005, **15**, 023903.
11. S. Martignoli, F. Gomez, and R. Stoop, *Scientific reports*, 2013, 2676.
12. M. Bordet, S. Morfu, and P. Marquié, *Electron. Lett.*, 2014, **50**, 861–862.
13. L.G. Silva, O.A. Rosso, M.V.D. Vermelho, and M.L. Lyra, *Commun Nonlinear Sci*., 2015, **22**, 641–649.
14. M. Bordet, S. Morfu, and P. Marquié, *Chaos, Soliton and Fractals*, 2015, **78**, 205–214.
15. P. Landa and P. McClintock, *J Phys A: Math Gen*; 2000, **33**, L433–L438.
16. E. Ullner, A. Zaikin, J. Garcia-Ojalvo, R. Bascones, and J. Kurths, *Phys Lett A*, 2003, **312**, 348–354.
17. V.N. Chizhevsky, *Phys Rev E* , 2014, **89**, 062914 and *Phys Rev E*, 2014, **90**, 042924.
18. M. Bordet and S. Morfu, *Electron Lett*, 2012, **48**, 903 and *Chaos, Solitons and Fractals*, 2013, **54**,82–89.
19. M. Bordet, S. Morfu, M. Rossé, and P. Marquié, *Electron. Lett.*, 2015, **51** (19), 1482.

Invited

CONSERVATION LAWS AND POTENTIAL SYSTEMS FOR A GENERAL FAMILY OF THIN FILM EQUATIONS

M.S. Bruzón[1] and **E. Recio**[2]

[1] University of Cádiz, Cádiz, Spain, m.bruzon@uca.es
[2] University of Cádiz, Cádiz, Spain

Abstract. We derive and investigate the first-level and second-level potential systems of a family of thin film equations. From the first-level system, we obtain a new nonlocal conservation law.

The motion of a liquid under the influence of surface tension and their interaction with adjacent hard surfaces is a phenomenon that arises in daily life and many industrial processes rely on the ability to control these interactions [1]. Long-wave unstable equations are ubiquitous in the modeling of pattern formation in physical systems that involve interfaces [2]. In [5] the lubrication approximation was obtained from systematic rescaling and asymptotic expansion of the Navier-Stokes equations

$$u_t + \nabla\Big(f(u)\big(\nabla\Delta u - \nabla g(u)\big)\Big) = 0 \tag{1}$$

where u is the thickness of the film $f(u) = u^3 + b^{3-p}u^p$, $g(u) = (C_a)^{1/2}u + C\pi(u)$, b represents a dimensionless slip length, C_a is the capillary number, $\pi(u) = A_D u^{D-5}$, A_D is the Hamaker constant and C is a dimensionless parameter that depends on the Hamaker constant and the characteristic height of the film.

From equation (1) several equations have been considered by some authors [3–9]. In [10] the authors considered a generalization of equation (1) and they made a classification of symmetries

$$u_t + \nabla\Big(f(u)\big(\nabla\Delta u - \nabla g(u)\big)\Big) + h(u) = 0\,. \tag{2}$$

By using the multiplier method [11–14] we show that equation (2) admits conservation laws. From these conservation laws we obtain the associated first-level potential system and by using the Lie group method we classify the point symmetries. From each potential system we deduce the integrated equation and for these equations we investigate conservation laws. These conservation laws yield second level potential system and we make a point symmetry classification of this system.

Acknowledgements

The authors acknowledge the financial support from Junta de Andalucía group FQM-201, Universidad de Cádiz and they express their sincere thanks to the Plan Propio de Investigación de la Universidad Cádiz

References

1. A.L. Bertozzi, *Notices Amer. Math. Soc*., 1998, **45**, 689–697.
2. A. L. Bertozzi and M. Pugh, *Comm. Pur. Appl. Math*., 1998, **LI**, 625–661.
3. M.L. Gandarias and E. Medina *Proc. NEEDS*, 1999.
4. M.L. Gandarias and E. Medina Europhys. Letts., 2001, **55**, 143.
5. M.L. Gandarias, *Proc. XXXIII Summer School Advanced Problems in Mechanics*, APM, 2005.
6. M.L. Gandarias and M. Bruzón, *Proc. in Applied, Mathematics and Mechanics*, PAMM WILEY, 2007, 267–274.
7. E. Recio, S. Anco, and M.S. Bruzón, *Proc. in Int. Conf. of Numerical Analysis and Applied Mathematics*, AIP, 2016, preprint.
8. R. Tracinà, *Proc. 4th Workshop "Group Analysis of Differential Equations and Integrable Systems*, 2008, 2009, 26–30.
9. R. Tracinà, M.S. Bruzón, and M. Gandarias, *Appl. Math. and Comp.*, 2016, **275**, 299–304.
10. R. Cherniha and L. Myroniuk, *J. Phys. Math*, 2010, **2**, 1–19.
11. S. Anco and G. Bluman, *Phys. Rev. Lett.*, 1997, **78**, 2869–2873.
12. S. Anco and G. Bluman, *Euro. J. Appl. Math*., 2002, **13**, 545–566.
13. S. Anco and G. Bluman, *Euro. J. Appl. Math*., 2002, **41**, 567–585.
14. S. Anco, *Recent progress and Modern Challenges in Applied Mathematics, Modeling and Computational Science*, Fields Institute Communications, 2016, p. 1.

Invited

RESPIRATORY NEURAL NETWORK: ACTIVITY, CONNECTIVITY AND SYNCHRONNIZATION

M. Courbage, L. Mangin, and **F. Rozi**

University Paris-Diderot, Paris, France
e-mail: maurice.courbage@univ-paris-diderot.fr

Chaos in the rhythmic activity is a major issue that has been discussed in many studies of neuroscience and physiology, and especially in the respiratory air flow. Here, we present the results of two studies concerning the activity and the connectivity of the respiratory neural network in healthy humans and patients with obstructive lung disease. Our results show an increase in the dynamic chaos of airway flow in patients, focusing on expiratory flow. We then seak for the reasons for this augmentation in analyzing the activity of neural centers involved in respiratory rhythmogenesis, using functional brain imaging of the automatic neural networks, the first group generating inspiration (pre-Bötzinger complex) and the second in charge of expiration (the parafacial group). Brain imaging reveals in healthy humans a significant activation of the pre-Bötzinger complex linked to a high active inspiration while patients have a higher expiratory parafacial excitability leading to an active expiration. We also propose a theoretical model of respiratory rhythmoge- nesis which reproduces the synchronized respiratory neural network from two chaotic pacemakers, the first modelling the pre-Bötzinger complex and the second modelling the expiration. Our model reveals how the synchronized chaotic activity of this network reproduced the experimental data of the activity of the respi- ratory nerve centers both in healthy humans and the patients. We are able to reproduce fMRI signal after hemodynamic convolution of the simulated synchronized neural network. Besides, the respiratory neural network comprises the automatic brainstem and voluntary cortical network. The extension of the study to other important aspects such as functional connectivity and Granger causality allow to better understand the com- munication within the network with the aim to develop new therapeutic strategies involving the modulation of brain oscillation.

Invited

LOOK AT THE WORLD IN A DIFFERENT LIGHT: RADIO ILLUMINATION USING MICROWAVE DYNAMIC CHAOS

A.S. Dmitriev, E.V. Efremova, M.Yu. Gerasimov, and **V.V. Itskov**

Kotel'nikov Institute of Radio-engineering and Electronics of RAS, Moscow, Russia, chaos@cplire.ru

Abstract. The problem of wideband illumination of objects and surfaces by radiation from artificial noncoherent microwave sources with the aim of subsequent observation by radiometric equipment is considered. The main problem in solving this task consists in creating efficient microwave generators analogous to available sources of lighting in the visible spectral range. We propose to use generators of ultrawideband chaotic oscillations as sources of noncoherent microwave radiation.

By radio-illumination we imply artificially created noiselike field of wideband (or ultrawideband, UWB) spatially and temporarily noncoherent radiation in the radio-frequency or microwave spectral range. Radioillumination can be provided using one or more noncoherent UWB microwave sources. Being incident on surrounding objects and surfaces, this microwave radiation is partly absorbed, transmitted, and reflected, after which the subsequently propagating radiation bears information about the medium with which it interacted. In this respect, the situation is analogous to that with standard visible light. The essential difference consists in involving different frequency range and different laws of radiation–medium interaction.

The observation of objects with the aid of noncoherent microwave radiation and other noncoherent signals in frequency intervals different from that of visible light has been successfully used for a long time, e.g., in space research, monitoring of the Earth from space, and in medical diagnostics. These observations employ either the noncoherent microwave radiation generated by natural processes such as intrinsic thermal radiation of physical bodies or the scattering of microwave radiation emitted by highpower natural sources (e.g., by the Sun). Another extensively developing field of using noncoherent microwave radiation for the observation of objects is related to radiometric systems with noiselike illumination. In these systems, the radiometer contains a directional source of artificial noncoherent electromagnetic radiation that illuminates the examined part of space by analogy with a projector in the visible spectral range.

The existing microwave technology employs noiselike signal sources of two types: gas-discharge tubes and semiconductor p–n diodes operating in the avalanche breakdown regime. The main parameter of these devices is the so-called excess noise ratio (ENR, expressed in dB), defined as the ratio of the generated noise power to the noise power in a resistor matched with a particular transmission line at the given temperature of environment. The ENR of gas-discharge tubes is typically on a level of 15 dB, which is about 30times the thermal noise power in a matched resistor at the ambient temperature of 290 K. Thus, a gas-discharge tube generates noise corresponding to a temperature of $9 \cdot 10^3$ K. The ENR of diode sources reaches 30 dB and their noise temperature is about $3 \cdot 10^5$ K, which corresponds to a spectral power density of $p \approx 4 \cdot 10^{-9}$ mW/MHz (–84 dBm/MHz). Further increase in the ENR level can be achieved by using amplifiers. However, a significant increase in the power would require using rather complicated and expensive equipment. Thus, neither of the two types of noise sources can provide appropriate solution for radio-illumination tasks. We propose to use dynamic chaos generators for radio-illumination sources (lamps of radiolight), which can be treated as sources of noiselike analog signals in the corresponding frequency range.

An experimental prototype of this device developed using the chaos microgenerator. This lamp design comprises a chip with electronic components, antenna, and a secondary power supply unit that transforms 220-V ac mains voltage into a 5-V dc bias. The frequency band of the lamp is 3–5 GHz. The upper metal-coated chip side with a cone-shaped element forms a disk polycone emitter antenna. In addition, the upper chip side bears an LED indicator of the device on/off state. The electronic circuitry is arranged in a standard case for LED lamps with a radio-transparent plastic hemisphere and E27-type base. The secondary power supply source also is located in the base. The lamp radiates within a broad angular range symmetric relative to the longitudinal axis. Radio-illumination of a room or open space is provided by screwing the lamp into a standard socket and switching on the mains voltage.

Acknowledgements

The study was supported by the Russian Science Foundation, project no. 16-19-00084.

Invited

SELF-INDUCED SWITCHINGS BETWEEN MULTIPLE SPACE–TIME PATTERNS ON COMPLEX NETWORKS OF EXCITABLE UNITS

U. Feudel[1], **G. Ansmann**[2], and **K. Lehnertz**[2]

[1] Theoretical Physics/Complex Systems, ICBM, Carl von Ossietzky University Oldenburg, Carl-von-Ossietzky-Straße 9–11, Box 2503, 26111 Oldenburg, Germany
[2] Department of Epileptology, University Bonn, Sigmund-Freud-Straße 25, 53105 Bonn, Germany

Abstract. We report on self-induced switchings between multiple distinct space–time patterns in the dynamics of a spatially extended excitable system. These switchings between low-amplitude oscillations, nonlinear waves, and extreme events strongly resemble a random process, although the system is deterministic. We show that a chaotic saddle – which contains all the patterns as well as channel-like structures that mediate the transitions between them – is the backbone of such a pattern switching dynamics.

We study inhomogeneous small-world networks of excitable systems. As a paradigmatic model for excitability, we consider diffusively coupled FitzHugh-Nagumo oscillators. The inhomogeneity is realized by choosing different parameter values for each FitzHugh-Nagumo unit in the network. The topology of our network is determined by two properties: the number of long-range connections, which is controlled by the rewiring probability p, and the range of short-range connections, which can be manipulated by resizing the sphere of local influence (via the number of neighbors m involved in the coupling).

For a large range of parameter values we observe a switching between three different types of space-time patterns, which are manifested as low-amplitude oscillations, nonlinear waves and extreme events. We study this pattern switching from different points of view – phenomenologically, statistically, as well as dynamically and geometrically, which yields a coherent picture of the possible underlying ingredients and mechanisms.

Our investigations revealed two properties that are essential for the pattern switching as observed in our system to occur:

- The units have inhomogeneous control parameters, but are all in the oscillatory regime and, if coupled, they are capable of self-generating localized excitations.
- The coupling topology is dominated by connections that are short-ranged with respect to at least a two-dimensional geometry, but also contains random long-range connections.

From a dynamical point of view, our findings suggest that the observed pattern switching is a very long transient on a chaotic saddle, which contains all three distinct space-time patterns. This structure of the transient chaotic behavior extends the usual notion of a chaotic saddle in the sense that it does not need to exhibit one type of spatiotemporal dynamics only as in many examples studied previously but can be characterized by an irregular switching between different space-time patterns. We identified channel-like structures in phase space through which the trajectory switches from one particular pattern to the next. The observed pattern switching has proven to be robust against moderate changes of the number of long-range connections and parameter inhomogeneity. Moreover, the phenomenon is not tied to a specific system size.

With our findings, we present an alternative to the well-known ways to obtain self-induced pattern switching, namely noise-induced attractor hopping, heteroclinic orbits, and adaptation to an external signal. This alternative way can be expected to improve our understanding of pattern switchings in spatially extended natural dynamical systems like the brain and the heart.

References

1. G. Ansmann, K. Lehnertz, and U. Feudel, *Phys. Rev. X*, **6**, 011030.

MEAN-FIELD ANALYSIS OF STABILITY AND SLOW RATE FLUCTUATIONS IN A NETWORK OF NOISY NEURONS WITH COUPLING DELAY

I. Franović[1] and **V.V. Klinshov**[2]

[1] Scientific Computing Laboratory, Center for the Study of Complex Systems, Institute of Physics Belgrade, University of Belgrade - Pregrevica 118, 11080 Belgrade, Serbia, franovic@ipb.ac.rs
[2] Institute of Applied Physics of the Russian Academy of Sciences
46 Ulyanov Street, 603950 Nizhny Novgorod, Russia

Abstract. We analyze the emergence of slow rate fluctuations and rate oscillations in random neuronal networks influenced by external and internal noise, as well as coupling delay. The second-order stochastic mean-field model is derived to examine (i) network's stability and bifurcations in the thermodynamic limit and (ii) fluctuations associated to finite-size effects. Regarding (i), external and internal noise are found to affect macroscopic dynamics in a fundamentally different fashion. Considering (ii), we demonstrate that slow rate fluctuations between two quasi-stationary states may be understood as noise-driven transitions in a double-well potential, whereas delay-noise interplay can yield fluctuations involving two oscillatory regimes.

In recent years, the issue of how fluctuations and correlations affecting individual neurons are reflected at the network level has become a focal point of research in neuroscience. The external and/or internal sources of noise, combined with other ingredients, such as the coupling delay, play an important part in self-organization of collective behavior. One of the points attracting particular interest is that the spontaneous activity of cortical neurons comprises a doubly stochastic process, involving highly variable spike-trains on a short timescale, and slow irregular firing rate fluctuations on much longer timescales. The slow rate fluctuations (0.4–2 Hz) constitute emergent macroscopic events, consisting of "on" episodes of high spiking activity interspersed with "off" episodes of relative quiescence, and have been indicated to mediate certain forms of learning and memory, as well as to contribute to cortical response variability.

In order to gain an insight into the described phenomena, we introduce a model of a sparse random network of excitatory rate-based neurons [1, 2], where the local dynamics is influenced by external and internal noise, while the interactions include coupling delay. Our approach to analysis of network dynamics is based on deriving the second-order stochastic mean-field (MF) model which incorporates an implicit Gaussian closure hypothesis [3], in a sense that the macroscopic behavior is characterized by the mean (network-averaged) rate and the associated variance. MF dynamics is deterministic in the thermodynamic limit (TDL), while the stochastic terms make up the finite-size effect.

Using bifurcation analysis, we demonstrate that the MF model can (i) predict the network's stationary states, (ii) anticipate the delay-controlled onset of mean-rate oscillations, and (iii) qualitatively account for the generic mechanisms underlying slow fluctuations of the mean-rate.

Concerning (i), an important result is that the internal noise does not influence the MF dynamics at all, while the external noise may change the number of stationary states and their levels.

Regarding (iii), the slow rate fluctuations are shown to emerge via two scenarios. In the delay-free case, the leading mechanism can be seen as noise-driven transitions of a particle in a double-well potential. Then, the MF model in the TDL displays bistability between the "up" and the "down" state, whereas the finite-size effect gives rise to stochastic transitions between two metastable states. The second scenario for slow rate fluctuations involves cooperative action of noise and delay, where the fluctuations can be interpreted as stochastic mixing between two different oscillatory regimes.

Acknowledgements

This work was supported by the Ministry of Education, Science and Technological Development of the Republic of Serbia under project No. 171017, the Russian Foundation for Basic Research within Grants Nos. 14-02-00042 and 15-02-04245, as well as the Ministry of Education and Science of the Russian Federation, Agreement No. MK-8460.2016.2.

References

1. I. Franović and V. Klinshov, *Europhys. Lett.*, 2016, **116**, 48002.
2. V. Klinshov and I. Franović, *Phys. Rev. E,* 2015, **92**, 062813.
3. I. Franović, K. Todorović, N. Vasović, and N. Burić, *Phys. Rev. E,* 2014, **89**, 022926.

Invited

CHUNKING BY MUTUAL SUPERVISION IN RESERVOIR COMPUTING

T. Asabuki[1], N. Hiratani[1,2], and **T. Fukai[1,3]**

[1] Department of Complexity Science and Engineering, Univ. of Tokyo, Kashiwa, Chiba, Japan
[2] Gatsby Computational Neuroscience Unit, Univ. College London, London, UK
[3] RIKEN Brain Science Institute, Wako, Saitama, Japan, tfukai@riken.jp

Abstract. Many higher-order functions of the brain such as language acquisition and motor learning require sequence learning. Chunking enables the brain to generate compact representations of complex sequential events, and hence plays a pivotal role in the modeling of the external world by the brain and artificial intelligence. Several mechanisms have been proposed for chunking in the literature of computational neuroscience and computer science. However, the performance of the previous models was limited to relatively simple sequences, and the neural mechanisms underlying chunking in complex sequences remain elusive. Here, we propose a recurrent network model that is capable of learning chunks in such complex sequences.

Chunking refers to a process by which pieces of information (e.g., characters) are bound together into a meaningful whole (e.g., words). Chunking is thought to occur through two processes. Long and complex sequences are first segmented into shorter and simpler sequences. Then, frequently repeated segments may be concatenated into a single unit. While various approaches to chunking mechanisms have been proposed [1–3], chunking is still a challenge in such sequences as alternately repeat multiple chunks and random sequences of arbitrary length. I will present a novel mechanism of chunk learning in recurrent neural networks. The key is to use independent multiple reservoir computing systems that supervise each other during learning. The reservoir computing consists of a recurrent neural network and readout neurons, and has been known as a basic model of cortical information processing [3]. Although several extensions of the system, for instance to spiking neuron networks [4], have been attempted, their applications have been typically limited to motor sequence learning and control through supervised learning. In our model, while each reservoir is trained in a supervised manner, as in the original model for motor learning and control, the entire system learns multiple chunks in an unsupervised fashion. Through this learning, the system converges to a state of stable operations when each reservoir computing system produces teaching signals that are consistent with the temporal structure of input sequences. Thus, our model extends the reservoir computing system to a more flexible unsupervised learning system for chunking. Interestingly, readout neurons in our model behave like “stop cells” which have been discovered in the basal ganglia after motor sequence learning. This result suggests the biological relevance of our model.

Acknowledgements

This work was partly supported by KAKENHI (nos. 15H04265 and 16H01289) to T.F.

References

1. S.J. Kiebel, K. Von Kriegstein, J. Daunizeau, K.J. Friston, *PLoS computational biology*, 2009, **5**(8), e1000464.
2. M. Rabinovich, P. Varona, I. Tristan and V. Afraimovich, *Frontiers Comput. Neurosci*., 2014, **8**, 22.
3. T. Taniguchi, S. Nagasaka and R. Nakashima, *IEEE Trans. Cog. Dev. Systems*, 2016, **8**(3), 171–185.
4. D. Sussillo and L.F. Abbott, *Neuron*, 2009, **63**(4), 544–557.

Invited

ON CONSERVATION LAWS FOR SOME EQUATIONS THAT ADMIT COMPACTON SOLUTIONS

M.L. Gandarias

University of Cadiz, Spain
marialuz.gandarias@uca.es

We consider a generalized equation admitting compacton solutions induced by a non-convex convection. A complete classification of low-order conservation laws is obtained for this equation.

Invited

AMPLITUDE DEATH AND CHIMERA PATTERNS IN COMPLEX NETWORKS WITH TIME DELAYS

A. Gjurchinovski[1], E. Schöll[2], and **A. Zakharova[2]**

[1] Institute of Physics, Faculty of Natural Sciences and Mathematics, Sts. Cyril and Methodius University Skopje, Macedonia, E-mail:aleksandar.gjurchinovski@gmail.com
[2] Institut für Theoretische Physik, Technische Universität Berlin, Berlin, Germany

Abstract. We study the conditions of amplitude death in a network of delay-coupled limit cycle oscillators with time-varying delay coupling. By generalizing the master stability function formalism, we analyze the amplitude death regimes in a ring and a multiplex network of Stuart-Landau oscillators. We further investigate the influence of time delay (constant, time-varying, or distributed) on the dynamical regimes and the lifetime of amplitude chimera states in the case when coupling breaks the rotational S^1 symmetry. We demonstrate that the lifetime of amplitude chimeras and related incoherent states can be deliberately reduced or increased, depending upon the type of coupling delay.

In this talk, we first describe a method to control amplitude death in networks of delay-coupled limit cycle oscillators [1]. We consider the impact of the variability of the time delay in the node interconnections, as well as in the self-feedback, either at each node or at a single node only. The variability of the coupling delay in real networks is often due to random fluctuations induced by the environment, or due to imperfections of the system. In these cases, the delay varies stochastically in time, being distributed over an interval of values and characterized by a distribution function. To investigate analytically the regions of amplitude death in the parameter space, we generalize the formalism of the master stability function, which is a method originally used to analyze the synchronous dynamics of complex networks. At high-frequency delay modulation, analytical results for the occurrence of amplitude death can be obtained by approximating the variable-delay coupling terms by distributed delay with delay-distribution kernels matching the probability density function. The superiority of the proposed method with respect to the constant delay case is demonstrated both numerically and analytically for a regular ring network consisting of Stuart-Landau limit cycle oscillators in the regime near a Hopf bifurcation. We have shown that controllability of the network fixed point is strongly limited by the local node dynamics, which could be removed in certain cases by including a variable-delay self-feedback. In addition, we have shown that amplitude death can even be induced if the self-feedback is applied at a single node only, for certain control parameter intervals and not too large networks. We also apply our control method to investigate amplitude death patterns in more complex situations of multiplex network topologies.

Next, we report on our investigations of a ring network of Stuart-Landau oscillators coupled non-locally and through the real part of the complex variable [2–4]. While analyzing various space-time patterns observed in this network, we focus on the transition from transient amplitude chimera states to phase-lag synchronization (traveling waves) and higher-order coherent structures. Since the Kuramoto order parameter cannot be used as an indicator for such a transition, we have developed a measure which generalizes the global Kuramoto mean-field order parameter and allows us to detect the transition from partially incoherent states (e.g., amplitude chimeras) to any type of coherent structures. We have systematically studied the impact of time delay in the coupling on the dynamics of the system, comparing the results for constant, distributed, and time-varying delays with different modulation types. We have shown numerically that at high-frequency delay modulation, the system with time-varying delay coupling is equivalent to distributed delay coupling with related delay-distribution kernels.

Acknowledgements

This work was supported by DFG in the framework of SFB 910.

References

1. A. Gjurchinovski, A. Zakharova, and E. Schöll, *Phys. Rev. E*, 2014, **89**, 032915.
2. E. Schöll, *Eur. Phys. J. Spec. Top*., 2016, **225**, 891.
3. A. Zakharova, S. Loos, J. Siebert, A. Gjurchinovski, J. C. Claussen, and E. Schöll, *Controlling chimera patterns in networks: interplay of structure, noise, and delay*, in *Control of Self-Organizing Nonlinear Systems*, edited by E. Schöll, S. H. L. Klapp, and P. Hövel (Springer, Berlin, Heidelberg, 2016).
4. A. Gjurchinovski, E. Schöll, and A. Zakharova, 2017, arXiv:1702.05326v2.

Invited

MACROSCOPIC AND MICROSCOPIC SPECTRAL PROPERTIES OF MULTILAYER EPILEPTIC BRAIN NETWORKS DURING LOCAL AND GLOBAL SYNCHRONIZATION

A.E. Hramov[1], V.A. Maksimenko[1], V.V. Makarov[1], A. Luttjohann[2], M.V. Goremyko[1], A.A. Koronovskii[3], A.E. Runnova[1], G. van Luijtelaar[4], and **S. Boccaletti[5,6]**

[1] Yuri Gagarin State Technical University of Saratov, REC "Nonlinear Dynamics of Complex Systems", Saratov, 410054, Russia
[2] University of Munster, Institute of Physiology I, Munster, 48149, Germany
[3] Saratov State University, Faculty of Nonlinear Processes, Saratov, 410012, Russia
[4] Radboud University, Donders Centre for Cognition, Nijmegen, 6525 HR , Netherlands
[5] CNR-Institute for complex systems, Sesto Fiorentino, 50019, Italy
[6] The Italian Embassy in Tel Aviv, Tel Aviv, 68125, Israel

Abstract. We introduce a practical and computationally undemanding technique for inferring interactions at various microscopic levels between the units of a complex network with adaptive links from the measurements and the processing of macroscopic signals. Our methodology is then applied for taking a look at the microscopic interactions occurring in a neurophysiological system, namely, in the thalamo-cortical neural network of an epileptic brain, where the group electrical activity is registered by means of EEG. We demonstrate that it is possible to infer the degree of interaction between the interconnected regions of the brain during different types of brain activities, and to estimate the regions' participation in the generation of the different levels of consciousness.

The current trends in neuroscience and neurophysiology relate to the analysis of brain networks which interact with each other to perform different types of cognitive tasks such as, e.g., the formation of a memory trace, the processing of a visual object, or the development (on a clinical level) of pathological rhythms like epileptic seizures. These interactions are often quantified by means of the degree of synchrony, which can be measured both locally (i.e. within the same brain structure), or over a more global scale (i.e. in between brain structures).

In this talk, we introduce a practical and computationally undemanding technique for inferring interactions at various microscopic levels between the units of a complex network with adaptive links from the measurements and the processing of macroscopic signals. Starting from a network model of Kuramoto phase oscillators which evolve adaptively according to homophilic and homeostatic adaptive principles, we give evidence that the increase of synchronization within groups of nodes (and the corresponding formation of synchronous clusters) causes also the defragmentation of the wavelet energy spectrum of the macroscopic signal.

Our methodology is then applied for taking a look at the microscopic interactions occurring in a neurophysiological system, namely, in the thalamo-cortical neural network of an epileptic brain of a WAG/Rij rat, where the group electrical activity is registered by means of multichannel electroencephalograms. We demonstrate that it is possible to infer the degree of interaction between the interconnected regions of the brain during different types of brain activities, and to estimate the regions' participation in the generation of the different levels of consciousness. We compare our approach with wavelet coherence calculations and show the advantages of our method. We apply our approach to develop the brain-computer interface for prediction and prevention of epileptic seizure [1].

References

1. V.A. Maksimenko, S. Heukelum, V.V. Makarov, J. Kelderhuis, A. Lüttjohann, A.A. Koronovskii, A.E. Hramov, G. Luijtelaar, "Absence Seizure Control by a Brain Computer Interface", *Scientific Reports*, 2017, **7**, 2487.

MODEL OF HUMAN CARDIOVASCULAR SYSTEM

A.S. Karavaev, J.M. Ishbulatov, A.R. Kiselev, V.I. Ponomarenko, and **M.D. Prokhorov**

Saratov Branch of the Institute of Radio Engineering and Electronics of Russian Academy of Sciences, Saratov, Russia, karavaevas@gmail.com

Abstract. We propose a model of human cardiovascular system which describes the main heart rhythm, the regulation of heart function and blood vessels by the autonomic nervous system, baroreflex, and the formation of arterial blood pressure. The proposed model demonstrates the phenomenon of synchronization of mean arterial pressure regulatory system by the signal of respiration with the basic period close to 10 s, which is observed in the physiological experiments.

The studies of complex multicomponent systems of the real world are usually accompanied by consistent improvement of the model. Starting with the simple block diagrams that only qualitatively describe the behavior of the real system, the models are developed and grow more complex as new knowledge becomes available. These more complicated models offer both qualitative and quantitative description of the observed phenomena. Simulation is of particular importance in physiology, biology, and medicine, where the possibilities of experimental invasive research and the range of acceptable impacts on the object under investigation are fundamentally limited [1].

A model of human cardiovascular system is proposed which describes the main heart rhythm, the regulation of heart function and blood vessels by the autonomic nervous system, baroreflex, and the formation of arterial blood pressure [2]. The model takes into account the impact of respiration on these processes.

Its capabilities and the boundaries of applicability were compared to the experimental results and the model proposed earlier by Kotani [3]. For this purpose spectral analysis of heart rate variability (HRV) signals was carried out. Also, frequency synchronization between 0.1 Hz oscillations in HRV signals and respiration with linearly changing frequency was detected.

It was shown that the addition of baroreflex regulation loop of mean arterial pressure (AP) in the form of self-sustained oscillator with time delay [4] in the proposed model allows one to reproduce the power spectra, the values of statistical indices of HRV, and the ratio of systolic and diastolic blood pressure typical for healthy subjects at rest. Besides, the proposed model demonstrated the ability to simulate the phenomenon of phase synchronization of 0.1 Hz rhythm of mean AP baroreflex regulation and respiration with linearly changing frequency that was previously observed in our experiments. Moreover, it is possible to reproduce the autonomous blockade and arterial hypertension by the choice of the model parameter values [5].

Acknowledgements

This work was supported by the Russian Science Foundation, Grant No. 14-12-00291.

References

1. B.P. Bezruchko and D.A. Smirnov, https://doi.org/10.1007/978-3-642-12601-7.
2. A.S. Karavaev *et al*., *J. of Am. Society of Hypertension*, 2016, **10**(3), 235–243.
3. K. Kotani *et al*., *Phys. Rev. E*, 2005, **72**, 041904.
4. J.V. Ringwood and S.C. Malpas, *Am. J. of Physiology*, 2001, **280**, R1105–R1115.
5. P.P. Jones *et al*., *Circulation*, 2001, **104**, 2424–2429.

Invited

LIE GROUP ANALYSIS AND CONSERVATION LAWS OF THE ZOOMERON EQUATION

C.M. Khalique

North-West University, Mmabatho, South Africa
Masood.Khalique@nwu.ac.za

In this talk, we study the (2 + 1)-dimensional Zoomeron equation which is an extension of the well-known (1 + 1)-dimensional Zoomeron equation that has been studied extensively in the literature. We determine the classical Lie point symmetries admitted by the equation and compute an optimal system of one-dimensional subalgebras. Based on this optimal system, we obtain symmetry reductions and new group-invariant solutions. Furthermore we construct the conservation laws of the underlying equation using the multiplier method**.**

SELECTIVE PROPERTIES OF NEURONS WITH DYNAMIC THRESHOLD OF EXCITABILITY

S.Yu. Kirillov and **V.I. Nekorkin**

Institute of Applied Physics of the Russian Academy of Sciences, Nizhny Novgorod, Russia
skirillov@neuron.appl.sci-nnov.ru

Abstract. A model neuron with slow synaptic input demonstrates high variability of its excitability threshold properties. This allows the neuron to receive and transform fast external synaptic signals in a complicated nontrivial manner. The slow modulation of the threshold properties not only changes the number of spikes in the response, but also makes the number of spikes from the fast pulse amplitude nonmonotonic.

The study of systems modeling the properties of nerve cells is one of the intensively developing areas of modern nonlinear physics [1]. The neural modeling on the one hand allows us to understand the basic mechanisms of the brain and on the other to develop new ways of processing and transmitting information.

An important place in the research of neural activity is occupied by the identification of mechanisms of action potential generation in an individual neuron under the influence of an external stimulus. The change in the membrane potential of a neuron is determined by the sum of different incoming synaptic currents that can be either pulsed relaxation or slowly monotonically increasing or decreasing [2]. Here we study the dynamics of a model neuron with a complex-threshold excitation [3, 4] under the additive effect of weak slow and fast pulsed synaptic currents. The processes of short pulse transformation are investigated depending on the characteristics of the slow stimulus and the state of the neuron itself. It is shown that the response of the model has selective properties in terms of the amplitude of the incoming pulse. Depending on the parameters of the model the response can be either single action potential or a series of several action potentials called bursts.

A key role in the formation of the neuron response to a pulsed signal is played by the presence of a complex threshold of excitability. In the absence of slow synaptic input the threshold properties are determined in the model phase space by the oscillating separatrix of the saddle equilibrium state. The presence of a slowly varying synaptic current leads to a significant change in the shape and location of the threshold manifold. Threshold transformation with an increase in the rate of the slow synaptic current occurs in a complex nonlinear manner. Its distinctive feature is the appearance of structures in the form of folds on the threshold manifold. The appearance of folds is a purely dynamic effect. Its existence can't be established directly from the classical methods of analysis of slow-fast systems. Thus, the threshold of neural excitability has a complex nonstationary structure, which can't be obtained directly on the basis of static threshold analysis. It is shown that with simultaneous action of fast and slow synaptic currents on a neuron, a fast pulse current excites spike-burst oscillations, while a slow synaptic current has a modulating effect on them. Activating a weak slow current not only changes the number of spikes in the response, but also makes the number of spikes from the fast current amplitude nonmonotonic. The established regularities of the action potential sequence emergence are of considerable interest for the construction of neuroinspired sensory systems capable of processing or transmitting information at relatively short time intervals of the order of several action potentials.

Acknowledgements

This work has been funded by the Russian Foundation for Basic Research (grants 15-42-02353, 15-02-04245, 17-02-00904 and 17-02-00874).

References

1. P.E. Kloeden, C. Potzsche (Eds.), *Nonautonomous dynamical systems in the life sciences*, Springer, London, 2013, p. 314.
2. J.G. Nicholls *et al.*, *From Neuron to Brain*, 5-th ed., Sunderland MA: Sinauer Associates, Inc., 2011, p. 621.
3. S. Binczak, S. Jacquir, J.M. Bilbault, V. Kasantsev, and V. Nekorkin, *Neural Networks*, 2006, **19**(5), 684–693.
4. S.Y. Kirillov, V.I. Nekorkin, *Radiophys. Quantum. El.*, 2015, **57**(11), 837–847.

MULTI-JITTERING REGIMES IN NETWORKS WITH PULSE DELAYED COUPLING

V.V. Klinshov[1], D.S. Shchapin[1], S. Yanchuk[2], and **V.I. Nekorkin[1]**

[1] Institute of Applied Physics, Nizhny Novgorod, Russia, vladimir.klinshov@ipfran.ru
[2] Technical University Berlin, Germany

Abstract. We report a novel type of the dynamics in oscillatory networks with pulse delayed coupling. In such networks the regular low-periodic oscillations may destabilize giving birth to the higher-periodic ones, the so-called "jittering" regimes. The period of the emergent regimes is proportional to the value of the coupling delay. Another characteristic feature is high multistability of these regimes. At the bifurcation point, the low-periodic regime destabilizes, and a bunch of higher-periodic ones appear at once. The number of the coexisting "jittering" regimes grows exponentially with the coupling delay.

Interaction via short signals, or pulses, is a characteristic feature of many types of dynamical networks. Delayed interaction is typical for many of them as well. A prototypical example is neural networks where neurons interchange spikes which propagate with finite speed leading to coupling delays. Numerous researches have shown that the introduction of time delays may lead to significant changes in the dynamics of a system, the reason for which is the increase of its dimensionality.

Here we report a novel type of the dynamics that emerges in oscillatory networks with pulse delayed coupling. Recently we showed that in such networks the regular low-periodic oscillations may destabilize giving birth to the higher-periodic ones, the so-called "jittering" regimes. The period of the emergent regimes is proportional to the value of the coupling delay and may be arbitrarily large. Another characteristic feature of such regimes is their high multistability. At the bifurcation point, the low-periodic regime destabilizes, and a bunch of higher-periodic ones appear at once. The number of the coexisting "jittering" regimes grows exponentially with coupling delay.

The jittering regimes are observed in networks of various configurations, such as a single oscillator with feedback, a pair of oscillators, rings with unidirectional coupling and small motifs of various topology. The onset of the "multi-jittering" bifurcation is determined by the form of the coupling function and can be predicted analytically.

Acknowledgements

The research is supported by the Ministry of Education and Science of the Russian Federation (Agreement No. MK-8460.2016.2) and the Russian Foundation for Basic Research (grant 17-02-00904).

References

1. V.V. Klinshov, D.S. Shchapin, S. Yanchuk, and V.I. Nekorkin, *Phys. Rev. E*, 2016, **94**, 12206.
2. V.V. Klinshov, L. Lücken, D.S. Shchapin, S. Yanchuk, and V.I. Nekorkin, *Phys. Rev. Lett*., 2015, **114**, 178103.
3. V.V. Klinshov, L. Lücken, D.S. Shchapin, S. Yanchuk, and V.I. Nekorkin, *Phys. Rev. E*, 2015, **92**, 42914.

Invited

CHARACTERISTICS OF NOISE-INDUCED INTERMITTENCY IN BISTABLE SYSTEMS

A.A. Koronovskii

Saratov State University, Saratov, Russia
alexey.koronovskii@gmail.com

The irregular alternation of two different regimes in time, while all system parameters are fixed, has been observed and studied intensively in many dynamical systems, from electrical circuits [1] and lasers [2] to immensely complex living objects [3–7]. Recently, the notion of intermittency was extended to multistable systems (multistate intermittency) manifested as the alternation between coexisting periodic or chaotic behaviors [8, 9]. In bistable and multistable dynamical systems, irregular switches between coexisting states can be induced by noise resulting in so called noise-induced intermittency, also known as multistate intermittency, or noise-induced attractor hopping [10–13].

Despite of some achievements in the study of noise-induced intermittency, there remain several problems demanding consideration and discussion. One of them is the lack of an appropriate theory which would reveal the main characteristics of noise-induced intermittency, including the case of a bistable dynamical system.

The aim of this talk is to develop a quantitative theory of noise-induced intermittency in a system with two coexisting regimes, and prove it with several different systems, from the point of view of the proposed theory comparing the statistical characteristics of the behavior of these systems with the theoretical predictions. We consider several systems where the noise-induced intermittency is observed, namely, the bistable energy model, erbium-doped fiber laser and the brain dynamics in perception of ambiguous images.

Acknowledgements

This work has been supported by Russian Science Foundation (project 14-12-00224).

References

1. I.M. Kyprianidis, M.L. Petrani, J.A. Kalomiros, and A.N. Anagnostopoulos, *Phys. Rev. E*, 1995, **52**, 2268.
2. A.N. Pisarchik, A.V. Kir'yanov, Y.O. Barmenkov, and R. Jaimes-Reategui, *J. Opt. Soc. Am. B*, 2005, **22**, 2107.
3. J.L. Perez Velazquez *et al*., *Eur. J. Neurosci*., 1999, **11**, 2571.
4. J.L. Cabrera and J.G. Milton, *Phys. Rev. Lett*., 2002, **89**, 158702.
5. C. Park, R.M. Worth, and L.L. Rubchinsky, *Phys. Rev. E*, 2011, **83**, 042901.
6. P. Gong, A. R. Nikolaev, and C. van Leeuwen, *Phys. Rev. E*, 2007, **76**, 011904.
7. S. Ahn, C. Park, and L.L. Rubchinsky, *Phys. Rev. E*, 2011, **84**, 016201.
8. A.N. Pisarchik, R. Jaimes-Reategui, R. Sevilla-Escoboza, and G. Huerta-Cuellar, *Phys. Rev. E*, 2012, **86**, 056219.
9. R. Sevilla-Escoboza, J.M. Buldu, A.N. Pisarchik, S. Boccaletti, and R. Gutierrez, *Phys. Rev. E*, 2015, **91**, 032902.
10. F.T. Arecchi, R. Badii, and A. Politi, *Phys. Rev. A*, 1985, **32**, 402.
11. K. Wiesenfeld and P. Hadley, *Phys. Rev. Lett*., 1989, **62**, 1335.
12. S. Kraut and U. Feudel, *Phys. Rev. E*, 2002, **66**, 015207.
13. A.N. Pisarchik, R. Jaimes-Reategui, R. Sevilla-Escoboza, G. Huerta-Cuellar, and M. Taki, *Phys. Rev. Lett.*, 2011, **107**, 274101.

Invited

DESIGN PRINCIPLES AND ILLUSTRATIONS OF HYPERBOLIC CHAOS IN MECHANICAL AND ELECTRONIC SYSTEMS

S.P. Kuznetsov[1,2]

[1] Kotel'nikov Institute of Radio-Engineering and Electronics, Saratov Branch, Russia, spkuz@yandex.ru
[2] Udmurt State University, Izhevsk, Russia

Abstract. The report contains an overview of approaches to constructing systems of electronic and mechanical nature manifesting the hyperbolic chaos.

Hyperbolic chaos has fundamental advantages for applications. First, it is characterized by roughness, or structural stability, i.e. insensitivity of chaos to slight variations of parameters and to a form of the evolution operator. Second, presence of a well-elaborated mathematical theory is attractive for developing profound opportunities for applications, for example, in communication systems. Until recently, however, hyperbolic chaos was represented exclusively by mathematical constructions (Smale-Williams attractor, Plykin attractor, and Anosov dynamics). If mathematicians develop their examples using geometric, topological, algebraic methods, a physicist for design of mechanical or electronic models with hyperbolic chaos should use another toolbox: oscillators, particles, interactions, feedback loops etc. [1].

The simplest approach is to consider a mechanical system, for example, a particle in a plane or in space, under periodic kicks, the magnitude and direction of which depend on the instantaneous position of the particle, implementing such conditions that the mapping over the period would correspond to some mathematically constructed map with a hyperbolic attractor [2].

The second approach is based on the use of two or more oscillators, which pass the excitation of each other so that the complete cycle of the transfer corresponds to the expanding map for the angular variable, which corresponds to the phase of the oscillations [3]. A similar method may be applied to distributed systems, where the expanding map is subjected to a phase of spatial patterns, such as Turing structures or parametrically excited standing waves on a nonlinear string [4].

Several approaches are based on the purposeful design of models in the form of differential equations with right parts of periodically switched form. In particular, this made it possible to indicate an example of a system where an attractor of the Plykin type is realized [5].

One more recently developed direction is constructing mechanical systems starting from Anosov's dynamics on a surface of negative curvature. In particular, such dynamics are realized in the Thurston-Wicks-McKay-Hunt triple-linkage hinge mechanism. Several versions have been considered, where the mechanical constraint through hinges and pivots is replaced by potential interaction for the three rotators [6]. Introducing dissipation and feedback makes the system with hyperbolic chaos self-oscillatory. The Anosov type dynamics occurs on an attractive set in the phase space but the attractor retains the hyperbolic nature due to the inherent structural stability. Being inspired by the mechanical system, it appears possible to implement an electronic circuit operating as a hyperbolic chaos generator, where a phase-locked loop is used as an analog of the mechanical rotator.

All the mentioned principles of design of systems with hyperbolic chaos are illustrated by concrete examples represented by differential equations or electronic circuits, and results of simulation of their functioning are presented.

Acknowledgements

The research is supported partially by RSF grant No 15-12-00235 (mechanical models) and by RFBR grant No 16-02-00135 (design and simulation of electronic systems).

References

1. S.P. Kuznetsov, *Physics-Uspekhi*, 2011, **54**(3), 119–144.
2. S.P. Kuznetsov, V.P. Kruglov, *Regular and Chaotic Dynamics*, 2016, **21**(2), 160–174.
3. S.P. Kuznetsov, *Phys. Rev. Lett.*, 2005, **95**, 144101.
4. V.P. Kruglov, S.P. Kuznetsov, A. Pikovsky, *Regular and Chaotic Dynamics*, 2014, **19** (4), 483–494.
5. S.P. Kuznetsov, *Chaos*, 2011, **21**, 043105.
6. S.P. Kuznetsov, *Regular and Chaotic Dynamics*, 2015, **20**(6), 649–666.

Invited

DYNAMICS OF SYSTEMS WITH MANY DEGREES OF FREEDOM FROM LONG RANGE-INTERACTIONS TO COMPLEX NETWORKS

X. Leoncini

Aix-Marseille Université, Marseille, France
xavier.leoncini@cpt.univ-mrs.fr

In this talk I will discuss the dynamics of systems with many degrees of freedom. We first will consider some results obtained in the case of long-range interacting systems with Hamiltonian dynamics. Starting from these we shall see how some of the properties can be transferred to the dynamics on networks, either on regular lattices or more complex networks.

Finally if I have time, I will briefly present some simple models of the growth of a network itself (mainly with a tree like structure at this stage) and discuss some of the obtained results with possible comparison to real trees.

Invited

ON PERIOD-1 MOTIONS TO CHAOS IN A PARAMETRICALLY EXCITED PENDULUM

Y. Guo[1] and **A.C.J. Luo**[2]

[1] McCoy School of Engineering, Midwestern State University, Wichita Falls, TX 76308, USA
yu.guo@mwsu.edu
[2] Department of Mechanical and Industrial Engineering, Southern Illinois University Edwardsville
Edwardsville, IL 62026-1805, USA
aluo@siue.edu

In this paper, bifurcation trees of period-1 motions to chaos in a parametrically excited pendulum are predicted semi-analytically. To construct discrete mapping structure of periodic motions, implicit discrete maps are developed from the discretized differential equation of such a parametric pendulum. The bifurcation tree of period-1 motions to chaos is presented via the complete bifurcation trees of period-1 to period-4 motions. The corresponding stability and bifurcation analysis are carried out through eigenvalue analysis. Finally, numerical simulations of various periodic motions are completed, and such simulations are illustrated over the analytically predicted trajectories for verifications.

MEAN-FIELD MODEL FOR A NETWORK OF GLOBALLY COUPLED STOCHASTIC MAP-BASED NEURONS

O.V. Maslennikov[1], **I. Franović**[2], and **V.I. Nekorkin**[3]

[1] Institute of Applied Physics of the RAS, Nizhny Novgorod, Russia, e-mail: olmaov@ipfran.ru
[2] Institute of Physics, University of Belgrade, Belgrade, Serbia
[3] Institute of Applied Physics of the RAS, Nizhny Novgorod, Russia

Abstract. We analyze the emergent regimes and the stimulus-response relationship of a population of stochastic spiking neurons modeled by discrete-time systems by means of a mean-field (MF) model, derived within the framework of cumulant approach complemented by the Gaussian closure hypothesis. It is demonstrated that the MF model can qualitatively account for stability and bifurcations of the exact system, capturing all the generic forms of collective behavior, including macroscopic excitability, subthreshold oscillations, periodic or chaotic spiking, and chaotic bursting dynamics. Apart from qualitative analogies, we find a substantial quantitative agreement between the exact and the approximate system, as reflected in matching of the parameter domains admitting the different dynamical regimes, as well as the characteristic properties of the associated time series. The effective model is further shown to reproduce with sufficient accuracy the phase response curves of the exact system and the assembly's response to external stimulation of finite amplitude and duration.

In this talk we present results on the systematic analysis of the emergent dynamics and the stimulus-response relationship of a network of globally-coupled map-based neurons using a mean-field (MF) approach. The considered map neurons can exhibit a variety of regimes, including excitability, subthreshold oscillations, regular and chaotic spiking or bursting, as well as mixed spiking-bursting oscillations. Despite the extensive studies of collective motion of spiking neurons subjected to noise using different models of discrete local dynamics, a MF theory for a population of noisy map neurons is obtained here for the first time. Our derivation of the effective model relies on Gaussian approximation, which is introduced within the framework of a Gaussian closure hypothesis. In physical terms, such an approximation suggests that the local variables at an arbitrary moment of time are independent and conform to a normal distribution centered about the assembly mean and characterized by the associated assembly variance.

Within the MF framework we have demonstrated that the effective model can qualitatively capture all the bifurcations of the exact system leading to the onset of different generic regimes of collective behavior. As far as the quantitative agreement is concerned, we have established substantial matching between the parameter domains admitting the respective dynamical regimes for the exact and the approximate system. Moreover, the typical features of the associated regimes, such as the average interspike interval or the average bursting cycle, exhibit analogous changes with parameter variation, and in many parameter domains display numerically similar values.

Apart from considering asymptotic dynamics, we have verified that the MF model is capable of capturing the stimulus-response features of the exact system. For short pulse-like perturbations, it has been found that the approximate system reproduces the phase response curves of the exact system for both the spiking and bursting regimes of collective activity with high accuracy. Substantial analogies have also been observed in case of macroscopic excitable regime for scenarios where the assembly is stimulated by rectangular pulse perturbations of finite amplitude and duration.

Acknowledgements

This work is supported by the Russian Foundation for Basic Research within Grants No. 15-02-04245 and 17-02-00904, and by the Ministry of Education, Science and Technological Development of Republic of Serbia under project No. 171017.

Reference

1. I. Franovic, O.V. Maslennikov, I. Bacic, & V.I. Nekorkin. *ArXiv preprint*, 2017, *arXiv:1703.01964*.

Invited

SUBTHRESHOLD SIGNAL ENCODING AND TRANSMISSION IN COUPLED FITZHUGH-NAGUMO NEURONS

M. Masoliver and **C. Masoller**

Universitat Politecnica de Catalunya, Terrassa, Barcelona, Spain
cristina.masoller@upc.edu

Abstract. We study two coupled neurons using the FitzHugh-Nagumo model. We analyze how mutual coupling affects the detection and transmission of a periodic, subthreshold signal that is applied to only one of the neurons. Recent work has shown that, in a single neuron, the interplay of noise and modulation induces temporal ordering in the spike sequence. We analyze under which conditions the coupling to a second neuron further enhances the temporal order of the spikes of the first neuron, improving signal encoding. We also study which conditions enhance temporal order in the spikes of the second neuron, improving signal transmission.

In sensory neurons the presence of noise can facilitate the detection of weak signals, which are encoded and transmitted via temporally correlated sequences of spikes. In a recent work [1] the dynamics of a stochastic FitzHugh-Nagumo (FHN) neuron was studied, when a weak periodic signal was applied to the neuron (the amplitude of the signal was kept below the excitable threshold, such that by itself, in the absence of noise, the signal did not generate spikes and the response of the neuron was a subthreshold oscillation). In the presence of noise, however, spikes were generated which encoded information about the applied subthreshold signal. By using a symbolic method of time-series analysis known as ordinal analysis [2] applied to the sequence of inter-spike-intervals (ISIs), it was shown that the interplay of noise and the periodic signal induced the emergence of relative temporal ordering in the timing of the spikes (i.e., induced temporal correlations among several consecutive ISIs). Different types of temporal ordering were found, in the form of preferred and infrequent ordinal patterns that depended on both, the strength of the noise and the period of the input signal. A resonance-like behavior was also found, as the probabilities of the preferred/infrequent patterns were maximum/minimum for certain periods of the input signal and noise strengths. In contrast, the spike rate was found to be nearly independent of the period of the signal. These results suggest that single sensory neurons in noisy environments might encode information about weak periodic stimuli not in the rate of the generated spikes ("rate coding") but rather in the relative timing of the spikes ("temporal coding"), in the form of more/less frequent ordinal patterns, which vary with the period of the input signal.

Here we analyze under which conditions the coupling to a second neuron, which is assumed to be mutual, linear and instantaneous, can further enhance the temporal ordering in the spike sequence of the first neuron, improving the encoding of the weak, subthreshold external signal. As in [1], we apply the method of ordinal analysis to the output sequence of inter-spike intervals of the first neuron. We find that for certain periods and amplitudes of the external signal, the coupling to the second neuron changes the preferred (and also the infrequent) ordinal patterns. A detailed study of how the ordinal probabilities vary with the coupling strength is performed. In a second step, we analyze which coupling conditions enhance temporal order in the spikes of the second neuron, improving the transmission of the signal.

Acknowledgements

This work was supported in part by Spanish MINECO/FEDER (FIS2015-66503-C3-2-P) and ICREA ACADEMIA, Generalitat de Catalunya..

References

1. J.A. Reinoso, M.C. Torrent, and C. Masoller, "Emergence of spike correlations in periodically forced excitable systems", *Phys. Rev. E*, 2016, **94**, 032218.
2. C. Bandt and B. Pompe, "Permutation entropy: a natural complexity measure for time series", *Phys. Rev. Lett.*, 2002, **88**, 174102.

EMERGENT TRAFFIC IN A HYPERNETWORK GENERATED BY AN ADAPTIVE NEURON NETWORK

V.I. Nekorkin[*], **O.V. Maslennikov,** and **D.S. Shchapin**

Institute of Applied Physics of the RAS, Nizhny Novgorod, Russia
[*] e-mail: vnekorkin@neuron.appl.sci-nnov.ru

Abstract. We propose a model of an adaptive network of spiking neurons that gives rise to a hypernetwork of its dynamic states at the upper level of description. Left to itself, the network exhibits a sequence of transient clustering which relates to a traffic in the hypernetwork in the form of random switching between different states. Receiving inputs the system is able to generate reproducible sequences corresponding to stimulus-specific paths in the hypernetwork. We illustrate these basic notions by a simple network of discrete-time spiking neurons together with its FPGA realization and analyze their properties.

We propose a paradigmatic model of how network dynamics and structure evolution can lead to the emergence of a new level of description which may be considered as an emergence of functions from evolving dynamical structures [1, 2]. The outline of the model is the following. First, we consider a neuronal population as a network of interacting nodes-oscillators coupled by directed links. This is the bottom level. The nodal dynamics as well as the activity of links are governed by some deterministic evolutionary operators. Depending on nodal dynamics the links become active or inactive thus forming different structural patterns in the network. Physiologically this can mean that some synaptic links become strong while others tend to be weak. A structural pattern results in a specific spatiotemporal activity in the form of synchronous or asynchronous clusters. Depending on the internal state as well as external conditions the network can adapt to different stimuli and reconfigure the structure of strong and weak couplings thus changing the spatiotemporal pattern. Different perception stimuli or cognitive tasks give rise to the activation of different distributed neuronal groups or to a different order of sequential activation of various brain areas. We relate this distributed neuronal group specified by the common task to a corresponding hypersimplex. *Hypersimplices* are ordered, or structured, sets of nodes with an explicit relation; in other words, they exist at a higher level of representation than network's nodes. In our model, hypersimplices are specified by the coupling topology that leads to a certain cluster activity. A structured set of hypersimplices determines a hypernetwork where the connections between hypersimplices describe their functional relations. In our model, we assume that two hypersimplices are connected if the network can change its state from one hypersimplex to another due to the evolutionary rules governing its structure and dynamics. Internal as well as external conditions usually tend to slowly evolve or drastically change which causes the network to adapt by reconfiguring the structure of its links. In general, this leads to rewiring and a new hypersimplex appears in the system. Hence the coevolution of structure and dynamics at the bottom-level network gives rise to a kind of traffic at the upper level–in the hypernetwork. The complexity of the hypernetwork and potential transitions in it depend on the dynamical principles and evolutionary rules that govern the constituents of the basic network. An actual path in the hypernetwork depends on the joint action of external inputs and the network's internal state. Sensory information and task requirements activate some subset in the hypernetwork thus transforming it to a simpler structure that enables to move along the hypernetwork by a specific path. Each such path is a unique pattern of transient cluster activity for a given task performance and is robust in non-stationary environments.

Acknowledgements

This work is supported by the Russian Foundation for Basic Research within Grants No. 15-02-04245 and 17-02-00904.

References

1. O.V. Maslennikov, D.S. Shchapin, and V.I. Nekorkin, *Phil. Trans. R. Soc. A*, 2017, **375**(2096), 20160288.
2. O.V. Maslennikov and V.I. Nekorkin, *Commun. Nonlin. Sci. Numeric. Simulat.*, 2015, **23**(1), 10–16.

Invited

CHIMERA STATES IN CONTINUOUS MEDIA

Z.G. Nicolaou, H. Riecke, and **A.E. Motter**

Northwestern University, Evanston, IL, USA, zachary.nicolaou@northwestern.edu

Abstract. The defining property of chimera states is the coexistence of coherent and incoherent domains in symmetric coupled systems. The recent realization that such states might be common in oscillator networks raises the question of whether an analogous phenomenon can occur in continuous media. Using the complex Ginzburg-Landau equation as a model system, we characterize continuous chimera states consisting of a coherent domain of a frozen spiral structure and an incoherent domain of amplitude turbulence. In contrast with discrete network systems, fluctuations in the local coupling field here play a crucial role in limiting the coherent regions.

Chimera states are spatiotemporal patterns resulting from symmetry breaking. The discovery of such states in oscillator networks demonstrated that even in systems of identically-coupled identical oscillators, mutually synchronized oscillators can coexist with desynchronized ones [1]. Chimera states were initially identified in networks of phase oscillators with nonlocal coupling [1, 2], but they have been recently demonstrated for a wide range of oscillator networks [3]. Yet with very few exceptions, previous, previous work has focused exclusively on chimeras in (discrete) network systems. It is thus natural to ask the extent to which chimera states can exist and have salient properties in continuous systems. To address this question, we consider as a model system the complex Ginzburg-Landau equation, $\frac{\partial A}{\partial t} = A + (1 + ic_1)\nabla^2 A - (1 - ic_3)|A|^2 A$, which describes the universal behavior of a homogenous oscillatory medium in the vicinity of a supercritical Hopf bifurcation [4]. This system exhibits different dynamical phases depending on the parameters c_1 and c_3. Relevant phases for our study include amplitude turubulence, consisting of a disordered and finite density of defects, and frozen vortex glasses, consisting of multiple domains of slowly evolving spiral structures with time-independent amplitude near the spiral cores.

By studying the previously under-explored parameter regime between vortex glasses and amplitude turbulence, we report novel frozen vortex chimera states, consisting of a frozen spiral structure coexisting with surrounding amplitude turbulence, as shown in Figure 1. We characterize these frozen vortex chimeras using a local coupling field analysis inspired by the Kuramoto-Battogtokh approach [1]. We find that, in contrast to the fluctuations in chimera states in nonlocally coupled discrete systems, fluctuations in the local coupling field in these continuous chimeras cannot be neglected, and we conjecture that such fluctuations are key to understanding the coexistence of order and disorder in these state. This mechanism provides insights into experimental observations [5, 6] of coexisting order and disorder in continuous media.

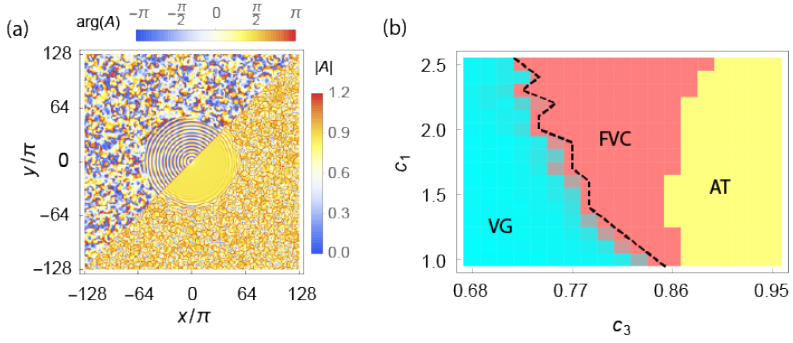

Fig. 1. Frozen vortex chimeras (FVC) (a) consist of a coherent spiral structure surrounded by amplitude turbulence and (b) are found in an under-explored parameter regime between vortex glasses (VG) and amplitude turbulence (AT).

Acknowledgements

Support from ARO Award No. W911NF-15-1-0272 and NSF Award No. NSF-CMMI-1435358.

References

1. Y. Kuramoto and D. Battogtokh, *Nonlinear Phenom. Complex Syst.*, 2002, **5**(4), 380–385.
2. D.M. Abrams and S.H. Strogatz, *Phys. Rev. Lett.*, 2004, **93**(17), 174102.
3. M.J. Panaggio and D.M. Abrams, *Nonlinearity*, 2015, **28**(3), R67–R87.
4. I.S. Aranson and L. Kramer, *Rev. Mod. Phys.*, 2002, **74**(1), 99–143.
5. Q. Ouyang and J.M. Flesselles, *Nature*, 1996, **379**(6561), 143–146.
6. F. Hayot and Y. Pomeau, *Phys. Rev. E.*, 1994, **50**(3), 2019–2021.

Invited

STATISTICAL SYMMETRIES IN TURBULENCE – RECENT RESULTS FOR 2D FLOWS

M. Oberlack[1,2], V. Grebenev[3,4], and M. Waclawczyk[5]

[1] Chair of Fluid Dynamics, Dep. Mech. Eng., TU Darmstadt, Germany, Oberlack@fdy.tu-darmstadt.de
[2] Graduate School of Computational Engineering, TU Darmstadt, Germany, 64293 Darmstadt, Germany
[3] Universidade Federal do Amazonas, Manaus AM, 69067-005, Brazil
[4] Institute of Computational Technologies, Russian Academy of Sciences, Lavrentjev ave. 6, 630090 Novosibirsk, Russia
[5] Institute of Geophysics, Faculty of Physics, University of Warsaw, Pasteura 7, 02-093 Warsaw, Poland

Abstract. Turbulence is inherently statistical in nature. Further, from large-scale direct numerical simulations we have an overwhelming evidence, that the Navier-Stokes equations are an excellent model to describe turbulence. Independent of this, from a group theoretical point of view the Navier-Stokes equations admit the classical Galilean symmetry group extended by a scaling group, which gives a deep understanding on the physical properties together with the link to the underlying conservation laws.

Interesting enough, the three complete statistical theories of turbulence all derived from Navier-Stokes equations, i.e. the infinite hierarchy of multi-point moments, the infinite Lundgren-Monin-Novikov hierarchy of the probability density function and the Hopf characteristic functional theory, all admit the above mentioned classical Galilean group. However, and most important, they all admit additional symmetries so-called statistical symmetries. These are in particular two statistical symmetry groups, which quantify two important properties of turbulence: intermittency and non-gaussianity (Waclawczyk et al. 2014).

Very recently, these results were significantly extended for turbulence in two dimensions. Though in 2D the key mechanism of vortex stretching is absent and, hence, the generation of small scales does not exist, it is still an important model for many theories and applications.

The new finding of additional statistical symmetries in 2D traces back to a conjecture by Polyakov (1993) and Falkovich (2007) that the probability density function (PDF), or more precisely the probability measure of vorticity, is invariant under the conformal group (CG). This conjecture has recently been proven by the present authors, though interesting enough the CG is only "visible" if the PDF is based on the vorticity (and not the velocity), which for 2D flows is a scalar function.

As the CG is infinite dimensional, it may have important implications, though details have not been explored yet. Still, due to its infinite dimensionality, an infinite number of conserved quantities exist and, hence, the system is integrable – at least in principle (Schottenloher, 2008).

References

1. M. Wacławczyk, N. Staffolani, M. Oberlack, A. Rosteck, M. Wilczek, and R. Friedrich, *Phys. Rev. E*, 2014, **90**, 013022.
2. A.M. Polyakov, *Nuclear Phys. B*, 1993, **396**(23), 367–385.
3. G. Falkovich, *Russian Math. Surveys*, 2007, **63**, 497–510.
4. M. Schottenloher, *Mathematical Introduction to Conformal Field Theory*, 2nd edition, Springer, Berlin, 2008, **759**.

Invited

PATTERNS FORMED BEFORE THE ONSET OF SUBCRITICAL TURING BIFURCATION

A.A. Polezhaev and **M.B. Kuznetsov**

P.N. Lebedev Physical Institute, Moscow, Russia, e-mail: apol@lpi.ru

Abstract. We investigate numerically the behavior of a two-component reaction-diffusion system of FitzHugh-Nagumo type before the onset of subcritical Turing bifurcation in response to local rigid perturbation. In a large region of parameters, initial perturbation evolves into a localized structure. In a part of that region, closer to the bifurcation line, this structure turns out to be unstable and undergoes self-completion covering all the available space in the course of time. Depending on the parameter values in two-dimensional space this process happens either through generation and evolution of new structures or through the elongation, deformation and rupture of initial structure, leading to space-filling non-branching snake-like patterns.

Spatio-temporal patterns formed in systems far from thermodynamic equilibrium are widely spread in nature. They are observed in systems of different nature: physical, chemical, biological. In experiments, two major types of spatially non-uniform structures are observed: non-localized patterns that occupy the whole available space, and localized structures, that do not spread far away from the place of their origin. While in the region of Turing instability non-localized dissipative structures are always formed, localized structures can arise rigidly in the prebifurcation region of subcritical Turing instability due to large enough initial local excitation. Under appropriate parameter values, these structures may evolve into non-localized ones due to perturbations.

We investigate numerically the behavior of a two-component reaction-diffusion system of FitzHugh-Nagumo type with two control parameters: the ratio of diffusion coefficients D and the reaction parameter α:

$$\begin{aligned} \dot{u} &= D\Delta u - u(u+\alpha)(u-1) - v, \\ \dot{v} &= \Delta v + u - v. \end{aligned} \tag{1}$$

Turing bifurcation takes place when $1 > \alpha > 2D^{1/2} - D$. Using week nonlinear analysis we show that the bifurcation becomes subcritical for sufficiently small diffusion coefficient: $D < 0.094$.

Close to the line of Turing bifurcation in parameter space before the onset of bifurcation, similar structures arise in the same manner as in the region of instability. New spots arise around the initial localized structure because of rotational symmetry breaking. They build up to new localized deformed spots the whole process resulting in a dissipative structure covering the whole available space.

When moving away from the bifurcation line at small values of D another type of self-completion takes place – the initial spot deforms and starts elongating in one direction. The growing structure folds and corrugates, but never branches, densely occupying all the available space in course of time. The first elongating patterns, which appear with the increase $\Delta\alpha$, accidentally rupture during their development, but further from the bifurcation line, they become more rigid.

Moving away from the bifurcation line, the rate of self-completion process decreases and its behavior qualitatively changes. The nature of this change differs for different values of D. When D is less than ~0.002, with the growth of $\Delta\alpha$ the rigidity of the line structures continues to grow, until the region in parametric space is reached where self-completion ceases and initially arisen structures remain localized. However, for larger values of D with the increase of $\Delta\alpha$ the line structures rupture more frequently and quite near the edge of the self-completion region they begin to break apart soon after initial deformation into spot-like structures, which then elongate into perpendicular direction.

Numerical simulations for one- and two-dimensional spatial cases detected essential difference between them in the behavior of FitzHugh-Nagumo type model. For 2D case the parametric domain within which non-localized patterns are formed is significantly larger. Parameter values, under which in 2D case self-completion of initial localized structures takes place through elongation, in 1D case correspond to stable localized structures. The reason of this striking difference is apparently due to the break of cylindrical symmetry of the initial circular spot, which is impossible in 1D.

Acknowledgements

The authors are thankful for partial support from the RFBR grant No.17-01-00070.

Invited

CHAOTIC AND QUASIPERIODIC OSCILLATIONS IN THE SYSTEM OF COUPLED SELF-GENERATORS AND MULTI-CONTOURS SELF-GENERATOR

E.P. Seleznev[1,2], **O.V. Astakhov**[2], and **N.V. Stankevich**[3,4]

[1] Kotel'nikov's Institute of Radio-Engineering and Electronics of RAS, Russian Federation, e-mail: evgenii_seleznev@mail.ru
[2] Chernyshevsky Saratov State University, Russian Federation
[3] Yuri Gagarin State Technical University of Saratov, Russian Federation
[4] University of Jyväskylä, Finland

Abstract. In the present paper, formation of multi-modes chaotic attractor, based on the multi-dimensional quasiperiodic torus observed in numerical and radiophysical experiments is reported. Characteristic phase portraits are shown.

One of the promising directions of practical application of radiophysical generators of chaotic signals is to use them for secure communication systems [1–4]. This direction has been developing for quite a long time, however, there are a number of problems, not allowing to use these generators in applications. Such problems include: the dependence of generation mode of chaotic signal on the parameters and initial conditions, sensitivity to noise, the problem of confidentiality of transmitted information, etc. In general, all these problems are connected with different properties of chaotic attractors.

Investigation of multi-frequency quasi-periodic oscillations is a topical and important problem in different areas of science [5–7], including systems of secure communication.

In the present paper we would like to present numerical and experimental investigation of the systems, such as a system of coupled self-generators and a system of multi-contours self-generator with common controlling circuit. The starting point of our investigation was the dynamics of five coupled van der Pol oscillators. Recently a model of five globally coupled oscillators of van der Pol type was proposed, in which the Landau-Hopf scenario was observed: a sequence of the birth of torus of high dimension. For such a system a special topology of coupling was found, when one can observe the transition between high-dimensional torus as a result of quasiperiodic saddle-node bifurcation (it is a typical situation), but also as a result of quasiperiodic Hopf bifurcation (this bifurcation is typical for the Landau-Hopf scenario). Then the multicontour self-generator is suggested. This multicontour generator consists of several oscillating circuits (contours) with independent control circuits responding for excitation of oscillatory mode. The interaction of different modes leads to chaotic dynamics with a different amount of modes. We have studied chaotic and quasiperiodic regimes in such systems numerically and experimentally.

Acknowledgements

This research was supported by the grant of the President of the Russian Federation for young candidates of science MK-661.2017.8.

References

1. A.S. Dmitriev, A.I. Panas, S.O. Starkov, and L.V. Kuzmin, *International Journal of Bifurcation and Chaos*, 1997, **7**(11), 2511–2527.
2. A.A. Koronovskii, O.I. Moskalenko, and A.E. Hramov, *Phys. Usp*., 2009, **52**, 1213–1238.
3. R. Suyama, *Chaotic signals in digital communications*, CRC Press, 2013.
4. A.S. Karavaev, D.D. Kulminskii, V.I. Ponomarenko, and M.D. Prokhorov, *Technical Physics Letters*, 2015, **41**(1), 1–4.
5. B.P. Bezruchko, S.P. Kuznetsov, and E.P. Seleznev, *Phys. Rev. E.*, 2000, **62**(6), 78287830.
6. A.P. Kuznetsov, S.P. Kuznetsov, I.R. Sataev, and L.V. Turukina, *Phys. Lett. A*, 2013, **377**, 32913295.
7. N.V. Stankevich, A.P. Kuznetsov, E.S. Popova, and E.P. Seleznev, *Comm. Nonlin. Sci. Num. Sim.*, 2017, **43**, 200–210.

DETECTION OF COUPLINGS BETWEEN OSCILLATORS BASED ON THE PHASE DYNAMICS ANALYSIS IN CASE OF HIDDEN INTERACTIONS

E.V. Sidak[1,2], **D.A. Smirnov**[2], and **B.P. Bezruchko**[1,2]

[1] Saratov State University, Saratov, Russia, e-mail: sidakev@gmail.com
[2] Saratov Branch of V.A. Kotel'nikov Institute of Radioengineering and Electronics RAS, Saratov

Abstract. We investigate the possibilities of the phase dynamics analysis-based method for detection of directional and time-delayed couplings between two oscillators from their time series (exhibiting multiple spectral peaks) in case of hidden third oscillator influencing both the observed ones. We have shown that application of the method of phase dynamics modeling to such a situation leads to false coupling detections. We have suggested a diagnostic criterion of possible errors and modified the technique of couplings detection. The effectiveness of the proposed modification is shown in numerical experiments.

The problem of revealing couplings (causal influences) between elements in complex systems from observed time series appears in different fields including neurophysiology and climatology (e.g. [1] and references therein). In [2] the method for detection of directional couplings between two oscillators from phase time series is proposed. The method is based on fitting empirical phase dynamics models. In [3] this method was modified for estimation of directional couplings from noisy and short time series and in [4] was modified for estimation of couplings delay time.

According to the techniques developed earlier, one computes phases of the observed signals e.g. using the analytic signal construction and obtains the time series $\varphi_1(t_n)$ and $\varphi_2(t_n)$ where t_n is a discrete time. Then, to determine the influence of the second oscillator on the first one (and vice versa, by analogy) and estimate couplings delay time, one fits the phase dynamics model of the second oscillator in the form of a stochastic difference equation:

$$\varphi_1(t+\tau) - \varphi_1(t) = F_1(\varphi_1(t), \quad \varphi_2(t-\Delta_{2\to1})) + \varepsilon_1(t), \tag{1}$$

where the phase increments are taken on a time interval of fixed length τ, ε is the τ-integrated phase noise, Δ is a trial time delay and F is a trigonometric polynomial, which describes both individual phase nonlinearity of the oscillators and coupling between them. The estimations of directional coupling indexes and of couplings delay time one gets through assessments of polynomial coefficients and minimum of model errors correspondingly. This method is effective for an analysis of couplings between oscillators with well-defined phases (narrow-band signals). However, in practice, often real signals exhibit multiple spectral peaks and one needs modified estimators applicable to such situations.

In this work we investigate the potential of the above method for detecting directional and time-delayed couplings between two oscillators from wideband signals. As an exemplary mathematical system we consider the case of a hidden third oscillator influencing both the observed ones. In numerical experiment we analyzed ensembles of time series from three coupled Van der Pol oscillators with different coupling structures and noise levels. Application of the method of phase dynamics modeling to such a situation is shown to lead to false detections of coupling and its delay time. We have proposed a diagnostic criterion of the possible false conclusions which is based on the autocorrelation function of the residual errors of the phase dynamics model. We have modified the method in such way that the phases of the oscillators are calculated after a rejection filter eliminates spectral components in the frequency band containing the basic spectral peak of the hidden oscillator. We have shown that this modification is effective for detecting couplings in a wide range of parameters of oscillators (the influence intensity of the hidden oscillator, the coupling strength between the observed oscillators and noise level of oscillators).

Acknowledgements

This work was supported by the Russian Science Foundation (grant No. 14-12-00291).

References

1. B.P. Bezruchko and D.A.Smirnov, "Extracting knowledge from time series: An introduction to nonlinear empirical modeling", Springer-Verlag: Berlin, Heidelberg, 2010.
2. M.G. Rosenblum and A.S. Pikovsky, *Phys. Rev. E*, 2001, **64**, 045202R.
3. D.A. Smirnov and B.P. Bezruchko, *Phys. Rev. E*, 2003, **68**, 046209.
4. D.A. Smirnov, E.V. Sidak, and B.P. Bezruchko, *Tech. Phys. Lett.*, 2011, **37**, 30–33.

Invited

EXPERIMENTS IN NEURONAL CULTURES: CONNECTIVITY, DYNAMICS AND COMPLEXITY IN A DISH

Ll. Hernández-Navarro, S. Teller, E. Tibau, J.G. Orlandi, J. Casademunt, E. Vives, and **J. Soriano**

Universitat de Barcelona, Barcelona, Spain, jordi.soriano@ub.edu, www.soriano-lab.eu
Universitat de Barcelona Institute of Complex Systems (UBICS), Barcelona, Spain

Abstract. Neuronal cultures provide a versatile experimental platform to explore living neuronal networks, and model them through physico-mathematical toolboxes such as dynamical systems, network theory, or information theory. Here we present different examples on the use of neuronal cultures to address important questions in neuroscience, specifically spontaneous activity patterns, the importance of spatial embedding, and the resilience of circuits to damage. The studies combine experiments with numerical simulations.

Neuronal cultures are prepared by plating an ensemble of neurons over a substrate. Plated neurons quickly connect to one another and shape within a week a *de novo* assembly with rich activity. Data is acquired through fluorescence calcium imaging, which allows the simultaneous monitoring of thousands of neurons in the field of view (Fig. 1A–B). Images are processed to obtain, for each neuron, the fluorescence profile along time (Fig. 1C). The analysis of this data allows the investigation of coherent dynamics (yellow box in Fig. 1C); or the tracking of activity propagation (Fig. 1D).

In our studies, two kinds of neuronal cultures are of special interest, namely homogeneous and aggregated. For the former, about 5000 neurons cover uniformly the substrate [1, 2]. For the latter, neurons form compact aggregates – about 50 in number – connected to one another (Fig. 1E), leading to a network in which both the aggregates and their connections are well visible and accessible [3].

Our cultures grow on a two-dimensional substrate, which imposes strong metric correlations in the connectivity that, in turn, shape the properties of the spatiotemporal activity fronts [1]. For the particular case of homogeneous cultures, by using modeling scenarios from dynamical systems and statistical physics, we link the macroscopic properties of the observed activity fronts with the microscopic, network-level traits [1, 2, 4].

The aggregated networks exhibit an activity in which aggregates tend to fire in small groups, shaping dynamical modules of varying size. Additionally, network dynamics show a strong sensitivity to the details of the connectivity among aggregates. We have used such a trait to investigate network resilience to damage, for instance by quantifying the changes in the network dynamics before and after a biochemical attack, and to assess which network configurations are more resistant to damage [3].

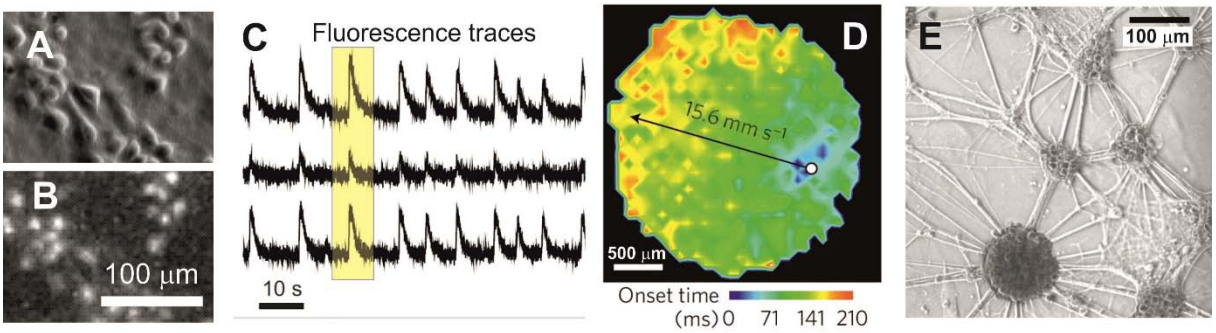

Fig. 1. (A) Neurons in culture. (B) Corresponding fluorescence image. Bright objects are firing neurons. (C) Typical spontaneous fluorescence activity traces. (D) Propagating front. (E) Culture of aggregated neurons

Acknowledgements

This work was supported by the Spanish Ministerio de Economia y Competitividad through project FIS2013-41144-P, and by the Generalitat de Catalunya through grant 2014-SGR-878.

References

1. Ll. Hernández-Navarro, J. G. Orlandi, B. Cerruti, E.Vives, and J. Soriano. *Phys. Rev. Lett*. (in press).
2. J. G. Orlandi, J. Soriano, E. Álvarez-Lacalle, S. Teller, and J. Casademunt, *Nat Phys*, 2013, **9**, 582.
3. S. Teller, I. B. Tahirbegi, M. Mir, J. Samitier, and J. Soriano, *Sci Rep 5*, 2015 article 17261.
4. E. Tibau, M. Valencia, J. Soriano, *Front. Neur. Circ. 7*, 2013, article 199.

COEXISTENCE BETWEEN BURSTING AND SILENT STATES IN A BETA-CELL MODEL

N.V. Stankevich[1,2] and **E. Mosekilde**[3]

[1] Yuri Gagarin State Technical University of Saratov, Russian Federation, e-mail: stankevichnv@mail.ru
[2] University of Jyväskylä, Finland
[3] Technical University of Denmark, Denmark

Abstract. In the present paper a modified version of the well-known pancreatic cell model is suggested. The considered modification only produces minor changes of the model and thus allows for a stable state to arise and develop inside the bursting dynamics. In this way the model becomes an example of coexisting stable and bursting dynamics in a biophysical model. We present a series of numerical simulations with the model and describe some of the main scenarios associated with the observed form of multistability.

Multistability, or coexistence of dynamical regimes, is a characteristic feature of many types of biological cells, neural networks [1–4], and other forms of oscillatory biophysical systems. This feature is particularly significant in connection with the study of interacting ensembles of many, nearly identical subsystems. It is well-known, for instance, that a variety of unusual phenomena that emerge in ensembles of coupled oscillators can lead to major reconstructions of an oscillator population, or to its total collapse. It is broadly accepted, for instance, that synchronization plays an important role in the pathogenesis of neurological diseases such as Parkinson's disease and essential tremor.

In line with the recent survey paper by Dudkowski et al. [5], an attracting state may be classified as either 'hidden' or 'self-excited', with hidden attractors representing all those attractors that do not connect to a stable equilibrium state. At the present, the mechanisms that allow bistability, such as the coexistence of tonic spiking and silence or the coexistence of tonic spiking and bursting, appear to be relatively well described. On the other hand, the dynamical mechanisms that support bistability between bursting and silence have not yet been examined to the same extent [4]. Classification of mechanisms that support the coexistence of oscillatory and silent regimes is so far incomplete, and this remains a challenge both in relation to the progress of dynamical systems theory and in relation to important issues in neuroscience. An example of a system that displays coexistence of silence and bursting oscillations was presented in the recent paper by Malashchenko et al. [4]. However, further examples of this type of coexistence are clearly desirable.

In this paper we introduce a modified version of the pancreatic beta-cell model obtained by introducing a new type of potassium-like ion with its characteristic set of channel parameters selected in accordance with a standard Hodgkin-Huxley formalism. The suggested modification is designed to be local and small enough to allow for the existence of an attracting state to live inside the regime of stable bursting dynamics. This provides for the presence of multistability in the modified beta-cell model and, at the same time, serves as an example of a biophysical system that allows for the coexistence of stable silence with large amplitude bursting.

References

1. P. Heyward, M. Ennis, A. Keller, and M.T. Shipley, *J. Neurosci*., 2001, **21**, 5311–5320.
2. Y. Loewenstein, S. Mahon, P. Chadderton, K. Kitamura, H. Sompolinsky, Y. Yarom, and M. Häusser, *Nature Neuroscience*, 2005, **8**, 202–211.
3. E.M. Izhikevich, *Int. J. Bif. Chaos*, 2000, **10**, 1171–1266.
4. T. Malashchenko, A. Shilnikov, and G. Cymbalyuk, *PloS One*, 2011, **6**, e21782.
5. D. Dudkowski, S. Jafari, T. Kapitaniak, N.V. Kuznetsov, G.A. Leonov, and A. Prasad, *Phys. Rep.*, 2016, **637**, 1–50.

EFFECT OF SWITCHINGS BETWEEN CHIMERA STATES IN AN ENSEMBLE OF COUPLED CHAOTIC MAPS

G.I. Strelkova, N.I. Semenova, and **V.S. Anishchenko**

Saratov National Research State University, Saratov, Russia
strelkovagi@info.sgu.ru

Abstract. We study numerically the dynamics of a network of nonlocally coupled Henon maps. Temporal random switchings between amplitude and phase chimera states are reported and studied for the first time. It is shown that in the autonomous ensemble, a nonstationary switching process has a finite lifetime and is a transient towards the stationary regime of phase chimera. By applying short-term noise perturbations the lifetime of the switching regime can be increased to infinity.

We present numerical results for the dynamics of a network of nonlocally coupled Henon maps [1] in a chaotic regime of partial elements. The ensemble is described by the following equations [2]:

$$\begin{aligned} x_i^{t+1} &= f(x_i^t, y_i^t) + \frac{\sigma}{2P} \sum_{j=i-P}^{i+P} \left[f(x_j^t, y_i^t) - f(x_i^t, y_i^t) \right], \\ y_i^{t+1} &= \beta x_i^t, \qquad i = 1, 2, ..., N, \end{aligned} \tag{1}$$

where x_i and y_i are real dynamical variables, $N = 1000$ is the number of ensemble elements, $f(x_i, y_i) = 1 - \alpha x_i^2 + y_i$, the parameters $\alpha = 1.4$ and $\beta = 0.3$ are fixed, σ is the coupling strength, P denotes the number of neighbors from both sides of the ith oscillator, and $r = P/N$ is the coupling radius (range). The dynamics of the ensemble (1) is studied for randomly distributed initial conditions and when the coupling strength and the coupling range are varied.

The analysis of time series $x_i(t)$ indicates that there are nonstationary effects which are characterized by random switchings between amplitude and phase chimeras [3]. It is shown that the lifetime of these switchings is sufficiently long (about 10^5 iterations) but finite. This nonstationary process is completed by the transition to the stationary regime of phase chimera. The amplitude chimera regime is nonstationary and has a finite lifetime.

We also demonstrate that in this case, the lifetime of nonstationary processes of switchings can be increased to infinity by applying very short-term noise perturbations to the all ensemble elements. If such kind of noise influences is added to the ensemble in a certain, sufficiently large, time interval, then the switching process is never ended. It is shown that the stationary phase chimera regime seems to be strongly stable in the presence of noise influence.

Acknowledgements

This research is partly supported by the RFBR (grant No. 15-02-02288) and the Russian Ministry of Education and Science (project code 3.8616.2017).

References

1. V.S. Anishchenko, T.E. Vadivasova, and G.I. Strelkova, *Deterministic Nonlinear Systems. A Short Course*, Springer, Heidelberg, New York, London, 2014.
2. N. Semenova, A. Zakharova, E. Schöll, and V. Anishchenko, *Europhysics Lett.*, 2015, **112**, 40002.
3. S.A. Bogomolov, G.I. Strelkova, E. Schöll, and V.S. Anishchenko, *Tech. Phys. Lett.*, 2016, **42**(7), 763–766.

MODULATED-WAVE SOLUTIONS FOR AN ANHARMONIC LATTICE

G.M. Nkeumaleu[1], A.S. Tchakoutio Nguetcho[1,2], and **J.M. Bilbault[1]**

[1] Laboratoire LE2I UMR FRE 2005, Arts et Métiers, Université de Bourgogne Franche-Comté, Dijon-France
[2] Laboratoire Interdisciplinaire des Sciences et Sciences Appliquées du Sahel (LISSAS),
Département de Physique, Faculté des Sciences, Université de Maroua, BP 814, Maroua-Cameroun,
nkeumaleu@yahoo.fr, nguetchoserge@yahoo.fr, bilbault@u-bourgogne.fr

Abstract. Using the theory of bifurcations, we provide and find travelling wave dynamics, in a nonlinear Klein Gordon model with anharmonic, cubic and quartic interactions, immersed in a parameterized on-site substrate potential. The case of an anharmonic interactions and a deformable substrate potential allow theoretical adaptation of the model to various physical situations. Non-convex interactions in lattice systems lead to the existence of singular straight lines in phase space and thus, allow the appearance of a number of interesting phenomena that cannot be produced with linear coupling alone. By investigating the dynamical behavior and bifurcations of solutions of the planar dynamical systems, we derive a variety of exotic (peakons, compactons, bright and dark solitary waves, cups, different families of periodic solutions and others) solutions corresponding to the phase trajectories under different parameter conditions. Moreover, we demonstrate how and why travelling waves lose their smoothness and develop into solutions with compact support or breaking.

Summary

An example of universal models, which can be used to describe a variety of different phenomena is the Nonlinear Klein-Gordon (NKG) model. In our model, the potential energies consist of the substrate external potential along the chain and the quite general interparticle interactions. Because in real physical systems, the shape of the substrate potential can deviate from the standard one (sinusoidal or rigid) and affect strongly the transport properties of the system, we generalized the standard NKG model by a Peyrard and Remoissenet potentials [1]. Modelling the interaction potential of the n^{th} particle has greatly influenced the pioneering works on the dynamics of nonlinear lattices and related solitonic exaltations. For that purpose, we connect us in this work on the Taylor expansion of the potential at the equilibrium position in a power series of the displacements to fourth order. Thus, we obtain an approximate $k_2 - k_3 - k_4$ potential [2–4]. For a finite medium, standing waves are expected and the transmissivity can be characterized. Now, we restrict ourselves to the weakly nonlinear coupling and the envelope part, is found to obey by a new type of extended nonlinear Schrödinger equation.

$$j\frac{\partial\Psi}{\partial\tau}+P\frac{\partial^2\Psi}{\partial X^2}+Q\left|\Psi\right|^2\Psi=$$

$$=jr_1\left|\Psi\right|^2\frac{\partial\Psi}{\partial X}+r_2\left(\left(\frac{\partial\Psi}{\partial X}\right)^2\Psi^*+\left|\Psi\right|^2\frac{\partial^2\Psi}{\partial X^2}\right)+r_3\left(\Psi^2\frac{\partial^2\Psi^*}{\partial X^2}+2\Psi\frac{\partial\Psi}{\partial X}\frac{\partial\Psi^*}{\partial X}+\left|\Psi\right|^2\frac{\partial^2\Psi}{\partial X^2}\right).$$

Looking solution at the form $\Psi\left(X,\tau\right)=a\left(z\right)\exp\left[\,j\left(\theta\left(z\right)+\Omega_0\tau\right)\right]$, we obtained the following planar dynamical system

$$\frac{d\varphi}{dz}=y,\quad \frac{dy}{dz}=\frac{P\left(P-r_2\varphi\right)^2y^2+4\varphi^2f_3\left(\varphi\right)}{2\varphi\left(P-\left(2r_3+r_2\right)\varphi\right)\left(P-r_2\varphi\right)^2},$$

where $f_3\left(\varphi\right)$ is a polynomial of degree three in φ and $a^2=\varphi$. This system is a singular traveling wave system of the first class with three invariant singular straight line solutions and it depends on eight-parameter group [5–7]. It is worth mentioning that the nonlinear equations with singular straight lines may have abundant and interesting new kinds of traveling wave solution.

Our aim is not only to consider all travelling wave solutions in the parameter space by using the theory of bifurcations of dynamical systems but also to study the effects of singular straight lines in nonlinear wave equations. We are interested in a more complete study of the existence of travelling wave solutions of this NKG model in every parameter region and in finding why travelling waves lose their smoothness and developed into breaking waves.

References

1. M. Peyrard and M. Remoissenet, "Solitonlike excitations in a one-dimensional atomic chain with a nonlinear deformable substrate potential", *Phys. Rev. B*, 1982, **26**, 2886.

2. O.M. Braun and Y.S. Kivshar, "The Frenkel-Kontorova Model", Concepts, Methods, and Applications, Springer-Verlag: Heidelberg New York, 2004.
3. H. Guoxiang and H. Bambi, "Asymmetric gap soliton modes in diatomic lattices with cubic and quartic nonlinearity", 75 *Phys. Rev. B*, 1998, **57**, 5746.
4. L.S. Brizhik, A.P. Chetverikov, W. Ebeling, G. Ropke, and M.G. Velarde, "Bound States of Electrons in Harmonic and Anharmonic Crystal Lattices", Chapter in Quodons in Mica, Volume 221 of the series Springer Series in Materials Science, 2015.
5. A.S. Tchakoutio Nguetcho, J.B. Li, and J.M. Bilbault, "Bifurcations of phase portraits of a singular nonlinear equation of the second class", *Commun. Nonlinear. Sci. Numer. Simulat.*, 2014, **19**, 2590.
6. J.B. Li, F. Chen, and A.S. Tchakoutio Nguetcho, "Bifurcations and exact solutions in a model of hydrogen-bondedchains", *Int. J. Bifurcation and Chaos*, 2015, **25**, 1550062.
7. J.B. Li, "Singular nonlinear traveling wave equations: bifurcations and exact solutions", Beijing: Science Press, 2013.

Invited

COMPLEX ROUTES TO UNUSUAL COLLECTIVE CHAOS IN INDIRECTLY COUPLED IDENTICAL RING OSCILLATORS

E. Volkov[1] and **E. Hellen**[2]

[1] Lebedev Physical Institute, Moscow, Russia, volkov@lpi.ru
[2] Dept. of Physics & Astronomy UNC-Greensboro ehhellen@uncg.edu

Abstract. Synthetic genetic networks of identical ring oscillators with nonlinear conjugate coupling that simulates bacterial "quorum sensing" provide unusual examples of multistability between regular attractors, the appearance of symmetric chaos via period doubling of complex limit cycle or via torus destruction and uncommon spatially inhomogeneous collective chaos over very large parameter areas. A study of routes to the regions occupied by symmetric and asymmetric chaotic regimes demonstrates the presence of broad parts with coexisting regular and chaotic oscillations, which enhances the multistability of the coupled system.

In the last decade the ring oscillator has become very popular in studies of synthetic genetic networks. Genetic oscillators play important roles in cell life regulation. The regulatory efficiency usually depends strongly on the emergence of stable collective dynamic modes, which requires designing the interactions between genetic networks. We investigate the dynamics of two identical synthetic genetic ring oscillators, called Repressilators, coupled by bacterial-type "quorum sensing (QS)" in each oscillator, which supports global nonlinear coupling via the fast diffusion of small molecules. In a basic genetic ring oscillator network (in which three genes inhibit each other in a unidirectional manner), QS stimulates the transcriptional activity of chosen genes providing for competition between inhibitory and stimulatory activities localized in those genes. The "promoter strength", Hill cooperativity coefficient of transcription repression, and the coupling strength, i.e., parameters controlling the basic rates of genetic reactions, were chosen for extensive bifurcation analysis. The results of numerical bifurcation analysis are presented as a map of dynamic regimes and routes to them. We found that the remarkable multistability of the anti-phase limit cycle and stable homogeneous and inhomogeneous steady states exists over broad ranges of control parameters. We studied the anti-phase limit cycle stability and the evolution of irregular oscillatory regimes in the parameter areas where the anti-phase cycle loses stability. In these regions we observed torus formation, collective chaos, and multistability between regular limit cycles and quasiperiodic oscillations over remarkably large intervals of coupling strength. In spite of the identical nature of the oscillators, QS-coupling stimulates the appearance of intrachaotic periodic windows with spatially symmetric and asymmetric partial limit cycles which, in turn, change the type of chaos from a simple anti-phase character into chaos composed of pieces of the trajectories having alternating polarity. We found that for large values of promoter strength the main regime is an inhomogeneous limit cycle in which oscillators are synchronized in 1:2 limit cycle which generates strongly inhomogeneous chaos. The very rich dynamics discovered in the system of two identical simple ring oscillators may serve as a possible background for biological phenotypic diversification, as well as a stimulator to search for similar coupling in oscillator arrays in other areas of nature, e.g. in neurobiology, ecology and other systems with the domination of indirect coupling.

Invited

NOISE-RESISTANCE OF OSCILLATORY NEURAL NETWORKS WITH ADAPTIVE COUPLING

S. Yanchuk

Technical University of Berlin, Berlin, Germany
yanchuk@math.tu-berlin.de

In my presentation, I will review the results obtained in publications [1, 2]. They show that oscillatory neural populations with adaptive synaptic weights governed by spike timing-dependent plasticity (STDP) exhibit a natural resistance to noise. With the increase of the noise intensity, we observe a dramatic increase of the mean synaptic coupling. These findings suggest that there is an optimal noise level, where the amount of synaptic coupling is maximal. In addition to the numerical and statistical analysis of large systems of Hodgkin-Huxley neurons and phase oscillators, we study theoretically the influence of noise for a minimal model by considering just two coupled neurons. It is shown how a strong bidirectional coupling, which is not present in the noise-free situation, can be stabilized by the noise.

References

1. L. Lücken, O. Popovych, P. Tass, and S. Yanchuk, *Phys. Rev. E*, 2016, **93**, 032210.
2. O.V. Popovych, S. Yanchuk, and P.A. Tass, *Sci. Rep*., 2013, **3**, 2926.

CHIMERA STATES IN MULTIPLEX NETWORKS

A. Zakharova

Institut für Theoretische Physik
Technische Universität Berlin, Hardenbergstraße 36, 10623 Berlin, Germany
e-mail: anna.zakharova@tu-berlin.de

We investigate the occurrence of coherence-incoherence patterns in multiplex networks where the nodes are distributed in different layers according to the type of the relation they share. For instance, in the case of a neuronal network the neurons can form different layers depending on their connectivity through a chemical link or by an ionic channel. The prime objective of multiplex networks is to study multiple levels of interactions where functions of one layer get affected by the properties of other layers. In the present work we particularly aim to understand the interplay of multiplexity and communication delay on emergence of chimera state in which the system splits into coexisting domains of spatially coherent (synchronized) and incoherent (desynchronized) dynamics. Focusing on a multiplex network of nonlocally coupled identical chaotic maps with delayed interactions we show that the interplay of delay and multiplexing results in an enhanced or suppressed appearance of the chimera state. Additionally, we report a layer chimera state where one layer exhibits coherent and another layer incoherent dynamical evolution.

Joint work together with Saptarshi Ghosh, Anil Kumar, and Sarika Jalan.

References

1. S. Ghosh, A. Kumar, A. Zakharova, and S. Jalan, "Birth and Death of Chimera: Interplay of Delay and Multiplexing", *EPL*, 2016, **115**, 60005.

Invited

STUDYING PATTERN DYNAMICS IN AERODYNAMICS USING LAGRANGIAN COHERENT STRUCTURES

J. Zhang[1], Y. Liu[2], S. Cao[1], and **W. Wang[2]**

[1] School of Energy and Power Engineering, Xi'an Jiaotong University, Xi'an, 710049, P. R. China
jzzhang@mail.xjtu.edu.cn
[2] School of Mechanical Engineering, Northwestern Polytechnical University, Xi'an 710072, P. R. China

Abstract. For the flow around a body in aerospace engineering, there exists a rich variety of nonlinear phenomena. For example, the breaking of a separation bubble is the main route to vortex shedding, which is a complex unsteady flow. Moreover, it has an important influence on the aerodynamic performance of airfoil near stall. Recently, experiments show that some kind of separation bubbles and their breakings, which are induced by some unsteady perturbations or excitations, can lead to the improvement of the aerodynamic performance in a sense. In other words, such improvement is relevant to the generating, developing and breaking of the separation bubble. However, the nature for such phenomenon is still unclear, and hence it is necessary to study the evolution of the bubble breaking in depth.

For such dynamic behavior, Lagrangian Coherent Structures (LCS) are introduced to study the breaking of separation bubble in the flow around airfoil with low Reynolds number, from the viewpoint of nonlinear dynamics. In particular, the flowing inherent modes and the transitions between them are analyzed in detail, and then the mass and momentum transfers between modes are studied further, the influences of breaking modes on the aerodynamic performance are obtained finally.

The results show that there exists a transition from steady flow to unsteady flow, with a bifurcation in the flow pattern, as the breaking of separation bubble occurs. For such an unsteady flow, the traditional Eulerian description is no longer available to describe such dynamics, which is related to mass and momentum transfers. To this end, LCS is used to describe the Lagrangian dynamics, and the Lagrangian patterns, which are inherent following their definitions, are captured. Then, the breaking of heteroclinic orbit is studied in the breaking of separation bubble, as well as the mass and momentum transfers, following pattern dynamics. As the results, it is shows that the studies above are the key understanding of the breaking of separation bubble. Moreover, LCS is used to study the modes in such a complex flow, in order to find the fundamental modes which are dominant in the flow pattern and aerodynamic performance. Also, the mode jumping or mode transition and internal resonance between modes are studied further, so that the nature of bubble breaking is gained. Finally, the mass and momentum transfer in the evolution of the bubble are investigated following the LCS, and the influence of breaking of bubble on the aerodynamic performance is studied.

As a conclusion, the results show that the numerical method presented is a powerful tool for the stability and bifurcation analysis of the complicated flows around body, and some nonlinear phenomena can be captured and analyzed by the method.

International Symposium

TOPICAL PROBLEMS OF NONLINEAR WAVE PHYSICS

Lasers with High Peak and High Average Power

Cremlin Workshop: Key technological issues in construction and exploitation of 100 PW class lasers

Chairs

Efim Khazanov, Institute of Applied Physics RAS, Russia
Ken-ichi Ueda, Institute for Laser Science,
the University of Electro Communications, Japan

Alexander Sergeev, Institute of Applied Physics RAS, Russia
Catalin Miron, ELI, Romania

Program Committee

Jean-Claude Kieffer, Institut National de la Recherche Scientifique,
Université du Québec, Canada
Oleg Palashov, Institute of Applied Physics RAS, Russia
Alexander Pukhov, Institut für Theoretische Physik I,
University of Düsseldorf, Germany
Christophe Simon-Boisson, THALES, France
Vladimir Yashin, S.I. Vavilov State Optical Institute, Russia

INCREASING OF FRONT END SYSTEM STABILITY FOR PARAMETRIC PETAWATT LASERS

K.F. Burdonov, **I.B. Mukhin**, and **A.A. Soloviev**

Institute of Applied Physics RAS, Nizhny Novgorod, Russia, kfb.iap@gmail.com

Abstract. Here we present the results of upgrade of the FRONT END system for nanosecond pump laser of petawatt parametric facilities. A discharge lamp based pump of a single-mode Q-switched Nd:YLF master oscillator was replaced by a diode end-pumping system, which provides an opportunity to increase frequency from 1 Hz to more than 20 Hz and also to increase energy stability and control laser pulse shape. A new Nd:YLF laser at the wavelength of 1054 nm with duration 1 ns, energy 1 mJ, repetition rate more than 20 Hz and external synchronization with temporal jitter less than 100 ps was developed and optimized. A new FRONT END system will replace the existing one at the PEARL facility.

One of the main principle difficulties of OPCPA systems is the need for accurate (tens of ps) synchronization of the signal pulse with the pump pulse. Since pumping is carried out at a different wavelength, an individual pulse laser source is used to create the initial pulse, which usually operates by the Q-switching principle. Jitter in Q-switched systems leads to the inability to provide sufficient stability with commercial pulsed lasers. Typical jitter of commercial systems is 200 ps, which will result in 20% modulation of the amplified emission spectrum. The experience of using the existing original master oscillator [1] with acceptable jitter shows stability not better than 10% in energy, which is substantially dependent on the tuning quality of the master oscillator, which is not satisfactory for applications in the laser facility PEARL [2], especially when it concerns nonlinear laser-plasma interaction modes [3–5].

We propose to change the lamp pumping of the master oscillator active element to the end diode pumping. Due to a noticeable shortening of the active element, this will lead to the necessity of switching to the Q-switching mode with cavity damping which consists of two stages. At the first stage, the quality factor of the resonator is made as high as possible for the generation of a giant pulse, at the second stage, at the time when the field in the cavity is maximal, all radiation leaves the cavity with the help of a fast Pockels cell in one cavity roundtrip. In this case, synchronization is determined only by electrical jitter (which can be increased to several tens of ps), and the pulse amplitude stability can correspond to commercial analogs (usually, not worse than 1%).

To solve this problem we made a prototype of a new master oscillator. The active element was 1 cm long Nd:YLF cut in σ-orientation at an angle of 3 degrees to the optical axis to suppress generation at 1047 nm. The master oscillator operated at a wavelength of 1054 nm. Pumping was carried out by a diode laser at a wavelength of 808 nm co-axially with the mode of generation from the end of a cylindrical active element. Peak pumping power was about 150 W. Q-switching and formation of the leading edge of the pulse were attained by Pockels cell. The master oscillator worked on the principle of Q-switching with cavity damping. In such a concept the luminescence of the active element was used as a starter (in fact ‘start from noise’). The longitudinal mode was selected by means of an interferometric narrow-band mirror with a spectral width of 0.1 nm. The prototype we made showed the following parameters: single-mode generation at a wavelength of 1054 nm, repetition rate of more than 20 Hz, pulse duration 2 ns, energy not less than 0.8 mJ, external synchronization with jitter not worse than 100 ps. In the future we plan to optimize parameters of this prototype master oscillator for the purpose of its subsequent integration into the existing laser facility PEARL.

Acknowledgements

This work was supported by the Ministry of Education and Science of the Russian Federation under Contract No.14.Z50.31.0007.

References

1. E. Katin *et al*., *Quant. Electron*., 2003, **33**(9), 836–840.
2. V. Lozhkarev *et al*., *Laser Phys. Lett.*, 2007, **4** 421–427.
3. S. Hooker, *Nat. Photon.*, 2013, **7**, 775–782.
4. H. Daido *et al*., *Rep. Prog. Phys.*, 2012, **75**, 056401.
5. G. Mourou *et al*., *Eur. Phys. J. Special Topics*, 2014, **223**, 1181–1188.

QED CASCADE SATURATION AND ELECTRON-POSITRON JET FORMATION FROM AN ULTRASTRONG LASER-IRRADIATED THIN FOIL

M. Chen[2, 4, +], **W. Luo**[1, 3, *], **W.-Yu. Liu**[1, 2, 4], **T. Yuan**[2, 4], **Ji-Ye Yu**[2, 4], **F.-Yu Li**[3], **D. Del Sorbo**[5], **C.P. Ridgers**[5], **Zh.-M. Sheng**[2, 3, 4]

[1] School of Nuclear Science and Technology, University of South China, Hengyang 421001, China
[2] Key Laboratory for Laser Plasmas (Ministry of Education), School of Physics and Astronomy, Shanghai Jiao Tong University, Shanghai 200240, China
[3] SUPA, Department of Physics, University of Strathclyde, Glasgow G40NG, United Kingdom
[4] IFSA Collaborative Innovation Center, Shanghai Jiao Tong University, Shanghai 200240, China
[5] York Plasma Institute, Physics Department, University of York, York YO10 5DQ, United Kingdom
[+]Email: minchen@sjtu.edu.cn; [*]Email: wenluo-ok@163.com

Abstract. QED cascade saturation and relativistic electron-positron (e^-e^+) jet formation in a thin foil irradiated by two counter-propagating ultraintense laser pulses are studied. A scaling of QED cascade growth with laser intensity is found, which shows clear cascade saturation above threshold intensity of ~10^{24} W/cm^2. This saturation enables the production of high-yield ($\gtrsim 10^{13}$) ultradense (10^{24} cm^{-3}) e^-e^+ pair plasma and significant laser energy depletion. In the same intensity regime, the formed pair plasma is found to be further squeezed toward the initial thin-foil location, where finally relativistic e^-e^+ jets are formed and ejected transversely along the laser electric field directions.

With the development of ultraintense laser facilities, laser plasma interaction enters a completely new regime, where new phenomena such as copious gamma photon generation, electron-positron (e−e+) pair production and QED cascade, etc. are expected to occur [1]. Moreover, these ultra-high power laser facilities may allow one to study some extreme astrophysical phenomena in lab, such as relativistic e−e+ jet formation. They are ubiquitously found in black holes (BHs), pulsars and quasars, and are associated with violent emission of short-duration (milliseconds up to a few minutes) gamma-ray bursts.

By investigating the QED cascade and consequent relativistic e^-e^+ formation from counter-propagating laser-irradiated ultrathin foils, a scaling law of QED cascade growth with laser intensity is found which shows that QED cascade saturation occurs at laser intensities exceeding 10^{24} W/cm^2. QED cascade saturation results in highly efficient conversion from laser photons to pairs with an efficiency of the order of 10%. A high-yield ($\gtrsim 10^{13}$) ultradense (10^{24} cm^{-3}) e^-e^+ bunch is produced, causing the plasma to become opaque to incident lasers leading to QED pair-plasma squeezing. Consequent relativistic e^-e^+ jet formation along the transverse direction and high-harmonic generation (HHG) along the longitudinal direction have been observed [2]. The laser-driven relativistic jets formation opens up the opportunity to study energetic astrophysical phenomena in laboratory, and the HHG discovered here provides an easy way to experimentally identify these phenomena.

Acknowledgements

This work was supported by the National Basic Research Program of China (Grant No. 2013CBA01504) and the National Natural Science Foundation of China (Grant Nos. 11347028, 11405083, 11421064, and 11675075). W.L. appreciates the support from China Scholarship Council and Young Talent Project of the University of South China. M.C. appreciates the support from National 1000 Youth Talent Project of China. Z.M.S. acknowledges the support of a Leverhulme Trust Research Project Grant and the U.K. EPSRC (Grant No. EP/N028694/1).

References

1. A. Di Piazza, *et al*., *Rev. Mod. Phys.*, 2012, **84**, 1177.
2. W. Luo, W.Y. Liu, T. Yuan, M. Chen, *et al*., *to be submitted*, 2017.

DEORBITING OF SPACE DEBRIS BY LASER ABLATION

T. Ebisuzaki[1] and **S. Wada**[2]

[1] RIKEN, Wako, Japan, ebisu@postman.riken.jp
[2] RIKEN, Wako, Japan, swada@postman.riken.jp

Abstract. Recent years deorbiting by the laser ablation attracts increasing attentions as an almost unique effective method to remediate cm-sized space debris. According to Ebisuzaki et al., 2014, the deorbiting operation is divided into three steps. First, a super-wide field telescope detects the reflection signal of the solar light by space debris and roughly determines its position and moving direction. Second, laser beams are ejected to the directions of the debris to determine the position and velocity precisely as well as its distance. Finally, a high intensity laser beam is focused onto the debris surface to induce laser ablation on the surface. The reaction force of the ablation leads the debris to the deorbiting to the Earth's atmosphere. In this talk, we will discuss the technical challenges to achieve the mission and propose the step-by-step approach for the technical demonstration of the mission.

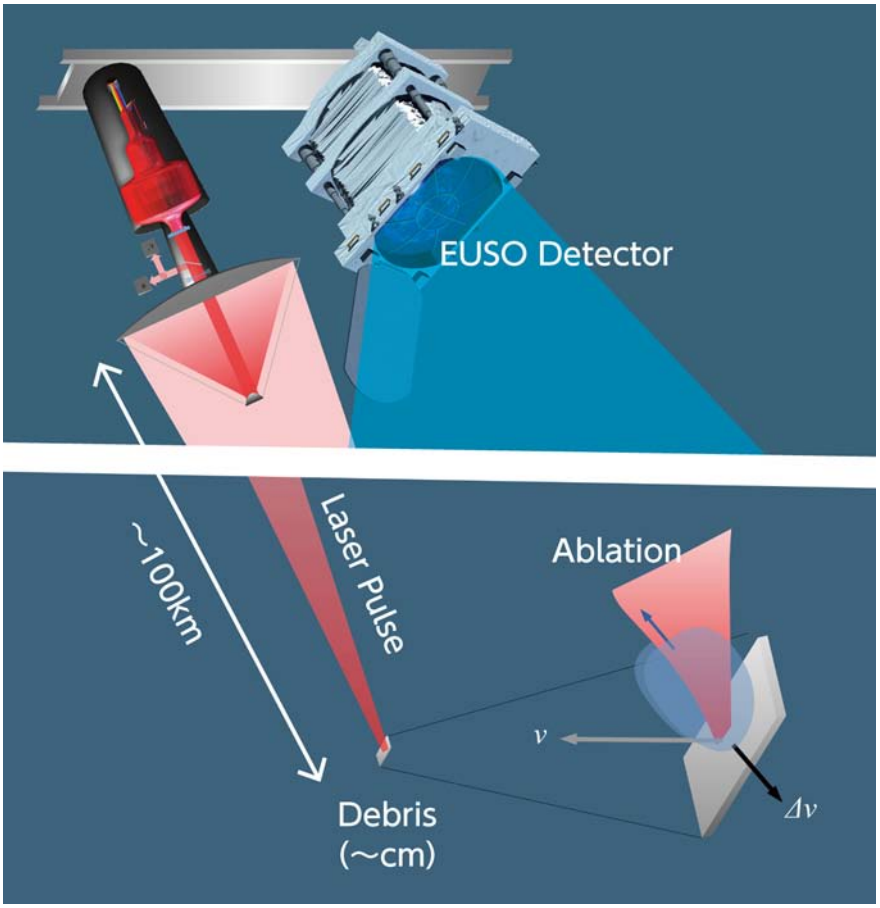

References

1. T. Ebisuzaki, *et al*., "Demonstration designs for the remediation of space debris from the International Space Station", *Acta Astronautica*, 2015, **112**, 102–113.

HORIZONS OF SCIENCE, DRIVEN BY SUPER-POWER LASERS

J. Fuchs

LULI, Ecole Polytechnique, 91128 Palaiseau cedex, France
julien.fuchs@polytechnique.edu

Abstract. During this presentation, I will discuss both the enormous progress that has been made since the inception of the laser with respect to its parameters and its capacity to deliver the highest concentration of energy in time and space, the highest ever achieved by man, but also the vast possibilities this has opened in terms of applications whether in science and progress of our fundamental knowledge of matter and the Universe, or for society at large, in energy, or medicine.

STUDY OF SELF-FILTERING AND SMALL-SCALE SELF-FOCUSING SUPPRESSION OF HIGH-INTENSITY LASER BEAMS

V.N. Ginzburg, A.A. Kochetkov, and **E.A. Khazanov**

IAP RAS, Nizhny Novgorod, Russian Federation

Abstract. Free space propagation of laser radiation with intensities over several hundred GW/cm^2 can act as a filter for spatial noise harmonics in an instability band of small-scale self-focusing (SSSF). Here we report on the results of experimental study of intense radiation self-filtering and SSSF suppression based on direct and indirect measurements of spatial noise gain of intense radiation propagating in a glass plate.

There is a great interest to use thin transmission optical elements to control the parameters of petawatt laser radiation. Such elements can be used for generation of the second harmonic aimed at increasing time contrast, time recompression of femtosecond pulses after spectral broadening by self-phase modulation, optical polarization transformation from linear to a circular one, radiation with intensities over several hundred GW/cm^2. The intensity of unfocused petawatt radiation is several TW/cm^2. In these conditions, small-scale self-focusing (SSSF) is the principal restriction in using transmission optical elements. SSSF is induced by cubic nonlinearity of the medium and leads to enhanced spatial perturbations and laser beam filamentation and, consequently, to damage of optical elements. The SSSF impact may be reduced by minimizing the accumulated nonlinear phase (B-integral), as well as by reducing spatial noise.

According to the SSSF theory [1, 2] the noise transverse wave vector at which the amplification coefficient is maximal is proportional to the square root of radiation intensity. In [3] it was proposed to use free space for filtering harmonic perturbations of laser beams having intensity of several TW/cm^2. Here we report on the results of experimental study of intense radiation self-filtering and SSSF suppression based on direct and indirect measurements [4] of spatial noise gain of intense radiation propagating in a glass plate. This investigation confirms the beam self-filtering and reduction of amplified spatial noise when the distance from a nonlinear element to noise source becomes large enough for the angle of vision of the element to be much smaller than the instability band.

References

1. V.I. Bespalov and V.I. Talanov, *JETP Letters*, 1966, **3**, 307–310.
2. N.N. Rozanov and V.A. Smirnov, *Soviet Journal of Quantum Electronics*, 1980, **10**, 232–237.
3. S.Y. Mironov, V.V. Lozhkarev, G.A. Luchinin, A.A. Shaykin, and E.A. Khazanov, *Appl. Phys. B*, 2013, **113**, 147–151.
4. A.K. Poteomkin, M.A. Martyanov, M.S. Kochetkova, E.A. Khazanov, *IEEE Journal of Quantum Electronics*, 2009, **45**, 336.

ANALYTIC MODEL FOR ELECTROMAGNETIC FIELDS IN THE BUBBLE REGIME OF PLASMA WAKEFIELD

A.A. Golovanov[1], **I.Yu. Kostyukov**[1], **J. Thomas**[2], and **A.M. Pukhov**[2]

[1] Institute of Applied Physics RAS, Nizhny Novgorod, Russia, e-mail: agolovanov@appl.sci-nnov.ru
[2] Institut für Theoretische Physik, Heinrich-Heine-Universität Düsseldorf, Düsseldorf, Germany

Abstract. We consider a model of a strongly nonlinear plasma wakefield (a bubble) excited by an intense laser pulse or a relativistic electron bunch propagating in plasma with transverse inhomogeneity. Assuming the general shape of the electron sheath on the border of the bubble, we obtain a second-order ordinary differential equation for the boundary of the bubble. We find approximations when this equation is significantly simplified. We develop a lowest-order perturbation theory for the components of electromagnetic fields inside and outside the bubble. The results are verified with 3D particle-in-cell simulations.

Acceleration in plasma wakefields is a prospective method of electron acceleration, as it allows acceleration rates several orders of magnitude higher than in conventional accelerators. Plasma wakefields can be driven by an intense laser pulse or a relativistic electron bunch. The most interesting is the so-called strongly nonlinear (or bubble) regime of plasma wakefield [1]. In this regime, the driver (either a laser pulse or an electron bunch) completely ejects plasma electrons, leading to the formation of an electron-free region behind the driver. This electron-free cavity has the shape of a sphere and is commonly referred to as a "bubble". The feature of this regime is the electron self-injection: background plasma electrons can be trapped and accelerated in the wakefield, which allows obtaining accelerated electron bunches without using external electron sources. However, the properties of such bunches are usually insufficient for applications, and there is a difficulty of obtaining electron bunches with low energy spread and low transversal emittance, which requires further development of plasma methods both in experiments and in theory.

Due to its complexity, the bubble regime of the wakefield is commonly studied using 3D particle-in-cell (PIC) simulations. However, theoretical analysis is also of huge interest. Based on existing theoretical models for the shape of the bubble in homogeneous [2] and radially inhomogeneous plasmas [3], we develop a new model in which we make no a priori assumptions about the transversal profile of the electron sheath on the border of the bubble and, similarly to [2, 3], obtain a second-order equation for the boundary of the bubble. When the width of the electron sheath is small compared to the size of the bubble, this equation is significantly simplified and no longer depends on the shape of the electron sheath [4].

In order to study the electron injection and the electron dynamics in the bubble, it is important to know the electromagnetic field spatial distribution. Knowledge of the bubble boundary together with the model for electron sheath are sufficient to reconstruct all components of the electromagnetic field inside and outside the bubble [5]. However, this reconstruction can be done only numerically due to the complexity of equations describing the fields. In our work, we present a simpler model for electromagnetic field, in which we obtain explicit expressions for its components. Our analysis is based on the assumption that the electron sheath on the boundary of the bubble is thin enough. This allows us to use the perturbation theory to simplify the equations. We show that the fields inside the bubble do not depend on the shape and the width of the electron sheath. For the fields outside the bubble, we find the laws of their decrease to zero depending on the particular model of the electron sheath. The analytical results are confirmed by 3D PIC simulations.

Acknowledgements

This work has been supported by the Russian Science Foundation through Grant No. 16-12-10383.

References

1. A. Pukhov and J. Meyer-ter-Vehn, *Appl. Phys. B*, 2002, **74**, 355.
2. W. Lu, C. Huang, M. Zhou, W.B. Mori, and T. Katsouleas, *Phys. Rev. Lett.*, 2006, **96**, 165002.
3. J. Thomas, I.Yu. Kostyukov, J. Pronold, A. Golovanov, and A. Pukhov, *Phys. Plasmas*, 2016, **23**, 053108.
4. A.A. Golovanov, I.Yu. Kostyukov, A.M. Pukhov, and J. Thomas, *Quantum Electron.*, 2016, **46**, 295.
5. S.A. Yi, V. Khudik, C. Siemon, and G. Shvets, *Phys. Plasmas*, 2013, **20**, 013108.

DEEP UV MONOCYCLE LASER FOR SEEDING OF NEXT GENERATION XFEL

Y. Kida [1,2]

[1] JST PREST, 4-1-8 Honcho, Kawaguchi, Saitama, 332-0012, Japan, kida@spring8.or.jp
[2] RIKEN SPring-8 Center, 1-1-1 Koto, Sayo, Hyogo, 679-5148, Japan

Abstract. In 2015, an approach was reported that potentially leads to free-electron lasers generating isolated X-ray pulses with durations orders of magnitude shorter than the state-of-the-art free-electron lasers. Called mono-cycle harmonic generation, it shortens X-ray pulses to their fundamental shortest limits of mono-cycle durations. The scheme requires stable mono-cycle seed laser pulses with high pulse energies for the density modulation of electrons in free-electron lasers. In this project, an approach is investigated to generate such a mono-cycle seed pulse in the deep-ultraviolet for the initiation of the mono-cycle harmonic generation scheme.

Hard X-ray free-electron lasers (XFELs) are becoming available in several facilities in the world, generating hard X-ray pulses with gigawatt peak powers and pulse durations shorter than 10 fs. XFELs have various applications in nonlinear optics, time-resolved X-ray diffraction, and X-ray structure analysis without radiation-induced deformations. Although, the pulse duration is extremely short, it is still far beyond the fundamental shortest limit: the mono-cycle pulse duration or a zeptosecond duration within which the electric field oscillates only once.

Various schemes have been proposed for shorter durations of XFELs. Among them, the one called mono-cycle harmonic generation (MCHG) is remarkable since it potentially generates isolated mono-cycle pulses in FELs [1]. The scheme up-converts a mono-cycle pulse to a shorter wavelength while retaining the mono-cycle pulse feature. After applying several times the MCHG scheme, it may be possible to generate a mono-cycle pulse in the hard x-ray as illustrated in Fig. 1.

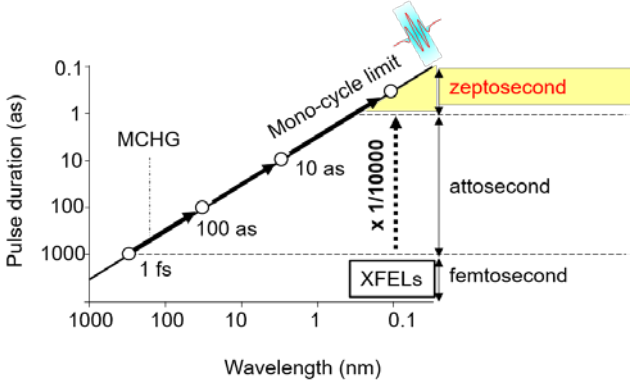

Fig. 1. Pulse durations of the state-of-the-art XFELs and the mono-cycle limits. The arrows indicate multiple MCHG schemes for mono-cycle XFELs with intermediate mono-cycle pulses (open circles)

To initiate the above scenario, a mono-cycle seed laser pulse is necessary with a high pulse energy. Although isolated attosecond pulses are generated in the extreme ultraviolet via high-harmonic generation, no free-electron laser seeded by the harmonics has sufficient stability for practical applications [2, 3]. On the other hand, seeding at a longer wavelength in the deep-ultraviolet has enabled FEL radiations with stable intensities. Seeding the MCHG scheme in the deep-ultraviolet may therefore be promising, although a mono-cycle pulse has never been generated in the ultraviolet.

In this research, an approach is proposed to generate such isolated mono-cycle pulses in the deep-ultraviolet. Since the mono-cycle laser pulse should have a high pulse energy for effective seeding of the MCHG scheme, the scheme relies on use of multiple multi-cycle laser pulses in longer wavelength ranges with energy scalabilities. The third-order nonlinear optical effects generate mono-cycle ultraviolet radiations, which is numerically simulated and will be discussed in detail.

Acknowledgements

This work was supported by JST PREST Grant Number JPMJPR16P5, Japan.

References

1. T. Tanaka, *Phys. Rev. Lett.*, 2015, **114**, 044801.
2. S. Ackermann *et al.*, *Phys. Rev. Lett.*, 2013, **111**, 114801.
3. H. Tomizawa *et al.*, *High Power Laser Science and Engineering*, 2015, **3**, e14.

HIGH PEAK POWER LASERS AT INRS AND APPLICATIONS OF LASER-WAKEFIELD-BASED X-RAY SOURCES: FROM BIO-MEDICAL TO GLOBAL FOOD SECURITY

J.C. Kieffer[1*], S. Fourmaux[1], and **E. Hallin[2]**

[1] INRS-EMT, Varennes, Québec, Canada, kieffer@emt.inrs.ca
[2] Global Institute on Food Security, U. of Saskatchewan, Saskatoon, Canada

We upgraded over the past two years the INRS high peak power laser facility from 200 TW (5 J, 25 fs) to 600 TW (11 J, 18 fs). The experimental programs have been restarted at the beginning of 2017 in the continuity of our previous scientific directions, i.e. high intensity laser-matter interaction and ultrafast X-ray sources. In this talk we will present and discuss the first experiments realized with our new laser facility, with a particular emphasis on the generation of ultrafast bright hard X-rays.

We discussed previously [1, 2] the potential impact of ultrafast laser-based X-ray sources. We will present here the generation of high throughput hard X-ray radiation by Laser Wakefield Acceleration (LWFA) process [3], which could allow a paradigm shift in a wide range of applications [4]. Ultrafast laser wakefield accelerated electrons perform wiggler-like oscillations creating a very bright micrometer-sized highly directional emission x-ray source. Such a laser-based betatron x-ray source is very attractive due to its ultrahigh brilliance, microscopic effective size, and cone beam geometry offering a large field of view for imaging.

We demonstrated in 2011 at INRS [5], and simultaneously similar results were obtained at U. of Michigan [6], that one phase contrast hard x-ray image could be produced in one X-ray pulse with a reasonable signal to noise ratio. This is opening a new route for fast 3D imaging of various objects [7]. These X-ray sources have also a unique duration characteristics, since they are as short as the optical driving laser pulses, offering extraordinary potential for femtosecond molecular imaging and Warm Dense Matter probing [8].

We will present the characterization of our upgraded LWFA betatron beam line coupled to our new laser system. X-ray source parameters are around 10^9 photons/0:1% bandwidth/sr/shot at 40 keV, a critical energy between 40 and 70 keV, an effective X-ray source size of 1 µm, a divergence between 10 and 50 mrads (FWHM), an X-ray beam pointing stability and an X-ray energy stability in the 2% rms range.

We will describe our funded program in developing high throughput phase contrast screening system based on LWFA X-ray sources for plant imaging through an initiative led by the Global Institute on Food Security (GIFS) at the U of Saskatchewan that aims to elucidate that part of the functional that maps specific environmental inputs onto specific plant phenotypes. X-ray images realized with the betatron source will be compared to thermal neutron images of same plants realized at the Canadian Nuclear Laboratory N5 Beam line. This program is the first of this kind in the world and we will show the very promising advantages of LWFA based betatron X-ray sources for the Agriculture sector and for the Global Food Security challenge.

References

1. J.C. Kieffer *et al*., *Appl. Phys. B*, 2002, **74**, S75.
2. J.C. Kieffer *et al*., 19th International Conference and School on Quantum Electronics: Laser Physics and Applications, edited by Tanja Dreischuh, Sanka Gateva, Albena Daskalova, Alexandros Serafetinides, *Proc. of SPIE*, 2017, **10226**, 1022612.
3. S. Corde *et al., Rev. Mod. Phys*., 2013, **85**, 1.
4. J.C. Kieffer *et al., SPIE Newsroom*, 2016, 10.1117/2.1201610.006713.
5. S. Fourmaux *et al., Opt. Lett*., 2011, **36**, 2426.
6. S. Kneip *et al., Appl. Phys. Lett*., 2011, **99**, 093701.
7. J. Wenz *et al*., *Nature Communications*, 2015, 6:7568 doi: 10.1038/ncomms8568.
8. M. Mo *et al*., *Rev. Sci. Instrum*., 2013, **84**, 123106.

THIRD-ORDER-NONLINEAR EFFECTS IN SINGLE CRYSTALS WITH ARBITRARY ORIENTATION AND IN CERAMICS

E.A. Khazanov, O.V. Maslennikov, V.N. Ginzburg, A.A. Kochetkov, and **V.I. Nekorkin**

Institute of Applied Physics, Nizhny Novgorod, Russia, efimkhazanov@gmail.com

Abstract. The influence of cubic crystal orientation on the generation of cross-polarization, self-phase modulation and laser beam self-focusing is investigated. The orientations at which these effects are maximal and minimal have been found. The qualitative and quantitative difference of these effects in ceramics from those in single crystals and glass has been determined. Random small-scale (of order grain size) spatial modulation of laser beam polarization and phase has been predicted. This effect has no analogs in glasses or in single crystals.

Laser ceramics is an ensemble of densely packed grains having characteristic size ranging from several microns to 100 microns. The orientation of crystallographic axes in each grain is random. Crystals with cubic symmetry have a unitary linear tensor of dielectric permittivity. Consequently, the index of refraction is the same for any single crystal orientation, as well as for ceramics. The nature of ceramics manifests itself in the presence of the effects dependent on crystal orientation, for instance, at thermally induced birefringence determined by the piezooptical tensor. Similarly to this tensor, the tensor of cubic nonlinearity $\chi^{(3)}$ of isotropic (cubic) crystals has a lower symmetry than $\chi^{(3)}$ of glasses; and it is defined by χ_{xxxx} and the parameter $\sigma = 1–3\chi_{xxyy}/\chi_{xxxx}$ that is equal to zero for glasses. As a result, the nonlinear effects related to cubic nonlinearity depend of crystal orientation; hence, they may be significantly different in ceramics and single crystals.

Of greatest interest are four $\chi^{(3)}$-effects: the generation of cross-polarization wave (XPW), self-phase modulation (SPM), whole-beam self-focusing (WBSF), and small-scale self-focusing (SSSF). The first thee effects may be both, parasitic and useful. SSSF is always a parasitic effect. The impact of single crystal orientation was studied only for XPW; it was shown that the XPW efficiency for the [110] orientation is higher than for the [001] orientation. SSSF was also studied only for three particular orientations: [001], [110] and [111]. To the best of our knowledge, none of these $\chi^{(3)}$-effects was discussed in the literature for ceramics. In the present work we undertook a detailed study of $\chi^{(3)}$-effects in single crystals and ceramics. The following results have been obtained.

1. The problem of changing wave polarization during propagation in an isotropic crystal with cubic nonlinearity is described by one equation and may be considered independent of changes of the wave phase.

2. It has been shown that, at small values of B-integral, the highest XPW efficiency may be achieved in a crystal having [110] orientation, and for large values of *B* optimal orientation depends on σ and *B*.

3. Cubic nonlinearity in ceramics gives rise to the effects that have no analogs in glass or in single crystals, namely, small-scale (of order grain size) spatial modulation of laser beam phase and polarization. The key parameter responsible for these effects is *N*, that is the ratio of the ceramics length to the average grain size. The standard deviation of the efficiency of XPW is inversely proportional to *N*, and standard deviation of nonlinear phase incursion D_Φ is inversely proportional to the root of *N*, see fig. 1.

4. In terms of nonlinear phase incursion Φ, on the average over beam cross-section, ceramics is equivalent to glass with effective nonlinearity $\chi_{eff} \approx (1–3\sigma/8)\chi_{xxxx}$.

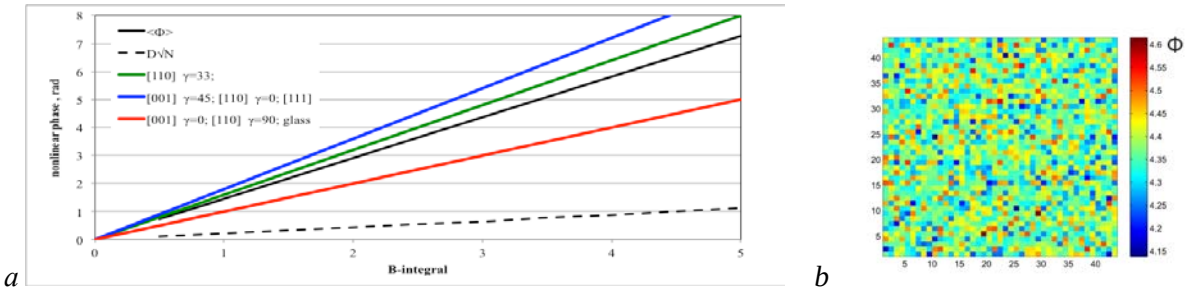

a *b*

Fig. 1. Average nonlinear phase <Φ> and $D_\Phi N^{1/2}$ (dashed line) for ceramics and nonlinear phase Φ for some single crystal orientations (γ is polarization inclination angle) *versus* B-integral (*a*), and value of Φ for 2000 random series for $N = 100$, $B = 3$ (*b*). Figure (*b*) models the profile of wave front of the beam passed through ceramics

EXPERIMENTAL RESEARCH OF SMALL-SCALE SELF-FOCUSING IN ISOTROPIC CRYSTALS

A.A. Kochetkov, V.N. Ginzburg, M.S. Kuzmina, A.A. Shaykin, and **E.A. Khazanov**

IAP RAS, Nizhny Novgorod, Russian Federation

Abstract. Direct measurements of spatial noise gain in an intense wave propagating in [001]-oriented BaF_2 were performed. Significant dependence of gain on the angle between the radiation polarization and the crystallographic axis predicted earlier was demonstrated.

Isotropic (cubic) crystals are currently widely used for creating high-power lasers. The optical element thickness as a rule varies from several millimeters to several centimeters, which imposes restrictions on the magnitude of the intensity of transmitted laser radiation increasing due to cubic nonlinearity of spatial perturbations. This results in small-scale self-focusing (SSSF) [1]. The maximum instability increment [2] is proportional to the B-integral. For large increments, SSSF leads to strong beam intensity modulation and to destruction of optical elements. Direct measurements of spatial perturbations amplification were first made in [3] and fully confirmed the theoretical predictions. However, the first study of SSSF in isotropic (cubic) crystals was undertaken only in 2016 [4]. A cubic crystal is a medium with isotropic linear properties but with anisotropic nonlinearity. As a result, two important parameters appear: crystal orientation and tilt angle of radiation polarization. The authors of [4] found out that in crystals with [001] and [101] orientations the instability increment greatly depends on radiation polarization, hence, SSSF may be suppressed substantially by choosing optimal polarization. In the present work we performed direct measurements of noise gain in a BaF_2 crystal with [001] orientation. The results obtained confirmed the predictions of the work [4].

Pulses with a duration of 60 fs, energy of 4 mJ and beam diameter of 6 mm were used as a source of powerful optical radiation. The radiation was fed into a 6 mm-thick BaF_2 crystal of [001] orientation. After passing the crystal the radiation was focused on a flat mirror with a drilled aperture 1.5 mm in diameter to cut-off a noise-free beam. As a result, only noise radiation was reflected at the mirror from which the image was transferred to the CCD camera registering the angular noise spectrum. A thin (200 μm) slightly matted glass plate placed at a distance of 17 mm in front of the BaF_2 crystal was used as a source of spatial noise. According to the SSSF theory, both in glass [2] and in an isotropic crystal [4] spatial perturbations gain depends not only on the angle α between the wave vector and the z-axis, but also on the phase difference between the strong wave and the perturbation wave at the nonlinear medium input. For the chosen geometry of the experiment, the angular spectrum of gain is modulated, i.e., there appear rings in the intensity distribution of the amplified noise in the far field, which was measured in the BaF_2 crystal (see fig. 1). The experimental dependence of noise gain corresponds to the theoretical predictions.

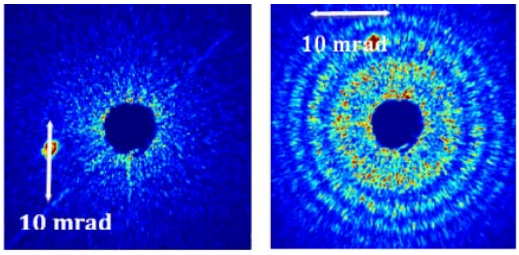

As was predicted in [4], unlike glass, noise gain in an isotropic crystal depends on the angle φ between the electric field vector and the crystallographic axis. The integral, i.e. averaged over the spatial spectrum noise gain as a function of the angle φ is plotted in fig. 2. The solid curves show the theoretical dependences for two values of the B-integral: $B = 0.75$ and $B = 0.9$.

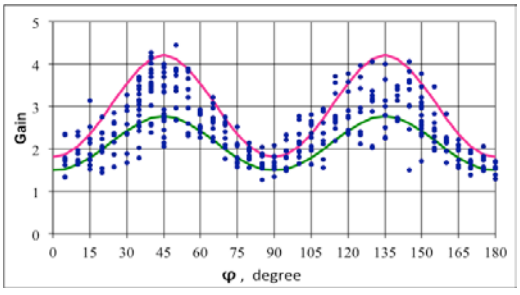

References

1. V.I. Bespalov and V.I. Talanov, *JETP Letters*, 1966, **3**, 307–310.
2. N.N. Rozanov and V.A. Smirnov, *Soviet Journal of Quantum Electronics*, 1980, **10**, 232–237.
3. A.K. Poteomkin, M.A. Martyanov, M.S. Kochetkova, and E.A. Khazanov, *IEEE Journal of Quantum Electronics*, 2009, **45**, 336–344.
4. M.S. Kuz'mina and E.A. Khazanov, *Radiophysics and Quantum Electronics*, 2016, **59**, 596–604.

MATHEMATICAL MODEL OF AN ADDITIONAL LASER PULSE GENERATING PROCESS IN A Q-SWITCHED GENERATOR

A.P. Korobeynikova, A.A. Shaykin, I.V. Koryukin, and **E.A. Khazanov**

IAP RAS, Nizhny Novgorod, Russia, nastya.k2594@gmail.com

Abstract. In this work a mathematical model is presented, that describes the generation of a laser pulse in a Q-switched generator taking into account the possibility of generating other modes. The modeling implies the formation of two neighbor longitudal modes with different losses of free running pulses and time variation of the population inversion in different areas of the active element due to light intensity. It is shown that in the Q-switched regime a second so-called postpulse can be generated after generation of the main giant pulse.

In the earlier published work [1, 2] the effect of the second giant pulse generation after the main pulse was observed in a pulse-pumped generator with Nd:YLF active element (wavelength 1054 nm) in a Q-switched single-mode regime. The simulation results presented in this work explain this effect and allow analyzing the behavior of pulse generation for different resonator parameters. The process of the population inversion changing in different layers of the active element is also clearly visible.

The simulation of the pulse evolution and the dependence of inversion on longitudinal coordinate and time is based on the equations

$$\begin{cases} \dfrac{dm_i}{d\tau} = Gm_i\left(g_i \cdot dz \sum_{k=1}^{N_n} n_k \left[\sin\left(\dfrac{\pi}{L}(k_0 + i - 1) z_k \right) \right]^2 - 1 - \beta_i \right) \\ \dfrac{dn_k}{d\tau} = A - n_k \left(1 + \sum_{i=1}^{N_m} g_i m_i \left[\sin\left(\dfrac{\pi}{L}(k_0 + i - 1) z_k \right) \right]^2 \right) \end{cases}, \quad (1)$$

where m_i is the field intensity of the resonator i-th mode, n_k is the population inversion in the k-th layer of the active element, $G = T_n/T_{ph}$ (T_n is the population inversion relaxation time, T_{ph} is the lifetime of a photon in a resonator), $\tau = t/T_n$ is normalized time, z_k is the coordinate of the k-th layer, $dz = \lambda/10$ is layer width, g_i is the ratio of the gain of the i-th mode to the gain of the mode closest to the center of the gain band ($g_i \le 1$), k_0 is central mode number, β_i are losses for the i-th mode, L is resonator length.

In the right-hand side of this system of differential equations, a running wave component was added to the standing wave, allowing more accurate description of the real processes in the generator:

$$\begin{cases} \dfrac{dm_i}{d\tau} = Gm_i\left(g_i \cdot dz \sum_{k=1}^{N_n} n_k \left[a \cdot \sin\left(\dfrac{\pi}{L}(k_0 + i - 1) z_k \right) + b \cdot \sin\left(\dfrac{\pi}{L}(k_0 + i - 1)(z_k - c\tau) \right) \right]^2 - 1 - \beta_i \right) \\ \dfrac{dn_k}{d\tau} = A - n_k \left(1 + \sum_{i=1}^{N_m} g_i m_i \left[a \cdot \sin\left(\dfrac{\pi}{L}(k_0 + i - 1) z_k \right) + b \cdot \sin\left(\dfrac{\pi}{L}(k_0 + i - 1)(z_k - c\tau) \right) \right]^2 \right) \end{cases} \quad (2)$$

It was shown that this simulation explains well the generation of the second giant pulse in the Q-switching regime. There are areas in the active element where population inversion is retained after generation of the first giant pulse. This is the cause of the nearby longitudinal mode generation.

References

1. A.P. Korobeynikova, K.F. Burdonov, A.A. Shaykin, and E.A. Khazanov, *Conf. Nonlinear waves-2016*, Bor, Russia, 2016, p. 78.
2. K.F. Burdonov, A.A. Shaykin, and E.A. Khazanov, *Laser Optics 2016*, Saint-Petersburg, Russia, 2016, p. 49.

DESIGN AND SPECIFICATIONS OF 630-MM PHASE SHIFTING INTERFEROMETER FOR THE QUALIFICATION OF LARGE APERTURE OPTICS

I.E. Kozhevatov, D.E. Silin, A.V. Pigasin, E.H. Kulikova, and **S.B. Speransky**

IAP RAS, Nizhny Novgorod, Russia, kozh-ie@mail.ru

Abstract. A specialized phase shifting interferometer for qualification of large optics for extremely high-power laser systems has been designed and tested at IAP RAS. The interferometer will be used to assess homogeneity of blank material as well as in-process inspection information and final inspection qualification data. The 630 mm system is one of the largest Fizeau phase shifting interferometers ever manufactured in Russia. The interferometer has a high lateral resolution, but the most notable feature of this device is its high absolute precission. In this presentation we consider vibration and distortion control of interferometer optical elements and optical transfer function optimization. We also address the effects in the test cavity arising from measuring transmitted and reflected wavefronts of optics mounted at various angles, including the Brewster's angles.

Introduction

Construction of an extremely high power laser system requires fabricating lots of large planar optics having apertures of approximately 600 cm. Some elements such as laser amplifier slabs and glass polarizer plates are used at Brewster's angle. Besides these optics must be measured both at full aperture and at reduced aperture to provide higher resolution and high precision. Analysis of markets [1, 2] showed that conventional commercial interferometers do not meet the needed requirements. For this reason a special-purpose large aperture phase shifting interferometer has been developed and manufactured at IAP RAS in Nizhny Novgorod.

Measurement parameters

The IAP RAS interferometer enables:

– qualifying the forms of flat surfaces for diameters up to 630 mm;

– testing the wavefront distortions of the transmitted and reflected wavefronts of optics mounted at various angles;

– measuring homogeneity of blank material;

– simultaneous imaging of the wavefront distortions on two scales: 630 mm per 1024 camera pixels, 100 mm per 1024 camera pixels.

Basic characteristics

The IAP RAS interferometer has the following basic characteristics:

– repeatability	$\lambda/3000$ (λ = 630 nm)
– absolute precision	$\lambda/1000$ (for scale 630 ÷ 2.5 mm)
	$\lambda/500$ (for scale 2.5 ÷ 0,1 mm)
– lateral resolution	up to 0.1 mm
– maximal sample sizes	diameter = 630 mm, thickness = 800 mm.

References

1. J. Lamb, J. Semrad, J. Wyant, Ch. Ai, R. Knowiden, E. Novak, J. Downie, and R. Wolfe, *SPIE*, **3047**, 415.
2. https://www.zygo.com/?sup=/resource/manuals.cgi?type=interferometers.

LARGE BIMORPH FLEXIBLE MIRROR FOR PETA-WATT LASER BEAM CORRECTION

A. Kudryashov[1,2,4], **V. Samarkin**[1,4], **A. Aleksandrov**[1], **G. Borsoni**[2], **T. Jitsuno**[3], and **J. Sheldakova**[4]

[1] Moscow Polytech, Bolshaya Semenovskaya str., 38, Moscow, Russia, 107023, kud@akaoptics.com
[2] AKA Optics SAS, 2 rue Marc Donadille, Marseille, 13013 France
[3] Institute of Laser Engineering, Osaka University, 2-6 Yamada-oka, Suita, Osaka 565-0871, Japan
[4] Institute of Geosphere Dynamics, Russian Academy of Sciences, Leninskiy Avenue 38, Bld. 1, Moscow, Russia

Abstract. Two types of large bimorph deformable mirrors with the size of 410×468 mm and 320 mm were developed and tested. The results of the measurements of the response functions of all the actuators and of the surface shape of the deformable mirror are presented in this paper. The possibility of correction of the aberrations in high power lasers was demonstrated experimentally (to get Strehl number up to 0.7) and numerically.

There are various solid state pulse lasers based on Nd:glass with the output beam power of the PW level, such as the National Ignition Facility (NIF) in the USA, the MEGAJOULE (LMJ) in France, the LFEX in Japan, Lutch in Russia and etc. The increasing of the laser pumping power leads to an increase of the inhomogeneities in the active media and the distortions of the reflective and refractive surfaces of the optical elements primarily due to heating. As a result the wavefront of the output beam is distorted significantly. To obtain the beam intensities of $\sim 10^{+22}$ W/cm^2 and more at the target-laser interaction spot, the large scale and the low frequency wavefront aberrations have to be corrected. This is only possible with adaptive optical systems. Of course, the deformable mirror is the main element of any adaptive optical system. Correction efficiency depends first of all on the technology implemented on the deformable mirror. Different measurements performed in high power lasers have shown that the real wavefront aberrations are mainly low order ones [1]. Deformable mirrors based on bimorph technology can perform a precise correction of low order wavefront aberrations using a small number of the controlled electrodes (called bimorph actuators) [2]. A traditional semi-passive bimorph mirror consists of a comparatively thick glass substrate firmly glued to a flat thin actuator disk made of piezoelectric ceramic. The key problem of all wide aperture bimorph mirrors is their attachment in the housing – the larger the mirror the closer its behavior is to a simple membrane. For larger apertures, the problems with the initial mirror quality before and also after coating will even increase. This is why we have designed and manufactured a so-called combined deformable mirror, which includes both bimorph electrodes and piezo-stack actuators. The clear aperture of the mirror manufactured with this technology was 410×468 mm [3]. This mirror was designed to correct the wavefront distortions of a laser beam with a size up to 400×400 mm and with an angle of incidence on the mirror of 28 degrees. The amplitude of the deformation of the mirror surface ranged from –8 to +12 μm for each bimorph electrode with a control voltage applied ranging from –300 to +500 V. The roughness of the mirror after polishing was better than 2 nm (RMS). The flatness of the surface before assembling it in its mounting was better than 1.5 μm, it contained mostly defocus, because P-V decreased to 0.5 μm after analytically subtracting the total curvature. The dielectric coating offered a reflection coefficient of 99.9% at the wavelength of neodymium phosphate glass laser radiation, λ = 1.053 μm, and the damage threshold was better than 50 J/cm^2. In order to minimize the initial mirror aberrations caused by the mechanical tension after placing it into its mounting, we used the piezoelectric actuators glued on the edge of the mirror. The initial surface error after the bimorph mirror was attached to its mounting was about 30 μm (P-V). While using a standard correction procedure in a closed loop system with a Shack-Hartmann wavefront sensor [4], using only the stacked actuators, the aberration decreased to 1.517 μm (P-V). A deformable mirror with such a surface quality would initially introduce small phase aberrations in the laser beam, which need to be corrected. This additional wavefront error can be compensated by bimorph electrodes. Indeed, in the last step, when the bimorph electrodes were also activated by the closed loop the flatness obtained was equal to 0.162 μm (P-V) and 0.033 μm (RMS). Every voltage applied to electrodes was under 50 V that is no more than 10% of the dynamic range of the control voltage. This will save almost full control range for correction of the big amplitude aberrations of the high power laser beam.

Acknowledgements

The work was supported under RFBR grant #15-08-07986.

References

1. A.G. Alexandrov, V.E. Zavalova, A.V. Kudryashov, *et al*., *Quantum Electronics*, 2010, **40**, 321.
2. V. Samarkin, A. Kudryashov, *Proc. SPIE*, 2010, **7789**, 77890B.
3. Samarkin V., Alexandrov A., Borsoni G., *et al*., *High Power Laser Science and Engineering*, 2016, **4**, e4.
4. A. Rukosuev, A. Kudryashov, A. Lylova, *et al*., *Atmospheric and Oceanic Optics*, 2015, **28** (2), 189–195.

FORMATION OF THE LASER BEAM WITH THE HELP OF DIFFERENT TYPES OF DEFORMABLE MIRRORS

A. Lylova[1,2], J. Sheldakova[1], A. Kudryashov[1,2], V. Samarkin[1], and **A. Rukosuev[1]**

[1] Active Optics NightN Ltd., Moscow, Russia, lylova@activeoptics.ru
[2] Moscow Polytech, Moscow, Russia

Abstract. Adaptive optics allows transforming intensity distribution from Gaussian to flattop, doughnut etc. In this work, two types of the wavefront correctors for the beam shaping were used: bimorph deformable mirror and stacked-actuator deformable mirror. The flattop and doughnut beam formation results with the use of adaptive optics are also presented.

In some laser applications, it is necessary to optimize the beam parameters to transform the shape of the beam on the target [1] from Gaussian one to a flattop, doughnut etc. Adaptive optical systems are used to modify the wavefront to obtain the desired intensity distribution in the far-field. They could be also used for beam shaping. The modification of beam intensity in the far-field is important for high-quality laser beam cutting, laser fusion, laser thermal processing etc.

To get the desired shape of the focal spot we designed an adaptive optical system that included the collimated beam source, wavefront corrector, wavefront sensor and PC to control the beam shaping process.

In this work, we investigated two types of the desired intensity distribution: flattop and doughnut. To model the intensity distribution, we used the following algorithm:

1. Defined the desired wavefront through Zernike polynomials using hill-climbing algorithm [2].
2. Calculated voltages to be applied to the deformable mirror electrodes to form the wavefront with calculated Zernike polynomials coefficients.
3. Checked far-field with CCD camera placed at the focal plane of focusing lens.
4. Changed the wavefront through a slight change of Zernike coefficients to make the focal spot closer to the flattop or doughnut one.

Experimental Results

In our work, we used two deformable mirrors: bimorph mirror [3] with 48 electrodes and stacked-actuator mirror [3] with 37 actuators. Using this wavefront correctors, we calculated the estimated reconstruction of the desired beam shape. The residual error of the estimated reconstruction with the use of the bimorph mirror was 0.003 μ for flattop intensity distribution and 0.004 μ for doughnut intensity distribution. The residual error of the estimated reconstruction with the use of the stacked-actuator mirror was 0.005 μ for flattop intensity distribution and 0.007 μ for doughnut intensity distribution.

The experimental results of the beam shaping are also presented in this work. It may be noticed that the real focal spot contains some extra aberrations like astigmatism and coma. It means that the setup is not ideal and these extra aberrations should be also compensated for. For this purpose, it is better to use the bimorph mirror due to its ability to obtain good reconstruction of the low-order aberrations. The residual error of the experimental reconstruction was about 0.04 μ.

Acknowledgements

The work was supported by the FRBR grant №16-07-01097.

References

1. J. Sheldakova, A. Kudryashov, A. Lylova, V. Samarkin, and A. Rukosuev, *Proc. SPIE*, 2016, **2927**, 97271V.
2. D.B. Skalak, *Proc. of the eleventh international conference on machine learning*, 1994.
3. A. Lylova, A. Kudryashov, J. Sheldakova, and G. Borsoni, *Proc. SPIE*, 2015, 9641, 96410K.

THERMO-OPTICAL CHARACTERISTICS OF UNIAXIAL CRYSTALS

E.A. Mironov and **O.V. Palashov**

Institute of Applied Physics of the Russian Academy of Sciences, Nizhny Novgorod, Russia
miea209@rambler.ru

Abstract. Thermally induced distortions of laser radiation caused by the photoelastic effect during high-power beam propagation through optical elements cut along the optical axis of uniaxial crystals have been investigated. The optical anisotropy parameter ξ and thermo-optical constants Q and P specifying the magnitude of thermally induced depolarization and thermal lens, respectively, have been defined for uniaxial crystals of all three syngony types. The introduced thermo-optical characteristics may be used as applicability criteria of various uniaxial crystals for work with high-power laser radiation.

Uniaxial crystals are currently widely used for developing high-power laser systems, despite certain difficulties in working with them. This is explained by the advantages some of them have over their optically isotropic analogs.

Heat release accompanying the transmission of a high-power laser beam through optical elements may give rise to thermally induced phase and polarization distortions. These effects have been well studied for elastic isotropic optical media and are described fully enough by three thermo-optical characteristics: optical anisotropic parameter ξ [1] specifying the direction of the axes of thermally induced birefringence and the thermo-optical constants Q and P determining the magnitude of thermally induced depolarization and thermal lens strength, respectively [2]. Introduction of such characteristics for uniaxial optical media will also be useful for describing thermally induced optical distortions in these media and their measurement will allow assessing applicability of one or another crystal for work with high-power laser radiation.

In this work the problem of finding the distributions of the axes of thermally induced birefringence and the phase difference of eigenpolarizations in uniaxial crystals cut along optical axis was solved. In the case of trigonal and hexagonal crystals these distributions are the same as in the case of media with isotropic elastic and piezo-optical properties and in the case of tetragonal crystals, they are similar to the case of cubic crystals with [001] orientation assuming that their elastic properties are isotropic.

Formulas describing polarization and phase distortions of radiation are the same up to notations of thermo-optical characteristics ξ, Q and P. Thermo-optical characteristics of uniaxial crystals of all three syngony types were introduced in this way analogously to cubic crystals in elastically isotropic approximation. The obtained expressions take on the known form in corresponding particular cases.

The optical anisotropy parameter ξ of trigonal and hexagonal crystals has been found to be equal to unity by virtue of the isotropy of their piezo-optical properties in a plane perpendicular to the optical axis.

We have analyzed by way of example thermally induced polarization distortions in a tetragonal DKDP crystal [3] and in a trigonal CeF_3 crystal [4]. The distributions and dependences observed in experiment fully agree with the theoretical considerations.

Acknowledgements

This work was supported by the mega-grant of the Government of the Russian Federation No. 14.B25.31.0024 executed at the Institute of Applied Physics of the Russian Academy of Sciences.

References

1. R.E. Joiner, J. Marburger, and W.H. Steier, *Appl. Phys. Lett.*, 1977, **30**, 485–486.
2. A.V. Mezenov, L.N. Soms, and A.I. Stepanov, *Thermooptics of solid-state lasers*, Mashinostroenie, Leningrad, 1986.
3. E.A. Mironov, A.G. Vyatkin, A.V. Starobor, and O.V. Palashov, *Laser Phys. Lett.*, 2017, **14**(3), 035801.
4. E.A. Mironov, A.V. Starobor, I.L. Snetkov, O.V. Palashov, H. Furuse, S. Tokita, and R. Yasuhara, *Optical Materials* (to be published).

CONTROL OF TEMPORAL INTENSITY PROFILE FOR PW LASER PULSES

S.Yu. Mironov[1], J. Wheeler[2], E.A. Khazanov[1], and **G. Mourou[2]**

[1] IAP RAS, Nizhny Novgorod, Russia, Sergey.Mironov@mail.ru
[2] International Center for Zetta-Exawatt Science and Technology (IZEST), Ecole Polytechnique, France

Abstract. A possibility of using self-phase modulation and cascaded quadratic nonlinearity effects for enhancement temporal parameters of PW laser pulses was demonstrated with the help of numerical simulations. Pulse duration can be shortened and intensity contrast ratio can be increased after a standard grating compressor. Implementation of the techniques to output radiation of TW and PW laser systems will multiply peak power in times.

Present day technologies allow generating PW-level laser pulses. The focused radiation finds applications in different experiments devoted to investigation of the behavior of matter in a strong electromagnetic fields, acceleration of electron and proton bunches. Further increasing of peak power of pulses can be done by enlarging the energy level and/or reducing pulse duration after a standard grating compressor. The first way requires development of laser amplifiers with big aperture (>10 cm) and wide spectral band. It requires significant investments to modernization of powerful laser systems and development of technologies for producing laser amplifiers. The second approach to peak power increasing is more promising and simple. It is based on using the self-phase modulation effect, which appears in powerful beams during their propagation through a thin (less 1mm) plane parallel plate and and due to the consequent correction of spectral phase with the help of chirped mirrors. Cubic nonlinearity effects modify parameters of the laser pulses (spectra broaden and nonlinear spectral phase appears). The correction of the quadratic component of the phase allows compressing the pulse and increasing the peak power. The technique was verified experimentally [1, 2].

It is mostly attractive to use the technique for high-energy (kJ-level) pulses from PW glass lasers. The bright example of the system is PETAL (1 kJ, 500 fs, 40 cm beam diameter, 1054 nm). Peak intensity at the beam is about 1.5 TW/cm^2. Numerical simulations demonstrate possible pulse compression down to 108 fs at accumulated B-integral 6.5 in 3 mm fused silica plane parallel plate. In this case, peak intensity will be increased up to 6 TW/cm^2.

The use of cascaded quadratic nonlinearity in a KDP crystal allows implementing the idea without chirped mirrors and realizes a pulse self-compression regime. A KDP crystal is optimal for high power laser beams as it may be grown up to apertures of more than 10 cm with thicknesses 1 mm and less. The value of accumulated phase in the process of second harmonic generation depends on the value and the sign of wave vector mismatch Δk and is linearly proportional to the intensity of the fundamental pulse as well as the phase obtained due to self-action effects. As a result, the cascaded quadratic nonlinearity can be used for compensation or magnification of cubic polarization effects. Numerical simulations show the possibility of pulse shortening down to 220 fs in 1 mm KDP crystal.

The mentioned methods do not result in enhancement of intensity contrast ratio. The use of KDP crystals for second harmonic generation can improve it significantly on pulse wings. Optimal (more that 80%) energy conversion can be experimentally obtained for the same 1 mm KDP crystal. Moreover, with the use of chirped mirrors for second harmonic beam leads to pulse shortening down to 200 fs and peak power in SH beam will be more than in the fundamental one.

It is also worthy of notice that a couple of KDP crystals can be used for pulse contrast cleaning. The fundamental beam should be linearly (45 deg) polarized to have equal intensity in “o” and “e” components. The crystals should be placed so that the “o” wave in the first crystal should change for the “e” wave in the second crystal and vice versa. The crystals should be detuned from the phase matching angle in the opposite directions. The waves participating in a low efficiency SHG process can accumulate nonlinear $\pm\pi/2$ phase shift. If at the end of the second crystal the phase difference between the waves is π, the component can be filtered by the polarizer. The phase shift appears only in the area where the intensity is sufficient for producing a nonlinear phase shift.

References

1. S.Yu. Mironov, J. Wheeler, R. Gonin, G. Cojocaru, R. Ungureanu, R. Banici, M. Serbanescu, R. Dabu, G. Mourou, and E.A. Khazanov, *Quantum electron*, 2017, **47** (3), 173–178.
2. P. Lassonde *et al.*, *Laser Phys. Lett.*, 2016, **13**, 075401.

INTEGRATING THE HIGH-ENERGY AND HIGH-INTENSITY LASERS FOR THE HED INSTRUMENT AT THE EUROPEAN XFEL

M. Nakatsutsumi[1], T. Toncian[2], G. Priebe[1], K. Appel[1], C. Baehtz[2], B. Chen[3], S. Göde[1], Z. Konopkova[1], M. Makita[1], A. Schmidt[1], K. Sukharnikov[1], I. Thorpe[1], A. Pelka[2], M. Lederer[1], T.E. Cowan[2], and **U. Zastrau[1]**

[1] European XFEL, Schenefeld, Germany
[2] Helmholtz-Zentrum Dresden-Rossendorf, Dresden, Germany
[3] Chinese Academy of Engineering Physics, Mianyang, People's Republic of China

The High Energy Density Science (HED) instrument at the European X-ray Free-Electron Laser Facility is dedicated to the investigation of a wide range of materials at extreme conditions of pressure, temperature, ionization or electro-magnetic field. Several separate optical laser systems (~5 J / 25 fs, ~100 J/ns, ~2 mJ / 15 fs and ~45 mJ / 1 ps) will be available for warm- to hot-dense-matter creation, dynamic compression, relativistic laser-plasma interaction and more.

The instrument is designed to enable the application of various x-ray probing techniques including spectroscopic, diffraction and imaging methods with 3 up to 25 keV photon energies. Being one of the 6 baseline instruments of the European XFEL, first user experiments are planned for the autumn of 2018. The installation of several high-power lasers, a dedicated diamond anvil cell setup and of the ~60 T pulsed magnets will be available through contributions by the Helmholtz International Beamline for Extreme Fields (HIBEF) User Consortium.

We present an overview of the experimental capabilities.

References

1. www.xfel.eu/research/instruments/hed
2. K. Appel *et al*., *Plasma phys. cntl. Fusion*, 2015, **57**, 014003.
3. M. Nakatsutsumi *et al*., *Plasma Phys. Control. Fusion*, 2017, 59, 014028.
4. www.hibef.de.

SPACE-TIME EMPIRICAL MODES AS AN INSTRUMENT FOR INVESTIGATION OF NONLINEAR PHENOMENA IN THE SUPERRADIANT LASERS

A. Seleznev, A. Gavrilov, E. Kocharovskaya, E. Loskutov, D. Mukhin, Vl. Kocharovsky, and **A. Feigin**

Institute of Applied Physics of the RAS, Nizhny Novgorod, Russia,
aseleznev@ipfran.ru

Abstract. The work is devoted to investigating spatial-temporal dynamics of the laser field in the low-Q cavities where photon lifetime is less than polarization relaxation time. We develop the spatial-temporal-dependent mode technique that takes into account strong coupling of standard cold or hot laser modes due to non-adiabatic and nonlinear effects. Its efficiency for the spectral-correlation analysis of the laser field is demonstrated.

Highly nonlinear spatial-temporal patterns are inevitable features of lasing in the low-Q (bad) cavities where a photon lifetime T_E is less than polarization relaxation time (lifetime of the optical dipole oscillations) T_2 [1]. Analysis of spatial-temporal dynamics of the field and its spectral and correlation features in such lasers, known as the superradiant lasers, cannot be based on a standard decomposition via 'cold' or 'hot' modes [2] because they have fixed spatial profiles and are defined by a cavity without or with taking into account the active medium, respectively. Progress in modern technologies, especially in the field of semiconductor heterostructures, leaves no doubts about near fabrication of superradiant lasers and their applications in the optical information processing, the wideband dynamical spectroscopy, and diagnostics of many-particle systems in condensed active media. Thus, the efficient method to unveil the fundamental nonlinear phenomena in these lasers is needed.

In this work we suggest an approach of *Space-Time Empirical Modes* (STEMs) based on the singular spectrum analysis technique [3] instead of analyses of nonlinear coupling of cold and/or hot modes. The method is applied to investigate the regimes of 1D model of low-Q hybrid Fabry-Perot cavity and an active medium with a distributed feedback of the counter-propagating waves. By their nature STEMs assumes taking into account not only spatial, but also temporal correlation of the gridded data set of complex fields of the counter-propagating waves, taken at the discrete points along a cavity z_j at the discrete moments of time t_k within a common time interval $[t,t+T]$, which is defined by a characteristic time scale T under consideration. On the basis of the STEM approach, we describe in details possible dynamical spectra and qualitatively different lasing regimes including quasi-stationary, self-modulated, regular pulsed, irregular bunched and quasi-chaotic ones. In particular, we demonstrate that it is possible to separate the components of laser emission with different timescales even if the respective field components are not separable in frequency domain due to a complicated dynamical spectrum of radiation.

Acknowledgements

The study is supported by the Russian Foundation for Basic Research (grant # 16-02-00714).

References

1. Vl.V. Kocharovsky, A.A. Belyanin, E.R. Kocharovskaya, and V.V. Kocharovsky, "Superradiant lasing and collective dynamics of active centers with polarization lifetime exceeding photon lifetime", *Advanced Lasers: Laser Physics and Technology for Applied and Fundamental Science Series*: *Springer Series in Optical Sciences*, V. 193. Shulika, Oleksiy; Sukhoivanov, Igor (Eds.) 2015, Ch. 4. p. 49.
2. E.R. Kocharovskaya, A.S. Gavrilov, V.V. Kocharovsky, E.M. Loskutov, D.N. Mukhin, A.M. Feigin, and Vl.V. Kocharovsky, "Empirical mode with a variable spatial-temporal structure and the dynamics of superradiant lasers", *Journal of Physics: Conference Series*, 2016, **740**, 012007.
3. D. Mukhin, D. Kondrashov, E. Loskutov, A. Gavrilov, A. Feigin, & M. Ghil, "Predicting Critical Transitions in ENSO models. Part II: Spatially Dependent Models", *Journal of Climate*, 2015, **28**(5), 1962–1976.

MODEL FOR HARD X-RAY GENERATION AND ELECTRON ACCELERATION DURING GRAZING INCIDENCE OF A LASER PULSE ONTO A PLANAR TARGET

D.A. Serebryakov, E.N. Nerush, and **I.Yu. Kostyukov**

Institute of Applied Physics RAS, Nizhny Novgorod, Russia
dms@appl.sci-nnov.ru

Abstract. When a laser pulse with dimensionless amplitude a_0 ~ 2–8 is incident onto a solid-density planar target under small angles to the surface (~5–15 degrees), the superposition of the incident and the reflected waves results in appearance of strong longitudinal force at a certain distance from the target. The electrons (coming from, for example, a preplasma) can accelerate in the presence of this force up to tens of MeVs. PIC simulations also reveal that this effect is even enhanced if *a* reaches 30–50 because of nonlinear alteration of the target surface. As a result, the electrons produce hard X-ray or even gamma-ray flash in the direction of their propagation. We study this process by means of both theoretical model and numerical simulations and determine the optimal parameters for the most efficient electron acceleration x-ray generation.

Femtosecond laser pulses are known to provide ultrastrong electric fields so that the electrons during laser-plasma interaction can be accelerated up to hundreds of MeVs using both complicated techniques such as laser wake field acceleration (LWFA) and more simple ones like direct laser acceleration. These fields also force the electrons to emit synchrotron photons with energies in the hard X-ray and gamma-ray range. There is an actively ongoing search for new configurations that would yield better electron and photon beam characteristics for the given laser parameters. In some aspects, considering normal [1] and oblique [2] incidence of laser pulses onto solid planar targets looks very promising.

If we consider a laser pulse incident onto a highly-reflective solid-density planar target under small angles to the surface (so-called grazing incidence regime), we will see that under approximation of perfect reflection, the incident and reflected waves form a wave structure which is a standing wave in the transverse (*y*) direction and running in the *x* direction:

$$E_x = -2E_0 \sin\theta \cos(kx\cos\theta)\exp(iky\sin\theta - i\omega t + i\phi_0)$$
$$E_y = 2E_0 \cos\theta \sin(kx\cos\theta)\exp(iky\sin\theta - i\omega t + i\phi_0 + i\pi/2)$$
$$B_z = 2B_0 \cos(kx\cos\theta)\exp(iky\sin\theta - i\omega t + i\phi_0)$$

Field superposition makes the electric field purely longitudinal at a certain distance from the target, and the magnetic field at this point vanishes. Theoretical modeling shows that if the initial conditions are close to this point, then the electrons can be efficiently accelerated (to much higher energies that would be under moderate incidence angles). Depending on the electron initial position and momentum, the acceleration rate significantly differs, and the corresponding phase space appears to be very complicated (fractal-like).

It can be shown that the electrons with multi-MeV energies efficiently emit synchrotron photons because their trajectory is curved for the most part. Modeling shows that the phase space regions corresponding to the most efficient X-ray generation are not necessarily the same as for maximum electron acceleration.

We have also conducted a series of particle-in-cell simulations – it turns out that the described regime may be implemented if there is a small preplasma near the surface that acts as an electron injector. We have also found the parameters where the simplified theoretical models better align with the simulations. It also turns out that if the dimensionless laser amplitude a_0 is increased up to 30–50, the target surface shape begins to significantly alter, and in this process the longitudinal electric field is even increased so the electron acceleration and X-ray emission rate is improved

Acknowledgements

This work was supported by the Russian Science Foundation (Grant No. 16-12-1038).

References

1. D.A. Serebryakov *et al*., *Phys. Plasmas*, 2015, **22**, 123119.
2. D.A. Serebryakov and E. N. Nerush, *Quantum Electronics*, 2016, **46**(4), 299–304.

PUMP LASER FOR MULTISTAGE PARAMETRICAL AMPLFIER

I. Shaikin, A. Kuzmin, and **A. Shaykin**

IAP RAS, Nizhny Novgorod, Russia
ilya.shaikin@gmail.com

Abstract. This work is devoted to the PEARL-X setup pumping laser and improvements of the laser made in the last few years. A few problems are discussed: compactification of the scheme by using short spatial filters, pumping pulse energy increase by increasing beam aperture, efficient use of the energy stored in amplifiers due to the injection of an additional pulse into the pump pulse amplification system, ways to reduce the spatial and temporal inhomogeneity of the pump pulse.

A pump pulse for parametrical amplifiers in the petawatt laser complex PEARL-X is produced by a single-mode generator with Nd:YLF active element. The wavelength is 1054 nm, the duration is about 1 ns. Then it passes through several Nd:YLF rod amplifiers and is divided into two parts. The first one after frequency doubling (wavelength 527 nm) becomes a pump pulse for the input cascades of parametrical amplification. The second part is injected into the pump pulse amplification system and then it is used to pump a wide-aperture (130 mm) parametrical amplifier.

The object of consideration of this work is the pump pulse amplification system. It consists of several consecutive Nd:glass rod amplifiers. The diameter of the active elements gradually increases from 10 to 100 mm; the amplifiers are separated by Kepler telescopes.

Short spatial filters

Compactness of installation is an important parameter. Due to the replacement of the previously used aberration-free spatial filters by shorter ones [1], it becomes possible to reduce the area of the optical tables occupied by the pump pulse amplification system. This made it possible to upgrade the system in several directions. We used the shortest filters, which allowed keeping the spherical aberrations introduced by the lenses within acceptable limits.

Aperture increase

One of the directions of the upgrade is to increase the energy of the pump pulse by increasing the aperture of the amplified pulse. The compaction of the scheme permitted us to install an additional amplification cascade with a 150 mm diameter active element [2].

Injection of the second pulse into the amplification system

The maximum energy of the pump pulse is limited by optical breakdown in the elements and by small-scale self-focusing. It is about 300 J for a beam of 100 mm diameter and 1 ns duration. However, a significant portion of the energy stored in the amplifiers remains unused. It can be used by injecting a replica of the input pulse into the same system. The energy of the second pulse in this case is comparable with the energy of the first one. In the future, these pulses will be used to pump two successive parametric amplifiers.

References

1. K.F. Burdonov, A.A. Soloviev, A.A. Shaikin, A.K. Potemkin, and A.S. Egorov, *Quantum Electronics*, 2013, **43**(11), 1082–1087.
2. A. Shaykin, A. Soloviev, A. Kuzmin, I. Shaikin, K. Burdonov, and E. Khazanov, *Proceedings of SPIE*, 2014, **9238**, 923809.

TOWARD "DEFECT-FREE" OPTICS: WHERE TO START?

J. Shao[1], Zh. Wu[2], Sh. Liu[1], J. Chen[2], Yu. Zhao[1], and **M. Huang[2]**

[1] Shanghai Institute of Optics and Fine Mechanics, Chinese Academy of Sciences, Shanghai, P R China, jdshao@mail.shcnc.ac.cn

[2] ZC Optoelectronic Technologies, Ltd, Hefei, P R China

Abstract. To characterize the defects in optical materials is of great importance for high power laser applications. In this paper, recent progress in defect characterization of various optics is presented by using different imaging techniques, including photothermal microscopy and optical scattering microscopy. A multimodal microscopic technique was proposed for a more comprehensive evaluation of the defects over the surface of the large optics, so as to have a better understanding of the laser damage behaviors and to provide clues to eliminate defects during manufacturing process.

The laser based inertial confinement fusion (ICF) research devices, typically represented by the National Ignition Facility (NIF) are striving to seek a new energy source for human-being. However, until now NIF still faces several obstacles. One of them is the limitation of laser damage resistance of large optics and some optics should be regularly recycled or replaced when the damage sites on optics grow up. Various defects generated in the optics manufacture processes are critical factors to reduce the laser damage threshold of optics. Therefore, obtaining “defect-free” optics is the ultimate dream of optical engineers, which is also a promising way to improve the laser damage resistance and to reduce the running cost of large high-power lasers.

Precision metrology techniques of surface defects for optics applied in high-power lasers are critical to realize “defect-free” large optics with high damage threshold. Generally, surface defects of large optics with modern fabrication methods can be classified into two types: “visible defects” and “invisible defects”. The former includes scratches, digs, cracks, particles and surface blemishes. It was reported that the optics applied in the most of global ICF high-power laser systems were measured by naked-eyes on surface defects [1, 2]. The automatic optical inspection (AOI) method [3] can quantitatively measure the length and width of surface defect and greatly reduce the subjective error from naked-eyes. Even though these methods can obtain the distribution of surface defects over meter-size surface of large optics, they have the problem of low efficiency and can’t precisely distinguish various defects. The other type of defects generated in the manufacture processes of large optics is “invisible defects”, including non-homogeneity, impurity and dislocation. Most of these defects are absorptive and can be detected by photo-thermal based metrology technologies [4]. However, the existing methods can only measure small samples and cannot quickly find the absorbing defects.

To study the relation between the defects and laser damage, most of the researchers usually employ microscopical methods, i.e. SEM, AFM, PTM, etc., to magnify the structural characteristics of defects in the limited local areas. By this way, the damage mechanisms initiated from defects were proposed and the LIDT of specific defect can be derived from simulation [5]. However, surface defects are various in properties and randomly distributed over the surface of large optics, which makes damage behaviors and the lifetime of the optics unexpected.

Due to the fact that the existing metrologies can’t directly build the relation between damage and defects statistically, it is necessary to fill the blank of defect metrology methods in the mesoscopical dimension, a bridge between existing microscopic and macroscopic metrology methods. In this paper, the conception of high-speed, high-sensitivity multi-mode metrology technology, as far as we know, is first proposed for surface defects of large optics. The technology is a compressive integration of super-smoothing surface laser scattering method, high sensitive weak absorbing method and total internal reflection microscopy. The proposed technology can detect the surface defect with high-speed, high-sensitivity and non-destruction in the mesoscopical dimension. It is hopeful to provide a novel tool for mapping the defects in meter size optics and provide clues to eliminate defects during fabracations

References

1. P. Baisden, L. Atherton, and R. Hawley *et. al*., *Fusion Science and Technology*, 2016, **69**, 295–351.
2. D. Daurios, S. Bouillet and G. Gaborit, *Proc. of SPIE*, 2007, **6616**, 661645.
3. F. Wu, P. Cao, Yo. Yang, *et. al*., *Proc. of SPIE*, 2016, **10023**, 10023T-1.
4. J. Chen, J. Dong, Zh. Wu, *Proc. of SPIE*, 2013, **8786**, 87861M-1.
5. H. Wang, H. Qi, W. Zhang, *et. al*., *Optics Letters*, 2016, **41**(6), 1209–1211.

200 W CONTINUOUS WAVE DISK-LASER ON Yb:LuAG CERAMICS

I.L. Snetkov[1], **D. Zhou**[2], **A.I. Yakovlev**[1], **I.B. Mukhin**[1], **I.I. Kuznetsov**[1], **O.V. Palashov**[1], and **K.I. Ueda**[3]

[1] Institute of Applied Physics of the Russian Academy of Sciences, Nizhny Novgorod, Russia, snetkov@appl.sci-nnov.ru
[2] School of Material Science and Engineering, Shanghai University, Shanghai, China
[3] Institute for Laser Science, University of Electro-communications, Tokyo, Japan

Abstract. The optical and laser properties of Yb:LuAG ceramic sample made by nanocrystalline pressure-less sintering in H_2 (NC-PLSH) were investigated. An active element of a disk laser was manufactured and continuous generation with maximum output power of 200 W and slope efficiency of 40% was demonstrated.

Laser radiation with high average power is increasingly more frequently used in various fields of human activity: in applied fields (welding, cutting, drilling, material processing, 3d printing of complex metal products) and for scientific purposes (detection of gravitational waves, generation of MIR and THz radiation, as a pump of parametric amplifiers of lasers with a high peak power). The main requirements for lasers that generate such radiation are high efficiency, stability of operation while maintaining the quality of the generated radiation close to diffraction. This significantly limits the choice of the type of laser, the active ion, the method of its pumping, and the material of the active element. An active ion should have a small quantum defect, the geometry of the active element should allow organizing efficient heat sink and material of the active element should have high thermal conductivity and good thermo-optical properties.

In this study, the sample of 3at% Yb:LuAG ceramics made by nanocrystalline pressure-less sintering in H_2 (NC-PLSH) [1] in Shanghai University (China) was investigated and efficient laser generation in disk laser geometry was observed. The Yb doped LuAG powders were synthesized by a wet chemical approach, then were preformed into green compacts in a stainless steel die, and were cold isostatic pressed (CIP) under 200 MPa. Finally, green bodies were sintered in a furnace with a tungsten-mesh heater at 1750 C for 10 hours in flowing H_2 atmosphere. After sintering, the ceramic sample was optically polished. The transmission spectrum, the luminescence spectrum at 940 nm pumping and a life time of the laser level were measured. After that, the thickness of the sample was reduced to 300 microns and the sample faces were coated with dielectric layers (an antireflection layer on one side and a mirror layer on the other side for the pump λ_{pump} = 940 nm and laser wavelengths λ_{laser} = 1030 nm). For effective cooling, the active element with dielectric coatings was mounted on a water-cooled diamond heat sink. The active element on the heat sink was placed in a V-shaped resonator formed by the rear face of the active element and two dielectric mirrors: spherical mirror (2) with a radius of 30 mm and a reflectance R ~100% at a wavelength of 1030 nm and output mirror (3). For the output mirror we used mirrors with reflectance of 90%, 95% and 97% at 1030 nm. Pumping was performed by a fibre-coupled diode laser (Laserline LDM 2000) emitting at a wavelength of 940 nm. 12 passages of pump radiation through the active element were organized in the resonator and at continuous pumping laser generation with maximum output power 200W and 40% slope efficiency was observed.

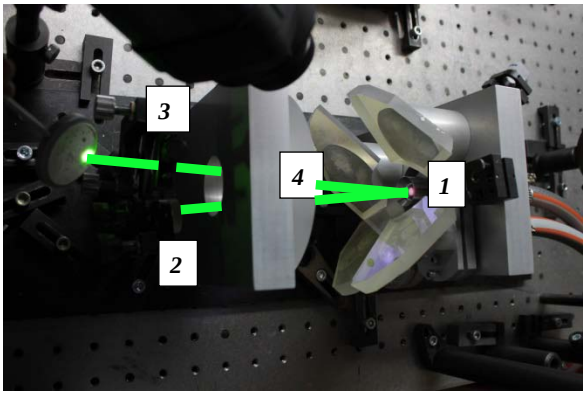

Fig. 1. Photo of laser experiment. *1* – active element; *2* – spherical mirror; *3* – output plane mirror; *4* – system of mirrors for organization of multi-pass pumping scheme

Acknowledgements

This work was supported by the mega-grant of the Government of the Russian Federation No. 14.B25.31.0024 executed at the Institute of Applied Physics of the Russian Academy of Sciences.

References

1. D. Zhou, Y. Shi, J. Xie, D. Chen, J. Dong, K.-i. Ueda, J. Xu, "Laser grade Yb:LuAG transparent ceramic prepared by nanocrystalline pressure-less sintering in reducing H_2", *Opt. Mater. Express*, 2017, **7**, 1274–1280.

LASER DRIVEN ION ACCELERATION AT PEARL LASER FACILITY

A. Soloviev[1], K. Burdonov[1], S.N. Chen[1,2], A. Eremeev[1], S. Pikuz[3], G.V. Pokrovskiy[3], T.A. Pikuz[3], G. Revet[1,2], A. Sladkov[1], V. Ginzburg[1], E. Khazanov[1], A. Kuzmin[1], D.K. Batheja[4], S. Mironov[1], R. Osmanov[1], I. Shaykin[1], A. Shaykin[1], I. Yakovlev[1], M. Starodubtsev[1], and **J. Fuchs[1,2]**

[1] Institute of Applied Physics of the Russian Academy of Sciences, Nizhny Novgorod, Russia, 7oloviev@gmail.com

[2] LULI - CNRS, Ecole Polytechnique, CEA: Université Paris-Saclay; UPMC Univ Paris 06: Sorbonne Universities - F-91128 Palaiseau cedex, France

[3] Joint Institute for High Temperatures Russian Academy of Science (RAS), Moscow 125412, Russia

[4] Institute of Physics of the Czech Academy of Sciences, 252 41 Dolní Břežany, Czech Republic

Abstract. The talk presents experimental investigation of the interaction of the femtosecond sub-PW laser pulse from PEARL laser facility and plasmas. The experimentally realized conditions are close to optimal in terms of effective laser energy deposition into the solid target leading to NTSA proton beams accelerated up to 43 MeV cut-off energy. The characterization of the interaction parameters is achieved by combining X-ray spectrometry and proton spectra measurements, complimented by detailed laser prepulse characterization. The ways to improve the cut-off energy for the laser driven protons as well as application perspectives are considered.

The experiments were conducted at the PEARL laser facility (IAP RAS, Nizhny Novgorod, Russia). PEARL is an OPCPA laser system [1] with a wavelength of 910 nm and the record reported power of 0.56 PW [2]. The temporal contrast of the laser systems after compression and over a 1 ns frame before the main pulse was estimated to be $1/(2\cdot10^8)$ [3]. By means of an off-axis parabolic f /4 mirror the laser pulse was focused on the target surface (aluminium foil 10 mm thick) making an angle of 45° with the direction of incident radiation.

Using two complementary diagnostics, we have been able to characterize the interaction of an ultra-high intensity, and ultra-high contrast laser with a thin Al solid slab. We have shown that at the time of the main laser pulse interaction, the target front and rear surfaces are gradient-free. This ensures a very efficient coupling between the laser energy and the target, and the generation of a very dense population of hot electrons at high temperature (as diagnosed by the accelerated protons). They couple very efficiently to the bulk electrons and ions heating them (as diagnosed by x-ray spectrometry) to ~300 eV, which is in good agreement with 1D modeling of such coupling using the hot electron parameters as an input.

Such efficient, gradient-free, heating to high temperatures opens up opportunities for probing various materials, using a much smaller-scale and relatively low-cost facility compared to FEL. We note that for such a mid-scale laser, the employed technology is a key to allow high-contrast interactions without the need to resort to contrast enhancement techniques. The work is considered in the aspect of possible applications in laboratory astrophysics, medicine and homeland security.

Acknowledgements

This work was supported by the Ministry of Education and Science of the Russian Federation under Contract No.14.Z50.31.0007. The work has been supported by the Russian Foundation for Basic Research under the project 16-32-60183.

References

1. I. Ross, P. Matousek, M. Towrie, A. Langley, & J. Collier, "The prospects for ultrashort pulse duration and ultrahigh intensity using optical parametric chirped pulse amplifiers", *Optics Communications*, 1997, **144**, 125–133.
2. V.V. Lozhkarev, *et al.*, "Compact 0.56 Petawatt laser system based on optical parametric chirped pulse amplification in KD*P crystals", *Laser Physics Letters*, 2007, **4**, 421–427.
3. V.N. Ginzburg, *et al.*, "Third-order correlator for measuring the time profile of petawatt laser pulses", *Quantum Electronics*, 2008, **38**, 1027–1032.

PERSPECTIVES OF ION ACCELERATION WITH PW-ULTRASHORT LASER PULSE

S. Ter-Avetisyan

ELI-ALPS, Szeged H-6720, Hungary

Abstract. This presentation will discuss the ion acceleration obtained on 1.5 PW laser and different issuers connected with ion source and beam properties. The newly found scenario of ion acceleration offers more favorable proton energy scaling with laser intensity than it is known for an “ordinary” so-called TNSA regime. Another challenge is the laser beam back reflection from interaction region, which was measured to be of the order of 1% of laser energy. Our findings pave a way to achieving an ion source and desired beam parameters and they encourage further activities for optimisation of laser plasma-based accelerators.

The unique exploratory mission of laser driven ion acceleration research is to build the scientific foundation needed to develop high energy laser-particle accelerators.

This presentation will discuss the ion acceleration obtained on 1.5 PW laser. The newly found scenario of ion acceleration offers more favorable proton energy scaling with laser intensity than it is known for “ordinary” so-called Target-Normal-Sheath-Acceleration. For the first time the ion energy scaling law for acceleration process in the ultra-short regime was extend beyond 10^{20} W/cm^2.

Ion source and beam properties at PW laser power offers unique features which will be discussed in details. The latter are essential for potential applications of laser driven ion beams.

Another challenge is the laser beam back reflection from interaction region. It was found that at ultrahigh contrast of the laser pulse on the electron density profile at the target surface a regular structure is generated during the interaction which acts as a grating and some of the diffraction maxima are under back reflection angle [1]. This back reflection of the order of 1% of laser energy, measured in the experiments, can lead to serious constraints on both the laser operation (cause damage) and the conditions of interaction.

These investigations are closely related to recent development or imminently anticipated development of laser technology to bring the existing laser systems to a multi-PW level. Our findings pave a way to achieving an ion source and beam desire parameters and they encourage further activities for optimisation of laser plasma-based accelerators.

References

1. S. Ter-Avetisyan *et al*., *Optics Express*, 2016, **24**, 28104.

GENERATION OF STRONG TERAHERTZ SURFACE WAVES ON METAL WIRES BY RELATIVISTIC-INTENSITY LASER PULSES

S. Tokita[1], K. Teramoto[2], T. Terao[1], S. Inoue[2], R. Yasuhara[3], T. Nagashima[4], M. Hashida[2], J. Kawanaka[1], N. Miyanaga[1], and **S. Sakabe[2]**

[1] Institute of Laser Engineering (ILE), Osaka University, Japan
[2] Institute for Chemical Research (ICR), Kyoto University, Japan
[3] National Institute for Fusion Science (NIFS), Japan
[4] Setsunan University, Japan
Email: tokita-s@ile.osaka-u.ac.jp

Abstract. We report an efficient method for strong terahertz surface wave generation by relativistic-intensity ($>10^{18}$ W/cm^2) laser pulses. Ultrafast field propagation along a metal wire driven by a femtosecond laser pulse with a relativistic intensity is characterized by femtosecond electron deflectometry and electro-optic sampling. We found that the field propagating at the speed of light is a half-cycle transverse-magnetic surface wave excited on the wire and a considerable portion of the kinetic energy of laser-produced fast electrons can be transferred to the surface wave.

Intense ultrashort terahertz (THz) pulses are now utilized not only as probe pulses, but also as ultrafast driving pulses in modern experimental studies on topics such as carrier dynamics in semiconductors [1]. Such investigations rely on picosecond or sub-picosecond THz pulses with electric field strength greater than 100 kV/cm. The development of waveguides for intense ultrashort THz pulses will offer new methodologies for many applications. In particular, to achieve low loss and low dispersion, the use of a metal wire as a waveguide has attracted considerable attention [2]. A THz pulse trapped as a surface wave (surface plasmon polaritons) on a metal wire can be flexibly transmitted and focused to sub-wavelength dimensions by techniques such as using a tapered tip [3]. However, the generation of intense THz surface waves remains a challenge due to inefficient coupling between free-space waves and surface waves.

Here, we review highly efficient generation and characterization of a THz surface wave directly on a wire waveguide. We have developed a technique for measuring THz waveforms by using laser-accelerated femtosecond electron pulses [4, 5]. As a result, we have observed an intense half-cycle THz surface wave with field strength exceeding 1 MV/cm upon driving ultrafast electron current on a metal wire by irradiating a femtosecond laser pulse with pulse energy of 70 mJ [~~6~~8]. We also report recent experimental results of electro-optic sampling measurement of THz surface waves.

Acknowledgements

This work was supported by Japan Science and Technology Agency (JST), Basic Research Programs "PRESTO", and supported by Japan Society for the Promotion of Science (JSPS), Grants-in-Aid for Scientific Research (Grant Numbers 22654050, 24540537, 23226002, and 25600138).

References

1. M. C. Hoffmann and J. Fülöp, *J. Phys. D: Appl. Phys.*, 2011, **44**, 083001.
2. K. Wang and D. M. Mittleman, *Nature*, 2004, **432**, 376–379.
3. V. Astley, R. Mendis, and D. M. Mittleman, *Appl. Phys. Lett.*, 2009, **95**, 031104.
4. S. Tokita *et al.*, *Phys. Rev. Lett.*, 2010, **105**, 215004.
5. S. Inoue, S. Tokita *et al.*, *Phys. Rev. Lett.*, 2012, **109**, 185001.
6. S. Tokita *et al.*, *Phys. Rev. Lett.*, 2011, **106**, 255001.
7. H. Nakajima, S. Tokita *et al.*, *Phys. Rev. Lett.*, 2013, **110**, 155001.
8. S. Tokita *et al.*, *Scientific Reports*, 2015, **5**, 8268.

THERMAL-LENS-FREE HEAT CAPACITIVE ACTIVE MIRROR

K. Ueda[1,2,3,4,5]

[1] Institute for Laser Science, Univ. of Electro-Communications, Chofu, Tokyo 182-8585, Japan
[2] Institute of Laser Engineering, Osaka University, Osaka, Japan
[3] Hamamatsu Photonics K.K., Hamamatsu, Japan
[4] JST, PRESTO, Tokyo, Japan
[5] Institute of Applied Physics, RAS, Nizhny Novgorod, Russia
* e-mail: ueda@ils.uec.ac.jp

Abstract. A new concept for thermal-lens-free solid state lasers, Heat Capacitive Active Mirror (HCAM), is proposed according to the systematic calculation of temperature profile and thermal-induced phase shift on 0.25–5 mm thick active mirrors of 10-mm diameter with 5-mm area pumping. Three orders of magnitude of thermal-lens reduction under the efficient cooling condition is possible. This is the first proposal for the paradigm shifting technology of thermal-lens-free active mirror available for coherent beam combination.

How to generate super-high power by the solid state lasers? Power scaling law of a laser is changing from the aperture scaling to the beam number scaling. Coherent beam combining has been a dream of the laser technology since 1960. Thermal-lens is a difficult problem to solve for solid state laser technology for a long time. There are two kinds of solution. One is the development of thermal laser ceramics using mixed solid solution to tune the optical parameter. And another is the thermal-lens compensation inside the laser material.

We propose a simple and efficient idea of Heat Capacitive Active Mirror (HCAM) capable of reducing the thermal-lens-effect by three orders with respect to 100% bottom cooled case.

HCAM in thermal equilibrium condition is shown in Fig. 1. The bottom cooling area is tuned to the pumping volume, typically 50% radius pumping and 50% bottom cooled (B-cool). Top to the bottom heat flow in the pumping volume gives us an efficient cooling almost equivalent to the 100 B-cool case. Most important point is the constant temperature halo area in the unpumped outer edge. This is a heat capacitive volume because there is no heat generation and heat sink. Thermal insulation on the heat capacitive volume reduces the non-flat wave component less than 1/50 over a wide range of disk thickness as shown in Fig. 2. When we tune the bottom surface temperature of heat capacitive volume to be constant to the average temperature of pumping volume, the thermal-shift decreases less than 1/1000 for thin disk (t = 0.25 mm) to thick disk (1 mm < t < 5 mm) range. Even a thick active mirror shows the order of magnitude smaller thermal shift than a typical thin disk. HCAM design relaxes the requirement on the doping concentration and pumping optics significantly. This is a simple solution toward thermal-lens-free solid state lasers for the coherent beam combining under CW and high rep. rate operation. The detailed properties of HCAM will be discussed in the presentation.

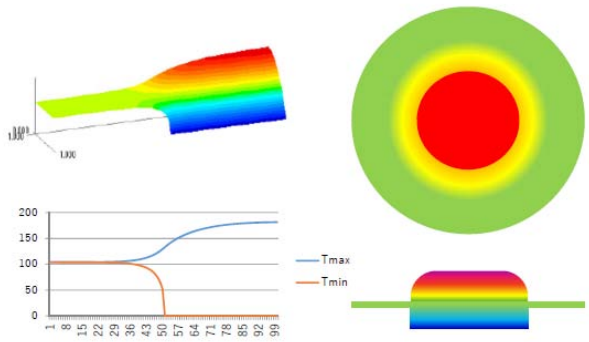

Fig. 1. Temperature profile of a HCAM laser

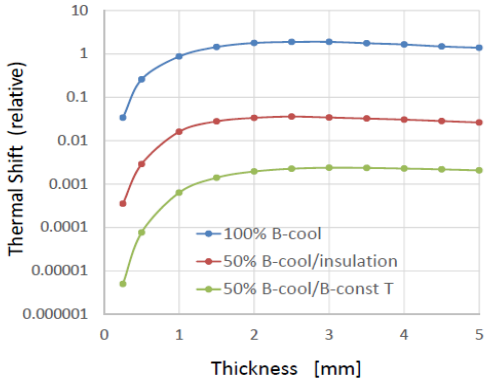

Fig. 2. Thermal-lens reduction curve

Acknowledgements

This work is partially supported by Toyota Physical and Chemical Research Institute and Mega Grant Program of Russian Federation No. 14.B25.31.0024.

ANALYSIS OF ELECTRONS ACCELERATED FROM ULTRA-THIN FOILS FOR EVALUATION OF HIGH-POWER ULTRASHORT LASER PULSE INTENSITY

O.E. Vais and **V.Yu. Bychenkov**

P.N. Lebedev Physical Institute of the Russian Academy of Sciences, Moscow, Russia
e-mail:ovais@lebedev.ru

Abstract. In the present work we suggest a new method of diagnostics of relativistically strong ultrashort laser pulses that is based on the analysis of angular spectral distributions of electrons gaining their energy in the process of direct vacuum acceleration by the laser field. To describe laser fields near the diffraction limit we use Stratton-Chu integrals to model a laser beam with different spatial profiles sharply focused by an off-axis parabolic mirror.

Nowadays continuous increase of the laser power demands new methods of laser beam quality control and diagnostics of laser parameters. When laser intensities reach relativistic values, the promising way for these purposes is to use measurements of laser-accelerated electrons [1, 2] and corresponding nonlinear Thomson scattering [3]. If the contribution of collective field effects as compared to the laser-particle interaction is negligible, the characteristics of charge particles are determined by parameters of the laser beam. This approach permits using the test particle method, when electron dynamics is ruled by the standard relativistic motion equations given by:

$$\frac{d\gamma m\mathbf{v}}{dt} = \mathbf{F}_L = -e\mathbf{E} - \frac{e\left[\mathbf{v}\times\mathbf{B}\right]}{c}, \frac{d\mathbf{R}}{dt} = \mathbf{u}, \quad (1)$$

where $\mathbf{R}$, $\mathbf{v}$, γ are radius-vector, velocity and gamma-factor of the test particle, respectively. Here we omit the radiation reaction force that can be possible for laser intensity of less than 10^{23} W/cm^2 [4].

In the current work we offer laser pulse diagnostics via angular-spectral distributions of accelerated electrons. Our calculations based on Stratton-Chu integrals [5] for the laser pulses (as example: linearly polarized, 30 fs, 800 nm) with the square spatial profile and Gaussian beams focused by the off-axis parabolic mirror (with $\varphi_{off} = 60°$ and radius r = 15 cm) have been performed and compared for different focal spot sizes and peak powers. In the recent work [2] the flat intensity distribution was shown to be more effective for electron acceleration as compared with Gaussian profile. After reflection by off-axis parabolic mirror the pulse interacts with thin layer of electrons that mimics an ultrathin foil, which is proposed to be used in diagnostic experiments.

The results show that electron distributions are sensitive to such laser parameters as the laser intensity and the focal spot size. Decreasing of the laser intensity due to changing of the laser power leads to decreasing of maximum electron energies, while defocusing of the tightly focused laser beam, at first, enhances maximum electron energies but after reaching an optimum value of the focal spot size starts to decrease them. Our calculations display anisotropic angular distributions under tight laser focusing which depend on the pulse parameters and become isotropic in paraxial limit that emphasize the need for accurate description of the tight focused laser beam. Comparison of these characteristics with the same from experiments is proposed for diagnostics of the laser parameters such as peak intensity and focal spot diameter.

Acknowledgements

This work was supported by RFBR (grant # 15-02-03042).

References

1. M. Kalashnikov, A. Andreev, K. Ivanov, *et al*., *Laser Part. Beams*, 2015, **31**, 361.
2. O.E. Vais, S.G. Bochkarev, S. Ter-Avetisyan, V.Yu. Bychenkov, *Quantum Electron.*, 2017, **47**(1), 38–41.
3. O.E. Vais, S.G. Bochkarev, and V.Yu. Bychenkov, *Plasma Phys.Reports*, 2016, **42**, 818–833; *Bull. Lebedev Phys.Inst.*, 2016, **43**, 12.
4. A. Di Piazza, K.Z. Hatsagortsyan, and C.H. Keitel, *Phys. Rev.Lett.*, 2009, **102**, 254802.
5. J.A. Stratton, L.J. Chu, *Phys. Rev*., 1939, **56**, 99; P. Varga, P. Torok, *J. Opt. Soc. Am. A*, 2000, **17**, 2081.

HOLOGRAPHIC WAVEFRONT SENSORS AND HIGH-POWER LASERS

V.Yu. Venediktov [1,2]

[1] St.-Petersburg Electrotechnical University, St.-Petersburg, Russia
vlad.venediktov@mail.ru
[2] Faculty of Physics, St.-Petersburg State University, St.-Petersburg, Russia

Abstract. Holographic wavefront sensors provide a fast and computations-free tool for measurement of the wavefront distortions. We consider the basic schemes of such devices, the recent progress in their development, related first of all to the use of Fourier holography, and special features of such devices, which make them especially interesting for application in various laser systems, including the high-power laser systems.

Holographic wavefront sensors represent the new generation of wavefront sensors (WFS), i.e. of the devices, providing the real-time measurement of wavefront shape and its deviation from some ideal sphere or plane. Traditionally such measurements are carried out with the use of computation-abundant techniques like interferometery or “traditional” WFS (Shack-Hartmann, curvature sensor etc.), all of which are implementing the multi-megapixel CCD, CMOS and other matrix sensors. In many cases – for instance, in the case of atmospheric adaptive optics, when distortions’ refreshment time is ~1 ms, the use of such devices requires processing of many GByte of data per second.

The principle of the holographic WFS performance is much simpler (see, for instance, [1]). Special holographic filters select from the incident wavefront this or that specific component (e.g., this or that Zernike polynomial, this or that vortex structure etc.). Such a holographic filter output represents the plane wave signal, whose direction or, in another design, intensity is proportional to the depth of Zernike polynomial etc. The response time of such a device is determined only by the response time of photodetector, which can, in principle, fill into mcs or even ns time range.

However, until recently, the use of such devices was tantalized by the severe noise of the overlapped holograms. Our recent theoretical and experimental studies, which are reported in the paper, have shown that the use of Fourier holography promise the solution of these problems and thus open the way to implementation of real holographic WFS in various applied systems.

The holographic WFS have some features which differ them from the more traditional Shack-Hartmann WFS. In particular, they are more appropriate for the use in systems dealing with the monochrome light rather than the polychrome one. In addition, the energy losses in such WFS are comparatively higher than in the traditional WFS. So one can say that the laser systems are the best field of application for the holographic WFS. In our paper we consider some possible applications of such WFS in high peak or high average power lasers and laser systems.

References

1. V. Venediktov, *Photonics*, 2016, **1**(55), 132–143.

HIGH-PEAK AND HIGH-AVERAGE POWER YB-DOPED FEMTOSECOND LASERS FOR VARIOUS APPLICATIONS

V. Yashin[1], B. Lee[2], B. Jeong[2], J. Yang[2], E. Sall[2], S. Chizhov[2], and **G.H. Kim[2]**

[1] JSC "S.I. Vavilov State optical Institute", St. Petersburg, Russia
vyashin@yandex.ru
[2] Advanced Medical Device Research Division, Korea Electrotechnology Research Institute, Ansan-si, Republic of Korea

Abstract. A diode-pumped, ultrafast Yb:KGW laser system utilizing chirped-pulse amplification (CPA) in a dual-slab regenerative amplifier (RA) with spectral shaping of seeding pulse from a master oscillator (MO) has been developed. A train of compressed pulses with pulse length of 181 fs, repetition rate up to 500 kHz, and average power exceeding 15 W after compression and pulse picker was achieved.

Femtosecond laser sources based on Yb-doped laser materials became a promising tool for various scientific, technological and industrial applications including femtosecond lasers. Energetic optical pulses with femtosecond pulse lengths and hence ultra-high focused intensities in the range 10^{12} to 10^{16} Wcm^{-2} are capable for ablating a wide range of materials including metals, semi-conductors, ceramics, polymers, biological tissue and dielectrics. Femtosecond laser ablation has been demonstrated to be a powerful tool for various technologies [1]. Due to rapid energy delivery, the laser-plasma interaction is avoided and heat-affected zones in the irradiated targets are strongly localized with minimal residual damage. This allows generation of well-defined microstructures with high quality and reproducibility [1].

Among Yb-media ytterbium tungstates (Yb:KYW/Yb:KGW) crystals exhibit an attractive set of parameters that makes it one of the best choices for high-power fs lasers operating around 1 μm. Thwe bandwidth of Yb:KGW/Yb:KYW is sufficient for amplification of sub-200 fs pulses but typical pulse length on the output of Yb:KYW amplifier system is limited by the level 300–400 fs primarily due to gain narrowing [2]. A promising method to reduce the effect of gain narrowing and to increase the effective gain bandwidth is to combine laser media with separated gain maxima and to overlap broadband gain. Using Yb:KYW crystals with different orientation of crystallographic axes (the so-called Ng and Np cut orientation) this approach can be realized [3, 4]. Another way for increasing gain bandwidth is using special spectral filters introducing controlled losses at maximum of gain spectrum [2, 4].

In this report we present a combination of these approaches to a double-slab regenerative amplifier. Each slab is pumped separately, which enables additional possibility to control gain. Furthermore as a seed source, we used a high-power master oscillator based on Np-cut Yb:KYW crystal with output pulse length about 100 fs and central wavelength agreed well with spectral gain profile of regenerative amplifier. A highly efficient stretcher and compressor based on single transmitted diffraction grating are used for stretching and recompressing initial pulses after master oscillator.

The laser was realized as a chirped-pulse amplification (CPA) system [4]. The system consists of a femtosecond master oscillator (MO), a common module of stretcher and compressor based on a single diffraction grating, a spectral shaper based on Lyot filter, and a dual-slab regenerative amplifier (RA) with combined gain spectra. The system also includes two Faraday isolators: one for isolation of MO against leaking amplified pulses and the other for extraction of laser pulses from the system after RA. A train of compressed pulses with pulse length of 180 fs, repetition rate up to 500 kHz, and average power exceeding 15 W after compression and pulse picker was achieved.

References

1. F. Dausinger, F. Lichtner, and H. Lubatschowski, *Femtosecond Technology for Technical and Medical Applications*. Berlin: Springer, 2004.
2. C.P.J. Barty, G. Korn, F. Raksi, C. Rose-Petruck, J. Squier, A.-C. Tien, K. R. Wilson, V.V. Yakovlev, and K. Yamakawa, *Opt. Lett.*, 1996, **21**(3), 219–221.
3. A. Buettner, U. Buenting, D. Wandt, J. Neumann, and D. Kracht, *Opt. Express*, 2010, **18**(21), 21973–21980.
4. G.H. Kim, J. Yang, S.A. Chizhov, E.G. Sall, A.V. Kulik, V.E. Yashin, D.S. Lee, and U. Kang, *Opt Express*, 2012, **20**(4), 3434–3442.

LASER-ION ACCELERATION BOOSTED BY MULTI-PICOSECOND PULSES

A. Yogo[1,2], K. Mima[1,3], N. Iwata[1], S. Tosaki[1], A. Morace[1], Y. Arikawa[1], S. Fujioka[1], H. Nishimura[1], Y. Sentoku[1], T. Johzaki[4], K. Matsuo[1], N. Kamitsukasa[1], S. Kojima[1], H. Nagatomo[1], M. Nakai[1], H. Shiraga[1], M. Murakami[1], S. Tokita[1], J. Kawanaka[1], N. Miyanaga[1], K. Yamanoi[1], T. Norimatsu[1], A. Sagisaka[5], S.V. Bulanov[5], H. Sakagami[6], K. Kondo[5], and **H. Azechi[1]**

[1] Institute of Laser Engineering, Osaka University, Suita, Osaka, Japan
[2] PRESTO, Japan Science and Technology Agency, Kawaguchi, Saitama, Japan
[3] The Graduate School for the Creation of New Photon Industries, Hamamatsu, Shizuoka, Japan
[4] Graduate School of Engineering, Hiroshima University, Higashi-Hiroshima, Japan
[5] Kansai Photon Science Institute, National Institutes for Quantum and Radiological Science and Technology, Kizugawa, Kyoto, Japan
[6] National Institute for Fusion Science, Gifu, Japan

Abstract. We demonstrate that high-contrast multi-picosecond pulses are advantageous for proton acceleration. By extending the pulse duration from 1.5 to 6 ps with fixed laser intensity of 10^{18} Wcm^{-2}, the maximum proton energy is improved more than twice (from 13 to 33 MeV). The proton energies observed are discussed using a plasma expansion model newly developed that takes the electron temperature evolution beyond the ponderomotive energy in the over picoseconds interaction into account.

Laser-ion acceleration in a relativistic intensity (10^{18}–10^{21} Wcm^{-2}) regime is governed by the absorption mechanism of laser energy into electrons. Recently, it has been reported [1–3] that the plasma electrons are heated beyond the typical scaling low, ponderomotive potential [4] through the nonlinear motion of the electrons. In this paper, we experimentally investigate the electron heating in multi-picosecond (ps) time scale and its effect on the ion acceleration [5].

The experiment was performed using LFEX laser of ILE, Osaka University, which provides four beams of 1.5-ps (FWHM) duration. By setting intervals of 1.5 ps between the four pulses, we obtained duration-extended pulses of 3 ps, when we use two beams, and 6 ps, as the longest case using the four pulses. The maximum laser energy in total is 1 kJ (250 J for each laser beam), and the intensity is $2.3{\cdot}10^{18}$ Wcm^{-2} on the target. Note the focal spot diameter is set to be 60 μm (FWHM), which makes a beneficial effect on the electron recirculation around the target, mentioned later. The accelerated ions were analyzed by a Thomson Parabola (TP) at the normal direction of the target rear surface. The electrons generated from the plasma were also measured by an electron spectrometer (ESM) located at the target rear side. The angle between the TP and the ESM was 20.9°.

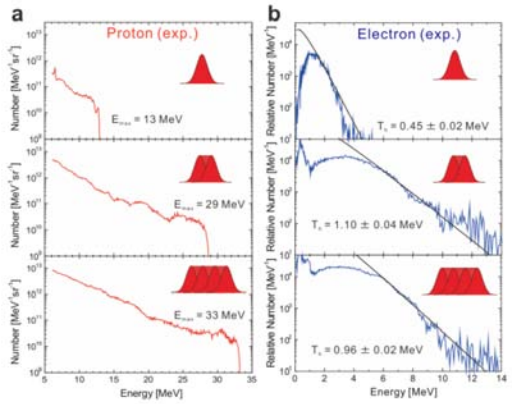

Fig. 1: The energies of protons (a) and electrons (b), temporally evoluting at the fixed laser intensity.

As shown in Fig. 1(b), when we expand the pulse duration of the laser from 1.5 ps to 3 ps at the fixed laser intensity, the electron temperature is drastically enhanced up to 1.1 MeV, which clearly exceeds the ponderomotive potential around 0.2 MeV for the laser intensity of $2.3{\cdot}10^{18}$ Wcm^{-2}. In addition, the proton energy, analyzed simultaneously with the electron temperature, reaches 29 MeV at 3 ps and saturates around 30 MeV at 6 ps. Our PIC simulation reveals that electrons continue to recirculate between the front and rear sides of the foil plasma during the laser incidence and are heated through the nonlinear mechanism depending on the laser pulse duration. The details will be discussed in the presentation.

Acknowledgements

This work was funded by Grant-in-Aid for Scientific Research (Nos 25420911 and 26246043) of MEXT, A-STEP (No. AS2721002c), JST and PRESTO, JST. The authors thank the technical support staff of ILE for their assistance with the laser operation, target fabrication and plasma diagnostics. This work was supported by the Collaboration Research Program of the National Institute for Fusion Science (Nos NIFS15KUGK096, NIFS12KUGK057) and ILE, Osaka University (2015A1-32).

References

1. A.J. Kemp & L. Divol, *PRL*, 2012, **109**, 1–5.
2. A. Yogo, *et al*., *PPCF*, 2016, **58**, 025003.
3. S.V. Bulanov, *et al*., *PoP*, 2015, **22**, 063108.
4. S. Wilks, *et al*., *PRL*, 1992**, 69**, 1383–1386.
5. A. Yogo *et al*., *Sci. Rep*., 2017, **7**, 42451.

THERMAL-DYNAMICAL ANALYSIS OF FEMTOSECOND LASER DAMAGE OF OPTICAL COATINGS

Yu. Zhao[1], J. Shao[1], Sh. Liu[1], M. Zhu[1], J. Chen[2], and **Zh. Wu[2]**

[1] Shanghai Institute of Optics and Fine Mechanics, Chinese Academy of Sciences, Shanghai, P R China
yazhao@siom.ac.cn
[2] ZC Optoelectronic Technologies, Ltd, Hefei, P R China

Abstract. Laser-induced damage behaviors of the HR coatings and chirped mirrors (CMs) are studied by 800 nm – 38 fs lasers. Interestingly, a circular blister feature appears in the CMs at a wide range of laserfluence. The damage threshold was simulated by multi-wavelength ionization, and an adiabatic expansion model of ideal gas is adopted to illustrate the formation dynamics of blisters. The evolution of blisters can be explained by partial evaporation of the film and a subsequent gas expansion, driving the bulging of the film stack up to the stress limit, where the blister fractures. According to this model, the energy absorption ratio of blisters increases monotonously with increasing laser fluence.

Nb_2O_5/SiO_2 dielectric stacks, 800 nm 0°AOI high-reflector (HR) and two kinds of optimized chirped mirrors (CMs), were fabricated by dual ion-beam sputtering technology on fused silica substrate. Sample damage was studied by single 800 nm – 38 fs Ti:S lasers. For the HR, CM1 and CM2, the LIDTs are 0.36, 0.11 and 0.08 J/cm^2, respectively. All the samples showed the blister damage morphologies at near LIDT. Blister of HR only exist for narrow fluence range (30–40% above LIDT), and that of CMs for wide range (2X-10X above LIDT). (Fig. 1).

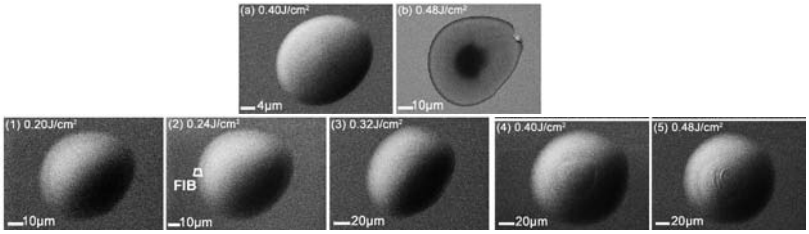

Fig. 1. Blister morphologies for HR (*up*) and CM (*down*)

In order to analyze the evolution law of blisters with the increasing of laser fluence, the blister volume as a function of laser fluence and the normalized blister amplitude (δ/h) as a function of normalized blister radius (R/h) are given in Fig. 2a and Fig. 2b, respectively.

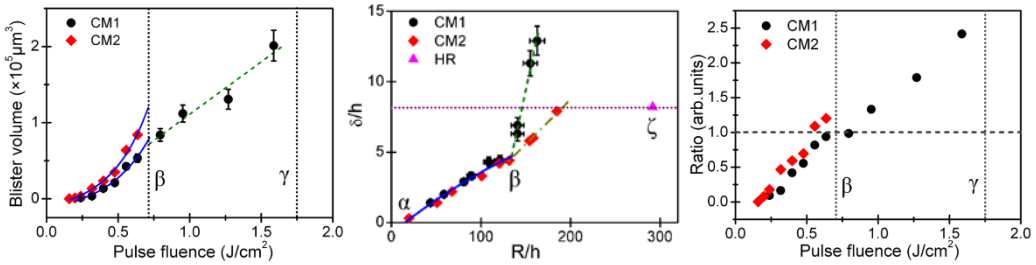

Fig. 2. (a) Blister volume as a function of laser fluence, (b) Normalized blister amplitude as a function of blister radius, and (c) Energy absorption ratio of blisters as a function of laser fluence

The adiabatic expansion model of ideal gas are as follows:

1) Irradiation and energy conservation: $Q_a = V_1\rho[c_p(T_b - T_0) + \Delta H]$

2) Absorption and ideal gas formation: $p_1 = (\rho / M_{mole})R_{mole}T_b$

3) Blister formation induced by film bulging due to adiabatic expansion of ideal gas: $V_2 = V_1(p_1 / p_2)^{1/k}$

4) Blister fracture at the stress limit: $p_2 = \dfrac{4h\delta\sigma_{in}}{R^2} + \dfrac{8h\delta^3 E}{3R^4(1-\upsilon)}$

The simple adiabatic expansion model is reasonable to elucidate the blister evolution in the CMs before the appearance of focal spot confinement effect (Fig. 2c). Meanwhile, this model in this format was not suitable to explain the blister formation when the incident laser fluence was more than 0.7 J/cm^2 (β position).

UPGRADE OF THE FRONT-END OF THE PETAWATT LASER COMPLEX PEARL

A.S. Zuev[1], **A.A. Kochetkov**[1], **A.A. Shaykin**[1], and **I.V. Yakovlev**[1,2]

[1] IAP RAS, Nizhny Novgorod, Russian Federation
[2] UNN, Nizhny Novgorod, Russian Federation

Abstract. The front-end of the laser system PEARL is currently upgraded at IAP RAS. A femtosecond Ti:Sapphire oscillator and a new stretcher will be installed aimed at reducing output pulse duration and increasing stability and reliable operation of the laser system.

The PEtawatt pARametric Laser system (PEARL) based on optical parametric chirped pulse amplification (OPCPA) [1] is operating at the Institute of Applied Physics of the Russian Academy of Sciences (IAP RAS). Stretched radiation with central wavelength of 1250 nm generated by a femtosecond Cr:Forsterite laser is injected into the first parametric amplification cascade, and radiation with central wavelength of 910 nm generated as a result of three-wave interaction is directed to the subsequent amplification cascades and to the compressor. As radiations of different wavelengths are stretched and compressed in the system, a unique prism-grating stretcher [2] is used to provide the condition of phase matching.

Currently, we are upgrading the front-end of the laser system PEARL. The Cr:Forsterite oscillator is to be replaced by a Ti:Sapphire oscillator radiating a broadband pulse with central wavelength of 910 nm. Thus, signal radiation that will be amplified in the subsequent cascades and then compressed in a compressor will be injected into the first cascade of the parametric amplifier. The condition of phase matching at compression and stretching of a broadband pulse will be fulfilled in a traditional scheme including Treacy compressor and stretcher with image inversion ensuring positive dispersion of group velocity.

The duration of the laser pulses at the femtosecond oscillator output has been measured to be 56 fs. According to the measured spectrum it was clear that the pulse is not Fourier-transform-limited. In the experiment we compensated the nonlinear phase by means of chirped mirrors. The measured pulse duration was 30.3 fs.

We present comparative analysis of the Martinez stretcher [3] and the Offner triplet stretcher [4] with parabolic and spherical mirrors from the viewpoint of their use in the PEARL system. Numerical computations show that the fourth-order phase dispersion will be minimal in the Offner triplet stretcher with spherical mirrors.

A single-grating Offner stretcher has been developed. A laser beam propagating through the stretcher hits the diffraction grating 8 times. To separate the input and output beams horizontal and vertical roof-mirrors are used. The stretcher's transmission band is 92 nm, pulse duration after stretcher reaches 0.6 ns. The stretcher characteristics are chosen so that the introduced nonlinear phase should correspond to the compressor phase: angle of incidence on the diffraction grating ~43°, effective base 133.7 cm, grating groove density 1200 l/mm.

The stretcher has been adjusted, including control of radiation propagation through the Offner triplet, control of the tilt angle and vertical deflection of diffraction grating grooves, as well as alignment of the vertical and horizontal roof-mirrors by means of autocollimator. After the stretcher, the radiation has been directed to the compressor to be compressed to 36 fs.

The broad spectrum of the radiation generated by a Ti:Sapphire laser, as well as the experiments on compressing pulses in a compressor enable us to expect that a duration not more than 37 fs will be obtained after compression of the amplified pulse, which will significantly increase the peak power of laser complex PEARL.

References

1. V.V. Lozhkarev, *et al.*, "Compact 0.56 Petawatt laser system based on optical parametric chirped pulse amplification in KD*P crystals", *Laser Phys. Lett.*, 2007, **4**, 421.
2. G.I. Freidman, I.V. Yakovlev, "New stretcher scheme for a parametric amplifier of chirped pulses with frequency conversion", *Quantum Electron.*, 2007, **37**, 147.
3. O.E. Martinez, "3000 Times Grating Compressor with Positive Group Velocity Dispersion: Application to Fiber Compensation in 1.3-1.6 um Region", *IEEE J. Quantum Electron.*, 1987, **23**, 59.
4. A. Offner, U.S. Patent 3,748,015; 1973.

International Symposium

TOPICAL PROBLEMS OF NONLINEAR WAVE PHYSICS

Nonlinear Phenomena in the Atmosphere and Ocean

Chairs

Henrik Dijkstra, Utrecht University, The Netherlands
Alexander Feigin, Institute of Applied Physics RAS, Russia
Juergen Kurths, Potsdam Institute for Climate Impact Research, Germany
Evgeny Mareev, Institute of Applied Physics RAS, Russia
Vladimir Rakov, University of Florida, USA

Program Committee

Alexander Babanin, University of Melbourne, Australia
Cristian Franzke, University of Hamburg, Germany
Andrey Gritsun, Institute of Numerical Mathematics RAS, Russia
Sergey Gulev, Institute of Oceanology RAS, Russia
Sergey Kravtsov, University of Wisconsin, Milwaukee, USA
Igor Mokhov, Institute of Atmospheric Physics RAS, Moscow
Colin Price, Tel Aviv University, Israel
Yuliya Troitskaya, Institute of Applied Physics RAS, Russia

DYNAMICALLY CONSISTENT PARAMETERIZATION OF MESOSCALE EDDIES

P. Berloff

Department of Mathematics, Imperial College London, London, United Kingdom
p.berloff@imperial.ac.uk

Abstract. Dynamically consistent, novel parameterization of oceanic mesoscale eddies is proposed, implemented and tested in the double-gyre ocean circulation model. The results are encouraging and providing the framework for further refinements of the parameterization.

This work aims at developing a framework for dynamically consistent parameterization of mesoscale eddy effects for use in non-eddy-resolving ocean circulation models. The proposed eddy parameterization framework is successfully tested on the classical, wind-driven double-gyre model, which is solved both with explicitly resolved vigorous eddy field and in the non-eddy-resolving configuration with the eddy parameterization replacing the eddy effects. The parameterization locally approximates transient eddy flux divergence by spatially localized and temporally periodic forcing, referred to as the *plunger*, and focuses on the linear-dynamics flow solution induced by it. The nonlinear self-interaction of this solution, referred to as the *footprint*, characterizes and quantifies the induced cumulative eddy forcing exerted on the large-scale flow. We find that spatial pattern and amplitude of the footprint strongly depend on the underlying large-scale and the corresponding relationships provide the basis for the eddy parameterization and its closure on the large-scale flow properties. Dependencies of the footprints on other important parameters of the problem are also systematically analyzed. The parameterization utilizes the local large-scale flow information, constructs and scales the corresponding footprints, and then sums them up over the gyres to produce the resulting eddy forcing field, which is interactively added to the model as an extra forcing. The parameterization framework is implemented in the simplest way, but it provides a systematic strategy for improving the implementation algorithm.

References

1. P. Berloff, "Dynamically consistent parameterization of mesoscale eddies". Part I: Simple model. *Ocean Modelling*, 2015, **87**, 1–19.
2. P. Berloff, "Dynamically consistent parameterization of mesoscale eddies". Part II: Eddy fluxes and diffusivity from transient impulses. *Fluids*, 2016. **1**, 22, doi:10.3390/fluids1030022.

BIDIRECTIONAL LEADER DEVELOPMENT NUMERICAL SIMULATION

A.A. Bulatov, A.A. Syssoev, S.S. Davydenko, and **D.I. Iudin**

Institute of Applied Physics of the Russian Academy of Sciences, Nizhny Novgorod, Russia
iudin@ipfran.ru

Abstract. An advanced 3D numerical model of lightning bidirectional leader initiation and development is presented. The key features of the model include probabilistic branching, streamer-to-leader transition, bidirectional propagation, non-zero internal electric field, simultaneous growth of multiple branches, physical timing, and, for the first time, probabilistic propagation field threshold and channel decay. Also, the proposed model takes into account the differences between initiation and propagation fields of positive and negative streamer discharges.

Our current understanding of macroscopic processes in lightning flashes is based on the concept of bidirectional leader propagation, proposed by Kasemirin in 1960 and explored further by Mazur and Ruhnke. The key concepts of bidirectional leader theory are that shortly after initiation, positive and negative leaders are two ends of one "tree" which move simultaneously into opposite polarity charges. The recently suggested advanced 3D numerical model of lightning development [1] was applied to studying the lightning initiation through the relatively unknown type of discharge, called fast positive breakdown, that is the cause of high-power discharges known as narrow bipolar events or compact intracloud discharges.

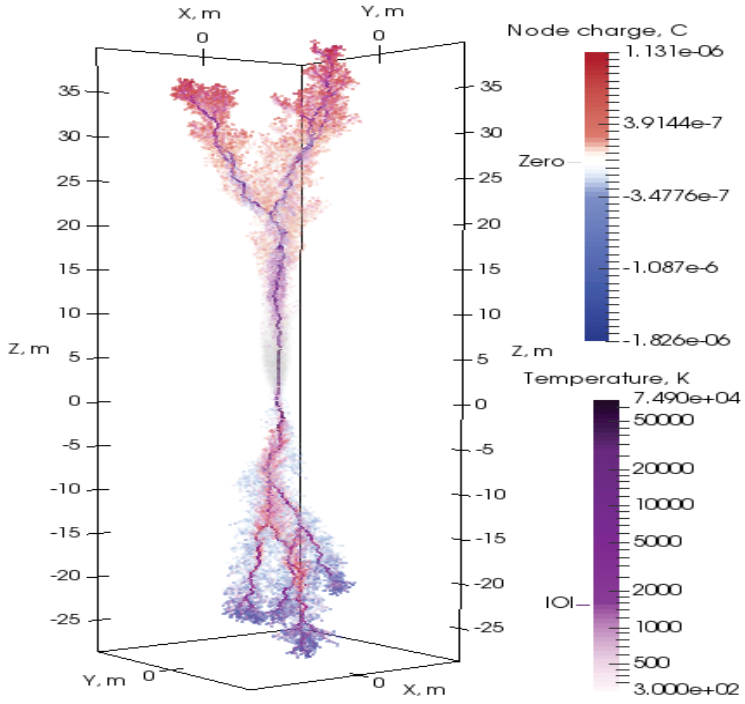

Fig. 1. Lightning bidirectional leader development final stage.
Two color bars are used to represent node charge and channel temperature distribution

Acknowledgements

This work was supported in part by the Government of the Russian Federation (contract No. 43414.B25.31.0023) and by the Russian Foundation for Basic Research (projects Nos 15-01-06612, and 16-05-01013).

References

1. D.I. Iudin, V.A. Rakov, E.A. Mareev, S.S. Davydenko, F.D. Iudin, and A.A. Syssoev, "Advanced numerical model of lightning development: Application to studying the role of LPCR in determining lightning type", *J. Geophys Res*., 2017, 2016JD026261R.

MACROSCOPIC PHYSICAL MODELS FOR LIGHTNING LEADERS AND RETURN STROKES

M. Chen, M.K. Chan, S. Cai, and **Y. Du**

The Hong Kong Polytechnic University, Hong Kong, China
mingli.chen@polyu.edu.hk

Abstract. Cloud-to-ground lightning includes downward flashes and upward flash. A downward flash usually starts in clouds with a downward-going leader followed by a return stroke. An upward flash usually starts from a tall grounded structure with an upward-going leader followed by one or more downward leader/return stroke processes. It is the leader process that determines the path of the return stroke. In the following, we firstly present a macroscopic physical model for upward leaders from tall grounded structures and then a leader-return stroke coupled model for return stroke current and electromagnetic field calculations.

A Macroscopic Model for Upward Leader from Tall Structure

In this session we present a macroscopic physical model that is able to simulate an upward leader initiated from a tall grounded object under thunderclouds. Based on a tri-layer leader channel structure and the energy conservation law, a new equation for estimating the upward leader propagation speed is proposed. Equations for modeling other physical parameters, such as the leader line charge density, leader core radius, leader corona sheath radius, leader current, leader electric field and leader conductance, are also proposed. Besides, a set of initiation and survival criteria for a steady self-initiated upward leader from a tall grounded object is suggested. Based on the suggested criteria and the proposed model, the critical corona and charge amount as well as the minimum height for successful initiation of an upward positive leader (UPL) from a tall grounded object are evaluated and discussed. The model is then used to investigate the general properties of UPLs self-initiated from tall grounded objects with and without the effect of corona space charge layer near the ground under different thunderstorm conditions. The modeling results can well explain the leader properties observed in literature. The model is further tested with two set of experiment data and very promising results are obtained.

A Macroscopic Model for Lightning Return Stroke

A return stroke is usually preceded by a downward leader process. It is the preceding downward leader that governs the return stroke property. Besides, the return stroke property evolves with height and time. These two aspects, however, are not well-addressed in most existing return stroke models. In this section, we present a leader-return stroke coupled model based the time domain electric field integral equation (TD-EFIE), which is a growth and modification of Kumar's microscopic model. The model is further extended to simulate the optical and electromagnetic emissions of a return stroke by introducing a set of equations relating the return stroke and conductance to the optical and electromagnetic emissions. With a presumed leader initiation potential, the model can then simulate the temporal and spatial evolution of the current, charge transfer, channel size and conductance of the return stroke, furthermore the optical and electromagnetic emissions. The model is tested with different leader initiation potentials ranging from –10 to –140 MV, resulting in different return stroke current peaks ranging from 2.6 to 209 kA with different return stroke speed peaks ranging from 0.2 to 0.8 speed of light and different line optical power peaks ranging from 4.76 to 248 MW/m. The larger of the leader initiation potential, the larger of the return stroke current and speed. Both the return stroke current and speed attenuate exponentially as it propagates upward. All these results are qualitatively and quantitatively consistent with those reported in literature.

Acknowledgements

The works leading to this paper is funded by The Hong Kong Polytechnic University and Research Grant Council of Hong Kong (Grants:PolyU5123/12E and PolyU152652/16E).

ENHANCED PARTICLE FLUXES DURING THE DECAY STAGE OF ARAGATS THUNDERSTORMS

A. Chilingarian

Yerevan Physics Institute, Yerevan, Armenia, chili@aragats.am
National Research Nuclear University MEPhI, Moscow, Russia
Space Research Institute of RAS, Moscow, Russia

Abstract. The bulk information on particle fluxes correlated with thunderstorm can be used to better understand the electrical structure of thunderclouds. The only very specific electric configuration of the lower part of the cloud can support the sustainable acceleration of the electrons. Our analysis is based on the thunderstorm data from the Aragats Mountain in Armenia, 3200 m above sea level Varieties of particle detectors located at Aragats Space Environmental Center are registering neutral and charged particle fluxes correlated with thunderstorms, so-called Thunderstorm Ground Enhancements (TGEs, [1]). In the present paper, we relate particle fluxes to the electrical structure of thunderclouds, namely, to an end-of-storm oscillation (EOSO) during the storm's decay phase.

Classification of the TGE events according to the near-surface electrical field disturbances. Examining disturbances of the near surface electric field during enhancement of particle fluxes (TGE), we outline the following most typical patterns accompanied by TGE [3]: electric field reversal from positive to negative; electric field reversal from negative to positive; electric field's abrupt decreases and multiple disturbances of a near-surface electrical field. Usually all four types of TGE events were accompanied with precipitation and lightning occurrences; however, sometimes lightning and rain are missing. During a multicellular storm in New Mexico, the electric field at the ground beneath a thunderstorm often exhibits an EOSO during the storm's decay phase in which field typically undergoes several polarity changes over a period of 30–75 minutes [2]. The pattern of the electric field changes in New Mexico is very close to the one we classify as a fourth type of the TGE initiation scenario (multiple disturbances of the field, see [3]. Therefore we identify this type of TGE initiation on Aragats also as EOSO, see Figs. 1 and 2.

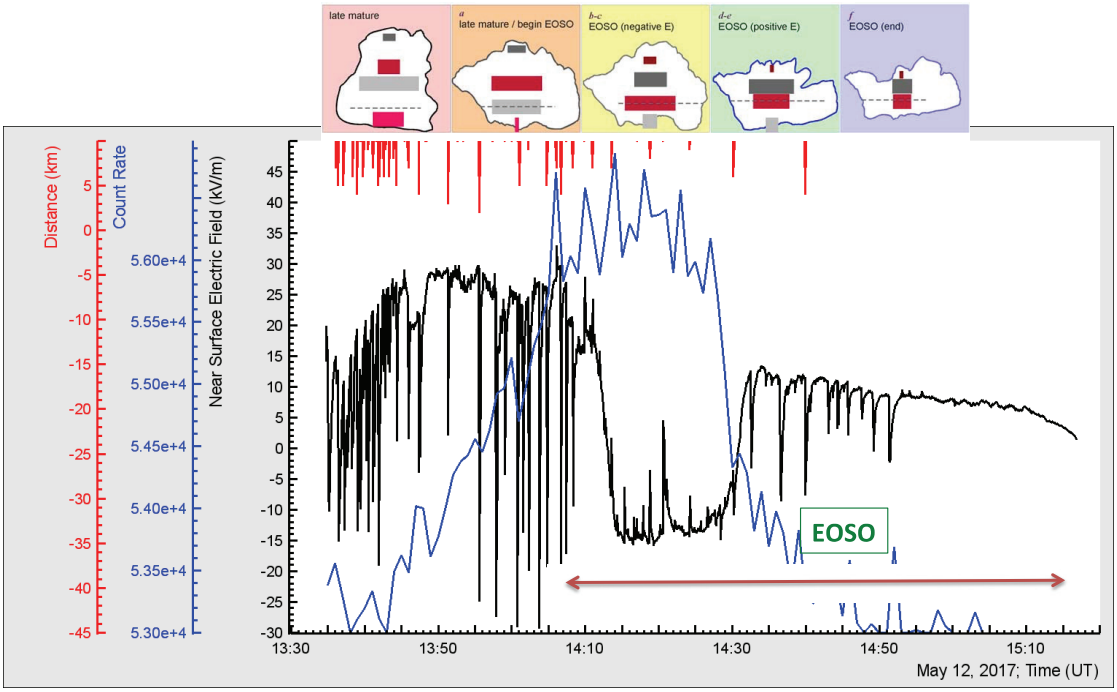

Fig. 1. Conceptual representation of the end-of-storm oscillation (EOSO) scenario. Red lines in upper part of panel show distance to lightning; black curve – disturbances of the near-surface electric field; blue – the particle 1-minute count rate measured by the 3-cm thick plastic scintillator. Boxes in the five upper panels are approximately 6 km in altitude (3.5–9.5 km) and 10 km in the horizontal dimension (taken from [2])

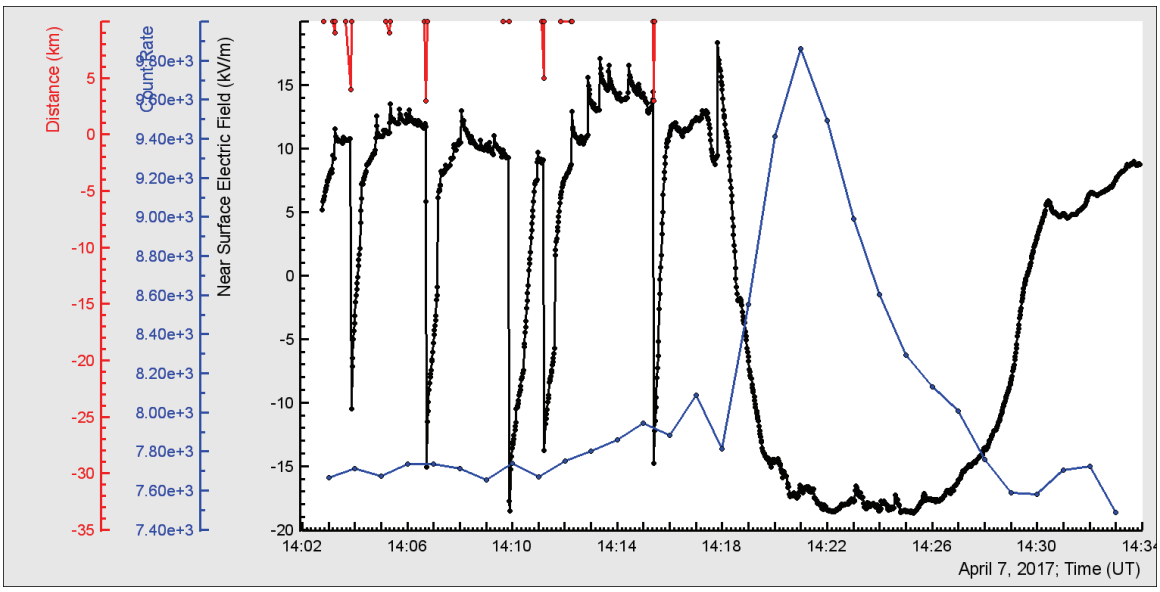

Fig. 2. Electrostatic field (black) and distance to lightning (red) was measured by electric mill EFM-100 located on 13 m long mast in the center of Aragats research station; Particle flux was measured by 3 cm thick plastic scintillator of the STAND3 detector (combination 1000 – low energy particles). Observed TGE does not relate to lightning flash – large negative electric field is required only

References

1. A. Chilingarian, A. Daryan, K. Arakelyan, *et al*., *Phys. Rev. D,* 2010, **82,** 043009.
2. T.C. Marshall, M. Stolzenburg, P.R. Krehbiel, *et al*., *JGR,* 2009, **114,** D02209.
3. A. Chilingarian and H. Mkrtchyan, *Physical Review D,* 2012, **86**, 072003.

THE RUNAWAY BREAKDOWN PARTICLES SPECTRA OBTAINED JUST BEFORE THE LIGHTNING STROKE

A. Chilingarian

Yerevan Physics Institute, Yerevan, Armenia, chili@aragats.am
National Research Nuclear University MEPhI, Moscow, Russia
Space Research Institute of RAS, Moscow, Russia

Abstract. The newly emerging field of high-energy physics in the atmosphere involves measuring as many parameters as possible, such as particle fluxes, electric-field disturbances, radio emissions from the thunder-clouds, and meteorological environments. The intensity of the Thunderstorm Ground Enhancement (TGE, [1]) analyzed in the present study was observed by 3 cm thick scintillators with a sensitive area of 1 m. sq. operated in the particle counter mode. The energy release spectra of gamma ray and electron content of avalanches unleashed in the cloud were measured by the 60 cm thick plastic scintillator equipped with veto system for charged particles. We estimate the height of cloud and compare the estimated maximal energy of electrons and gamma rays with simulated ones [2]. It is the first report on Runaway Breakdown (RB) electrons spectrum measured just before the lightning stroke.

Super TGE event occurred on October 4

The particle count rate of 3cm thick outdoor plastic scintillator reaches a maximum of 1808 counts per second at 14:12:14 (fine weather mean value is 525 counts per second, MSD ~23). The TGE particle flux enhancement was enormous; reaching 340% at the maximum flux second which is equivalent to the p-value of 53σ, see insert in fig. 1. The height of the cloud is calculated by the measured "spread" parameter – the difference between the surface temperature and the dew point. The clouds were very low above the earth's surface ~ 25 m. The maximal energy of the electrons was 20 MeV (Fig. 1), in the construction matter above the detector electron losses was estimated to be ~ 18 MeV. Thus we come to the maximal energy of electrons leaving the cloud 25 m above detector to be 40–45 MeV in good agreement with estimates obtained in [2]. The maximal energy of gamma rays equals 35 MeV also well agreed with "parent" electrons energy. Thus, this event (first reported in [3]) is a direct proof of the runaway avalanche process in the thunderclouds.

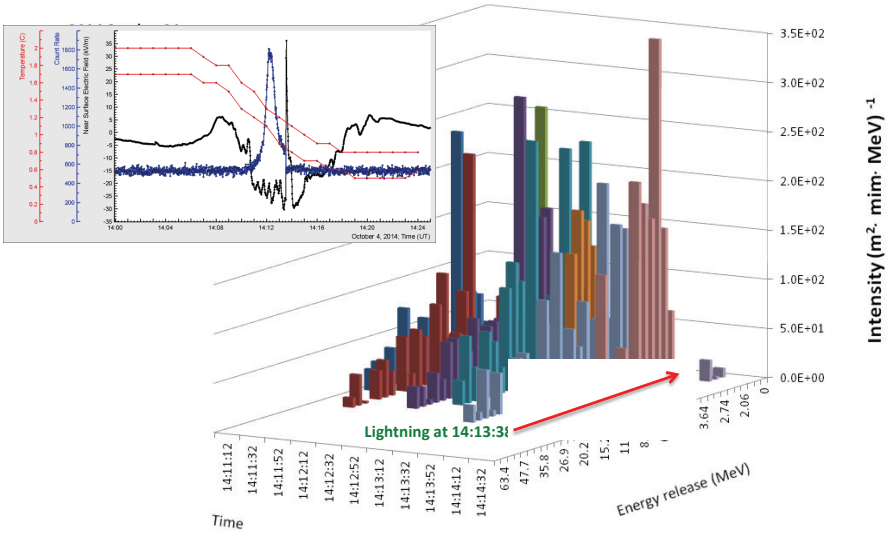

Fig. 1. Differential Energy spectra of RB electrons; in the insert 1-sec time series of count rate of 3 cm thick plastic scintillator (blue), near surface electric field (black) and temperature and dew point used for the spread calculation (red)

References

1. A. Chilingarian, A. Daryan, K. Arakelyan, *et al.*, *Phys. Rev. D,* 2010, **82,** 043009.
2. A. Chilingarian, B. Mailyan and L. Vanyan, *Atmospheric Research,* 2012, **114–115**, 1–16.
3. A. Chilingarian, G. Hovsepyan, Y. Khanikyanc, *et al.*, *EPL,* 2015, **110** 49001.

EFFECTS OF THE NORTH ATLANTIC THERMOHALINE CIRCULATION ON CLIMATE VARIABILITY AND ARCTIC CLIMATE CHANGE PROJECTIONS BASED ON THE COMBINED SCENARIO

N.A. Diansky[1,2,4], **I.V. Solomonova**[3], **A.V. Gusev**[1], and **T.Yu. Vyruchalkina**[3]

[1] Institute of Numerical Mathematics of the RAS, Moscow, Russia, nikolay.diansky@gmail.com
[2] N.N. Zubov State Oceanographic Institute, Moscow, Russia
[3] Institute of Water Problems of the RAS, Moscow, Russia
[4] Moscow State University, Moscow, Russia

Abstract. The combined scenario of climate change assessment is proposed based on the composition of "greenhouse" and "cyclic" effects. The forecast of atmospheric characteristics was made for 2010–2071 using the CORE datasets for 1948–2009. The prognostic run was made with the OGCM INMOM on reproducing thermohaline circulation and sea ice in the Atlantic and Arctic Oceans for 1948–2071. The interconnections were investigated amongst climate processes of the North Atlantic and Arctic.

Period of warming (1915–1949 and 1971 till now) and cooling (1950–1970) were observed in the global climate, which were more noticeable in the Arctic compared to other latitudes. These climate oscillations (Panin, 2009; Panin et al., 2015; Panin and Diansky, 2015; Semenov, 2008) are not well reproduced in simulations with the IPCC Earth system models (IPCC AR-4, 2013). Data on temperature measurements and reconstructions in the north polar zone (Panin, 2009) evidence on the significant contribution of cyclic (about 60 years) temperature variations in the Arctic climate. In (Gusev and Diansky, 2014) it was noted that in the temperature intrasecular regional (e.g. in the North Atlantic and Atlantic sector of the Arctic), hemispherical and global changes, as well as in the changes of ice content in the Arctic seas, the variations of periods about 60-yrs are noticeably presented, which are typical for the Atlantic Multidecadal Oscillation (AMO), connected, in turn, to the ocean thermohaline circulation. This behavior of the climate change allowed G.N. Panin (2009) to propose the simple approximation of climate changes based on composition of "greenhouse" and "cyclic" effects. The "greenhouse" climate change implies the ones caused by the external anthropogenic. In turn, the "cyclic" climate changes imply the internal climate oscillations in the joint system atmosphere-ocean-land. At the same time, it was supposed that the main frequency of the strongest cyclic climate oscillations fits to the period of 60 years, and the greenhouse climate changes are presented as a linear trend. It was shown that the boost of Arctic ice melting in the 70's–90's of the XX century is concerned with the variations in AMO and intensity of Atlantic meridional circulation. The latter reflects the climate changes in the heat flux from the North Atlantic surface to the Atmospere in midlatitudes (Gusev and Diansky, 2014).

The combined scenario of the climate change assessment is proposed based on the composition of the "greenhouse" and "cyclic" effects. On this basis, the forecast was made of near-surface characteristics of atmosphere circulation for 2010–2071 using the CORE data for 1948–2009 (Large and Yeager, 2009). Using the data, the prognostic run was made with the OGCM INMOM on reproducing thermohaline circulation and sea ice in the Atlantic and Arctic Oceans for 2010–2071. The interconnections were investigated amongst climate processes of the North Atlantic and Arctic. This approach allows one to describe temperature growth due to greenhouse gas emission and climate variability. The proposed combined scenario presents the possible cooling in the Arctic and decrease of navigation period in the North Sea Route for the next 15–20 years.

Acknowledgements

The main part of the research is supported by RFBR, grants №15-05-03127, 15-05-07539, 16-05-00534. Investigations of climate changes in the North Atlantic and Arctic is supported by RSF, grant 17-17-01295.

References

1. G.N. Panin, *Doklady Earth Sciences*, 2009, **427,** 397–402.
2. G.N. Panin, T.Yu. Vyruchalkina, I.V. Solomonova, *Fund. and Appl. Climatology*, 2015, **1**, 183–210.
3. G.N. Panin, N.A. Diansky, *Doklady Earth Sciences*, 2015, **462**(2), 217–222.
4. V.A. Semenov, *Doklady Earth Sciences*, 2008, **418**(1), 106–109.
5. A.V. Gusev and N.A. Diansky, *Izvestiya, Atmospheric and Oceanic Physics*, 2014, **50**(1), 3–15.
6. W. Large, S. Yeager, *Clim Dyn*, **33**, 341–364.

OBSERVATION AND TESTING PLATFORM FOR LIGHTNING TO THE 350M-TALL SHENZHEN METEOROLOGICAL TOWER

Y. Du[1], **M. Chen**[1], and **Yu. Yang**[2]

[1] The Hong Kong Polytechnic University, Kowloon, Hong Kong, ya-ping.du@polyu.edu.hk
[2] Shenzhen Meteorological Service Center, Shenzhen, China

Abstract. A 360m-tall meteorological gradient observation tower has been constructed in Shenzhen, China. As the tall tower is subject to lightning strikes, it has been considered to be a perfect site for measuring lightning-related parameters and carrying out field tests for lightning protection. A series of observation systems have been installed at the site for measuring natural lightning currents, electromagnetic fields, lightning electromagnetic impulses, lightning optical phenomena. It is expected that the results obtained from measurement and observation at the site will further enhance the research on lightning discharge characteristics, lightning effects on electronic/electrical systems, bonding and grounding for lightning protection.

Introduction

The steel-structure tower is 350 m tall with a 6m-height working platform on its top. It is erected on the RC cap supported with 4 pillars. The steel structure above the ground is stabilized with a large number of stay cables, which attach the cable foundations on the ground. These stay cables have a span of up to 550 m on the ground level. The tower foundation and stay cable foundations serve as a grounding system together with bonding conductors buried under the ground. An air termination conductor is provided on the tower top for lightning interception. Current probes are installed on tower for measuring the return stroke current on the top as well as on the ground. The currents on the stay cables as well as the bonding conductors are planned to measure as well. The data collected by sensors or probes are sent to data acquisition systems either via an optical link or a wireless communication link. Lightning optical observation is made by using a camera system set on the roof of a remote building. The system includes one high-speed camera and one normal-speed camera, and is capable of reconstructing the development of upward and downward leaders, as well as return strokes. Tower outriggers are provided onfive work platforms constructed along the tower. Sensors or probes are mounted on these outriggers to continuously monitor both meteorological parameters and electric fields or space charge distribution. Together with the data from lightning detection system, early waring or prediction on lightning and thunderstorm becomes more accurate.

Fig. 1. Steel Tower

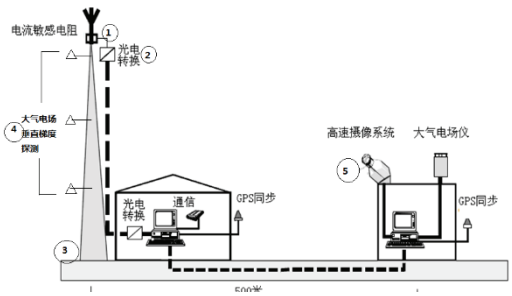

Fig. 2. Current measurement system

The observation system installed on the tower will operate in this coming thunderstorm season. The system will be continuously updated and more meaningful data will be collected for further study of lighting physics and further improvement of ligthning protection.The facilities installed at the site will be also intended to use for the development of new technologies and new methods for lightning protection in electric power industry, telecommunications industry, lightning protection of high-rise buildings.

Acknowledgements

The work leading to this paper was supported by grants from the Hong Kong Polytechnic University, and Research Grants Council of the HKSAR (Project No. 152044/14E and 152038/15E).

SUPERMODELING THE CLIMATE SYSTEM TO CAPTURE SELF-ORGANIZED CRITICALITY

G.S. Duane[1,2], **M.-L. Shen**[1], and **N.S. Keenlyside**[1]

[1] Geophysical Institute, University of Bergen, Bergen, Norway, gregory.duane@colorado.edu
[2] Department of Atmospheric and Oceanic Sciences, Univ. of Colorado, Boulder, CO, USA

Abstract. Differences in climate projections among state-of-the-art models can be resolved by connecting the models in run times. Even when the models err on the same side of truth, a supermodel formed from state-of-the-art climate models can compensate for the error, seemingly by learning to connect the constituent models (with positive connections) so as to mimic realistic *critical* behavior, as in blocked-zonal regime vacillation or the El Niño cycle.

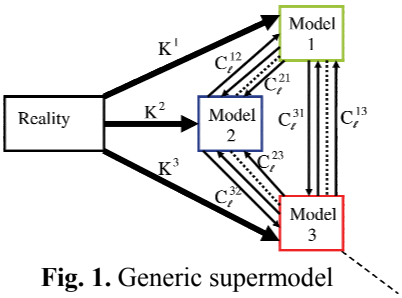

Fig. 1. Generic supermodel as it assimilates data from reality

Averaging climate model outputs results in improvement as compared to any individual model output, so averaged re-initializations as models run also seem appropriate. Continual re-initialization, e.g. by inter-model nudging, gives synchronization among models, which form a single "supermodel" (Fig. 1) [1, 2]. Supermodels can surpass output averages in a hierarchy of model types: simple ODE's [1, 2], quasigeostrophic models [3], simple primitive equation models [4], and full climate models [5].

Even when the imperfect constituent models all differ from reality *in the same way, with errors that have the same sign,* supermodeling can succeed. If the learned connection coefficients have negative values, such non-monotonic behavior can be easily explained. But we find improvement even with positive connections.

A hypothesis is that the inter-scale interactions typically drive the system to a critical state, differing from the mean states of all the constituent models in the same way. The critical state is not reached by guessing the model parameters. But when the supermodel is trained on real data, in a relatively small space of connection coefficients, it is possible to capture the criticality, as illustrated in a hierarchy of models: With quasigeostrophic models, a supermodel can learn blocked/zonal regime vacillation, starting from constituent models with no blocking. With versions of the mid-complexity SPEEDO model that exhibit similar bias patterns of the same sign relative to truth, a supermodel with positive coefficients can reduce the bias (unlike an *ex post facto* average). In a supermodel formed from two COSMOS full-complexity climate models by coupling the two atmosphere models to a common ocean through weighted fluxes [5], a normal Intertropical Convergence Zone (ITCZ) and El Nino cycle are reproduced, while the constituent models exhibit a double ITCZ and/or permanent El Niño (Fig. 2).

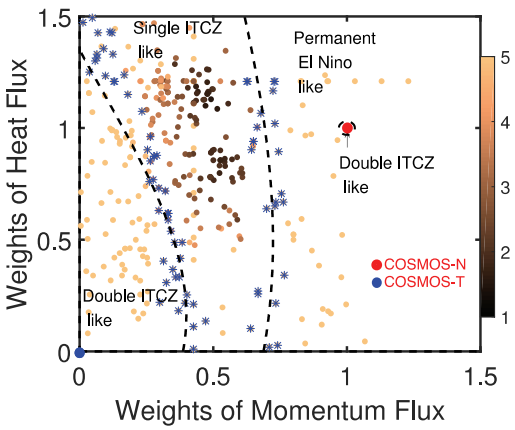

Fig. 2. Phases of the COSMOS supermodel. Optimal weights (dark circles) give critical El Niño and single ITCZ, unlike the constituent models COSMOS-N and COSMOS-T

Acknowledgements

The research reported here was supported by EC Grants 648982 and 658602.

References

1. L.A. Van den Berge, F.M. Selten, W. Wiegerinck, and G.S. Duane, *Earth Syst. Dynam.*, 2011, **2**, 161–177.
2. G.S. Duane, *Entropy,* 2015, **17**, 1701–1733.
3. G.S. Duane, http://www.sumoproject.eu/downloads/SUMO_WP3_yr2_deliverable3_2.pdf.
4. F.M. Selten, F.J. Schevenhoven, and G.S. Duane, in preparation for Focus Issue of *Chaos*, 2017, **27**(12).
5. M.-L. Shen, *et al.*, *Geophys. Res. Lett.*, 2016, **43**(1), 359–366.

LABORATORY MODELING OF HIGH-ALTITUDE DISCHARGES

A.A. Evtushenko, A.V. Strikovskiy, M.E. Gushchin, and **S.V. Korobkov**

Institute of Applied Physics RAS, Nizhny Novgorod, Russia
a_evtushenko@inbox.ru

Abstract. Sprites and jets are very interesting geophysical phenomena in the Earth's atmosphere, but their laboratory modeling is difficult. The vertical size of discharges is 30–40 km, this means that pressure at the top and at the bottom of discharges differs by about 2 orders of magnitude. Creation of such a high pressure difference in laboratory is a difficult technical problem. We create pressure difference up to 8 times and present our first results.

The vacuum chamber 1.9 m long and 1.6 m in diameter was taken for laboratory modeling. We create pressure difference between electrodes in the impulse regime (air valve is opened for 30 ms). Distribution of the pressure along the vacuum chamber at different points between the electrodes after air injection is shown in Fig. 1 (left). After 12.5 ms the pressure near the left electrode is the highest and near the right electrode it is still without perturbation. This is a time delay between air injection and voltage supply to the electrodes in all our experiments.

Photos of discharges in the absence and presence of air injection are shown in the first line of Fig. 1 (right). All other parameters are the same in both experiments: the background pressure is equal to 0.35 Torr, the discharge gap is equal to 81 cm, the voltage is equal to 6 kV. The negative electrode is seen as a peak on the left, the positive electrode is a disk on the right. Diffuse discharge forms in the whole volume between the electrodes without air injection. During the injection of the air the pressure difference between the electrodes reaches 8 times. Streamer discharge is formed in the left part of the discharge. The maximum current is about 700 A in both experiments, the discharge duration is no more than 20 μs. During increasing of the pressure, the diffuse part of the discharge becomes smaller and we have streamer discharge in the whole volume when the basic pressure is equal to 1.31 Torr.

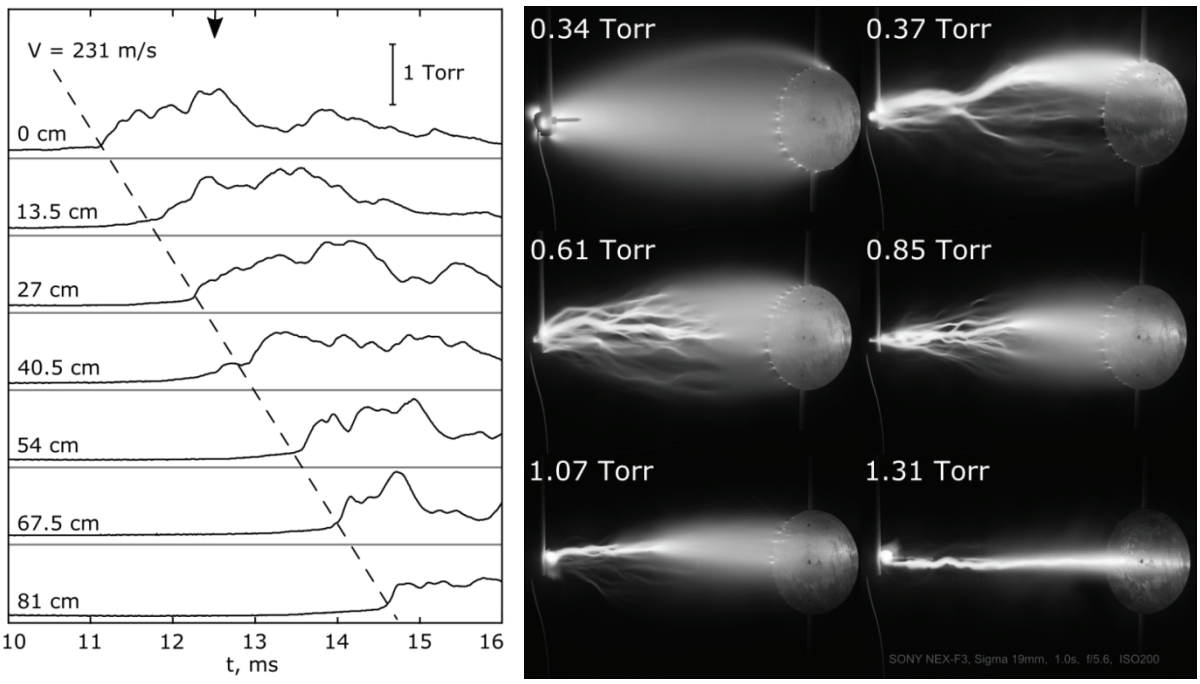

Fig. 1. Distribution of the pressure along the axis of the vacuum chamber during the impulse air injection (*left*). Discharges in the vacuum chamber with different basic pressure with impulse injection of air (except picture p = 0.34 Torr) (*right*)

Acknowledgements

This work was partially supported by the RFBR (project № 17-05-01182).

EMPIRICAL APPROACH TO MODELING & PROGNOSIS OF CLIMATE SYSTEMS

A.M. Feigin, D.N. Mukhin, E.M. Loskutov, A.S. Gavrilov, and **A.F. Seleznev**

Institute of Applied Physics of the Russian Academy of Sciences, Nizhny Novgorod, Russia
feigin@appl.sci-nnov.ru

The underlying objectives of the empirical (data-driven) approach are, first, derivation of as much as possible information about system function and, second, use this knowledge for prognosis of the system evolution. The talk focuses on the current problems posed by empirical modeling of climate:

i. Extraction of spatio-temporal pattern from climate data and their application to study functional features of climate systems;

ii. Construction of empirical models that are optimal for short-term prognosis of climate characteristics;

iii. Empirical prediction of critical transition.

Three interrelated talks of the same authors are devoted to detailed discussions of these issues.

REDUCED NONLINEAR DATA-DRIVEN PROGNOSTIC CLIMATE MODEL CONSTRUCTION

A.S. Gavrilov, A.F. Seleznev, D.N. Mukhin, E.M. Loskutov, and **A.M. Feigin**

Institute of Applied Physics of the Russian Academy of Sciences, Nizhny Novgorod, Russia
gavrilov@ipfran.ru

Abstract. A Bayesian approach to construction of evolution operator from high-dimensional climate data is presented. The method incorporates two key steps: (1) obtaining the time series of hidden variables by empirical reduction of observed data and (2) constructing an evolution operator for the hidden variables using the reduction of its time-embedded phase space. Both of these steps take into account the most significant spatial and temporal couplings which are crucial in climate system. Predictions of global SST field as well as particular climate indices (e.g. El Nino index) are demonstrated.

Nowadays an instantly growing amount of real-measured data leads to an increasing role of empirical methods in climate system modeling and forecasting. Meanwhile, construction of a data-driven prognostic model (evolution operator model) using universal approximating functions is statistically justified only if the dimension of its phase space is small enough. Therefore it is necessary to use efficient dimensionality reduction methods capable of capturing key dynamical properties of the system from observed data.

In our previous papers [1–3] a Bayesian approach to data-driven stochastic evolution operator retrieval from high-dimensional time series was elaborated which uses artificial neural networks as approximating functions. An important thing for this approach to perform well is construction of good model phase space embedding by choosing appropriate variables for the model. Here we further develop the method and incorporate into it two key steps: (1) obtaining the time series of hidden variables by empirical reduction of observed data and (2) constructing an evolution operator for the hidden variables using the reduction of its time-embedded phase space. Both of these steps should take into account the most significant spatial and temporal couplings which are crucial in climate system. Concerning this question, in we discuss and compare application of such reduction methods as standard empirical orthogonal function decomposition and recently developed nonlinear dynamical mode decomposition [4, 5] in the suggested method.

To performance of the approach is demonstrated on the predictions of global SST field as well as particular climate indices (e.g. El Nino index) taken form reanalysis.

Acknowledgements

The study is supported by the Government of the Russian Federation (agreement #14.Z50.31.0033 with the Institute of Applied Physics of RAS).

References

1. Y.I. Molkov, E.M. Loskutov, D.N. Mukhin, & A.M. Feigin, "Random dynamical models from time series", *Physical Review E*, 2012, **85**(3), 36216. http://doi.org/10.1103/PhysRevE.85.036216.
2. D. Mukhin, E. Loskutov, A. Mukhina, A. Feigin, I. Zaliapin, & M. Ghil, "Predicting Critical Transitions in ENSO Models". Part I: Methodology and Simple Models with Memory. *Journal of Climate*, 2015, **28**(5), 1940–1961. http://doi.org/10.1175/JCLI-D-14-00239.1.
3. D. Mukhin, D. Kondrashov, E. Loskutov, A. Gavrilov, A. Feigin, & M. Ghil, "Predicting Critical Transitions in ENSO models". Part II: Spatially Dependent Models. *Journal of Climate*, 2015, **28**(5), 1962–1976. http://doi.org/10.1175/JCLI-D-14-00240.1.
4. Gavrilov, A., Mukhin, D., Loskutov, E., Volodin, E., Feigin, A., &Kurths, J. (2016). Method for reconstructing nonlinear modes with adaptive structure from multidimensional data. Chaos: An Interdisciplinary Journal of Nonlinear Science, 26(12), 123101. http://doi.org/10.1063/1.4968852.
5. Mukhin, D., Gavrilov, A., Feigin, A., Loskutov, E., &Kurths, J. (2015). Principal nonlinear dynamical modes of climate variability. Scientific Reports, 5, 15510. http://doi.org/10.1038/srep15510.

INSTABILITY CHARACTERISTICS OF BLOCKING REGIMES IN A SIMPLE QUASI-GEOSTROPHIC ATMOSPHERIC MODEL

A. Gritsun[1] and **V. Lucarini**[2]

[1] Institute of Numerical Mathematics, Moscow, Russia, e-mail: asgrit@mail.com
[2] Department of Mathematics and Statistics, University of Reading, UK

Abstract. In this paper we study statistics and instability characteristics of blocking events in the three layer quasi-geostrophic model of atmosphere by Marshall and Molteni. It is shown that the model is able to produce reasonable longitudinal distribution of blocking events as well as simulate blocking events with lifetime of up to 40 days. Using covariant Lyapunov exponents we analyze predictability of onset, duration and decay of blockings. It is shown that on the average blockings are less predictable than the system trajectory with the blocking onset and decay being the most unstable. We verify our findings by looking at unstable periodic orbits (UPOs) of the system representing blocking and nonblocking events. It was found that blocking UPOs have 20% more positive (unstable) Lyapunov exponents than the system trajectory, and 50% larger leading exponent.

Blockings, weather regimes determining localized and persistent departures from the approx. zonal jet stream (Rossby 1951), are relevant parts of the atmospheric low frequency variability. The problem of blocking formation and predictability has been mathematically studied using low dimensional dynamical systems (DS), where the blocked/zonal conditions are fixed points, and the transitions result from the noise due to higher frequency variability (see Dymnikov 1990). In this study we adopt the viewpoint of modern DS theory suggesting that a blocking (or any other specific state of the system) occurs when the system is close to the specific UPO (Auerbach et.al. 1986). The DS theory tools like Lyapunov exponents (LEs) then allow for quantifying the anomalous predictability of blockings (Schubert and Lucarini 2016).

In this study we are considering blocking events modeled by the quasi-geostrophic model of the atmosphere (Marshall and Molteni 1993). To simplify calculation of UPOs and CLVs we reduced its dimension to T18 and increased boundary layer dissipation and hyper diffusion. For this model we were able to calculate 2500 UPOs some of them representing blocking events. The model gives reasonable longitudinal statistics of blocking events (Fig. 1a, green) that could be recovered using UPOs (Fig. 1a, black). The CLVs growth rate along system trajectory measures the average system predictability (Fig. 1b, green). However, during the onset and decay of the blocking (2 days before and after the blocking event) this quantity jumps by about 10%. Blocking itself is about 5% more unstable than the trajectory on the average with respect to this measure. This result is supported by the fact that UPOs having the form of blockings are considerably more unstable than "nonblockings" in terms of Kaplan-Yorke dimension (Fig. 1c), the value of the leading unstable Lyapunov exponent and dimension of unstable manifold.

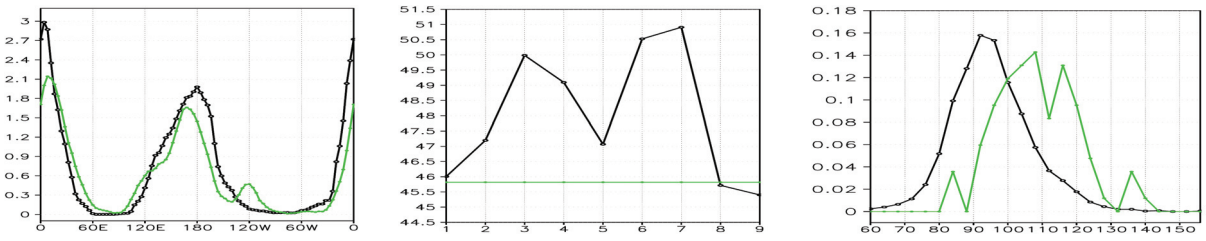

Fig. 1. (a) Longitudinal distribution of 5day+ blockings obtained from UPOs (black) and system trajectory (green) (% of the total). (b) Total average unstable CLVs growth rate for 5day+ blocking event: 6-4day, 4-2d and 2-0d before blocking event (black "1", "2" and "3"); during first, middle and final 1/3rd of the blocking ("4","5" and "6"); 2-0d, 4-2d and 6-4d after the blocking event ("7", "8" and "9"); attractor average CLVs growth rate (green). (c) Distribution of Kaplan-Yorke dimension for blocking UPOs (green) and all UPOs (black)

Acknowledgements

The work was supported by the Russian Foundation for Basic Research project no. 16-55-12015.

References

1. C.G. Rossby, *J. Chin. Geophys. Soc*., 1951, **2**, 1–13.
2. V.P. Dymnikov, *Sov. J. Numer. Anal. Math. Modelling*, 1990, **5**, 189–198.
3. D. Auerbach, P. Cvitanovic, J.-P. Eckmann, G. Gunaratne, I. Procaccia, *Phys. Rev. Lett*., 1987, **58**, 2387–2389.
4. S. Schubert, V. Lucarini, *Q.J.R. Met. Soc*., 2016, **142**, 2143–2158.
5. J. Marshall, F. Molteni, *J. Atmos. Sci*., 1993, **50**, 1792–1818.

NUMERICAL INVESTIGATIONS OF WAVE-INDUCED MIXING IN UPPER OCEAN LAYER

C. Guan[1] and **D. Zhu**[2]

[1] Ocean University of China, Qingdao, China, clguan@ouc.edu.cn
[2] Ocean University of China, Qingdao, China

Abstract The General Ocean Turbulence Model is employed to investigate the effects of the three mechanisms concerning wave-induced mixing. The numerical investigation is carried out for three turbulence closure schemes with the observational data from OSC Papa station and wave data from ECMWF. The mixing enhancement by various waved-induced mixing mechanisms is investigated and verified.

The upper ocean layer is playing an important role in ocean-atmosphere interaction. The typical characteristics depicting the upper ocean layer are the sea surface temperature (SST) and the mixed layer depth (MLD). So far, the existing ocean models tend to over-estimate SST and to under-estimate MLD [1], due to the inadequate mixing in the mixing layer, which is owing to that several processes related mixing in physics are ignored in these ocean models. The mixing induced by surface gravity wave is expected to be able to enhance the mixing in the upper ocean layer, and therefore the over-estimation of SST and the under-estimate of MLD could be improved by including wave-induced mixing [2] (Craig & Banner, 1994). The wave-induced mixing could be accomplished by the physical mechanisms, such as wave breaking [3] (Sun *et al*., 2008), wave-induced Reynolds stress [4–5] (Qiao *et al*., 2004; Babanin *et al*., 2009), and wave-turbulence interaction [6] (Huang *et al*., 2011). The General Ocean Turbulence Model (GOTM) is employed to investigate the effects of the three mechanisms concerning wave-induced mixing. The numerical investigation is carried out for three turbulence closure schemes, say, *k-epsilon*, *k-omega* and Mellor-Yamada (1982), with the observational data from OSC Papa station and wave data from ECMWF. The mixing enhancement by various waved-induced mixing mechanisms is investigated and verified.

Acknowledgements

This work is financially supported by the National Natural Science Foundation of China (No. U1406401).

References

1. L.H. Kantha and C.A. Clayson, *J. Geophys. Res*., 1994, **99**, 25235–25266.
2. P.D. Craig and M.L. Banner, *J. Phys. Oceanogr*., 1994, **24**, 2546–2559.
3. Q. Sun, C. Guan, and J. Song, *Chin. J. Oceanol. Limnol*., 2008, **26**(1), 9–13.
4. F. Qiao, Y. Yuan, Y. Yang, *et al*., *Geophys. Res. Lett*., **31**, L11303, doi:10.1029/2004GL019824.
5. A.V. Babanin, A. Ganopolski, and W.R.C. Phillips, *Ocean Modelling*, 2009, **29**, 189–197.
6. C. Huang, F. Qiao, and Z. Song, *et al*., *J. Geophys. Res*., **116**, C01007, doi:10.1029/2010JC006320.

THE ROLE OF ATMOSPHERE INTRASEASONAL VARIABILITY IN EL NINO FORCING

D.Yu. Gushchina[1] and **B. Dewitte**[2]

[1] Moscow State University, Faculty of Geography, Moscow, Russia, dasha155@mail.ru
[2] Laboratoire d'Etudes en Géophysique et Océanographie Spatiale, Toulouse, France

Abstract. The atmosphere disturbances of intraseasonal timescale (ITV) – Madden-Julian Oscillation (MJO) and equatorially Rossby waves (ER) were shown to participate in El Niño triggering with distinct contribution to conventional and Modoki El Niño. The ENSO/ITV relationship demonstrates a drastic seasonal dependence and is sensitive to the state of the tropical Pacific, particularly it is strongly correlated to the PDO and IPO index. This may have implication for ENSO seasonal forecasts.

El Niño Southern Oscillation (ENSO) is one of the most prominent patterns of climate variability at interannual scale. The ENSO evolution and mechanisms have been widely investigated, nevertheless key questions remain unresolved, in particular regarding its irregularity and strong diversity of the events. Here the focus is on the atmospheric disturbances of intraseasonal timescale (ITV) and its relationship with the two types of El Niño, the Eastern Pacific (EP) or conventional El Niño and Central Pacific (CP) or Modoki El Niño. The dominant intraseasonal mode in tropics – the Madden-Julian Oscillation (MJO) and convectively coupled equatorial Rossby waves (ER) were in particular shown to be tightly related to ENSO through their relationship to episodes of westerlies that can trigger downwelling intraseasonal Kelvin waves, a precursor to El Niño onset. The ENSO/ITV relationship exhibits a marked seasonal dependence: MJO induces the oceanic Kelvin wave in March-April preceding El Niño in the western Pacific while the ER intensification in June-July in the central Pacific serves the maintenance for Kelvin wave dissipating along its way through the Pacific. It is shown that MJO and ER activity have a distinct characteristics during the two types of El Niño. The most striking difference is that during conventional El Niño the MJO and equatorial Rossby waves activity are precursor signals, acting as a trigger of the event while during Modoki El Niño they contribute also to its persistence once it has appeared.

The ENSO/ITV relationship does not only demonstrate a drastic seasonal dependence, it is also sensitive to state of the tropical Pacific, which has implication for ENSO seasonal forecasts. Our results suggest that ER and MJO predictive score relative to the both types of El Niño drastically changes on the decadal timescale, with ER/ENSO relationship experiencing less low-frequency modulation than MJO. The predictive score of MJO relative to EP El Niño (to lesser extent to CP El Niño) is strongly correlated to the PDO and IPO index, suggesting the former is closely related to the mean zonal SST gradient across the equatorial Pacific: reduced (enhanced) SST gradient associated to positive (negative) IPO and PDO favors (decreases) the MJO contribution to the development of El Niño (Fig. 1). ER predictive score relative to ENSO is less dependent on decadal modulation of Pacific mean state, but ER/CP relationships is likely to be modulated by the meridional mode in the Pacific**.**

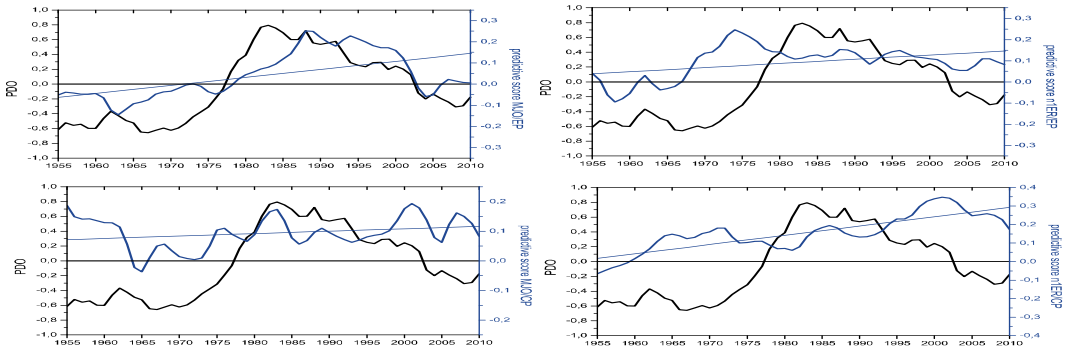

Fig. 1. The PDO index (black curve) and predictive score index (blue curve) calculated for EP El Niño (*upper panel*) and CP El Niño (*bottom panel*) for MJO (*left column*) and Rossby waves (*right column*). The trend of predictive score is indicated by blue line

Acknowledgements

The work is supported by RFBR, grant No.15-05-06693.

PREDICTION OF THE LIGHTNING ACTIVITY USING RADAR DATA AND MACHINE LEARNING TECHNIQUE

N.V. Ilin[1], F.A. Kuterin[1], and **C. Price[2]**

[1] Institute of Applied Physics RAS, Nizhny Novgorod, Russia, ilyin@appl.sci-nnov.ru
[2] Tel Aviv University, Tel Aviv, Israel

Abstract. Machine learning technique (MLT) is a very powerful mathematical tool with well-developed software infrastructure which is widely used for different applications, including geophysics and geosciences in general. In this paper MLT was applied for prediction of the lightning activity (mainly cloud-to-ground flashes) based on the WWLLN data training set and Doppler meteoradar records. Experiments with different classifiers showed sufficient prediction properties of MLT applicable for nowcasting of lightning activity.

Introduction

Prediction of lightning activity is a very complex and ambitious goal. The main difficulties of the lightning forecast are related to different-scale (both in space and time) phenomena and various physical processes (mechanics, hydrodynamics, electrodynamics, etc.). It is extremely difficult to unite such difficulties within the framework of one model.

There are some attempts to predict lightning activity using indirect nonelectrical parameters [1–5] and direct electric field calculations [6]. However, these algorithms don't provide sufficient accuracy.

In this paper, we suggested a new approach for prediction of lightning based on machine learning technique, namely supervised learning for binary classification.

Binary classification for the lightning prediction task

The binary classification is the task of classifying the elements of a given set into two groups on the basis of a classification rule. We consider the lightning activity in a map domain 200 × 200 km centered in the Nizhny Novgorod city. We divide the map domain into cells 4 × 4 km with height of 10 km. The radar reflectivity of each 1 km height layer (dBz0, dBz1, dBz2, dBz3, dBz4, dBz5, dBz6, dBz7, dBz8, dBz9, dBz10) at the time moment T for an individual cell creates a set of elements for classification.

The set of features (0 or 1) for each cell is created by WWLLN flashes in the follow way: if at least one flash is registered in the selected cell, during 20 minutes time period: (T-20 min) – (T), the feature is equal to one, otherwise, the feature is equal to zero.

Supervised learning for binary classification

There is a large number of binary classifiers: nearest neighbours, support vector machine, logistic regression, random forest and many others. The most successful classifier for our goal, the Multi-layer Perceptron classifier, was chosen based on the results of comparison with the experiments. The training set was assembled by the analysis of a very intense thunderstorm on June 1–2, 2015. During the 2nd of June WWLLN recorded about 2500 flash events for the selected map domain.

We analyzed three forecasting strategies:

One reference point strategy. It means that we analyzed radar data for time T only.

Reference point plus one support past point strategy. We analyzed radar data for time: T and T-10 min.

Reference point plus two support past points strategy. We analyzed radar data for three time steps: T, T-10 min, T-20 min.

Results of prediction

In order to assess the quality of the binary classifiers prediction, the following measures are used: *prediction score*, *recall score* and *F1 score*. The quality of the prediction can be carried out using gradations for all scores:

$0 < x < 0.5$ – bad prediction
$0.5 < x < 0.6$ – weak prediction
$0.6 < x < 0.8$ – good prediction
$0.8 < x < 1$ – overfitting or very simple correlation

Below are the results of the forecast for different strategies:

First strategy: prediction = 0.55, recall = 0.38, F1 = 0.45
Second strategy: prediction = 0.56, recall = 0.45, F1 = 0.50
Third strategy: prediction = 0.54, recall = 0.46, F1 = 0.50

The results show than the machine learning can't find strong correlation between radar and WWLLN data for 4 × 4 km cell. On the one hand, this can be explained by the complexity of the problem, on the other hand, by the insufficient accuracy of the positioning of flashes by WWLLN.

Let's apply the proposed approach for the 8 × 8 km cell:

First strategy: prediction = 0.61, recall = 0.63, F1 = 0.62
Second strategy: prediction = 0.64, recall = 0.64, F1 = 0.64
Third strategy: prediction = 0.77, recall = 0.76, F1 = 0.77

As can be seen from the results, the quality of the prediction has greatly increased for the 8 × 8 km cell, which really shows insufficient accuracy of WWLLN.

Thus, the machine learning technique shows good prediction properties, applicable for nowcasting of lightning activity using meteoradar data.

Example of the MLT prediction

Figure 1 shows comparison the third strategy prediction for 4 × 4 km cell for real case thunderstorm (b) and WWLLN data (a) for 24 may 2015 (events were not included in the training set).

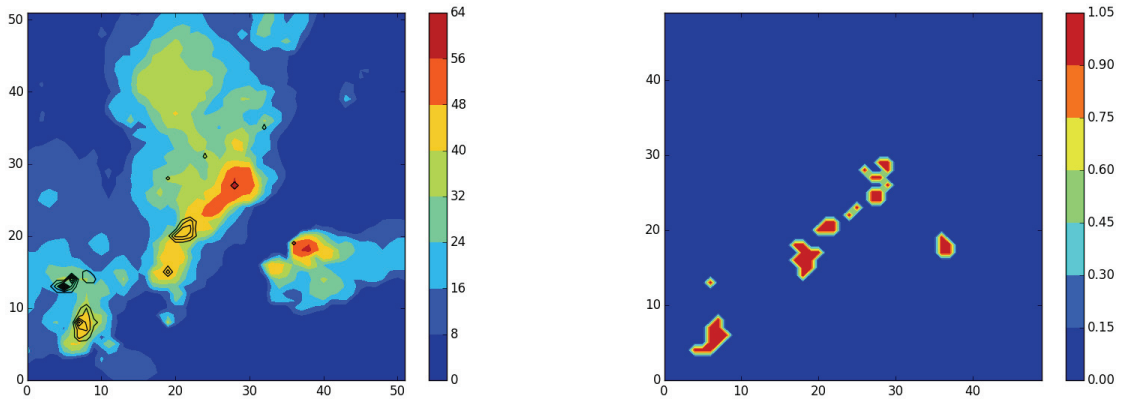

Fig. 1. Comparison of a real case thunderstorm on May 24, 2015 - 15:50 (a) and the MLT prediction (b). Colormap in fig (a) shows maximum of radar reflectivity, black lines show WWLLN flashes. Red aria in fig (b) shows the most possible areas of lightning activity predicted by MLT.

Acknowledgements

This research was supported by the Russian Science Foundation (Contract No. 16-17-00132).

References

1. W.A. Petersen and S.A. Rutledge, *J. Geophys. Res.: Atmos.,* 1998, **103**(D12), 14025–14040.
2. D.J. Cecil, S.J. Goodman, D.J. Boccippio, E.J. Zipser, and S.W. Nesbitt, *Mon. Weather Rev.*, 2005, **133**(3), 543–566.
3. W.A. Petersen, H.J. Christian and S.A. Rutledge, *Geophys. Res. Lett.*, 2005, **32**(14), L14819.
4. Y. Yair, B. Lynn, C. Price, V. Kotroni, K. Lagouvardos, E. Morin, A. Mugnai and M. del C. Llasat, *J. Geophys. Res.*, 2010, **115**(D4), D04205.
5. B. Lynn and Y. Yair, *Adv. Geosci.*, 2010, **23**, 11–16.
6. S.O. Dementyeva, N.V. Ilin, and E.A. Mareev, *Izv. Atmo. Ocean. Phys.,* 2015, **51**, 186–192.

DYNAMICS AND TRANSPORT CHARACTERISTICS OF ZONALLY ELONGATED TRANSIENTS IN THE OCEAN

I. Kamenkovich[1], **M. Rudko**[2], and **I. Rypina**[3]

[1] RSMAS, University of Miami, Miami, USA, ikamenkovich@miami.edu
[2] RSMAS, University of Miami, Miami, USA, mrudko@miami.edu
[3] Woods Hole Oceanographic Institution, Woods Hole, USA, irypina@whoi.edu

Abstract. Oceanic flows with mesoscale eddies (length scale of 10–100 km) contain zonally-elongated large-scale transients (ZELTs) that can be detected in pressure anomalies as a spectral peak corresponding to long zonal and short meridional length scales, or as leading Empirical Orthogonal Functions. These patterns are generated and maintained by transient nonlinear forcing, associated with mesoscale eddies, and are, therefore, nonlinear phenomena. ZELTs play a key role in anisotropic material transport and in large-scale tracer distributions.

Zonally elongated large-scale transients (ZELTs)

Multiple, predominantly zonal oceanic flows are detected in the ocean from the altimetry-based velocity estimates [1]. Most of these flow patterns are non-stationary and do not span the entire ocean basin. We refer to this type of flow structures as zonally-elongated large-scale transients (ZELTs) and define them in pressure anomalies as a spectral peak corresponding to long zonal and short meridional length scales (Fig. 1), or as leading Empirical Orthogonal Functions (EOFs).

Fig. 1. ZELTs in QG channel flows. (*left*) Wavenumber spectrum of the perturbation streamfunction (time-mean removed). X- and y-axis are the zonal and meridional wavenumber (non-dimensionalized by the Rossby deformation radius R_d). Note the presence of the anisotropic peak at long zonal wavelengths. (*right*) Leading EOF

Dynamics and transport characteristics of ZELTs

Analysis in a quasi-geostrophic zonal flow demonstrates that dynamics of ZELTs is governed by transient nonlinear forcing which has two parts: The part that is due to eddy-eddy interactions and the part that is due to eddy-mean flow interactions. The importance of each of these terms is established by simulations with artificially modified nonlinear forcing. The results indicate that neglecting the eddy-eddy interactions results in complete disappearance of ZELTs.

Eddy-induced transport in the North Atlantic flow is investigated using an idealized model of the double-gyre oceanic circulation and altimetry-derived velocities. The eddy diffusivity tensor varies geographically and is anisotropic, that is, it has a well-defined direction of the maximum transport [3]. ZELTs are particularly important for this transport anisotropy, which is demonstrated by numerical simulations with Lagrangian particles and idealized color dye tracers.

Conclusions

These results have implications for numerical ocean models. ZELTs are large enough to be resolved by numerical simulations even at relatively coarse spatial resolution, but such non mesoscale-resolving simulations will lack the dynamics necessary to simulate these zonal transients.

Acknowledgements

This work has been supported by the *NSF*OCE-1154923 and *NASA* Grant NNX14AH29G.

References

1. N. Maximenko, B. Bang, and H. Sasaki, *Geophys. Res. Lett.,* 2005, **32,** L12607.
2. I. Kamenkovich, I. Rypina, and P. Berloff, *J. Phys. Oceanogr.*, 2015*,* **45**, 778–791.
3. I. Rypina, I. Kamenkovich, P. Berloff, L. Pratt, *J. Phys. Oceanogr,* 2012*,* **42**, 2206–2228.

MICROPHYSICAL PROCESSES IN CLOUDS AFFECTING CHARGE SEPARATION

A.P. Khain and **M. Pinsky**

The Hebrew University of Jerusalem, Jerusalem, Israel
alexander.khain@mail.huji.ac.il

Abstract. We discuss microphysical processes in clouds such as effects of aerosols on formation of supercooled droplets, formation of crystals, graupel and hail at high levels. Possible role of breakup of snow by ice-ice collisions is considered. The state-of the art situation in cloud modeling is discussed.

Role of microphysical processes

It is believed that charge separation in clouds is caused by graupel (and hail) collisions with low density ice crystals. The collisions should take place in the presence of supercooled droplets. The coexistence of ice crystals, graupel/hail and supercooled water at low temperatures require the presence of high vertical velocities, when drops reach the upper levels without freezing, or in case clouds develop in a polluted air containing large concentration of aerosol particles. In this case concentration of droplets is small and the droplets ascend the upper levels without collisions.

Aerosol effects

Atmospheric aerosol particles (AP) give rise to formation of cloud droplets. The minimum size of AP size is determined by supersaturation values in clouds. Using the results of 1D and 2D cloud models, including those of the Hebrew University Cloud Model of Jerusalem (HUCM) we show that the aerosol effects on cloud microphysics depend on the APs size. Large APs are converted to droplets at cloud base. These drops rapidly grow and give rise to intense collisions and are responsible for rain formation. Very large values of supersaturation are reached in the zone of intense collisions and high vertical velocities (typically at 5–6 km). This supersaturation leads to nucleation of smallest APs. As a result, concentration of small supercooled drops is determined by smallest APs [1].

Aggregation and riming

Processes of aggregation lead to formation of snowflakes. Riming of these snowflakes leads to formation of graupel. Hail forms from frozen drops and grows by collection of supercooled water. We demonstrate these processes using the results of HUCM and other models with spectral bin microphysics.

The frequency of collisions depends on particle concentration and on the differences in the fall velocities. The frequency of collisions depends on the intensity of turbulence. The effect of turbulence can be significant, because turbulence near the cloud top is intense. The frequency of collisions also depends on the sticking efficiency, which, in turn, depends on particle type and temperature. We will discuss these problems in the talk.

Ice collisional breakup

It is known that the concentration of ice crystals in clouds is much larger than the concentration of ice nuclei. The difference can be attributed to the process of ice multiplication. It is shown that collisions between ice particles, especially between graupel/hail and snow lead to an increase in ice crystals and small aggregates by an order of magnitude [2].

Acknowledgements

This research was supported by the Israel Science Foundation (grant 1393/14), the Office of Science (BER), the US Department of Energy Award DE-SC0006788

References

1. A.P. Khain, V. Phillips, N. Benmoshe, and A. Pokrovsky, *J. Atmos. Sci*., 2012, **69**, 2787–2807.
2. V. Phillips, J-I. Yano, and A. Khain, *J. Atmos. Sci.* (in press).

ANALYSIS OF DAMPING OF SURFACE WAVES ON WATER WITH VISCOELASTIC FINITE-THICKNESS FILM

G.E. Khazanov and **S.A. Ermakov**

Institute of Applied Physics, Russian Academy of Sciences, N. Novgorod, Russia, gremugory@gmail.com

Abstract. The characteristics of surface waves on water covered with a viscoelastic finite-thickness film have been analyzed, and an analytical formula for gravity-capillary waves damping coefficient as a function of film thickness, viscosity and elasticity has been derived. The results are compared with the well-known case of monomolecular film in the context of remote observation and characterization of oil spills on sea surface.

A viscoelastic film on water surface may result in great changes in gravity capillary waves dynamics. The problem of surface waves in the presence of organic monomolecular film has been addressed in detail, for example, in [1]. But for the case of finite-thickness film, this problem is still not well understood. An important example of a finite-thickness film is crude oil which consists of a mixture of hydrocarbons and is able to form stable stationary films with quite large thickness ("thick film"). From a practical viewpoint the analysis of damping of gravity-capillary waves with "thick" film, particularly the relation between damping coefficient and film thickness is of particular interest when addressing the problem of remote observation and characterization of oil spills on sea surface. The solutions for velocity V and pressure p of low amplitude waves in a viscid water are

$$V_x = (ikAe^{kz} - lCe^{lz})e^{ikx+\alpha t}$$
$$V_z = (kAe^{kz} + ikCe^{lz})e^{ikx+\alpha t} \quad (1)$$
$$p = -\rho\alpha Ae^{kz}e^{ikx+\alpha t} - \rho gz,$$

where $l^2 = k^2 + \frac{\alpha}{\upsilon}$, υ is the kinematic viscosity coefficient, $\alpha = i\omega + \beta$, ω denotes the wave frequency, and Reβ is the wave damping coefficient which we are going to find. The solution is damped along the z axis exponentially. The $z = 0$ plane is chosen on water surface. The boundary conditions at the upper and lower interfaces may be written in form

$$-p + 2\mu\frac{\partial V_z}{\partial z} = p_\sigma \quad (2)$$
$$\mu\left(\frac{\partial V_x}{\partial z} + \frac{\partial V_z}{\partial x}\right) = p_t \quad (3)$$
$$p - 2\mu\frac{\partial V_z}{\partial z} = p_1 + 2\mu_1\frac{\partial U_z}{\partial z} + p_{\sigma 1} \quad (4)$$
$$\mu\left(\frac{\partial V_x}{\partial z} - \frac{\partial X_z}{\partial x}\right) = \mu_1\left(\frac{\partial U_x}{\partial z} - \frac{\partial U_z}{\partial x}\right) - p_{t1}\,, \quad (5)$$

where μ is the dynamic viscosity coefficient. By substituting solution (1) in (2–5) and taking into account that the wave frequency can be accurately described by the dispersion relation for potential gravity-capillary waves

$$\omega^2 = gk + \frac{\sigma k^3}{\rho}$$

we derived the following expression for the damping coefficient

$$Re\beta = -\frac{\omega}{2}\frac{\left(m+e^{kh}\left(-m-m_1+2me^{\delta h}\cos\delta h\right)+m_1e^{\delta h}C\right)2-\theta\sqrt{\frac{\eta}{2}}e^{\delta h}\left(e^{\delta h}(S+C)\left(1-e^{kh}\right)+e^{\delta h}(S-C)\left(2m+4m_1e^{kh}\right)\right)+\theta\sqrt{2\eta}me^{kh}+e^{\delta h}S\left(\theta e^{kh}-1+e\right.}{e^{\delta h}C\left(1+\theta\sqrt{\frac{\eta}{2}}e^{kh}\right)-e^{\delta h}S\theta e^{kh}\sqrt{\frac{\eta}{2}}}$$

where

$$\eta = \frac{\omega}{\upsilon k^2} = \frac{1}{m} \qquad \theta = \frac{\varepsilon}{\sigma} \qquad \delta = \sqrt{\frac{\omega}{2\upsilon}} \qquad S = \sin\delta h \qquad C = \cos\delta h$$

σ and ε are film tension and elasticity.

We'll discuss the relationship between the damping coefficient of gravity-capillary waves and film thickness, viscosity and elasticity. Comparisons with the known [1] case of monomolecular film will be made. In particular, the damping coefficient is larger than in the case of a monomolecular film. We discussed possible practical applications like remote observation and characterization of oil spills on sea surface.

References

1. B.G. Levich, *Physicochemical Hydrodynamics*, Prentice-Hall, Englewood Cliffs, NJ, 1962.

DATA-ADAPTIVE HARMONIC DECOMPOSITION AND MULTI-LAYER STUART-LANDAU STOCHASTIC MODELLING

D. Kondrashov

University of California, Los Angeles, USA, dkondras@atmos.ucla.edu

Abstract. Novel signal processing data-adaptive decomposition technique will be presented that estimates power and phase spectra of mutivariate datasets in geosciences and elsewhere. The key numerical features of the Data-adaptive Harmonic decomposition (DAH) method [1] rely on the construction of covariance matrix that exploits time-lagged cross-correlations. Eigenmodes associated with DAH covariance matrix form an orthogonal set of oscillating data-adaptive harmonic modes (DAHMs) that come in pairs and in exact phase quadrature for a given temporal Fourier frequency. Data-driven inverse modeling is greatly simplified by using DAHM basis [1].

The recently introduced Multilayer Stochastic Modeling (MSM) framework [2] emphasizes the ubiquitous role of nonlinear, stochastic as well as memory effects for the derivation of data-driven models with good skill in simulating and predicting main dynamical features of the targeted spatio-temporal field as an output of a nonlinear, high-dimensional geophysical model, or as a set of observations. However, if the input data are not numerous enough and exhibit mixture of different spatiotemporal scales, the analysis may reveal multiple predictors and complex model structure.

The DAH decomposition provides an attractive data-adaptive alternative that reduces the data-driven inverse modeling effort to elemental MSMs with fixed and much smaller number of coefficients to estimate [1]. In particular, the pairs of data-adaptive harmonic coefficients (DAHCs), obtained by projecting the input dataset onto DAHMs, can be effectively modeled within a universal parametric family of simple nonlinear stochastic models – coupled Stuart-Landau oscillators stacked per frequency, and synchronized at different frequencies by the same noise realization.

DAH-MSLM applications on didactic examples, as well as climate modeling and prediction will be presented. In all cases, the DAH decomposition allows for an extraction of spatio-temporal modes revealing key dynamical features in the embedded phase space. The DAH-MSLMs are shown to successfully model the typical patterns of the corresponding fields, as well as their key statistics.

In particular, DAH-MSLM has been successfully applied to a difficult problem of modeling Arctic sea ice data [3]. Decline in the Arctic sea ice extent (SIE) due to global warming has profound socio-economic implications and is a focus of active scientific research. Of particular interest is prediction of September SIE on subseasonal time scales, i.e., from early summer into fall, when sea ice coverage in Arctic reaches its minimum. Forecasting of September SIE is very challenging due to the high variability of ocean and atmosphere over Arctic in summer, as well as shortness of observational data and inadequacies of the physics-based models to simulate sea-ice dynamics. However, the real-time DAH-MSLM prediction outperformed most statistical models and physics-based models in 2016 Sea Ice Outlook [4] – a collaborative effort to facilitate and improve subseasonal prediction of September SIE: $4.79 \cdot 10^6$ km^2 vs. actually observed $4.7 \cdot 10^6$ km^2. The key success factor is associated with DAH-MSLM ability to efficiently disentangle and model complex spatiotemporal dynamics of SIE [5].

This is a joint work with Mickael D. Chekroun (UCLA) and Michael Ghil (UCLA,ENS).

Acknowledgements

This research was supported by grant N00014-16-1-2073 of the Office of Naval Research (USA), by grants OCE-1243175 and DMS-161698 of the National Science Foundation (USA), and Government of the Russian Federation (agreement #14.Z50.31.0033 with the Institute of Applied Physics of RAS).

References

1. M.D. Chekroun and D. Kondrashov, *Chaos,* 2017, submitted.
2. D. Kondrashov, M.D. Chekroun, and M. Ghil, *Physica D*, 2015**, 297**, 33–55.
3. D. Kondrashov, M.D. Chekroun, X. Yuan, and M. Ghil, 2017, *in Advances in Nonlinear Dynamics by Springer Nature*, Ed. A. Tsonis, in press.
4. Sea Ice Outlook: https://www.arcus.org/sipn/sea-ice-outlook/2016/.
5. D. Kondrashov, M.D. Chekroun, and M. Ghil, *Geophys. Res. Lett*, 2017**,** submitted.

PRONOUNCED DIFFERENCES BETWEEN THE OBSERVED AND CMIP5 SIMULATED CLIMATE VARIABILITY IN THE TWENTIETH CENTURY

S.V. Kravtsov

University of Wisconsin-Milwaukee, Milwaukee, USA, kravtsov@uwm.edu

Abstract. Identification and dynamical attribution of multidecadal climate undulations to either variations in external forcings or to internal sources is one of the most important topics of modern climate science, especially in conjunction with the issue of human induced global warming. Here we utilize ensembles of the 20th century climate simulations to isolate forced signal and residual internal variability in a network of observed and modeled climate indices. The observed internal variability so estimated exhibits a pronounced multidecadal mode with a distinctive spatiotemporal signature, which is altogether absent in model simulations. This single mode explains a major fraction of model–data differences over the entire climate-index network considered; it may reflect either biases in the models' forced response or models' lack of requisite internal dynamics, or a combination of both.

Previous work [1–3] detected considerable mismatches in both the magnitude and spatiotemporal structure of the twentieth century's multidecadal variability – defined via deviations from the long-term linear trend – in a network of observed and CMIP5 simulated indices characterizing the Northern Hemisphere climate. Here we apply a recent methodology [4] for (nonlinear) forced-signal identification to an extended set of oceanic and atmospheric climate indices and expand the analyses [3] to compare the resulting estimated internal components of the observed and CMIP5 simulated climate variability.

We find pronounced differences in the magnitude, time scale and spatial patterns of the observed and simulated variability, thus generalizing earlier conclusions of work [3] to the nonlinear forced signals and the entirety of the CMIP5 ensemble considered. We also show that the model–data differences are dominated by a low-order multidecadal mode of variability (Fig. 1), which appears to be altogether absent from the dynamical landscape of CMIP5 models.

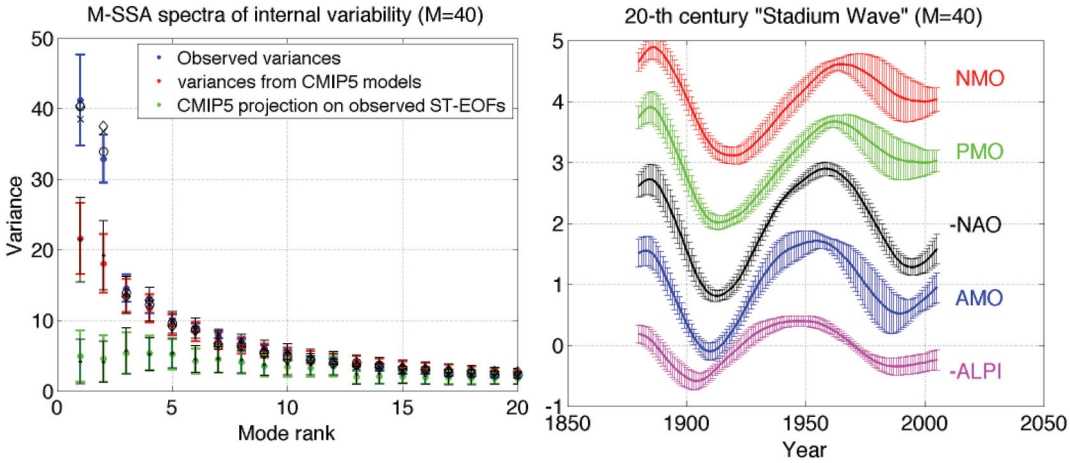

Fig. 1. The M-SSA analysis of the observed and simulated internal variability in the AMO–PMO–NMO–NAO–ALPI climate-index network

Acknowledgements

The author acknowledges the World Climate Research Programme's Working Group on Coupled Modeling, which is responsible for CMIP, and thanks the climate modeling groups for making their model output available. This research was supported by the NSF grants OCE-1243158 and AGS-1408897.

References

1. M. Wyatt, *et al.*, *Clim. Dyn.*, 2012, **38**(5–6), 929–949.
2. M. Wyatt and J. Peters, *Proc. SpringerPlus*, 2012, 1–68.
3. S. Kravtsov, *et al.*, *Geophys. Res. Lett.*, 2014, **41**, 6881–6888.
4. S. Kravtsov and D. Callicutt, *Int. J. Climatol.*, 2017, doi: 10.1002/joc.5096.

THE MAIN NEGATIVE LEADER TIP AND SPACE STEMS NUMERICAL MODELING

F.A. Kuterin, A.A. Syssoev, and **D.I. Iudin***

Institute of Applied Physics of the Russian Academy of Sciences, Nizhny Novgorod, Russia
* iudin@ipfran.ru

Abstract. Due to vigorous streamer development, various regions along the negative streamer tracks are heated and retain excess positive space charge. These regions are called space stems. The appearances of the stems in both laboratory discharge and lightning are successfully documented, but its origin remains still enigmatic. We consider the space stems appearance as a nonequilibrium kinetic transition provided by an external driving, the intensity of which is controlled by leader current.

The channel promotion mechanism and the streamer zone structure of the negative leader are much more complicated than in case of a positive one and, to date, are poorly understood. The active region of a negative laboratory leader has the same general anatomy as a positive laboratory leader, consisting of a leader channel, tip and streamer zone. There is, however, a significant addition to the negative laboratory leader extension process. In the negative laboratory leader case, an initial burst of negative streamers is emitted from the main leader tip and propagates through the strong local electric field for a few meters. Due to vigorous streamer development, various regions along the negative streamer tracks are heated and retain excess positive space charge. These regions are called space stems [1].We consider the space stems appearance as a nonequilibrium noise induced kinetic transition provided by an external stochastic driving, the intensity of which is controlled by leader current.

The physical processes that lead to branching, and the physical factors that affect branching features remain among several unresolved issues in our understanding of spark discharge development. In our study using directed percolation strategy we found a close relationship between the space stem formation and discharge tree branching process.

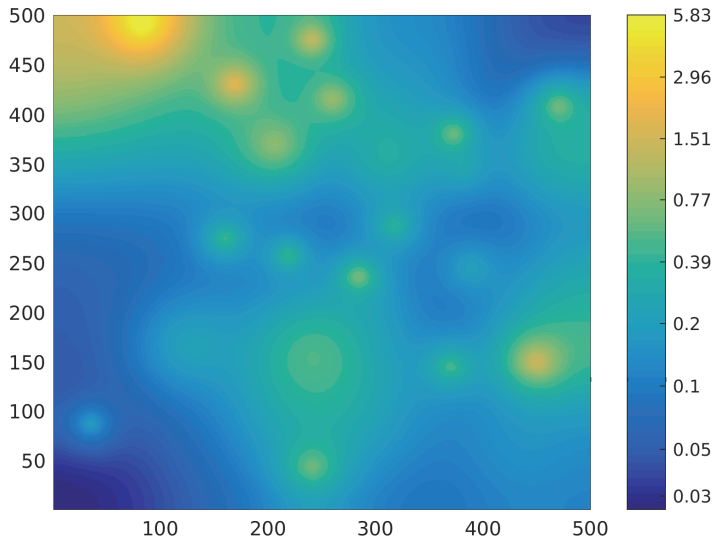

Fig. 1. The electron density model distribution is represented in the lateral cross section of the streamer corona of the negative leader. The simulation results are presented in arbitrary units

Acknowledgements

This work was supported in part by the Government of the Russian Federation (contract No. 43414.B25.31.0023) and by the Russian Foundation for Basic Research (projects Nos 15-01-06612, and 16-05-01013).

References

1. V.A. Rakov, and M.A. Uman, *Lightning: Physics and Effects*, Cambridge Univ. Press, New York. 2003, 687.

EFFECT OF NONLINEAR WAVE-WAVE INTERACTIONON ON APPARENT WAVE ATTENUATION IN ICE COVERED SEAS

J. Li[1], A.L. Kohout[2], H.H. Shen[3], and **C. Guan[1]**

[1] Ocean University of China, Qingdao, China, ljk1105@ouc.edu.cn
[2] National Institute of Water and Atmospheric Research, Christchurch, New Zealand
[3] Clarkson University, Potsdam, USA

Abstract. Studies of wave propagation in ice covered seas have become increasingly more important due to the rapid reduction of sea ice in the Arctic Ocean. However, in some cases, it is still problematic to interpret the behaviors of measured apparent wave attenuation only with current wave-ice models. Inspired by previous speculation, the effect of nonlinear four-wave interactions on apparent wave damping during a field observation in marginal Antarctic is tested with discrete interaction approximation. The results show that the nonlinear wave-wave interaction does offset wave damping during stormy cases and for short waves in ice covered waters.

Since the nineteenth century (Greenhill, 1886), wave propagation through ice-covered waters has been studied theoretically. The most recent review may be found in Squire (2007). Motivated by the dramatic ice cover reduction in the Arctic, theoretical development has advanced in the last 10 years. One of the key problems concerning wave propagation through ice covers is how much incoming waves are damped. Nearly all theories and observations demonstrate an exponential attenuation over distance, with higher frequencies corresponding to higher decay rates. However, during a field experiment that took place in the Antarctic marginal ice zone in 2012 (Kohout *et al.*, 2014), two interesting phenomena of apparent wave damping were observed which both don't follow the exponential decay.

1. Linear decay rate of large waves ($H_s > 3m$).

According to Kohout's data, apparent wave attenuation is a function of the significant wave height H_s. At low wave heights, i.e., calm conditions, the apparent wave decay over distance $-dH_s/dx$ was proportional to H_s, indicating that energy follows exponential decay. However, under storm conditions or large H_s, $-dH_s/dx$ became independent of H_s, indicating a linear attenuation with distance.

2. Rollover distribution of apparent wave attenuation.

Theoretically, attenuation coefficient of wave energy monotonically increases as wave period decreases. But in Kohout's measurement and several previous field observations (Wadhams *et al*., 1988; Doble *et al.*, 2015), the rollover phenomenon is observed. That is, as the wave period decreases the attenuation increases up to a point beyond which the opposite happens.

Both two phenomena cannot be explained only with current wave-ice models no matter applying scattering or continuum theories. It implies that other mechanisms may influence wave damping during propagation through ice covers. Therefore, nonlinear energy transfer is speculated as an important cause leading to overestimated attenuation by wave-ice theories for these two phenomena (Wadhams *et al.*, 1988; Kohout *et al*., 2014; Li *et al*., 2015).With improving capabilities of modelling waves in ice covered waters of WaveWatch III, it is possible to quantitatively study the effect of nonlinear wave-wave interaction on the basis of a satisfied wave hindcasting. By source term analysis, we find that the nonlinear wave-wave interaction (Hasselmann *et al.*, 1985) does offset wave damping during stormy cases, and for short waves in ice covered waters. This verifies that in interpreting measured apparent wave attenuation we should not ignore the contributions from nonlinear energy transfer.

References

1. A.G. Greenhill, *Am. J. Math.*, 1886, **9**(1), 62–96.
2. V.A. Squire, *Cold Reg. Sci. Technol.*, 2007, **49**, 110–133.
3. A.L. Kohout, M. J. M. Williams, S. M. Dean, and M. H. Meylan ,*Nature*, 2014, **509**(7502), 604–607.
4. P. Wadhams, V.A. Squire, D.J. Goodman, A.M. Cowan, and S.C. Moore, *J. Geophys. Res.*, 1988, **93**(C6), 6799–6818.
5. M.J. Doble, D.C. Giacomo, M.H. Meylan, B. Jean-Raymond, and W. Peter, *Geophys. Res. Lett*., 2015, **42**(11), 4473–4481.
6. J. Li, A.L. Kohout, and H.H. Shen, *Geophys. Res. Lett.*, 2015, **42**(14), 5935–5941.
7. S. Hasselmann, K. Hasselmann, J.H. Allender and T.P. Barnett, *J. Phys. Oceanogr.*, 1985, **15**, 1378–1391.

INVESTIGATION OF PALEOCLIMATE TRANSITIONS WITH DATA-DRIVEN MODELS

E.M. Loskutov, D.N. Mukhin, A.S. Gavrilov, and **A.M. Feigin**

Institute of Applied Physics of the RAS, Nizhny Novgorod, Russia
loskutov@ipfran.ru

Abstract. In this work we propose a data-driven model for the investigation of critical transitions on paleo time scales. Namely, we investigated the mid-Pleistocene transition which led to a change of dominate cycles of glacial variability in Pleistocene. We demonstrate that our data-driven model is a good tool for analysing paleoclimate variability. In particular, we discuss the possibility of detecting, identifying and predicting the mid-Pleistocene transition by means of nonlinear empirical modeling using the paleoclimate record time series.

At the present time there exist empirical methods of analysing complex spatially distributed systems, including methods of optimal phase variables retrieval and construction of empirical prognostic models by observed time series. One of them, the Bayesian approach to optimal evolution operator reconstruction by time series, has been developed by the authors. It is based on representation of evolution operator in the form of a nonlinear stochastic function represented by artificial neural networks [1, 2].

In this work we focus on the investigation of critical transitions – the abrupt changes in climate dynamics – on a much longer time scale. It is well known that there were a number of critical transitions on different time scales in the past. In this work, we demonstrate the first results of applying our empirical methods to analysis of paleoclimate variability. In particular, we discuss the possibility of revealing and indentifying the mid-Pleistocene transition (Fig. 1) by means of nonlinear empirical modeling by the paleoclimate record time series.

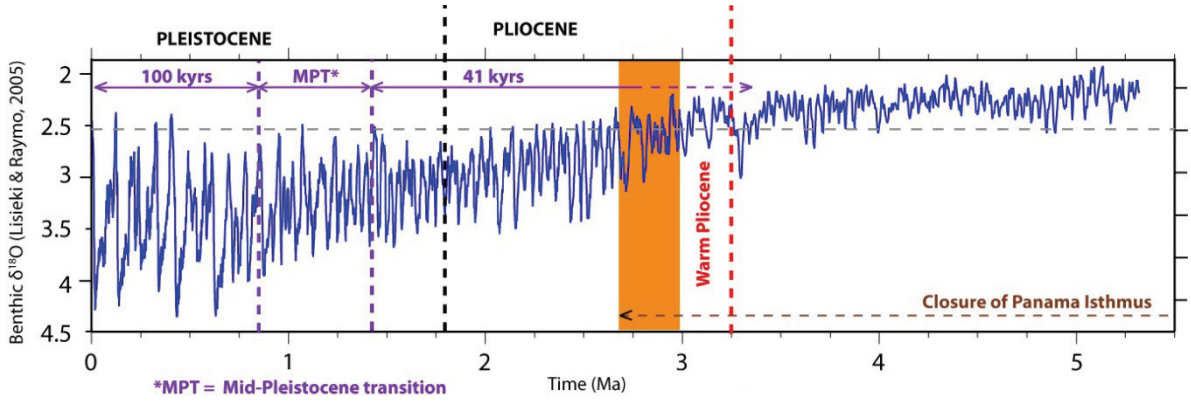

Fig. 1. Blue color is the LR04 stack [3] spans 5.3 million years and is an average of 57 globally distributed benthic d18O records. 100 kyrs and 40 kyrs correspond to the orbitally-driven glacial/interglacial cycles period. This period changed from 41 kyrs to 100 kyrs during the Mid-Pleistocene Transition toward 1 Ma (MPT)

Acknowledgements

The study is supported by the Government of the Russian Federation (agreement #14.Z50.31.0033 with the Institute of Applied Physics of RAS).

References

1. Y. Molkov, E. Loskutov, D. Mukhin, & A. Feigin, "Random dynamical models from time series", *Physical Review E*, 2012, **85**, 1–9.
2. D. Mukhin, D. Kondrashov, E. Loskutov, A. Gavrilov, A. Feigin, & M. Ghil, "Predicting Critical Transitions in ENSO models". Part II: Spatially Dependent Models. *Journal of Climate*, 2015, **28**(5), 1962–1976.
3. L.E. Lisiecki & M.E. Raymo, "A Pliocene-Pleistocene stack of 57 globally distributed benthic δ 18 O records", *Paleoceanography*, 2005, **20**(1).

ON THE ENERGY OF LIGHTNING FLASHES AND DISTRIBUTION OF THUNDERSTORM ACTIVITY OVER THE GLOBE

E.A. Mareev

Institute of Applied Physics RAS, Nizhny Novgorod, Russia
evgeny.mareev@gmail.com

The talk is devoted to the unsolved issues of lightning energy and parametrization of thunderstorm activity in weather and climate models. The main attention is paid to the physical processes and mechanisms that determine the statistical distributions of lightning flashes in current and energy, as well as the distribution of lightning activity over the globe. The problem of lightning with extreme parameters and their connection with the most intense meteorological phenomena and forest fires is also considered.

HILBERT ANALYSIS UNVEILS INTER-DECADAL CHANGES IN LARGE-SCALE PATTERNS OF SAT VARIABILITY

D.A. Zappala[1], M. Barreiro[2], and **C. Masoller[1]**

[1] Universitat Politecnica de Catalunya, Terrassa, Barcelona, Spain, cristina.masoller@upc.edu
[2] Universidad de la República, Iguá 4225, Montevideo 11400, Uruguay

Abstract. Climate change is a topic of great importance, and a lot of work is focused on quantifying significant variations in the properties of climatological variables, in particular, of surface air temperature (SAT). Although changes in local seasonal cycles (such as the amplitude and the phase lag to the insolation) have been investigated, changes in large-scale patterns of faster SAT variability (on a daily time-scale) remain poorly understood. Here we perform a Hilbert analysis of daily SAT reanalysis data covering the Earth's surface, and identify the geographical regions where inter-decadal changes are more pronounced.

Climate change is a topic of great importance, and a lot of work is focused on capturing relevant inter-decadal changes in the statistical properties of climatological variables, and understanding the causes and the significance of these changes. To further advance the field, it is important to develop reliable climate data analysis tools. Particularly important is to study variations of the Earth's surface air temperature (SAT). Although inter-decadal changes in the properties that characterize local seasonal SAT cycles have been investigated, a systematic study of how large-scale patterns of fast SAT variability (on a daily time-scale) changed in the last decades is still lacking.

Here we aim at filling this gap by applying Hilbert analysis to daily SAT in a regular grid over the Earth's surface (we analyze ERA-Interim and NCEP-DOE re-analysis, covering the period January 1979 – July 2016). Recently we computed the instantaneous Hilbert frequency time series and analyzed the resulting dataset by plotting the maps of (i) the average frequency <f>, and (ii) the standard deviation σ_f [1]. These maps revealed well-defined large-scale structures. In the extra-tropics, <f> tends to correspond to the expected one-year period of solar forcing, while in the tropics, it is generally faster. This was understood to be due to the small amplitude of the seasonal oscillation, with respect to oscillations induced by other climatological processes. Coherent structures were also found in the σ_f maps, which tend to be located over regions of strong annual precipitation.

Here we extend the analysis to also investigate the Hilbert amplitude. By computing the maps of <f>, <a>, σ_f and σ_a, in the first 10 years and in the last 10 years of the period covered by the reanalysis, as well as their difference, we perform a systematic characterization of the changes in the amplitude of the SAT cycle, and in the ``noisy-like'' daily fluctuations. As shown in Fig. 1, the analysis clearly identifies geographical regions where changes are most pronounced.

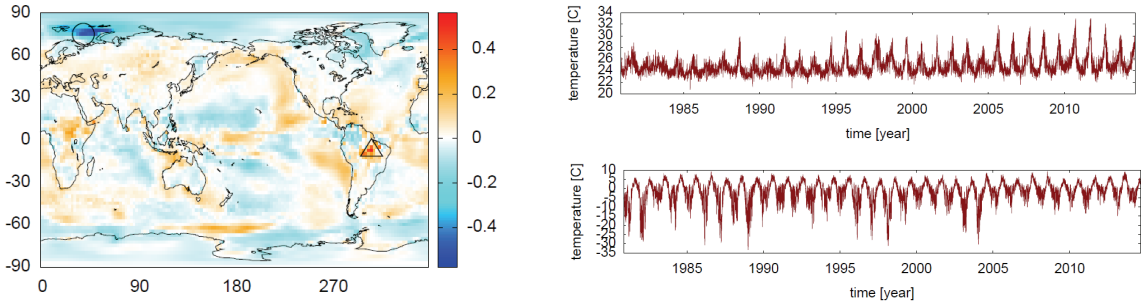

Fig. 1. *Left*: Variation of Hilbert amplitude statistics computed from ERA re-analysis. *Right*: SAT time series in two regions where large inter-decadal changes of Hilbert amplitude are detected. In the *top panel*, displaying daily SAT in the region indicated by a triangle (7.5 S, 307.5 E), one can notice that the amplitude of the SAT cycle in the last 10 years (July 2007 to June 2016) is larger than in the first 10 years(January 1979 to December 1988); in the *bottom panel*, displaying SAT in the region indicated by a circle (75 N, 40 E), the amplitude is smaller in the last 10 years than in the first 10 years.

Acknowledgements

This work was supported by MINECO/FEDER (FIS2015-66503-C3-2-P) and ICREA ACADEMIA.

References

1. D.A. Zappala, M. Barreiro, C. Masoller, "Global atmospheric dynamics investigated by using Hilbert frequency analysis", *Entropy*, 2016, **18**, 408.

LES AND DNS MODELLING OF STABLY STRATIFIED BOUNDARY LAYER TURBULENCE

A.V. Glazunov[1] and **E.V. Mortikov**[2]

[1] Institute of Numerical Mathematics RAS, Moscow, Russia, and.glas@gmail.com
[2] M.V. Lomonosov MSU Research Computing Center, Moscow, Russia

Abstract. Large-eddy simulation (LES) and direct numerical simulation (DNS) approaches were used for modelling boundary layer turbulence under stable stratification. We describe results for different boundary layer type flows and review their relevance for developing parameterizations of turbulent processes in large-scale models of atmosphere and ocean.

We review results of numerical modelling of stratified boundary layer turbulence based on two well-known approaches: large-eddy simulation (Glazunov *et al*., 2016) and direct numerical simulation (Mortikov *et al*., 2016).

Direct numerical simulation, in particular, was used to investigate intermittent turbulence in stably stratified plane Couette flow for Reynolds numbers based on the channel height and relative wall speed between top and bottom walls, up to 10^5. Results show that the transition to intermittent turbulence under strong stratification is associated with the formation of secondary counter-rotating roll-like structures elongated in the spanwise direction and organized in two rows corresponding to lower and upper walls of the channel. The ordering of rolls defines spatially confined alternating regions of laminar and turbulent flow. The spanwise length of these vortices increases with the increase of the bulk Richardson number and defines an additional constraint on the computational box size. We describe DNS results in spanwise-extended computational domains, where the turbulent intermittent regime is sustained without relaminarization for sufficiently higher bulk Richardson numbers than previously reported.

Large-eddy simulation and Lagrangian stochastic modeling of passive particle dispersion were applied to the scalar flux footprint determination in the stable atmospheric boundary layer. The sensitivity of the LES results to the spatial resolution and to the parametrizations of small-scale turbulence was investigated. It was shown that the resolved and partially resolved ("subfilter-scale") eddies are mainly responsible for particle dispersion in LES, implying that substantial improvement may be achieved by using recovering of small-scale velocity fluctuations. In LES with the explicit filtering, this recovering consists of the application of the known inverse filter operator. The footprint functions obtained in LES were compared with the functions calculated with the use of first-order single-particle Lagrangian stochastic models (LSMs) and zeroth-order Lagrangian stochastic models – the random displacement models (RDMs). According to the presented LES, the source area and footprints in the stable boundary layer can be substantially more extended than those predicted by the modern LSMs.

References

1. A. Glazunov, Ü. Rannik, V. Stepanenko, V. Lykosov, M. Auvinen, T. Vesala, and I. Mammarella, *Geosci. Model Dev*., 2016, **9**, 2925–2949.
2. E. Mortikov, *Izv. Atmos. Ocean. Phys*., 2016, **52**(1), 108–115.

EXTRACTION OF LEADING NONLINEAR DYNAMICAL MODES OF CLIMATE FROM DATA

D.N. Mukhin, A.S. Gavrilov, E.M. Loskutov, and **A.M. Feigin**

Institute of Applied Physics of the RAS, Nizhny Novgorod, Russia
mukhin@ipfran.ru

Abstract. A new nonlinear expansion of climatic data accounting for external forcing of different nature is suggested. It is applied to analysis of sea surface temperature anomalies over the globe aiming to extract leading climate modes. The structure of the obtained modes and their response to external factors are discussed.

A new method for principal mode extraction from climate data is presented. The method is based on the Nonlinear Dynamical Mode (NDM) expansion [1, 2], but takes into account a number of external forcings applied to the system. Each NDM is represented by hidden time series governing the observed variability, which, together with external forcing time series, are mapped onto data space. While forcing time series are considered to be known, the hidden unknown signals underlying the internal climate dynamics are extracted from observed data by the proposed method. In particular, it gives us an opportunity to study the evolution of principal system's mode structure in changing external conditions and separate the internal climate variability from trends forced by external perturbations. Furthermore, the as-obtained modes can be extrapolated beyond the observational time series, and long-term prognosis of modes' structure including characteristics of interconnections and responses to external perturbations, can be carried out.

In this work the method is used for reconstructing and studying the principal modes of SSTA variability on inter-annual and decadal time scales accounting for the external forcings such as anthropogenic emissions, variations of the solar activity and volcanic activity. The structure of the obtained modes as well as their response to external factors, e.g. possibility to forecast their change in the 21st century under different CO2 emission scenarios are discussed.

Acknowledgements

The study is supported by the Government of the Russian Federation (agreement #14.Z50.31.0033 with the Institute of Applied Physics of RAS).

References

1. D. Mukhin, A. Gavrilov, A. Feigin, E. Loskutov, & J. Kurths, "Principal nonlinear dynamical modes of climate variability", *Scientific Reports*, 2015, **5**, 15510. http://doi.org/10.1038/srep15510.
2. A. Gavrilov, D. Mukhin, E. Loskutov, E. Volodin, A. Feigin, & J. Kurths, "Method for reconstructing nonlinear modes with adaptive structure from multidimensional data", *Chaos: An Interdisciplinary Journal of Nonlinear Science*, 2016, **26**(12), 123101. http://doi.org/10.1063/1.4968852 .

DAYTIME PHOTOCHEMICAL EQUILIBRIUM OF OH, HO_2, AND O_3 AT THE ALTITUDES OF THE MESOSPHERE: IMPLICATION FOR MLS/AURA DATA VALIDATION

M.Yu. Kulikov, A.A. Nechaev, M.V. Belikovich, T.S. Ermakova, and **A.M. Feigin**

Institute of Applied Physics of the Russian Academy of Sciences, Nizhny Novgorod, Russia
porry@yandex.ru

Abstract. The technique of statistic validation for simultaneous mesospheric measurements of OH, HO_2 and O_3 in the daytime has been developed. It implies meeting the photochemical equilibrium equation and takes into account measurement error. The presentation shows the first results of applying the technique to MLS/Aura data.

The prominent feature of the Earth photochemical system is the presence of an essential number of chemical components with small life time. Thus, when calculating the evolution of the system, one may consider them to be in the state of instantaneous stable photochemical equilibrium. Moreover, the algebraic equations that represent the balance of sources and sinks for those components can be applied to determine poorly measured atmospheric species using other components' observations, validate results of distant measurements, and estimate reaction rates, which are known with a sufficient uncertainty, or other atmospheric characteristics.

In this paper, we consider simultaneous photochemical daytime equilibrium of OH, HO_2, and O_3 at the altitudes of the mesosphere. The reactions that represent sources and sinks in equilibrium are:

$$O_3 + h\nu \rightarrow O_2 + O(^1D, ^3P)$$
$$O + O_2 + M \rightarrow O_3 + M,\ M = O_2, N_2$$
$$O + OH \rightarrow O_2 + H$$
$$O + HO_2 \rightarrow O_2 + OH$$
$$O_2 + H + M \rightarrow HO_2 + M$$
$$O_3 + H \rightarrow O_2 + OH$$
$$O_3 + OH \rightarrow O_2 + HO_2$$
$$H + HO_2 \rightarrow 2OH$$

A simplified algebraic equation that describes the relationship between the local concentrations of the components at the altitudes of 50–100 km has been found. The only parameters of the equation are air temperature, air concentration, and the rates of the reactions mentioned above. The one-year simulation of the mesosphere and lower thermosphere based on a 3D chemical-transport model (atmospheric dynamics from CMAM [1]) shows that the discrepancy between the calculated evolution of the components and the equilibrium one given by the equation does not exceed 3–4% in the full range of altitudes, independent of a season or latitude.

We propose the technique of statistic Bayesian validation of simultaneous satellite measurements of OH, HO_2 andO_3. It uses the mentioned equilibrium equation and takes into account the satellite measurement error. The presentation includes the first results of the technique's application to MLS/Aura data [2]. It is found that the satellite data of HO_2 distribution regularly demonstrates essentially lower values of altitudes of this component's mesospheric maximum. These results confirm off-line retrieval of HO_2 from the MLS primary data [3].

Acknowledgements

This work was supported by the Russian Science Foundation (contract No. 15–17–10024).

References

1. J. de Grandpre, S.R. Beagley, V.I. Fomichev, E. Griffioen, J.C. McConnell, A.S. Medvedev, and T.G. Shepherd, *J. Geophys. Res.,* 2000, **105**, 26475–26491.
2. https://mls.jpl.nasa.gov/.
3. L. Millán, S. Wang, N. Livesey, D. Kinnison, H. Sagawa, and Y. Kasai, *Atmos. Chem. Phys.*, 2015, **15**, 2889–2902.

RADIATIONS IN LIGHTNING-LIKE ATMOSPHERIC DISCHARGES

A.V. Agafonov[1], I.S. Baidin[1], A.V. Oginov[1], A.A. Rodionov[1,2], and **K.V. Shpakov[1]**

[1] Lebedev Physical Institute of RAS, Moscow, Russian Federation, oginov@lebedev.ru
[2] Moscow Institute of Physics and Technology, Dolgoprudny, Russian Federation

Abstract. The recent results of investigation of laboratory high-voltage discharge in air are presented. X-ray and neutron emission detection is specially emphasized. Data were obtained with a combination of plastic scintillation detectors and Helium-3-filled counters of thermal neutrons. Strong dependence of the appearance of hard X-ray and neutron radiation on field strength near electrodes was found. A complicated temporal structure of neutron bursts observed during discharge was revealed. The anisotropy of bremsstrahlung X-rays was analyzed.

Atmospheric discharge was investigated on ERG installation [1]. Voltage pulse amplitude in the experiments reached 1.2 MV with a rise time of 150–200 ns and current amplitude of up to 15 kA. The discharge gap was from 0.3 to 0.7 m long. The electrodes allowing a variety of initial electric field distributions were used. A guided leader formation was modeled using thin wire explosion in interelectrode gap. The installation layout allowed receiving discharges of different polarities in the same conditions (voltage amplitude, energy, etc.). The present work covers the new results concerning different types of emissions of high voltage air discharge [2, 3]. Discharge parameters were registered by electrophysical diagnostics, an angular set of fast calibrated scintillation detectors, Helium-3 counter arrays, imaging visible range diagnostics based on electron-optical image converters. Spectral measurements of atmospheric discharge at optical wavelengths: near UV radiation sensors, integrated spectra obtained by CCD (185–920 nm) and imaging (with spatial resolution) spectrographs; time-based spectra obtained at a given wavelength (monochromator + PMT) and integrated with spatial collimation on a selected region of the discharge are presented.

The radiation in the visible region of the spectrum with the development of an extensive discharge in air in the interelectrode space carries information about the parameters of streamer-leader stage of the discharge, the discharge channel interaction with the electrode material, a stage of relaxation after the decay of the plasma channel of the discharge current. The visible spectra obtained are similar to those of the natural linear lightning obtained in [4], in the presence of the lines of N II ion in the shorter wavelengths range, and in the range of more 700 nm–lines of atomic nitrogen and oxygen. The electron temperature was about 3 eV. This corresponds to a significant degree of ionization. The formation of channel structures of different scales in near- and interelectrode space was noted. The resulting parameters are compared with the electrode properties and current-voltage characteristics of the discharge.

Combined character of radiations on the voltage rise was shown. The temporal structure of neutron generation shows the appearance of neutron bursts in the initial "dark" phase of the discharge [2, 3]. However, the temporal structure of neutron pulses was much more diverse. This may indicate different mechanisms for generating penetrating radiation during the formation and development of the atmospheric discharge. Direct evidence for the detection of neutron radiation was obtained with the use of ^{3}He neutron counters and the analog recording of neutron pulses generated at the time of discharge [3]. The close coincidence of measured and calculated neutron detection efficiencies of ^{3}He-counters, allows us to estimate the maximum value of the flux of neutrons emitted in shots at $1 \cdot 10^3$ to $5 \cdot 10^4$ in 4π sr, depending on the place of neutron generation (near the anode or near the cathode, respectively). Angular distribution of bremsstrahlung x-rays was analyzed.

Acknowledgements

The work was partially supported by the Russian Foundation for Basic Research, grant No. 17-08-01690.

References

1. A.V. Agafonov, A.V. Oginov, and K. V. Shpakov, *Phys. of Part. and Nucl. Lett.*, 2012, **9**, 380–383.
2. A.V. Agafonov, A.V. Bagulya, O.D. Dalkarov, M.A. Negodaev, A.V. Oginov, A.S. Rusetskiy, V.A. Ryabov, and K.V. Shpakov, *Phys. Rev. Lett.,* 2013, **111**, 115003.
3. A.V. Agafonov, V.A. Bogachenkov, A.P. Chubenko, and A.V. Oginov, A.A. Rodionov, A.S. Rusetskiy, V.A. Ryabov, A.L. Shepetov, K.V. Shpakov, *J. Phys. D: Appl. Phys*., 2017, **50**, 165202.
4. J. Cen, P. Yuan, and S. Xue, *Phys. Rev. Lett.*, 2014, **112**, 035001.

STOCHASTIC PARAMETRIZATION FOR 2-D TURBULENCE SIMULATION

P.A. Perezhogin[1,2], **A.V. Glazunov**[1], and **A.S. Gritsun**[1]

[1] Institute of numerical mathematics, Moscow, Russia, e-mail: pperezhogin@gmail.com
[2] Moscow institute of physics and technology, Moscow, Russia

Abstract. Stochastic subgrid parametrizations designed for coarse-grid numerical simulations of two-dimensional turbulence were investigated. These parametrizations require a-priori analysis of high resolution simulation data and take into account the properties of numerical schemes. The proposed parametrizations were tested under the modeling of bidirectional energy-enstrophy cascade in isotropic homogeneous 2-D turbulence. The energy generation spectrum induced by subgrid processes was obtained using high-resolution computation. This spectrum was used for the evaluation of subgrid stochastic model parameters. It was shown that the proposed model improves the large-scale dynamics. In particular, it restores the inverse energy cascade for different numerical schemes and improves the sensitivity of the coarse-grid numerical models to external forcing.

The simulations of isotropic homogeneous 2-D turbulence were earlier performed in [1] with the use of different numerical schemes. It was shown that the inverse energy cascade is suppressed in coarse-grid simulations and that the results strongly depend on the scheme if the spatial scale of the forcing is close to the grid step. These faults can be avoided by the use of stochastic kinetic energy backscatter parametrization. Similar parametrizations have been investigated in [2–4]. In contrast to these papers, we focus on the case of small-scale external forcing and on the improving of model dynamics in energy-containing spectral range. We use stochastic autoregressive parametrizations for the energy backscatter with the energy generation spectrum (see, e.g., fig. 1a), obtained from DNS and take into account numerical scheme of the coarse model. As a result the energy spectrum of the low resolution models fits DNS simulations much better (see, fig. 1b). The same is true for the lagged covariances of the model variables. It was also shown that stochastic parametrization improves the sensitivity of the coarse-grid numerical models to external forcing.

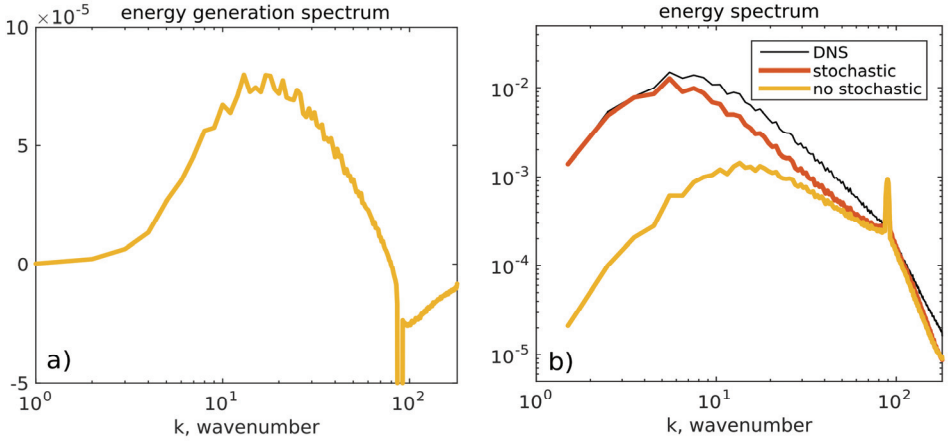

Fig. 1. Energy generation spectrum induced by subgrid processes in a-priori test (a) and coarse-grid simulation energy spectra vs DNS results (b). Yellow curve – simulation without stochastic backscatter. Red curve – simulation with the same numerical scheme and spatial resolution corrected by the proposed stochastic parametrization.

Acknowledgements

The work was performed in the INM RAS and supported by the Russian Foundation for Basic Research project no. 16-55-12015.

References

1. P. Perezhogin, A. Glazunov, E. Mortikov, and V. Dymnikov, *Russian Journal of Numerical Analysis and Mathematical Modelling*, 2017, **32**(1), 1–14.
2. J. Chasnov, *Physics of Fluids A: Fluid Dynamics (1989-1993),* 1991, **3**(1), 188–200.
3. G. Shutts, *Quarterly Journal of the Royal Meteorological Society,* 2005, **131**(612), 3079–3102.
4. J. Berner, G. Shutts, M. Leutbecher, and T. Palmer, *Journal of the Atmospheric Sciences,* 2009, **66**(3), 603–626.

WAVE TURBULENCE INTERACTION INDUCED VERTICAL MIXING AND ITS EFFECTS IN OCEAN AND CLIMATE MODELS

F. Qiao[1,2,3], Y. Yuan[1], C. Huang[1], D. Dai[1,2], J. Deng[1,2,3], and Z. Song[1,2]

[1] First Institute of Oceanography, Qingdao, China, qiaofl@fio.org.cn
[2] Laboratory for Regional Oceanography and Numerical Modeling, Qingdao National Laboratory for Marine Science and Technology, Qingdao, China
[3] Key Lab of Marine Science and Numerical Modeling, State Oceanic Administration, China

Heated from above, the oceans are stably stratified. Therefore, the performance of the general ocean circulation and climate studies through coupled atmosphere-ocean models depend critically on vertical mixing of energy and momentum in the water column. The surface wave, as its spatial scale is too far from that of ocean circulation, is treated as a separate stream from ocean circulation. As a result, oceanic general circulation models (OGCMs) face common problems, including too high simulated sea surface temperature, too cold subsurface temperature and too shallow mixed layer depth especially in summer time, all indicating lack of vertical mixing in OGCMs. We noticed that the surface wave is regarded irrotational mathematically, while real surface wave is rotational, and the surface wave can affect the upper ocean in the scale of wave length, in the order of 100 m, which is equivalent scale of upper mixed layer in OGCMs. We analytically expressed the non-breaking surface wave induced vertical mixing, Bv, as a function of wave number spectrum which can be exactly calculated from a wave numerical model (Qiao et al., 2004). Bv is then confirmed by laboratory experiments (Babanin and Haus, 2009; Dai et al., 2010), and field observations (Huang et al., 2012; Sutherland et al., 2013). Applying Bv into different OGCMs such as MOM4, POM, ROMS, NEMO, FESOM et al, the performances of all OGCMs are improved dramatically (Wu et al., 2015). And Bv can reduce about half the tropical biases of climate models. A specially designed field experimental results indicate that the wave-turbulence interaction induced enhancement of the background turbulence is indeed the predominant mechanism for turbulence generation and enhancement (Qiao et al., 2016).

References

1. F. Qiao, Y. Yuan, Y. Yang *et al*., *Geophysical Research Letter*, 2004, **31**, L11303, doi:10.1029/2004GL019824.
2. A.V. Babanin and B. K. Haus, *J. Phys. Oceangr.*, 2009, **39**, 2675–2679, doi: 10.1175/2009JPO4202.1.
3. D. Dai, F. Qiao, W. Sulisz, L. Han, and A. V. Babanin, *J. Phys. Oceangr.*, 2010, **40**, 2180–2188, doi: 10.1175/2010JPO4378.1.
4. C. Huang, F. Qiao, D. Dai, H. Ma, and J. Guo, *J. Geophys. Res*., 2012, **117**, C00J09, doi:10.1029/2011JC007806.
5. G. Sutherland, B.Ward, and K. H. Christensen, *Ocean Sci*., 2013, **9**, 597–608, doi:10.5194/os-9-597-2013.
6. L. Wu, A. Rutgersson, and E. Sahlee, *J. Geophys. Res*., 2015, **120**, 8210–8228, doi:10.1002/2015JC011329.
7. F. Qiao, Y. Yuan, J. Deng *et al.*, *Philosophical Transactions of the Royal Society of London Series A – Mathematical Physical and Engineering Sciences*, 2016, **374**, 20150201.http://dx. doi.org/10.1098/rsta.2015.0201.

A REVIEW OF GLOBAL AND REGIONAL LIGHTNING LOCATING SYSTEMS WITH EMPHASIS ON TESTING THEIR PERFORMANCE CHARACTERISTICS

V.A. Rakov

University of Florida, Gainesville, Florida, USA, rakov@ece.ufl.edu

Abstract. Both cloud-to-ground and cloud lightning discharges involve a number of processes that produce characteristic electromagnetic field signatures. In general, any observable electromagnetic signal from a lightning source can be used to detect and locate the lightning process that produced it. An overview of the various radio-frequency lightning locating techniques, including magnetic direction finding and time-of-arrival technique, is given. Lightning locating system performance characteristics are discussed. Both cloud and cloud-to-ground flashes are considered. Representative examples of modern lightning locating systems are reviewed. Besides general characterization of each system, the available information on its performance characteristics is given.

There exists a variety of lightning locating techniques that are based on the detection of lightning radio-frequency electromagnetic signals, with accurate locating being possible only by using multiple-station systems. When a single location per cloud-to-ground lightning stroke, typically the ground strike point, is required, magnetic direction finding, the long-baseline time-of-arrival technique, or a combination of the two can be employed. When electromagnetic imaging of the developing channels of any type of lightning flash is required, the VHF time-of-arrival technique or VHF interferometry can be used. Lightning locating systems operating on global scale utilize methods that are capable of extracting source information from electromagnetic signals dominated by ionospheric reflections.

Generally, a modern VLF-MF (MF indicates the medium frequency range, from 300 kHz to 3 MHz) lightning locating system (LLS) is expected to record, in separate categories, and locate over a certain area all or most cloud-to-ground strokes of either polarity, as well as cloud discharges. Also expected for each discharge is a measure of its intensity, usually in the form of peak current inferred from measured electric or magnetic field. Accordingly, system's performance can be evaluated using the following characteristics:

(a) cloud-to-ground (CG) flash detection efficiency;
(b) CG stroke detection efficiency;
(c) cloud discharge detection efficiency;
(d) percentage of misclassified events;
(e) location accuracy (or location error);
(f) peak current estimation error.

In general, the detection efficiency is the fraction (usually expressed in percent) of the total events occurred that are detected by the system and is ideally equal to 100%. In defining the CG flash detection efficiency, probably the most important performance characteristic for lightning locating systems used for the determination of ground flash density, a flash is considered to be detected when at least one stroke of the flash was detected.

The location error is the distance between the actual location and that reported by the system. In general, the location error consists of random and systematic components. The latter in some cases can be accounted for (e.g., site errors in magnetic direction finding systems).

The peak current estimation error is the difference between the actual peak current value and that reported by the system, usually expressed in percent of the actual peak current. Peak currents are estimated by lightning locating systems using either an empirical or model-based field-to-current conversion equation.

In order to evaluate the performance characteristics listed above, independent (ground-truth) data are needed. For example, discharges occurring at a precisely known location equipped with a current-measuring device (tall tower or lightning-triggering facility) can be used for estimating the location accuracy and peak current estimation error. Detection efficiencies and percentage of misclassified events are usually estimated using time-resolved optical recordings. As of today, only a limited number of ground-truth studies have been performed. Results of those studies will be reviewed in the present paper.

ESTIMATION OF THE CO_2 FLUXES BETWEEN THE OCEAN AND ATMOSPHERE FOR THE HURRICANE WIND FORCES USING REMOTE SENSING DATA

D.A. Sergeev, Yu.I. Troitskaya, and **G.N. Balandina**

Institute of Applied Physics, Russian Academy of Sciences, Nizhny Novgorod, Russia
daniil@hydro.appl.sci-nnov.ru

Abstract. CO_2 transfer between the hydrosphere and atmosphere in the boundary layer is an important part of the global cycle of the main greenhouse gas. Modern numerical models based on estimates of all components of the cycle, and taking into account the observed increase in concentration, often result an imbalance that varies over a wide range from year to year. It is comparable with estimates of the annual flux of carbon dioxide between the atmosphere and the ocean. It is customary to associate this imbalance with the problem of the flux correct estimation, since the error in its determination remains high in comparison with the other components of the global cycle. Direction and amplitude of continuous gases exchange in the boundary layer between the atmosphere and the hydrosphere, including carbon dioxide, vary greatly depending on geographical location, season, meteorological and hydrological conditions.

Description of the investigation

Gas flux is determined by the difference of the partial pressures of gas between the atmosphere and hydrosphere, near the border, as well as to a large extent by the processes involving turbulent boundary layer. The latter is usually characterized by power dependence on equivalent wind speed (10-m height). Hurricane-force winds lead to intensive wave breaking, with formation of spray in air and bubbles in water. Such multiphase turbulent processes at the interface strongly intensify gas transfer. Currently, data characterizing the dependence of the gas exchange of the wind speed for the hurricane conditions demonstrate a strong variation. On the other hand, there is an obvious problem of obtaining reliable data on wind speed. Widely used reanalysis data typically underestimate wind speed due to the low spatial and temporal resolution. One of the most promising ways to measure near water wind speed is the use of the data of remote sensing.

In the present study we employed the technique to obtain near water wind speed based on processing remote sensing of the ocean surface data obtained with C-band scattermeter of RADARSAT using the geophysical model function developed in laboratory conditions for a wide range of wind speeds, including hurricanes (see [1]). This function binds wind speed with effective radar cross-section in cross-polarized mode. We used two different parametrizations of gas transfer velocity of the wind speed: (1) used in [2], and (2) obtained by processing results of recent experiment in modeling winds up to hurricane on wind-wave facility [3]. The new method of calculations was tested by the example of hurricane Earl image (09.2010). Estimates showed 13–18 times excess CO2 fluxes rates in comparison with monitoring data NOAA (see. [4]).

Acknowledgements

This work was supported by the Russian Science Foundation projects #14-17-00667 (analysis results in situ measurements) and #15-17-20009 (processing of remote sensing data).

References

1. Yu. Troitskaya, V. Abramov, A. Ermoshkin, E. Zuikova, V. Kazakov, D. Sergeev, A. Kandaurov, O. Ermakova, "Laboratory study of cross-polarized radar return under gale-force wind conditions", *Int. J. Remote Sens*., 2016a, 37(9), 1981–1989.
2. M. Kanamitsu, W. Ebisuzaki, J. Woollen, S.K. Yang, J.J. Hnilo, M. Fiorino, G.L. Potter, NCEP-DOEAMIP-II reanalysis(R-2), *Bull. Am. Meteorol. Soc*., 2002, **83**, 1631–1643.
3. K.E. Krall and B. Jahne, "First laboratory study of air–sea gas exchange at hurricane wind speeds", *Ocean Sci*., 2014, **10**, 257–265.
4. ERDDAP EXPERIMENTAL. AOML Monthly Global Carbon Fluxes dataset. –: http://cwcgom.aoml.noaa.gov/erddap/griddap/aomlcarbonfluxes.graph.

WEAKLY SUPERCRITICAL DYNAMICS OF ROSSBY WAVE PACKETS IN BAROTROPICALLY UNSTABLE ZONAL JET FLOWS

S.V. Shagalov and **G.V. Rybushkina**

Institute of Applied Physics, Nizhny Novgorod, Russia, shagalov@appl.sci-nnov.ru

Abstract. This study explores the supercritical dynamics of Rossby wave packets comprised of unstable barotropic and baroclinic normal modes feeding on the common critical layers (CL) of a stratified barotropically unstable zonal jet flow. Nonlinear generation mechanisms of slowly modulated wave-trains and CL potential vorticity patterns are examined for the regimes of weakly nonlinear and strongly nonlinear dissipative CL.

Barotropic instability is one of the important dynamical processes in the atmosphere and is believed to play an important role in the onset of meandering in planetary jet streams. This study employs the approach developed in [1, 2] to explore the effects arising from stable (in the vertical z-direction) density stratification in a weakly dissipative barotropically unstable β-plane jet stream.

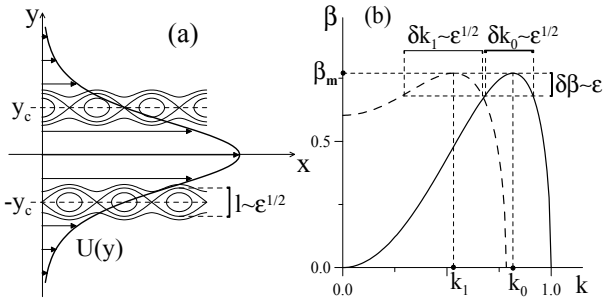

Fig. 1. (a) Streamline patterns in the CL of a zonal jet. (b) Stability boundaries of the barotropic mode (solid line) and the main baroclinic mode (dashed line) for the Bickley jet ($U(y)=\sec h^2 y$).

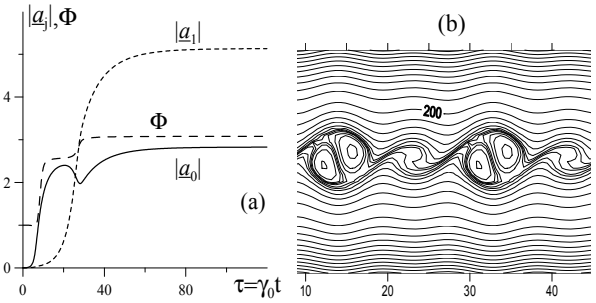

Fig. 2. (a) Evolution of mode amplitudes and phase-locking of resonantly coupled modes. (b) Potential-vorticity pattern formed in the CL from explosive growth of resonantly coupled modes.

Near the onset of the instability the gradient of the Coriolis parameter β is close to a critical value $\beta_m=(U'')_{\max}$ [1]. The basic barotropic flow is capable of supporting Rossby wave packets comprised of unstable barotropic and baroclinic normal modes limited to the narrow bands $\delta k_{0,1}=O(\varepsilon^{1/2})$ around critical wavenumbers $k_{0,1}$ and gaining the kinetic energy of the flow from common CL in the vicinity of latitudes $y=\pm y_c$, where $U(y)=c$ (c is a wave speed of marginal modes) (Fig. 1(a, b)). Employing the methods of multiple scales and matched asymptotic expansions [1, 2] leads to equations governing the evolution of the wave packets amplitudes $a_j(\xi,t)$ and the CL vorticity disturbances $\Omega_\pm(\xi,\eta,z,t)$:

$$\frac{\partial a_j}{\partial t}+(c_{jg}-c)\frac{\partial a_j}{\partial \xi}+i\alpha_j\frac{\partial^2 a_j}{\partial \xi^2}=i\varphi_c^2(j+1)\frac{k_j}{J}\sum_{\pm}\int_0^1\cos(\pi jz)\,dz\int_{-\infty}^{\infty}\left\langle\Omega_\pm e^{-ik_j\xi}\right\rangle d\eta_\pm \quad (j=0,1), \qquad (1),\ (2)$$

$$\frac{\partial\Omega_\pm}{\partial t}\pm U_c'\eta_\pm\frac{\partial\Omega_\pm}{\partial\xi}-2\,\mathrm{Re}\left\{\sum_{n=0,1}ik_n a_n\cos(\pi nz)e^{ik_n\xi}\right\}\frac{\partial\Omega_\pm}{\partial\eta_\pm}=F\left[a_j,\frac{\partial^2 a_j}{\partial\xi^2},\xi,z\right]+\nu\frac{\partial^2\Omega_\pm}{\partial\eta_\pm^{\,2}}, \qquad (3)$$

where $\xi=x-ct$ is a streamwise coordinate, $\eta_\pm=y\mp y_c$, ν is a small viscosity parameter. Under sufficiently small supercriticality with $\delta\beta\ll\nu^{2/3}$ the CL-flow evolves in a weakly nonlinear regime and equations (1)–(3) can be reduced to a set of two coupled Ginzburg-Landau envelope equations (GLE) describing suppression of the baroclinic modes and formation of spatially extended or localized barotropic patterns. In the presence of nonlinear resonant coupling of the modes through the condition $k_0=2k_1$, a nonlinear mechanism of explosive instability comes into play and the GLEs are no longer applicable, even if $\delta\beta\ll\nu^{2/3}$. It has been revealed with the aid of numerical analysis of eqs. (1)–(3) that the flow evolves toward a coherent steady state consisting of the phase-locked barotropic and baroclinic modes equilibrated in the regime of strongly nonlinear CL. This instability scenario is accompanied by the development of coherent potential-vorticity structures inside the common CL taking the form of a zonally modulated barotropic-baroclinic vortex chain (Fig. 2(a, b)).

Acknowledgements

The work was supported by Grant No. 17-05-00747 from the Russian Foundation for Basic Research.

References

1. S.V. Shagalov, V.P. Reutov, and G.V. Rybushkina, *Izv., Atmos. and Oceanic Phys.*, 2010, **46**(1), 95–108.
2. S.V. Shagalov, G.V. Rybushkina, *Progress in Turbulence V, Spring. Proc. in Phys.* 2014, **149**, 189–194.

ON THE DYNAMICAL CHAOS IN BAROTROPIC ZONAL JETS

V.P. Reutov, G.V. Rybushkina, and **S.V. Shagalov**

Institute of Applied Physics of RAS, Nizhny Novgorod, Russia; shagalov@appl.sci-nnov.ru

Abstract. The onset of dynamical chaos in the barotropic quasi-two-dimensional zonal flows is studied. The horizontal Bickley jet in a channel with rigid lateral walls is examined using numerical simulation. As soon as the flow velocity has exceeded the instability threshold, the mode alternation with hysteresis is revealed. It is found that the transition to the dynamical chaos occurs at fairly large supercriticality and may be regarded as the Ruelle-Takens scenario. The peculiarities of the transition due to modification of the flow velocity profile are elucidated.

The large-scale wave-vortex motions in zonal (directed along the Earth parallels) flows arising in the lower atmosphere and in the upper ocean are of interest in connection with weather and climate formation. Generation of such motions is frequently associated with barotropic instability of the horizontal jets [1]. The chains of the wave-vortex structures generated after a maximal jet velocity had exceeded the instability threshold were observed in natural conditions. Similar chains were realized experimentally in annular flows inside of a thin liquid layer [1]. The numerical simulation allows obtaining both vortex chains and quasi-turbulent flow regimes [2], however insuddicient attention was paid to the onset of the complex behavior of the wave field. In this paper the transition to chaotic wave motion in the model jet flows described within the beta-plane approximation [1, 3] is investigated. The influence of the differential rotation (the beta-effect) is assumed to be negligibly small.

We describe the quasi-two-dimensional jet flow in a thin liquid layer using the vertical vorticity component and the stream function [1]. The basic parameters of the problem are two Reynolds numbers: $\mathrm{R} = UL/\nu$ and $\mathrm{R}_\lambda = U/(\lambda L) = \mathrm{R}\nu/(\lambda L^2)$, where L is a transversal scale of the jet, U is a characteristic flow velocity, ν is an effective kinematic viscosity, and λ is an external friction coefficient. The jets are localized in a channel with rigid walls. Two steady-state velocity profiles in the form of the Bickley jet and an asymmetric jet having a small shelf are considered. The periodic boundary conditions are specified along the channel. The pseudospectral method with the discreet Fourier transform in the longitudinal coordinate (including 64 harmonics) and finite differences in the transversal direction (having 200 grid points) was employed. The evolution of the flow regimes due to the increase of U was investigated. The one-fold mode alternation and the hysteresis phenomenon were detected for the Bickley jet, while the continuous alteration of the main mode was obtained in the case of the asymmetric jet. The double vortex street appears in the jets at a critical value $\mathrm{R} = \mathrm{R}_c$ of the instability onset and, with increasing flow velocity, the vortex waves rapidly become nonlinear (containing large multiple harmonics). The longitudinal velocity perturbations and their time derivative were used for drawing the phase planes and the frequency spectra. The transition to chaos in the Bickley jet was found to be due to destruction of a quasi-periodic regime, which occurs at $\mathrm{R}/\mathrm{R}_c \approx 16.2$ and may be treated as the Ruelle and Takens scenario. Note that the same scenario was revealed in [3] within the asymptotic analysis in accord with the nonlinear critical layer concept. The satellites in the frequency spectrum are prooved to be produced by the modulational instability of a nonlinear vortex wave. The occurrence of the dynamical chaos is confirmed by the calculation of the maximal Lyapunov exponent. It is shown that the transition to the dynamical chaos in the asymmetric binary jet also obeys the Ruelle and Takens scenario, but it starts at a smaller supercriticality (when $\mathrm{R}/\mathrm{R}_c \approx 2.25$). Besides, in this case the transition becomes complicated due to the appearance of an interval of frequency synchronization inside which the multifrequency regimes of different complexity alternate.

Acknowledgements

The work was carried out with financial support from the Russian Foundation for Basic Research (project No. 17-05-00747).

References

1. F.V. Dolzhanskii, V.A. Krymov, and D.Y. Manin, *Sov. Phys. Usp.*, 1990, **33** (7), 495–520. https://doi.org/10.1070/PU1990v033n07ABEH002605.
2. H.J. Kwon and M. Mak, *J. Atmos. Sci.*, 1988, **45**(2), 294–308.
3. S.V. Shagalov, V.P. Reutov, and G.V. Rybushkina, *Izv., Atmos. Oceanic Phys.*, 2010, **46**(1), 95–108.

ON LARGE-SCALE LOW-FREQUENCY VARIABILITY OF THE WIND-DRIVEN MIDLATITUDE OCEAN GYRES

I.V. Shevchenko[1] and **P.S. Berloff**[2]

[1] Imperial College London, London, UK, i.shevchenko@imperial.ac.uk
[2] Imperial College London, London, UK

Abstract. We discuss the large-scale low-frequency variability of the midlatitude ocean gyres and their western boundary currents simulated by the eddy-resolving quasi-geostrophic model. We applied EOF analysis to turbulent solutions and extracted robust large-scale decadal variability modes. To interpret these statistical modes dynamically, we linearized the quasi-geostrophic equations around the time-mean circulation and solved the corresponding full set of linear eigenmodes with their eigenfrequencies. We then projected the extracted variability on the eigenmodes and found that this variability is a multi-modal coherent-pattern phenomenon rather than a single mode or a combination of several modes as in flows preceding developed turbulence.

The large-scale low-frequency variability (LFV) of the midlatitude ocean circulation on interannual to interdecadal timescales plays an important role in climate variability. Some of the LFV is imposed by the atmosphere or is due to the ocean-atmosphere coupling, but this study focuses on the intrinsic, oceanic LFV. Since the existence of the LFV was established observationally [1, 2], many studies attempted to determine its patterns and mechanisms. One of the main constraining factors is the computational cost of the eddy-resolving solutions that limited most of these studies to relatively viscous flow regimes characterized by transition to chaos rather than by developed turbulence. Nevertheless, we already know that in eddy-permitting quasi-geostrophic models of ocean gyres, the robust LFV pattern is characterized by changes in the position and shape of the eastward jet and its adjacent recirculation zones [3]. The authors of [4] argue that this LFV is a fundamentally turbulent phenomenon driven by a dynamical competition between the eddy rectification process and the potential vorticity anomalies induced by changes of the intergyre PV transport. This LFV pattern and mechanism have been named the Turbulent Oscillator.

In this work we study the LFV in an eddy-resolving flow regime and propose a new approach for its dynamical interpretation. The key idea is to project the LFV, described here statistically, by its leading Empirical Orthogonal Functions and their Principal Components, onto the dynamically consistent eigenmodes obtained from the governing quasi-geostrophic equations linearized around the underlying time-mean circulation, and, thus, to develop a dynamical interpretation of the LFV. The novelty here is that, by using advanced computational technology, we are able to solve for spatially inhomogeneous eigenmodes of a general 3-d flow with a large number of degrees of freedom, and to analyse and compare individual contributions of these modes to the LFV. The proposed approach can be extended to other idealized or comprehensive ocean models, as well as to highly turbulent flows.

Acknowledgements

The authors are thankful to the Natural Environment Research Council for the support of this work through the grant NE/J006602/1 and the use of ARCHER (the UK National Supercomputing Service).

References

1. C. Deser and M. Blackmon, *J. Climate,* 1993, **6**, 1743–1753.
2. Y. Kushnir, *J. Climate*, 1994, **7**, 141–157.
3. P. Berloff and J. McWilliams, *J. Phys. Oceanogr.*, 1999, **29**, 1925–1949.
4. P. Berloff, A. Hogg, and W. Dewar, *J. Phys. Oceanogr.,* 2007*,* **37**, 2363–2386.

DETERMINATION OF OPTICAL PROPERTIES OF TURBID MEDIA BY MONTE CARLO METHOD

V.V. Toporovsky[1], A.V. Kudryashov[1,2], J.V. Sheldakova[2], and **I.V. Galaktionov[3]**

[1] Moscow Polytechnic University, Moscow, Russia, topor@activeoptics.ru
[2] Institute of Geosphere Dynamics RAS, Moscow, Russia
[3]Active Optics NightN Ltd, Moscow, Russia

Abstract. The distribution of radiation in the turbid media and simulation of optical properties of the media are the most common tasks for description of interaction of incident radiation with scattering centers. Therefore, for description of the path of photons in the media different simulation methods are used: Kubelka-Munk method, diffusion approximation, Monte Carlo method. Among them the most optimal one is the Monte Carlo method, because it gives the most accurate and valid information about the distribution of the radiation inside the media.

The scattering causes decreasing of the sharpness, limiting of the resolution of the image, also blurring image. For enhancement of the modern methods of optical diagnostics of the tissue one should understand full patterns, underlying the photon path. Analysis of patterns can be obtained by computer simulation (Kubelka-Munk method, diffusion approximation, Monte Carlo method [1]). For description of optical properties of turbid media, the phase function ($p(\theta)$), absorption coefficient (μ_a) and scattering coefficient (μ_s) can be used, representing the pattern of photon motion in the media, i.e. showing the probability of either photon absorbed or scattered.

However, optical parameters of turbid media for different wavelengths are commonly unknown or have to be refined. Thus, computational algorithms are used for its determination (e.g. the reverse Monte Carlo method [2]), representing values of absorption coefficient and scattering coefficient. Data obtained after the simulation is compared with experimental results, after that we can estimate optical properties of the media. The Monte Carlo method is based on numerical simulation of the photon distribution. Photons are perpendicularly impinged on the border of the media, then for each step of the simulation, depending on optical properties of the media, the mean free path (random value), the probability of the absorption or the scattering of the photon by the media are calculated and, according to this the direction of the motion of the photon is defined [3].

This method allows splitting up scattering and absorbing parameters of certain biological tissues, that eventually is representing, for example, the value of melanin in the biological tissue [4]. It is necessary for estimation of the concentration and physicochemical features of melanin. It leads to development of new and more effective approaches for diagnostics and treatment of a wide range of skin diseases.

Finally, simulation allows finding the intensity distribution in the model structures corresponding to real experimental data in optical coherence tomography for acquisition of B-scan of the upper layers of dermis and deep blood vessels [5].

Acknowledgements

The work was supported by the Russian Foundation for Basic Research (Grant No. 16-07-01276a).

References

1. I. Sobol, "Numerical Monte Carlo methods", M.: Nauka, 1973.
2. V. Tuchin, S. Utz, and I. Yaroslavsky, "Tissue optics, light distribution, and spectroscopy", *Opt. Eng*., 1994, **33**, 3178.
3. I. Galaktionov, A. Kudryashov, J. Sheldakova, A. Byalko, and G. Borsoni, "Laser beam propagation and wavefront correction in turbid media", *Proc. Of SPIE*, 2015, **9617**, 96170D.
4. A. Bashkatov, E. Genina, V. Kochubey, and V. Tuchin, "Estimate of the melanin content in human hairs by the inverse Monte-Carlo method using a system for digital image analysis", *Quantum Electron*, 2006, **36**, 12.
5. D. Petrov, K.I.S. Galeb, and S. Proskurin, "Optical coherence tomography B-scan simulation using Monte Carlo method with voxel geometry representation of an object", *Fundamental research*, 2016, **5-2**.

WEATHER AND CLIMATE PREDICTABILITY AND ITS RELATION TO PREDICTIVE SKILL

J. Tribbia

NCAR, Boulder Colorado, USA
tribbia@lucar.edu

Traditional model twin predictability experiments lead to a straightforward method of estimating the predictability of both weather and climate variability on time scales of days to decades. Ensemble forecasts correspond to such identical model twin experiments and enable one to calibrate the reliability of predictions and permit the estimate of dynamically and predictability relevant quantities like local Lyapunov exponents and vectors. Predictability estimates for weather and climate variability and their comparison to forecast skill will be given using the NCAR CESM1. As is invariably the case such predictability estimates are useful estimates of predictive reliability only for a short time consistent with linear error and the ensemble estimates become inconsistent at longer forecast times. The nonlinear aspects of uncertainty growth that lead to such behavior will be examined and discussed.

INSIGHTS INTO DECADAL CLIMATE VARIBILITY FROM THE SYNCHRONIZATION OF A NETWORK OF MAJOR CLIMATE MODES

A.A. Tsonis[1,2] and **S. Kravtsov**[1]

[1] University of Wisconsin-Milwaukee, Milwaukee, USA, aatsonis@uwm.edu
[2] Hydrologic Research Center, San Diego, USA

Abstract. We apply ideas from the theory of synchronized chaos to analyze a network of a few major climate indices and show evidence of major climate regime shifts that accompany, and perhaps even define, the observed and simulated decadal climate variability. We also detect differences in the dynamical structure of this variability between the models and observations, which can eventually help understand the current limitations of climate models and guide their further development.

One aspect of climate variability is the synchronization of climate modes. These modes represent low-order subsystems of the climate system. An important element in the theory of synchronization between coupled nonlinear oscillators is the coupling strength. The theory of synchronized chaos [1, 2] predicts that in many cases when such systems synchronize, an increase in coupling strength between the oscillators may destroy the synchronous state and alter the system's behavior. These ideas were initially explored in a network of four climate oscillators, namely El Nino-Southern Oscillation (ENSO), the North Atlantic Oscillation (NAO), the North Pacific Index (NPI), and the Pacific Decadal Oscillation (PDO) [3–5]. Our results indicate that this network in the 20th century synchronized several times. It was then found that in those cases where the synchronous state was followed by a steady increase in the coupling strength between the indices, the synchronous state was destroyed, after which a new climate state emerged. These shifts are associated with significant changes in global temperature trend over decadal time scales. We also find the evidence for such type of behavior in three climate simulations (control and CO_2 forced) using state-of-the-art climate models, and in proxy climate records. Our results indicate that in the four-mode climate network, the direction of influences begins with the North Atlantic coupling to North Pacific, which then couples to the tropical Pacific and back to the North Atlantic [5, 6].

Finally, we show that there exist further significant differences in the dynamics between the different models [7], especially for the surface temperature and precipitation fields – the two fields of great interest in climate projections under increasing amounts of CO_2. This may impose a problem when synchronization between climate models is used to infer the most likely climate response.

Acknowledgements

AAT was supported by NSF grants ATM-0438612 and AGS-1408897; SK was supported by DOE grant DE-FG-03-01ER63260, NASA grant NNG-06-AG66G-1, and NSF grants OCE-1243158 and AGS-1408897.

References

1. L.M. Pecora, T.L. Carroll, G.A. Johnson, and D.J. Mar, *Chaos*, 1997, **7**, 520–543.
2. S. Boccaletti, J. Kurths, G. Osipov, D.J. Valladares, and C.S. Zhou, *Phys. Rep.*, 2002, **366**, 1–101.
3. A.A. Tsonis, K. Swanson, and S. Kravtsov, *Geophys. Res. Lett.*, 2007, **34**, L13705.
4. K.L. Swanson and A.A. Tsonis, *Geophys. Res. Lett.*, 2009, **36**, L06711.
5. G. Wang, K.L. Swanson, and A.A. Tsonis, *Geophys. Res. Lett.*, 2009, **36**, L07708.
6. S. Ineson, and A.A. Scaife, *Nat. Geosci.,* 2009, **2**, 32–36.
7. K. Steinhaeuser and A.A. Tsonis, *Clim. Dyn.,* 2014, **42**, 1665–1670.

International Symposium

TOPICAL PROBLEMS OF NONLINEAR WAVE PHYSICS

Magnetic Fields in Laboratory High Energy Density Plasmas (LaB)

Chair

Julien Fuchs, CNRS, Ecole Polytechnique, France

Coordinators

Andrea Ciardi,	Sorbonne University-UMPC, Observatoire de Paris, France
Dustin Froula,	Laboratory for Laser Energetics, University of Rochester, USA
Emmanuel d'Humières,	Univ. Bordeaux, CNRS, CEA, CELIA, France
Hantao Ji,	Princeton University, USA
Mattias Marklund,	Chalmers University of Technology, Sweden
Sergey Pikuz,	JIHT, RAS, Russia
Carlo Rizzo,	U. Toulouse, LNCMI-CNRS, France

Invited

GENERATION AND DETECTION OF SUPER-STRONG MAGNETIC FIELDS BY ULTRA-INTENSE LASER PULSES

A.A. Andreev[1,2] and **Z. Lech**[2]

[1] Sankt Petersburg State University, St. Petersburg, Russia
[2] ELI-ALPS, Szeged, Hungary

Magnetic fields are one of the fundamental entities which influence nature on all scales. Developments of laser technology stimulated exploration of methods for generating large magnetic fields from laser pulses directly or via interaction with plasma or solid targets. The generation of high amplitude solenoidal fields described in this presentation is based on the interaction of a screw-shaped laser pulse interacting with an under-dense plasma. This interaction creates a multi-gigaGauss magnetic field within a volume of 10s μm transverse dimensions, depending on the plasma density and laser pulse parameters. The detection of strong magnetic fields by laser accelerated particles is considered.

Invited

MODELLING OF ACCRETION PROCESSES IN MAGNETIZED BINARY STARS

D.V. Bisikalo

Institute of Astronomy of the RAS, Moscow, Russia

We present a review of physical processes occurring due the mass transfer between the components of close binary stars. To study the main properties of accretion disks and envelopes in various types of binaries we use results of three-dimensional HD and MHD numerical simulations. Special attention is paid to the description of the magnetic field influence on accretion processes. The main observational manifestations of the numerically found flow structure elements are also presented.

Invited

MECHANISMS OF ASTROPHYSICAL JET FORMATION, AND COMPARISON WITH LABORATORY EXPERIMENTS

G.S. Bisnovatyi-Kogan

Space Research Institute of RAS, Moscow, Russia
and
National Research Nuclear University MEPhI, Moscow, Russia
Email: gkogan@iki.rssi.ru

Jets are observed in young stellar objects, X-ray sources, and active galactic nuclei (AGN). The mechanisms of jet formation may be divided into regular, acting continuously for a long time, and explosive ones [1]. Continuous mechanisms are related to electrodynamics and radiation pressure acceleration, hydro- dynamical acceleration in the nozzle inside a thick disk, acceleration by relativistic beam of particles. Explosive jet formation is connected with supernovae, gamma ray bursts and explosive events in galactic nuclei. Mechanisms of jet collimation may be connected with magnetic confinement or pressure of external gas [2–4]. Explosive formation of jets in laboratory is modeled in the experiments with powerful laser beam, and plasma focus [5, 6].

References

1. G.S. Bisnovatyi-Kogan and R.V.L. Lovelace, *Astro.Ap*, 1995, **296**, L17.
2. G.S. Bisnovatyi-Kogan, B.V. Komberg, and A.M. Friedman, *Astron.Zh*., 1969, **46**, 465.
3. R.D. Blandford and M.J. Rees, *MNRAS*, 1974, **169**, 395.
4. G.S. Bisnovatyi-Kogan, *MNRAS*, 2007, **376**, 457.
5. V.I. Krauz *et al*., *Physics of Plasma*, 2010, **36**(11), 997.
6. V.S. Belyaev, *Quantum Electronics*, 2004, **34**(1), 41.

Invited

INVESTIGATING GUIDE FIELD RECONNECTION IN HED PLASMAS

S. Bolaños[1,2], **R. Smets**[3], **R. Riquier**[4], **A. Grisollet**[4], and **J. Fuchs**[1,2]

[1] LULI - CNRS, École Polytechnique, CEA: Université Paris-Saclay; UPMC Univ Paris 06: Sorbonne Universités - F-91128 Palaiseau cedex, France
[2] Institute of Applied Physics, 46 Ulyanov Street, 603950 Nizhny Novgorod, Russia
[3] LPP, University P. & M. Curie, CNRS, Ecole Polytechnique, F-91128 Palaiseau, France
[4] CEA, DIF, Bruyères-le-Chatel, France

Magnetic reconnection (MR) is a process which occurs in many astrophysical plasmas, e.g. in solar flares, in coronal mass ejecta, or at the outer boundary of the Earth magnetosphere. However, as of now, the fundamental microphysics implied in this process is far from being well understood. Most of the investigations on this long standing issue come from numerical studies and space observations. Laboratory modelling of plasmas, including those that can be generated by high-power lasers, offer now new perspectives to investigate MR and the processes governing it.

Investigating MR in high-energy-density plasmas (HEDP) such as those produced by lasers is also, beyond allowing progress on its fundamental understanding, an important issue for Inertial Confinement Fusion (ICF). In ICF, a number of laser spots irradiate the inner holhraum cavity and around each of these irradiated spots, a toroidal magnetic field is self-generated. Between the close-by magnetic ribbons, magnetic reconnections can occur and the process converts the magnetic potential in kinetic energy and heat which might affect the overall drive of the inner DT fuel.

We will present recent experiments, performed using the LULI2000 facility, aimed at investigating the dynamic of magnetic reconnection in a non-coplanar configuration between two magnetic toroids induced by two near-by laser spots irradiating solids targets. Despite being distinct from the astrophysical plasmas where the beta parameter is low (~10^{-3} in solar corona and ~1 in solar winds), such HEDP reconnection experiments are of interest to investigate fundamental issues in MR such as the influence of a guide field and of a quadrupolar Hall structure of the magnetic field on the dynamic of the MR. A non-coplanar configuration between the two laser-irradiated targets, as was investigated in our experiments, allows to initialize a guide field or a quadrupolar Hall structure of the magnetic field. The reconnection rate in the experiments has been diagnosed with proton radiography which provides a unique way to measure and map directly the distribution of the strong magnetic fields and their evolution. We observe that the Hall component and the guide field speed up or slow down the MR, depending on the setup between the two laser-irradiated targets, and hence between the two magnetic toroids that are made to interact. The measurements are compared to simulations performed by a hybrid simulation code, the 3D HECKLE code. This simulations have been initialized, with respect to the initial magnetic toroid, by calculations using a hydro-radiative code (FCI2) and experimental measurements.

Invited

RELATIVISTICALLY STRONG LASER PLASMA INTERACTION: ENERGETIC PARTICLES, GAMMA AND THZ RADIATION, MAGNETIC FIELDS

A.V.Brantov[1,2] and **V.Yu. Bychenkov**[1,2]

[1] P.N. Lebedev Physics Institute (LPI), Russian Academy of Science, Moscow, 119991, Russia
e-mail: brantov@sci.lebedev.ru
[2] Center of Fundamental and Applied Research (CFAR), VNIIA, ROSATOM, Moscow, 127055, Russia

Abstract. We review recent developments in LPI and CFAR research related to the production of energetic ions and electrons, generation of strong quasi-static magnetic fields, and emission of secondary electromagnetic radiation in the interaction of short relativistically intense laser pulses with different targets.We present theoretical models and 3D PIC simulations on optimization of charged particle acceleration from thin foils and low-dense targets and several schemes for generation of THz pulses, gamma radiation and quasi-static magnetic fields.

The laser-plasma methods of charged particle acceleration, production of secondary radiation from THz to gamma range, and generation of strong magnetic fields attract a lot of attention due to numerous potential applications for astrophysical science, inertial fusion, nuclear physics, material science, biology and medicine.

Ion acceleration. The 3D PIC simulations demonstrate effective ion acceleration from the interaction of intense ultrashort linearly polarized laser pulses with both ultrathin solid dense foils and low-density targets when the laser energy ranges from several millijoules to tens of joules. The optimum foil thickness and the corresponding maximum energy of the accelerated ions for a given energy of the laser pulse were found. A new, maximum proton energy scaling law with the laser pulse energy has been derived for solid density foils. A new effective scheme has been proposed for synchronized laser-triggered ion acceleration by a slow light pulse of relativistic intensity, which penetrates into a near-critical-density plasma, strongly slows, and then increases its group velocity during propagation within a target. The charge particle acceleration by linearly and circularly polarized laser pulses has been compared to find laser intensity for which circular polarization gives some advantage in particle acceleration.

Magnetic fields.We have studied by means of 3D PIC simulations and analytical theory magnetic field generation due to the inverse Faraday effect during the interaction of intense circularly polarized laser beams with underdense plasma in the regime of parameters corresponding to a relativistic self-focusing and laser pulse channeling. We have demonstrated for the cases of both full and without full evacuation of electrons that magnetic field generation results from inverse Faraday effect and the quasistationary magnetic field spatial distribution is well approximated by the solution to the theoretical model. We also studied magnetic field generation in interaction of short relativistically intense laser pulses with solid target of specially designed shape that that provides extremely strong field strength.

Electron acceleration and gamma radiation. Different regimes of electron acceleration from solid foils and low-density targets are investigated using 3D PIC simulations. The size of the plasma corona is shown to be the main parameter characterizing the temperature and number of hot electrons, which determine the yield of gamma radiation and its hardness. The latter has been studied from Bremsstrahlung by using different target-converters.

Terahertz emission. The theory of terahertz radiation in laser-induced charge separation in the planar plasma target has been developed. Both bulk and surface terahertz (THz) pulses can be generated by electron bunch leaving the target and/or by a moving front of the spatial charge separation of expanding plasma. These mechanisms responsible for generating bulk and surface THz radiation are refined and compared. We also performed both theoretical study and full-wave Maxwell simulation of laser-triggered excitation and following propagation of the terahertz pulse on the wire targets in the form of Sommerfeld surface waves. It has been shown that considerable fraction of the generated surface wave energy can be transported from the wire to the free space.

Acknowledgements

This work was supported by the Russian Foundation for Basic Research.

Invited

MAGNETIC FIELD AMPLIFICATION AND PARTICLE ACCELERATION IN LABORATORY ASTROPHYSICS

L. Chen

University of Oxford, UK

Cosmic rays have fascinated scientists for more than a century. One possibility is that cosmic rays are accelerated to such high energies through the process of Fermi acceleration, where particles gain energy by scattering off of magnetic field turbulence. The generation and amplification of magnetic fields is thus a crucial step in the understanding of cosmic ray acceleration. The standard model for the amplification of magnetic fields is via the stochastic tangling of small seed fields (either generated by plasma or primordial processes) – the turbulent dynamo mechanism. In this talk we will discuss the basic theory behind turbulent dynamo and its connection with particle acceleration in astrophysical environments. We will also discuss novel laboratory experiments that may help to shed lights in the understanding of these complex processes. The relatively new field of laboratory astrophysics aims at bringing together teams from around the world using the largest most powerful lasers in the world to create scaled astrophysical environments to look into magnetic field amplification and particle acceleration by turbulence.

Invited

ION INTERACTIONS WITH DENSE PLASMAS IN MAGNETIZED AND UNMAGNETIZED CONFIGURATIONS

J. Fuchs

LULI, Ecole Polytechnique, 91128 Palaiseau cedex, France
julien.fuchs@polytechnique.edu

I will present experimental work aimed at investigating the development of the streaming instability driven by the interaction of energetic ions -streaming along a magnetic field- with a background plasma, and its effects on the beam and background plasma. Beyond its interest as a fundamental phenomenon in plasma physics, the understanding of the streaming instability could be key to help explaining the observed anomalous ionization of dense clouds in the inter-stellar medium (ISM). Although numerical simulations underline the important role streaming instabilities play in space plasmas, the presence of a variety of growing and competitive modes, and the complex behaviour of such systems mean that our knowledge is still far from being complete.

To experimentally study this instability, we have exploited and coupled several experimental configurations that are well-assessed by our group: the generation of fast ion beams driven by short-pulse lasers, the generation and characterization of well-controlled background plasma in which the ions are propagated, and strong external magnetization of this system. Results will be presented and discussed.

Invited

LASER-DRIVEN ION ACCELERATIONS WITH SUBMICRON CLUSTER TARGETS: CONTRIBUTIONS OF MAGNETIC VORTEXES

Yu. Fukuda

Kansai Photon Science Institute (KPSI), National Institutes for Quantum and Radiological Science and Technology (QST), Kyoto, Japan
fukuda.yuji@qst.go.jp

Abstract. An approach for accelerating ions due to the formation of a strong dipole vortex structure in subcritical density plasmas, with the use of a cluster-gas target, is presented. Ions with energy 10–20 MeV per nucleon having a small divergence (full angle) of 3.4 are generated in the forward direction with an ultrashort pulse laser of 150-mJ energy and 40-fs duration, corresponding to approximately tenfold increase in the ion energies compared to the TNSA experiments using thin foil targets.

Laser-driven ion accelerations have been one of the most active areas of research during the last several years because the accelerated ion beams have unique properties such as ultrashort duration, high brilliance, and low emittance [1].

Here we present the tenfold enhancement of the accelerated ion energy due to the formation of a strong dipole vortex structure in subcritical density plasmas with the use of a cluster-gas target [2]. The experiment has been conducted using the JLITE-X 4 TW Ti:sapphire laser at KPSI. The laser delivers 40-fs pulses of 150 mJ energy at a 1 Hz repetition rate with a contrast ratio of 10^6. A pulsed solenoid valve connected to a specially designed circular nozzle was used to produce submicron-size CO_2 clusters embedded in He gas. Under the action of the prepulse accompanying the main laser pulse, the clusters are expected to be evaporated forming a near-critical inhomogeneous density plasma with its profile determined by the initial density distribution of the cluster-gas target. The high energy ions were generated when the laser beam was focused near the rear side of the gas jet.

The high energy ions were measured with a stack of CR-39 detectors. The energy range of the ions is determined quantitatively from the extent of the tracks recorded in the CR-39 stack by calculating their stopping ranges. We observe the ion tracks in CR-39 up to the 11th layer and none in the 12th layer. This penetration depth corresponds to maximum energies of 10, 17, and 20 MeV per nucleon for helium, carbon, and oxygen ions, respectively. Further evidence for high energy ion production was obtained from the time-of-flight (TOF) measurements, where the maximum ion energy is measured to be 18.5±1 MeV per nucleon. This corresponds to approximately tenfold improvement of the accelerated ion energy compared to the previous experiments with solid targets.

In order to elucidate the ion acceleration process, we formulate a simple model of the magnetic vortex acceleration which explains a high-energy ion generation from near-critical density plasmas [2, 3, 4]. Ultraintense laser pulses propagating in near-critical density plasmas generate magnetic dipole vortex structures. In the region of decreasing plasma density, the vortex expands both in forward and lateral directions. The gradient of magnetic field pressure leads to the formation of shell structure and column of ions surrounding the magnetic field. This also leads to the charge separation at the head of the dipole vortex and induces a longitudinal electric field. This structure moves together with the expanding dipole vortex. As shown in Fig. 1, the background ions located ahead of the electric field are accelerated to high energies.

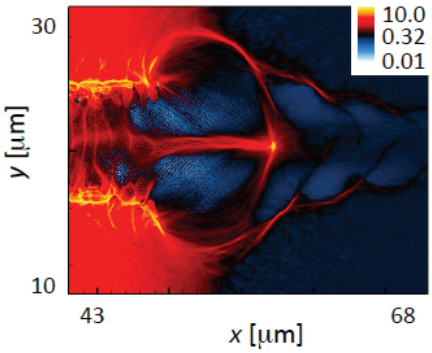

Fig. 1. Distribution of ion density normalized by the critical density ($n_c = 2{\cdot}10^{21}$ cm^{-3}) at t = 320 fs. An ion shell surrounding the vortex and an ion wall along the vortex axis are formed

The energy scaling of ions generated by this magnetic vortex acceleration mechanism is derived and corroborated using particle-in-cell (PIC) simulations. The scaling suggests that the magnetic vortex acceleration can enhance the ion energy by using near-critical density plasmas, and a 100 TW-class laser is capable to generate 200 MeV protons [4].

References

1. A. Macchi *et al*., *Rev. Mod. Phys*., 2013, **85**, 751.
2. Y. Fukuda *et al*., *Phys. Rev. Lett*., 2009, **103**, 165002.
3. S.V. Bulanov and T. Zh. Esirkepov, *Phys. Rev. Lett*., 2007, **98**, 049503.
4. T. Nakamura *et al*., *Phys. Rev. Lett*., 2010, **105**, 135002.

Invited

ON KINETIC APPROACH TO MAGNETIC RECONNECTION: FROM SPACE TO LASER HED PLASMA

V.M. Gubchenko

Institute of Applied Physics, Nizhny Novgorod, Russia, ua3thw@appl.sci-nnov.ru

Ideas of the magnetic reconnection (MR) first appeared in space physics, later in astrophysics as an explanation of the initial magnetic structure reconfiguration in a selfconsistent way due to some dissipation effects near weakly magnetized regions. Firstly, MR was treated in terms of nonideal MHD developed up to the level of application of the electron MHD dealing finally with temperature anisotropic plasma. Secondly, at the beginning with growing space probes power it was clear that the kinetic approach operating with the shape of the particle VDF (velocity distribution function) and in terms of the Vlasov equation is more adequate for the MR reality by providing the solar corona structuring and heating and for magnetosphere formation by solar wind flow. The argument is that plasma is collisionless and very hot but relatively slowly moving, which provides strong dissipative effects due to "resonant" electron acceleration. Here, 1D current sheet physics was the basis of analytics, and the e.m. PIC was the only instrument to move to the 3D MR. Recently, the 3D analytics in kinetics began its development for expanding plasma cases: it is based on new e.m. dimensionless plasma parameters and new resistive and diamagnetic plasma electromagnetic scales. The rebirth of the MR are the magnetic events in subcritical laser plasma which strongly corrected results of electrostatic consideration of plasma expansion perpendicular to the magnetic field. Theory shortly repeats now long time evolution of the space plasma methods from MHD to electron kinetics which correlates with the increase in laser power and with transition to consideration of the e.m. processes in the HED plasmas.

Acknowledgements

This work was supported by a megagrant (contract № 14.Z50.31.0007), by the RFBR (projects Nos. 14_02_00133 and 17_02_00910), and programs of the OFN and the Presidium of the RAS.

References

1. V.M. Gubchenko, http://www.vniitf.ru/images/zst/2012/s3/3-13.pdf .
2. V.M. Gubchenko, *Geomagnetism and Aeronomy*, 2015, **55**(7), 831-845 and **55**(8), 1009–1025. DOI: 10.1134/S0016793215070099, 10.1134/S0016793215080101.

Invited

LASER PLASMA EVOLUTION IN EXTERNAL 10 T MAGNETIC FIELD

Guang-yue Hu, Yi-han Liang, Hui-bo Tang, Yang Zuo, Yu-lin Wang, Bin Zhao, Ping Zhu, and **Jian Zheng**

Department of Modern Physics & CAS Key Laboratory of Geospace Environment,
University of Science and Technology of China (USTC), Hefei, Anhui Province, China
E-mail: gyhu@ustc.edu.cn

A Magnetized Laser Plasma Facility was built at USTC, which is composed of a nanosecond heating laser beam (6 J / 527 nm / 7 ns), a femtosecond detecting laser beam (2 mJ / 800 nm / 50 fs), and a 7-30T pulsed magnetic field generator. A series of laser plasma evolution experiments were performed at USTC.

(1) When a high-speed plasma stream, produced by laser ablated solid target,is expanding in an external transverse magnetic field, we found that the laser plasma forms an asymmetric hollow plasma bubble caused by the plasma accumulation at the plasma-magnetic field interface. The asymmetry of the plasma bubble can be reversed by turning the direction of the magnetic field. The plasma, streaming along the surface of the plasma bubble, converges at the head of the bubble and generates a plasma jet moving freely across the magnetic field. Hall MHD simulation shows that the asymmetry of the bubble is induced by the Hall effect. It indicates that the jet's movement is supported by the E×B drift that E is contributed by the self-polarization electric field –V×B.

(2) Plasma optical images and the ablation holes on the target show that the laser ablation is enhanced by using the external 7T magnetic field. The laser plasma is confined by the magnetic field and forms a plasma bubble surrounding the laser focus spot. The target surface, which contacts the plasma bubble, is heated by the energy transport along the surface of the plasma bubble. Thus the debris and the target surface surrounding the laser focus spot are ablated and increases the plasma generation.

(3) When an external magnetic field was added along the laser channel in underdense plasma, we found that the electron thermal transport was suppressed by the magnetic field, which enhanced the plasma temperature. It can be used to restrain the stimulated scattering process in laser fusion. We found that 20–30T external magnetic field is needed to mitigate the stimulated scattering process at the Shenguang-Ⅲ primary laser facility of China.

Invited

STUDY OF PHYSICAL PROCESSES AT HIGH ENERGY DENSITIES WITH THE USE OF EXPLOSIVE MAGNETIC GENERATORS

A.V. Ivanovsky

Russian Federal Nuclear Center – VNIIEF
37 Mira ave., 607188 Sarov, Nizhniy Novgorod region, Russia
ivanovsky@elph.vniief.ru

One of the methods to produce high energy density during modeling of physical processes and studies of material properties is to convert the kinetic energy of a high-speed shell or a liner. Traditionally, the liners are driven by:

– an explosive charge (HE) on gas-dynamic complexes;

– a current pulse on electrophysical facilities;

– radiation on laser facilities.

The paper will present these methods, will evaluate maximum attainable velocities and pressures, will compare the possibilities of providing symmetry and effect controlling, as well as recovery of the explored samples for subsequent analysis.

The electrophysical methods of research:

– provide better monitoring of parameters and obtained data in comparison with gas-dynamic complexes;

– allow studying the big-size samples (scale factor) in comparison with laser facilities.

The already realized and the planned experiments with the use of explosive magnetic generators (EMG) will be overviewed.

In the area of relatively low specific energies (to ~10 kJ/g) of interest are the studies of the rheological properties of matter, i.e. spall and shear strength, eject processes at shock wave release to the surface, etc. The use of EMG ensures high accuracy of control and reproducibility of loading parameters, and in some cases the recovery of the explored samples for further metallographic analysis.

In the intermediate region of specific energy (up to hundred kilojoules per gram) it would be interesting to investigate the equations-of-state of materials (EOS) and turbulent mixing. The paper will present the experimental test bench on the basis of a small-class disk EMG, making it possible to conduct high-precision measurements of the EOS (2–3%) at shock and isentropic compression by 2–3 Mbar pressure and to add significantly the existing experimental data (to 10^5 g_0) for turbulent mixing of substances at acceleration to 10^8–10^9 g_0.

Lasers are the most appropriate tool to conduct studies in the region of high (more than 1 MJ/g) energy densities. The laser facilities allow reaching the radiation temperatures of 250–300 eV. The experiments on Z-machine (SNL, USA) demonstrated that the electrophysical facilities, able to produce the currents of tens of MA for the time of ~100 ns, can be an alternative to lasers. The achieved level of energy generated by Z-pinch in the X-radiation compares well with lasers. However, in view of worse organization of energy for realization of radiation temperature of 250–300 eV it is necessary to construct the electrophysical facilities one order more powerful that Z-machine. To realize the above-mentioned temperatures, we need the energy of tens of megajoules in the X-radiation. At this the electrophysical facilities may add the lasers in scale effects modeling.

To achieve the laser energy densities using the EMG, it is necessary to resolve the problem of current pulse sharpening to 100 ns. The paper will discuss the ways to solve this problem. In case the current pulse sharpening technology is realized, the middle-class disk EMGs can serve the basis for a creation of an explosive analogue of Z facility, and this opens the way to realization of one-shot explosive experiments with the use of a super-power EMG and generation of Z-pinch X-radiation of tens of MJ.

Invited

CONFINEMENT OF HIGH ENERGY DENSITY PLASMA PRODUCED BY THE INTERACTION BETWEEN HIGH INTENSITY LASER AND STRUCTURED MEDIUM

Y. Kishimoto[1], D. Kawahito[1], T. Okihara[1], H. Sakaguchi[2], K. Fukami[3], and **Y. Fukuda[4]**

[1] Graduate School of Energy Science, Kyoto University, Uji, Kyoto, Japan, 611-0011
[2] Institute of Advanced Energy, Kyoto University, Uji, Kyoto, Japan, 611-0011
[3] Graduate School of Engineering, Sakyou-ku, Kyoto, Japan, 606-8501
[4] Kansai Photon Science Institute, National Institute for Quantum Radiation and Technology Kizu, Kyoto, Japan, 619-0215

We study a high energy density plasma produced by the interaction between high intensity short pulse laser and matter. Such a plasm is highly non-stationary and non-equilibrium regulated by multiply charged high-*Z* ions, high energy relativistic electrons, quasi-static and/or low frequency electromagnetic fields, and X-rays. Therefore, the plasma opens up many innovative applications including the study of astrophysics utilizing the nature of such an extreme state. However, the difficulty is the time scale that the plasma is sustained, i.e. the life time, which is very short and is determined by the inertia [1].

Here, we try to confine such a high energy density plasma exceeding the inertia time. For this purpose, we introduce a target having structures with sub-micro scale incorporating with an externally applied magnetic field. We refer to it as *structured medium* to which the high intensity short laser is irradiated. Here, by carefully choosing the strucure, we extract the function that the plasma is self-organized and then confined.

Here, we study the self-organization dynamics using the extended particle based integrated code (EPIC) [2], which includes atomic process and collisional relaxation process. We embed the medium in a magnetic field on the order of kT and irradiate it with the laser in the range of $10^{19–22}$ W/cm^2. High absorption of laser energy is achieved leading to a high energy density plasma. The applied ambient magnetic field is immediately scrambled by the complex plasma motion leading to a state dominated by magnetic turbulence. However, we found that the plasma is self-organized to a coherent structure regulated by magnetic vortices, which field strength is of the order of a magnitude higher than that of the initially applied magnetic field. The structure is similar to the z-pinch, where the high density plasma is confined on a longer time scale exceeding inertia time scale, so that it continues emitting high intensity X-rays.

Generation of magnetic vortices results from the flux transfer from the ambient open field line advected by the background plasma flows to the closed one around the rod through successive reconnections. This is similar to the interaction between magnetic field convected by the solar wind and Earth' magnetic field. Furthermore, collisions and merging of different magnetic vortices take place on a slower time scale through reconnection, which produce high density plasma acceleration.

References

1. T. Tajima, Y. Kishimoto, and M. Downer, *Physics of Plasmas*, 1999, **6**, 3759.
2. Y. Kishimoto, T. Masaki, and T. Tajima, *Phys. Plasmas*, 2002, **9**, 589.

Invited

LASER-PLASMA MAGNETIZATION FOR LABORATORY ASTROPHYSICS

Ph. Korneev[1], E. d'Humieres[2], V. Tikhonchuk[2], and **T. Pisarczyk[3]**

[1] NRNU MEPhI, Moscow, Russian Federation, korneev@theor.mephi.ru
[2] University of Bordeaux—CNRS—CEA, CELIA, Talence, France
[3] Institute of Plasma Physics and Laser Microfusion, Warsaw, Poland

Abstract. Spontaneous plasma magnetization is a common process in laser-plasma interaction. The magnetic field amplitudes depend on laser intensity, and may reach kilotesla and even higher level in relativistic regime. One of the most interesting features of these fields is that they can be "frozen" inside the laser-generated plasmas, hot, low collisional, or even relativistic and collisionless. This property makes such plasmas very attractive for studies of astrophysical-related laboratory studies. Here, we present some possibilities to facilitate the generation of the magnetized collisionless plasmas with controllable magnetization.

Magnetized plasmas is a usual object in Space. On the Earth, with the modern laser facilities, it became possible to perform experimental studies, which can reproduce some of the observations at least in simplified test models [1]. However, magnetization still is a tricky parameter, which demands normally powerful discharge banks or secondary discharge-coil targets and enough time during for target magnetization. However, there are several known self-magnetization mechanisms, which looks promising in the context. The most known correspond to plasma magnetization due to fast electron currents, discharge currents and Biermann battery effect.

In this work, we present several possible schemes, which may facilitate magnetization of laser-produced plasmas at the time of its preparation, i.e. these are the schemes for the production of a plasma with a controllable magnetization parameter. They deal with the relativistic directly accelerated electrons, discharge currents, and fast electron currents in sub-relativistic regimes.

With curved target, known as "snail" or "escargot"-shaped targets [2], the most important currents are directly accelerated electrons (at relativistic intensities) and discharge currents. The curved targets were already tested recently in different regimes, and demonstrated a very interesting physics. Within the scheme, it may become possible to produce hot collisionless plasma flow with magnetization parameter in wide range. Another scheme, based on the target chirality [3], uses mainly discharge currents, it may be interested in astrophysical context for generation of magnetized jets.

Also, in this work, within the frames of the sub-relativistic interaction, plasma magnetization mechanisms were revisited. It was found that kinetic magnetization due to fast electrons is crucially important and may provide quite interesting for astrophysical context magnetization level. In this concept, a possible generalization of the normal-incidence reconnection geometry [4] was considered.

As we show, a general approach of considering laser plasma magnetization to be a controllable parameter within self-magnetization scenario is reasonable and it opens wide possibilities in astrophysical-related research in laser laboratories.

Acknowledgements

The work is in part supported by the French National funding agency ANR within the project SILAMPA, it was granted access to the HPC resources of CINES under allocation 2016-056129 made by GENCI (Grand Equipement National de Calcul Intensif). Ph. Korneev was supported by RFBR 16-52-50019-JF. This work was also supported by the Access to the PALS RI under the EU LASERLAB IV project (Grant Agreement No. 654148), by the Ministry of Education, Youth and Sports of the Czech Republic, Grant No.: LM2015083 (PALS RI) and CZ COST Project LD14089, and by the Czech Science Foundation, project P205/11/P712.

References

1. Remington *et al*., *Physics of Plasmas*, 2000, **7**, 1641.
2. Korneev *et al*., *Phys. Rev. E*, 2015, **91**, 043107.
3. Korneev *et al*., *New Journal of Physics*, 2017, **19**, 033023.
4. Nilson *et al*., *Phys.Rev.Lett*., 2006, **97**, 255001.

Invited

EXPERIMENTAL STUDY OF ACCRETION PROCESSES IN X-RAY BINARY STARS USING AN EXTERNAL B-FIELD

F. Kroll[1,*], A. Pelka[1], B. Albertazzi[2], F. Brack[1], E. Brambrink[2], T. Cowan[1], P. Drake[3], E. Falize[4], E. Filipov[5], Y. Kuramitsu[6], C. Kuranz[3], D. Lamb[7], J. Levesque[3], C. Li[8], M. Manuel[3], T. Michel[2], T. Morita[9], N. Ozaki[10], S. Pikuz[5], G. Rigon[2], M. Rödel[1], Y. Sakawa[10], U. Schramm[1], H. Shimogawara[10], L. Van Box Som[4], and **M. Koenig[2]**

[1] Helmholtz-Zentrum Dresden - Rossendorf, Bautzner Landstraße 400, 01328 Dresden, Germany
[2] LULI - CNRS, Ecole Polytechnique, F-91128 Palaiseau cedex, France
[3] University of Michigan, Ann Arbor,MI 48109, USA
[4] CEA-DAM-DIF, F-91297 Arpajon, France
[5] JIHT-RAS, 13-2 Izhorskaya st., Moscow, 125412 Russia
[6] Department of Physics, National Central University, No. 300, Jhongda Rd., Jhongli, Taoyuan, 320, Taiwan
[7] Flash Center for Computational Science, University of Chicago, IL 60637, USA
[8] Plasma Science and Fusion Center, Massachusetts Institute of Technology, USA
[9] Department of Energy Engineering Science,Faculty of Engineering Sciences,Kyushu University, Japan
[10] Institute of Laser Engineering, Osaka University, Suita, Osaka 565-0871, Japan
* florian.kroll@hzdr.de

Abstract. Here we report on recent results from experiments carried out at LULI2000 using the nanosecond beam to generate a high-density plasma flow by laser-driven rear-side shock breakout. The sample was positioned inside a pulsed coil generating a magnet field of ~15T in order to study the influence of the magnetic field on the plasma flow. In addition, an obstacle was placed behind the sample to investigate the formation of a return shock. As diagnostics we used laser-driven X-ray point projection radioscopy driven by the pico2000 beam and optical Schlieren Imaging, shadowgraphy, and Streaked Optical Pyrometry from two sides.

Accretion processes are among the most important phenomena in high-energy astrophysics since they are widely believed to provide the power supply in various astrophysical objects and they are the main source of radiation in several binary systems [1]. Understanding the complex physical processes that allow releasing gravitational energy in the form of radiation is fundamental to interpret the high-energy astronomical observations [2]. Among the different X-ray binary systems are cataclysmic variable stars, close binary systems containing a white dwarf that accretes matter from a late type Roche-lobe filling secondary star [3]. They provide unique insight on accretion processes in extreme astrophysical regimes since sources of luminosity other than the accretion region itself are relatively weak.

In some cataclysmic variable stars, the magnetic field is strong enough (B >10MG) to prevent the formation of an accretion disk and to channel the accreting plasmas onto the compact object magnetic poles, leading to the formation of an accretion column and impacts the white dwarf atmosphere. By fulfilling similarity properties and scaling laws these processes can be scaled to laboratory length and time scales und thus can be studied using high energy laser-matter interactions. [4] Up to now experiments used a tube in order to collimate the plasma flow generated [5]. This induced spurious effects such as wall shocks and tube explosion that should be avoided. Here we instead applied a pulsed high-field magnetic coil in order to study the coupling of radiative processes in a supersonic plasma flow with magnetic effects. Both the dynamics of high-density and low-density regions of the flow were investigated by utilizing a combination of X-ray radiography and optical Schlieren imaging.

References

1. J. Frank, *et al*., *Cambridge University Press*, 2002.
2. J. M. Bonnet-Bidaud, *et al*., *Astronomy & Astrophysics*, 2015, 579.
3. B. Warner, *Cambridge Edition*, 2003.
4. E. Falize, *et al*., *Astrophysical Journal*, 2011, 730.
5. B. Loupias *et al*., Supersonic jet experiments using a high-energy laser, *Phys. Rev. Lett*., 99, 265001.

Invited

GENERATION OF SUB-MG QUASI-STATIONARY MAGNETIC FIELD USING CM SCALE CAPACITOR-COIL TARGETS

D. Kumar[1], S. Singh[1], H. Ahmed[2], R. Dudzak[3], J. Dostal[3], T. Chodukowski[4], L. Giuffrida[1], P. Hadjisolomu[2], T. Hodge[2], J. Hrebicek[3], L. Juha[3], Z. Kalinowska[4], E. Krousky[3], M. Krus[3], P. Lutoslawski[1], M. De Marco[1], M. Pfeifer[3], J. Skala[3], J. Ullschmeid[3], T. Pisarczyk[4], M. Borghesi[2], and **S. Kar[2]**

[1] ELI Beamlines, Dolni Brezany, Czech Republic, deepak.kumar@eli-beams.eu
[2] Queen's University Belfast, Belfast, United Kingdom
[3] Prague Asterix Laser Facility, Institute of Plasma Physics, Prague, Czech Republic
[4] Institute of Plasma Physics and Laser Microfusion, Warsaw, Poland

Abstract. A controlled and strong magnetic field is extremely useful in various laser plasma experiments with applications to fast ignition, laboratory astrophysics and charged particle beam lensing. Mega Gauss (MG) level quasi-stationary fields for such applications can be created by the interaction of a kJ-ns class laser with a capacitor-coil target. On a recent experiment at the Prague Asterix Laser (PALS) facility, cm scale macroscopic capacitor-coil targets were used to achieve fields up to 0.3 MG. The fields were diagnosed using polarimetry at two different wavelengths.

Traditional capacitor coil targets consist of two parallel foils with lateral dimension of several mm and a gap between the foils of a fraction of a mm [1, 2]. The duration of the laser pulse and the time scale of expansion of the plasma within the foils in such targets is of the order of a ns. In the experiment conducted at PALS facility, the Iodine laser (600 J, 350 ps, $I\lambda^2 = 10^{16} - 10^{17}$ W/cm^{2}μm^2) was used to irradiate much larger (up to 2 cm lateral dimension) macroscopic targets such that the plasma did not expand towards the second foil. With these large targets, the ablated plasma was about 3 cm from the center of the coil, thus preventing damage to the coil or to the TGG crystal used for polarimetry – an extremely desirable feature for developing future applications. Spatial distribution and temporal evolution of the magnetic field at the coil was characterized simultaneously by polarimetry technique at 2 different wavelengths – (a) imaging using a short pulse probe beam of duration 30 fs and center wavelength 810 nm and (b) streaked using the 2ω probe beam derived from the main pulse. Figure 1 shows an example of the data obtained from the fs polarimetry imaging diagnostic. For coils of 1 mm diameter, magnetic fields of up to 0.3 MG were measured in the experiment lasting for several ns. This presentation will summarize the experimental results obtained while varying the target geometry and related modeling.

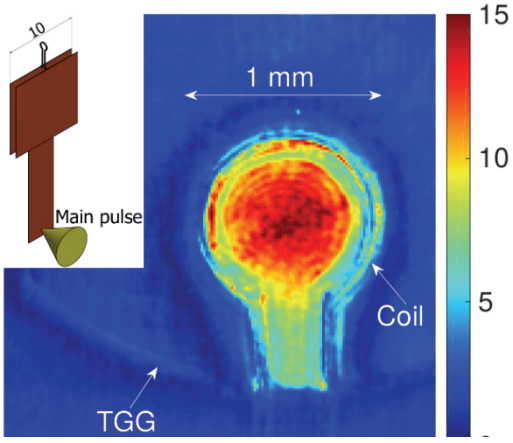

Fig. 1. Example of the measured Faraday rotation in degrees through a 0.5 mm thick TGG crystal placed about 0.3 mm behind the coil. Inset shows the target used for this shot

Acknowledgements

The authors acknowledge funding from EPSRC, UK [EP/J002550/1- Career Acceleration Fellowship held by S.K., EP/L002221/1, EP/K022415/1]. This work was also supported by the project ELI (Extreme Light Infrastructure) - phase 2 (Grant No. CZ.02.1.01/0.0/15_008/0000162), by the Access to the Research Infrastructure activity in the Horizon 2020 Framework Program of the EU, Grant Agreement No.: 654148 (Laser Lab Europe IV), by the Ministry of Education, Youth and Sports of the Czech Republic, project LM2015083 (PALS RI), by the Czech Science Foundation, project No.: P205/11/P712 and Ministry of Education, Youth and Sports as part of targeted support from the National Programme of Sustainability II (NPU II).

References

1. J.J. Santos *et al.*, *New J. Phys*., 2015, **17**, 083051.
2. L. Gao *et al.*, *Phys. Plasmas*, 2016, **23**, 043106.

Invited

DYNAMICS OF RELATIVISTIC ELECTRON VORTICES IN COLLISIONLESS PLASMAS

K.V. Lezhnin[1], **T.Zh. Esirkepov**[2], and **S.V. Bulanov**[2,3]

[1] Princeton University, Princeton, New Jersey, USA, klezhnin@princeton.edu
[2] National Institute for Quantum and Radiological Sciences and Technology, Kyoto, Japan
[3] A. M. Prokhorov General Phys. Inst. of RAS, Moscow, Russia

Abstract. Vortex dynamics is an important topic of physics of continuous media and plasma physics. In comparison to hydrodynamical vortices, the vortices in collisionless relativistic plasmas exhibit new properties, as the displacement current, two-fluid and kinetic effects come into play. Using 2D PIC simulations, we demonstrate how these effects appear during the single or binary vortex evolution, playing a huge role in stability of the electron vortices and ion acceleration.

Formation and evolution of localized nonlinear structures such as vortices and solitons play a crucial role in the physics of continuos media. For instance, drift wave dynamics in tokamak plasmas can be described in the framework of Hasegawa-Mima (HM) equation [1], which allows for the point-vortex solutions. The vortices may affect the energy and particle transport significantly [2]. In laser plasma interaction, we observe the formation of finite-radius relativistic electron vortex structures associated with the quasistatic magnetic field generation, which plays a significant role in the depletion of the electromagnetic field energy in laser plasmas [3]. The late stage of the vortex evolution resulting to strong plasma density modulations was observed with the use of proton radiography [4]. Understanding the dynamics of vortex structures is vital for developing the theory of the relativistic plasma turbulence [5]. In contrast to hydrodynamical vortices, which are sustained by non-charged fluids, vortices in plasma are sustained by the rotational motion of charged particles, which, generally speaking, leads to nonzero circular current. The associated magnetic flux is locked inside the vortex. In the point-vortex solutions of HM equations, the vortex internal energy is conserved during the interaction process. However, in the case of finite radius vortices, we expect the kinetic and electromagnetic interaction effects to step up, resulting in fast dissipation of the vortex energy with its transformation to the energy of fast particles.

Using 2D PIC simulations with the code REMP [6] and simple analytical models of electron vortex dynamics, we discuss the dynamics of single and binary relativistic electron vortices in collisionless plasma. On an ion timescale, a single vortex is subject to various effects, such as vortex boundary field intensification, multistream instabilities at the vortex boundary, and bending of the vortex boundary with the subsequent transformation into smaller electron vortices [7]. In immobile ion regime, we discuss the effects of binary vortex interaction. Among them, we demonstrate the mechanism of electron vortex dissipation into the fast electrons and electromagnetic waves. In ultrarelativistic electron vortex case, the dipole vortex forms a von Karman-like streets of secondary vortices in the wake region. The results obtained will be useful for understanding the super strong magnetic fields [8] and diagnostics of the results of the experiments with petawatt-class laser systems that are being build nowadays [9].

References

1. A. Hasegawa and K. Mima, *Phys. Fluids,* 1978, **21**, 97.
2. M. Kono and W. Horton, *Phys. Fluids,* 1991, **3**, 3255.
3. S. V. Bulanov *et al*., *Phys. Rev. Lett*., 1996, **76**, 3562.
4. L. Romagnani *et al*., *Phys. Rev. Lett*., 2010, **105**, 175002.
5. V. Zhdankin *et al*., *Phys. Rev. Lett.*, 2017, **118**, 055103.
6. T. Zh. Esirkepov, *Comput. Phys. Commun.*, 2001, **135**, 144.
7. K. V. Lezhnin *et al*., *Phys. Plasmas*, 2016, **23**, 093116.
8. G. Sarri *et al*., *Phys. Rev. Lett*., 2012, **109**, 205002.
9. G. A. Mourou, G. Korn, W. Sandner, and J. L. Collier, *ELI-Extreme Light Infrastructure Science and Technology with Ultra-Intense Lasers Whitebook*, THOSS Media, Berlin, 2011, p. 536.

Invited

MEASUREMENT OF SELF-GENERATED SPONTANEOUS FIELDS AND THEIR EFFECTS ON ICF ION KINETIC DYNAMICS

C.K. Li[1], F.H. Séguin[1], J.A. Frenje[1], R.D. Petrasso[1], P.-E. Masson-Labprde[2], S. Laffite[2], V. Tassin[2], P.A. Amendt[3], H.G. Rinderknecht[3], S.C. Wilks[3], N.M. Hoffman[4], A.B. Zylstra[4], S. Atzeni[5], R. Betti[6], M.J. Rosenberg[6], and **T.C. Sangster[6]**

[1] Massachusetts Institute of Technology, Cambridge, Massachusetts 02139, USA
[2] CEA, DAM, DIF, F-91297 Arpajon, France
[3] Lawrence Livermore National Laboratory, Livermore, California 94550, USA
[4] Los Alamos National Laboratory, Los Alamos, New Mexico 87545, USA
[5] Università di Roma "La Sapienza", Via A Scarpa, 14–16, I-00161 Roma, Italy
[6] University of Rochester, Rochester, New York 14623, USA

The plasma kinetic effects, which have been overlooked in the conventional single-spices-averaged hydrodynamic codes for inertial-confinement fusion (ICF), are attracting increasing attention. It has been realized that such effects are largely responsible for some disagreements between the experimental results and numerical simulations. Kinetic effects play an important role in the early ICF implosion phase and can potentially affect the dynamics in the later implosions. In particular, coupled with ion-kinetic processes, self-generated fields would have important effects on aspects of ion kinetic dynamics. For example, experiments at the OMEGA laser have shown that the interface between ICF hohlraum fill gas and Au wall blowoff is kinetically unstable, leading to formation of a diffusion layer and development of an ambipolar electric (E) field in the hohlraum radial direction. Such a field would enhance interpenetration and mixing between the Au blowoff and the gas plasma, changing hohlraum drive dynamics and then capsule implosions. We have recently conducted a series of indirect-drive and direct-drive ICF experiments on OMEGA. The experimental data, helped by the simulations, provide a new insight into the effects of self-generated fields on the interface structure in various ICF targets and ion kinetic dynamics.

Acknowledgements

The work described herein was performed in part at the LLE National Laser User's Facility (NLUF), and was supported in part by US DOE (Grant No. DE-FG03- 03SF22691), LLNL (subcontract Grant No. B504974) and LLE (subcontract Grant No. 412160-001G).

Invited

RELATIVISTIC MAGNETIC RECONNECTION DRIVEN BY HIGH INTENSITY LASERS

A. Maksimchuk[1], A. Raymond[1], C.F. Dong[2], A. McKelvey[1], C. Zulick[1], N. Alexander[3], A. Bhattachajee[2], P.T. Campbell[1], H. Chen[4], V. Chvykov[1], E. Del Rio[3], P. Fitzsimmons[3], W. Fox[2], B.X. Hou[1], C. Mileham[5], J. Nees[1], P.M. Nilson[5], C. Stoekl[5], A.G.R. Thomas[1], M.S. Wei[2], V. Yanovsky[1], L. Willingale[1], and **K. Krushelnick[1]**

[1] Center for Ultrafast Optical Science, University of Michigan, Ann Arbor, MI 48109, USA
[2] Princeton Plasma Physics Laboratory, Princeton, New Jersey 08543, USA
[3] General Atomics, San Diego, California 92121, USA
[4] Lawrence Livermore National Laboratory, Livermore, California 94551, USA
[5] Laboratory for Laser Energetics, University of Rochester, Rochester, NY 14623, USA

Magnetic reconnection is a fundamental plasma process involving a conversion of magnetic energy into plasma kinetic energy and plasma heating through changes in the magnetic field topology. Such events are widespread in astrophysics, space and laboratory plasmas. Here we present experimental studies using the OMEGA EP laser at the Laboratory for Laser Energetics and the HERCULES laser at the University of Michigan as well as numerical modeling which indicate that relativistic magnetic reconnection can be driven by two short-pulse, high-intensity laser pulses that produce relativistic plasma along with very strong magnetic fields. Evidence of magnetic reconnection in midplane diffusion region was identified by the plasma's X-ray emission patterns, changes to the electron energy spectrum, and by measuring the time over which reconnection occurs.

Acknowledgements

This work was supported by the National Nuclear Security Administration of the US Department of Energy under Award Number DE-NA0002727.

Invited

PIC SIMULATIONS FOR THE STUDY OF COLLISIONLESS SHOCKS FORMATION IN LABORATORY ASTROPHYSICS CONTEXT

Q. Moreno[1], M.E. Dieckmann[2], X. Ribeyre[1], S. Jequier[1], V.T. Tikhonchuk[1], L. Gremillet[3], and **E. d'Humières[1]**

[1] University of Bordeaux, Centre Lasers Intensases et Applications, CNRS, CEA, UMR 5107, France, Talence, Country, quentin.moreno@u-bordeaux.fr
[2] Departement of Science and Technology, Linköping University, Norrköping, Sweden
[3] CEA, DAM, DIF, France

Laboratory experiments are proposed to investigate collisionless shock formation in the interstellar medium [1–3]. These shocks are driven by different particle instabilities [4], which create a strong electromagnetic field, allowing the acceleration of particles [5]. Modeled with particle-in-cell simulations the shocks are created by the collision of two electron-ion clouds at a velocity that exceeds everywhere the threshold velocity for shock formation in a external magnetic field oriented perpendicularly/parallel to their flow velocity vectors, a setup that can accelerate the shock formation process (magnetic field perpendicular) or promotes particles acceleration (magnetic field parallel). Shock formation is a long process, and PIC simulations are very costly in numerical resources and time for such long studies. For these reasons the ion mass is thus reduced below 1836 electron masses, which can affect the plasma dynamics during the initial exponential growth phase of the instabilities and during the subsequent nonlinear saturation [6]. One part of this study is dedicated to assess how far the ion to electron mass ratio can be decreased,without changing qualitatively the physics and the second is the presentation of 2D simulations of shock formation with experimental parameters using a reduced ion mass.

References

1. Ph. Korneev, E. D'Humières, V. Tikhonchuk, D.P. Higgison, and J.Fuchs, *High Energy Density Physics*, 2015, **17**, 183–189.
2. Ph. Korneev, E. D'Humières, and V.Tikhonchuk, *Physics of Plasmas*, 2014, **17**, 022117.
3. H. Takabe *et al*., *Phys, Plasma*, 2008, **50**, 124057.
4. M.E. Dieckmann, A. Meli, P.K Shukla, L.O.C. Drury, and A. Mastichiadis, *Plasma Phys. Control, Fusion*, 2018, **50**.
5. L. Sironi and A. Spitkovsky, *The Astrophysical Journal*, 2011.
6. A. Bret and M.E. Dieckmann, *Phys, Plasmas*, 2010, **17**, 032109.

Invited

MAGNETIC INHIBITION OF LASER-DRIVEN, SHEATH-ACCELERATED HIGH-ENERGY PROTONS

M. Nakatsutsumi[1,2,6], Y. Sentoku[3], S.N. Chen[1,7], S. Buffechoux[1], A. Kon[4,6], A. Korzhimanov[7], L. Gremillet[8], B. Atherton[5], P. Audebert[1], M. Geissel[5], L. Hurd[1], M. Kimmel[5], P. Rambo[5], M. Schollmeier[5], J. Schwarz[5], M. Starodubtsev[7], R. Kodama[4,6], and **J. Fuchs[1,7]**

[1] LULI - CNRS, École Polytechnique, Palaiseau, France
[2] European XFEL, Schenefeld, Germany
[3] Department of Physics, University of Nevada, Reno, Nevada, USA
[4] Graduate School of Engineering, Osaka University, Suita, Osaka, Japan
[5] Sandia National Laboratories, Albuquerque, USA
[6] CREST, Japan Science and Technology Agency, Tokyo, Japan
[7] Institute of Applied Physics, Nizhny Novgorod, Russia
[8] CEA, DAM, DIF, Arpajon, France

Proton and ion beams accelerated in ultra-high-potential electron sheaths created on solid targets by ultrafast lasers have remarkable characteristics that have enabled unique applications. The current challenge is to increase the ion energy to 100 MeV and beyond, which is commonly thought to be possible by raising the on-target laser intensity. In this talk, we present experimental and numerical results demonstrating that magnetostatic fields self-generated on the target surface may pose a fundamental limit to acceleration for high enough laser intensities.

Poster

DENSITY BUMP FORMATION AT THE FRONT OF A COLLISIONLESS ELECTROSTATIC SHOCK WAVE IN A LASER ABLATED PLASMA

M.A. Garasev[1,2], V.V. Kocharovsky[1,2], A.A. Nechaev[1], and A.N. Stepanov[1]

[1] Institute of Applied Physics of the RAS, Nizhny Novgorod, Russia; e-mail: ant.a.nech@gmail.com
[2] Lobachevsky State University of Nizhny Novgorod, Nizhny Novgorod, Russia

Abstract. The collisionless expansion of a dual-temperature plasmoid through a cold and tenuous plasma is studied numerically. It is found that a density bump is formed at the front of a collisionless electrostatic shock wave propagating at nearly ion-acoustic velocity. 1D3V and 2D3V PIC-simulations suggest that the bump emerges due to the presence of the ionized background and differs from an ion-acoustic soliton, being exposed to a continuous flow of high-energy particles of the dense plasmoid. Electrons' thermal anisotropy, arising behind the shock, leads to the growth of quasi-static Weibel magnetic fields up to a level of magnetization of ~10%.

Recent experiments on thin foils ablation with powerful ultrashort laser pulses revealed unexpected features – density bumps – in the density profile of a hot laser plasma that collisionlessly expands into a rarefied ionized background [1, 2]. The latter is always present around the target, being either produced by the photoionization of a residual gas in the vacuum chamber, or ablated from the same foil by a laser prepulse. The bumps, observed on the plasma slope, are absent in the well-known case of expansion into vacuum. They propagate away from the target at nearly ion-acoustic velocity, so are most likely connected with a collisionless electrostatic shock wave arising in the system.

The solitary bump in [1] emerges at the shock's front, stays there throughout the expansion, and can not be treated as a free ion-acoustic soliton (cf. [2, 3]). Our 1D3V and 2D3V PIC-simulations with the code EPOCH [4] suggest that the bump arises when the differences in density and temperature between the hot expanding plasmoid and the background is strong, with the transition layer between them being quite narrow. According to the simulations, the continuous flow of energetic electrons from the dense plasmoid considerably impacts the ion-acoustic wave packet excited in plasma by the shock and prevents the formation of free solitons. In all cases when the bump is present these electrons have a non-Maxwellian velocity distribution with the skewness of the order or greater than 0.1.

A typical simulation is initiated with the configuration of a background plasma with a 10^{19} cm^{-3} density and electron (ion) temperature of 3 eV (50 eV), uniformly distributed in the simulation domain (with all boundaries open), and a semicircular plasmoid with a density of 10^{21} cm^{-3} (sub-critical for a 800 nm laser), placed near a domain's boundary. Electron and ion temperatures in the plasmoid are 2.5 keV and 3 eV, respectively. It is shown that during the expansion of the hot plasmoid a layer with a local density maximum of ~10^{19} cm^{-3} is formed, spanning ~10 Debye lengths of the dense plasma and moving at speed slightly higher than the ion-acoustic one.

We analyze the dynamics of plasma fractions' number density, particle trajectories and the evolution of their phase space, and trace the development of electric and magnetic fields generated meanwhile. We consider various parameters of both plasmas and different profiles of the transition layer between them, indicate the parameters domain corresponding to the bump formation and describe stages of its formation and dynamics. Thermal anisotropy of the dense plasma electrons behind the shock induces Weibel generation of magnetic fields, which have the energy eventually approaching ~10% of the total energy of particles and influence the long-term evolution of the bump.

Acknowledgements

This work was supported by the Russian Science Foundation grant No. 16-12-10528.

References

1. M.A. Garasev, A.I. Korytin, V.V. Kocharovsky, Yu.A. Mal'kov, A.A. Murzanev, A.A. Nechaev, and A.N. Stepanov, *JETP Letters*, 2017, **105**(3), 164–168.
2. L. Romagnani, S. V. Bulanov, M. Borghesi, P. Audebert, J. C. Gauthier, K. Lowenbruck, A.J. MacKinnon, P. Patel, G. Pretzler, T. Toncian, and O. Willi, *Phys. Rev. Lett.*, 2008, **101**, 025004.
3. G. Sarri, G.C. Murphy, M.E. Dieckmann, A. Bret, K. Quinn, I. Kourakis, M. Borghesi, L.O.C. Drury, and A. Ynnerman, *New J. Phys.*, 2011, **13**, 073023.
4. T.D. Arber, K. Bennett, C.S. Brady, A. Lawrence-Douglas, M.G. Ramsay, N.J. Sircombe, P. Gillies, R.G. Evans, H. Schmitz, A.R. Bell, and C.P. Ridgers, *Plasma Phys. Control. Fusion*, 2015, **57**, 113001.

Invited

X-RAY SPECTROSCOPY DIAGNOSTICS TO STUDY COMPLEX SUPERSONIC PLASMA FLOWS WITH ASTROPHYSICAL RELEVANCE IN LASER PLASMA

S.A. Pikuz[1,2], E.D. Filippov[1,2], S.N. Ryazantsev[1,3], I.Yu. Skobelev[1,2], G. Revet[4,5], D.P. Higginson[4,6], S.N. Chen[4], B. Albertazzi[4,7], A.A. Soloviev[5], J. Beard[8], B. Khiar[9], A. Ciardi[9], A.Ya. Faenov[1,10], H. Pepin[11], and **J. Fuchs[4,5]**

[1] Joint Institute for High Temperatures RAS, Moscow 125412, Russia
[2] National Research Nuclear University 'MEPhI', Moscow115409, Russia
[3] Lomonosov Moscow State University, Moscow 119991, Russia
[4] Laboratoire pour l'Utilisation des Lasers Intenses, CNRS-CEA-Ecole Polytechnique, Palaiseau 91128, France
[5] Institute of Applied Physics RAS, Nizhny Novgorod 603950, Russia
[6] Lawrence Livermore National Laboratory, Livermore, CA 94550, USA
[7] Graduate School of Engineering Osaka University, Suita, Osaka 565-087, Japan
[8] LNCMI, UPR 3228, CNRS-UJF-UPS-INSA, 31400 Toulouse, France
[9] LERMA, Observatoire de Paris, PSL Research University, CNRS, Paris 75014, France
[10] Institute for Academic Initiatives, Osaka University, Suita, Osaka 565-0871, Japan
[11] Centre Energie Materiaux Telecommunications INRS, Varennes J3X1S2, Quebec, Canada
spikuz@gmail.com

Remarkable plasma hydrodynamic phenomena such as supersonic jets have been observed to emerge from a wide variety of astrophysical systems, however the questions on their formation mechanisms and morphology are still open. Laboratory experiments employing the plasma produced by high power lasers can be scaled to astrophysical systems by matching dimensionless scaling parameters and thus providing the studies of astrophysical phenomena in controllable conditions. Particularly, laser produced jets are fully scalable to that one from young star objects, and the application of external magnetic field to plasma flows allows to investigate stable, large aspect ratio plasma jets.

While the laser produced plasma expands from the target surface, it becomes overcooled, *i.e.* recombining one, and with non-stationary ionization state in most cases. Accordingly, to improve diagnostic methods applicable for such plasma is a rather important task in laboratory astrophysics.

X-ray spectroscopy method considering the relative intensities of spectral lines emitted by He-like and H-like F and O ions is developed and implemented to determine electron temperature T_e and density N_e profiles of plasma jets along their propagation in vacuum, external magnetic field and ambient gas and precursor plasma. It is shown that N_e decreases monotonically in the case without B-field, but demonstrates an extended density profile when 20 T poloidal magnetic field is applied. While at target surface irradiated by 60 J 1 ns laser pulses the electron temperature peaks at 250–280 eV, at 3 mm distance it cools down to ~20 eV.

Then, due to the impact of B field providing the collimation of the jet, T_e and N_e are measured to keep at almost constant values for a long distance along the jet. Laboratory experiments reveal that the shaping of narrow jets emerging from young stars can be explained by axial magnetic fields in which the stars are embedded.

In the case of accretion phenomena modelling, the plasma flow interacts with solid obstacle making the plasma hydrodynamics and atomic kinetics more complex. With X-ray spectroscopy methods the creation of a two-component plasma near the obstacle is confirmed to be composed of several 100 eVs hot shell and few tens eV denser core. The combination of recombining and steady-state atomic kinetics modeling allows revealing the parameters of both shell and core plasma fractions, as well considering the effects of plasma self-absorption to the observed X-ray spectra.

Invited

MAGNETIC RECONNECTION IN THE HIGH-ENERGY-DENSITY AND RELATIVISTIC REGIME

B. Qiao, Z. Xu, W.P. Yao, and **X.T. He**

Peking University, Beijing, China
bqiao@pku.edu.cn

Magnetic reconnection (MR), breaking and reorganizing the topology of magnetic field dramatically, is a fundamental process observed in many space, laboratory and astrophysical plasmas. In this talk, I report recent theoretical investigations on MR in the high-energy-density and relativistic regime for high-β (β > 1) and relativistic plasmas. For MR in the high-β regime, comparing 2D and 3D PIC simulation results for the interactions of colliding laser-produced plasma bubbles with induced anti-parallel and parallel poloidal magnetic fields, we find that many of the previously-observed characteristics [2, 3], such as the quadrupole magnetic field, plasma heating and even the out-of-plane electric field, can be induced by the mere plasma bubble collision, which do not necessarily indicate MR occurrence in the high-β regime. The Lorentz-invariant scalar quantity $D_e = \gamma_e \mathbf{j}\cdot(\mathbf{E}+\mathbf{v}_e\times\mathbf{B})$ in the electron dissipation region is proposed as the key sign of MR occurrence in this regime. For MR in the relativistic regime, though the topology of magnetic field depends on the relativistic observer, we prove that the x-point of MR is conserved as well as o-point. Therefore, the reconnection physics still survives in the relativistic regime. In the global view, we propose two global Lorentz invariants $\int(c^2B^2-E^2)d^3x$, and $\int(E\cdot B)^2 d^3x$ to be more reasonable for the coarse description of the energy dissipation and the fields activity in multi-reconnection circumstances. Based on this, relativistic reconnection in the extreme near-Schwinger magnetic environment has also been investigated. We find that the MR dynamics is strongly coupled with and heavily influenced by the QED effects. In turn, gamma-ray emission and pair creation have a strong relevance with the MR configurations, i.e., X- and O-points.

References

1. M. Yamada, R. Kulsrud, and H. Ji, *Rev. Mod. Phys*., 2010, **82**, 603.
2. J. Zhong *et al*., *Nat. Phys*., 2010, **6**, 984.
3. W. Fox *et al*., *Phys. Rev. Lett*., 2011, **106**, 215003.

Invited

BEAM SELF-FOCUSING AND ELECTRON TRANSPORT EFFECTS IN MAGNETISED LASER-PLASMAS

M.P. Read[1], C.P. Ridgers[1], J.J. Bissell[2], and **R.J. Kingham[3]**

[1] York Plasma Institute, University of York, UK
[2] Department of Physics, University of Bath, UK
[3] Blackett Laboratory, Imperial College London, UK

Abstract. Strong magnetic fields can beneficially affect electron transport in under-dense laser-plasma interactions relevant to laboratory HEDP applications. For example, externally applied B-fields have been used to control low density plasma wave-guide formation [1], to improve laser coupling to gas-filled hohlraums [2], and will affect laser pre-heating in the MagLIF scheme [3]. Changes to electron transport under magnetised conditions cause heat-flow suppression across field lines but phenomena such as the Nernst effect can also lead to changes in B-field dynamics [4] which must be accounted for.

Previously we investigated the effects of magnetised electron transport on the focusing and channelling behaviour of a long-pulse (~1 ns) laser propagating under moderately magnetised plasma conditions ($\omega\tau$ ~1). The complicated interplay between hydrodynamics, thermal transport, B-field evolution and beam focusing dynamics was investigated computationally in 2D using an MHD code with full Braginskii electron transport coupled to a paraxial wave solving routine. We reported [5] that Nernst advection of B-fields appeared to have a disruptive effect on beam self-focusing but accounting for non-local effects using a full Vlasov-Fokker-Planck treatment resulted in long-time-scale beam channelling behaviour being retained. Further work is presented here comparing simulations with a range thermal flux-limiter values and considering appropriate Nernst flux limitation values by comparison to the results of kinetic simulations.

References

1. D.H. Froula *et al.*, *Plasma Physics and Controlled Fusion*, 2009, **51**.
2. D.S. Montgomery *et al.*, *Physics of Plasmas*, 2015. **22**.
3. A.J. Harvey-Thompson *et al.*, *Physical Review E*, 2016, **94**.
4. C.P. Ridgers *et al.*, *Physical Review Letters*, 2008, **100**.
5. M.P. Read *et al.*, *Journal of Physics: Conference Series*, 2016, **717**.

Invited

LABORATORY UNRAVELLING OF MATTER ACCRETION IN YOUNG LOW-MASS STARS

G. Revet[1,2], S.N. Chen[1,2], R. Bonito[3], B. Khiar[4], E. Filipov[5,6], C. Argiroffi[3], D.P. Higginson[2], S. Orlando[7], J. Béard[8], M. Blecher[9], M. Borghesi[10], K. Burdonov[1], D. Khaghani[11], K. Naughton[10], H. Pépin[12], O. Portugall[8], R. Riquier[2,13], R. Rodriguez[14], S.N. Ryazantsev[5,6], I.Yu. Skobelev[5,6], A. Soloviev[1], O. Willi[9], S. Pikuz[5,6], A. Ciardi[4], and **J. Fuchs[1,2,*]**

[1] Institute of Applied Physics, 46 Ulyanov Street, 603950 Nizhny Novgorod, Russia
[2] LULI - CNRS, École Polytechnique, CEA: Université Paris-Saclay; UPMC Univ Paris 06: Sorbonne Universités - F-91128 Palaiseau cedex, France
[3] Dipartimento di Fisica e Chimica Università di Palermo, Italy
[4] LERMA, Observatoire de Paris, CNRS UMR 8112, Paris France
[5] National Research Nuclear University 'MEPhI', 115409 Moscow, Russia
[6] Joint Institute for High Temperatures, RAS, 125412, Moscow, Russia
[7] INAF - Osservatorio Astronomico di Palermo, Italy
[8] LNCMI, UPR 3228, CNRS-UFJ-UPS-INSA, 31400 Toulouse, France
[9] Institut für Laser- und Plasmaphysik, Heinrich-Heine-Universität Düsseldorf, D-40225 Düsseldorf, Germany
[10] The Queen's University of Belfast, Belfast BT7 1NN, United Kingdom
[11] GSI Helmholtzzentrum für Schwerionenforschung GmbH, 64291 Darmstadt, Germany
[12] INRS-EMT, Varennes, Québec, Canada
[13] CEA, DAM, DIF, 91297 Arpajon, France
[14] Departamento de Fisica de la Universidad de Las Palmas de Gran Canaria, E-35017 Las Palmas de Gran Canaria, Spain

Accretion dynamics in forming young stars is still widely investigated because of limitations in observations and modelling. In our present understanding, matter from the accretion disk (10^{11}–10^{13} cm^{-3} / 2000 K) is connected to the star by the extended magnetosphere (0.1–1 kG) and falls down into the stellar surface at the free fall velocity (500 km.s^{-1}). At the impact, a shock is formed, leading to observable X-ray and UV emissions, the amount of each channel being still incompatible with the present shock dynamic modelling at the impact region.

Through scaled laboratory experiments of collimated plasma accretion onto a solid in the presence of a magnetic field, we open the first experimental window on this phenomenon by tracking, with spatial and temporal resolution, the dynamics of the system and simultaneously measuring multiband emissions. This is performed using a laser-created thermal plasma embedded in an external 20T pulsed magnetic field. As a result of the magnetized plasma expansion, a collimated jet is formed, having an aspect ratio >10, a temperature of tens of eV, an electron density of $1.5 \cdot 10^{18}$ cm^{-3} and propagating at 750 km.s^{-1}. This jet, acting as the accretion column following the magnetic field lines then impacts a solid obstacle located on its path, mimicking the stellar surface. This setup differs in many ways from previous experiments using unmagnetized shock-tube configurations having unwanted edge-constraints.

We observe in our experiment that matter, upon impact, is laterally ejected from the solid surface, then refocused by the magnetic field toward the incoming stream. Such ejected matter forms a plasma shell that envelops the shocked core, reducing escaped X-ray emission. Discussed in the light of 3D-MHD simulations in the laboratory conditions as well as 2D-MHD astrophysical-scaled simulations, these experimental results shed light on one possible structure reconciling current discrepancies between mass accretion rates derived from X-ray and optical observations.

Invited

FIRST EXPERIMENTAL DEMONSTRATION OF ISOCHORIC HEATING OF A DENSE PLASMA CORE WITH ASSISTANCE OF EXTERNAL KILO-TESLA MAGNETIC FIELD

S. Sakata[1], S. Lee[1], H. Sawada[2], Y. Iwasa[1], H. Morita[1], K. Matsuo[1], K.F.F. Law[1],T. Johzaki[3], H. Nagatomo[1], Y. Sentoku[1], A. Sunahara[4], A. Yao[1], Y. Arikawa[1], M. Hata[1], S. Kojima[1], Y. Abe[1], H. Kishimoto[1], K. Kanbayashi[1], A. Yogo[1], A. Morace[1], H. Sakagami[5], T. Ozaki[5], K. Yamanoi[1], T. Norimatsu[1], T. Shimizu[1], Y. Nakata[1], J. Kawanaka[1], S. Tokita[1], N. Miyanaga[1], M. Murakami[1], M. Nakai[1], H. Shiraga[1], H. Nishimura[1], K. Mima[6], H. Azechi[1], and **S. Fujioka[1]**

[1] Institute of Laser Engineering, Osaka University, Suita, Japan, sakata-s@ile.osaka-u.ac.jp
[2] Department of Physics, University of Nevada Reno, Reno, USA
[3] Graduate School of Engineering, Hiroshima University, Higashi-Hiroshima, Japan
[4] Institute for Laser Technology, Suita, Japan
[5] National Institute of Fusion Science, Toki, Japan
[6] The Graduate School for the Creation of New Photonics Industries, Hamamatsu, Japan

Abstract. We have demonstrated efficient heating of a compressed plasma by relativistic electron beams produced by LFEX laser with the assistance of external magnetic field. Emission from Cu tracer atoms contained in the compressed plasma was measured to infer the plasma temperature and the energy coupling efficiency from heating laser to core plasma. Li-like and He-like emission lines, which appeared only with assistance of the external magnetic field, suggest that the electron temperature was ~1.7 keV and density ~ 6 g/cc.

Introduction. Fast ignition (FI) [1] is an high-gain ignition scheme of the inertial confinement fusion, in which a compressed dense plasma is achieved by heating fuel with relativistic electron beam (REB) or fast ions produced by a high intensity short pulse laser. In electron based FI, large angular divergence of the REB is a critical issue, resulting in low coupling efficiency from heating laser to a core plasma [2]. Guidance of the REB using strong external magnetic field was proposed for efficient heating of a dense core plasma [3]. Recently, guiding of REB using strong magnetic field induced by a laser-driven capacitor-coil [4] has been demonstrated in a planar geometry [5].

Experimental results. The integrated experiment was conducted at ILE, Osaka University. A Cu (II) olate sphere was introduced to measure an electron temperature of a heated dense core plasma and visualize a REB transport [6]. Kilo-Tesla magnetic fields was induced by a laser-driven capacitor-coil, applied to the solid sphere, which was compressed by six GEKKO-XII laser beams. LFEX laser [7] was injected into a compressed core plasma to produce a REB. Li-like and He-like lines recoded with a flat HOPG crystal spectrometer appeared only when the external magnetic field was applied. The electron temperature and density of the heated plasma were evaluated to be ~1.7 keV and ~6 g/cc by comparing the measured X-ray spectra with FLYCHK calculations [8]. Details of analysis will be discussed in the presentation.

Acknowledgements

This research was supported by the Collaboration Research Program between the National Institute for Fusion Science (Grant Nos. NIFS12KUGK057, NIFS11KUGK053, and NIFS15KUGK087) and the Institute of Laser Engineering at Osaka University (2015A1-19 and 2015A1-31), and by the Japanese Ministry of Education, Science, Sports, and Culture through Grants-in-Aid for Young Scientists (Grant Nos. 24684044, 26820396, and 25630419), Bilateral Program for Supporting International Joint Research by JSPS, and Grants-in-Aid for Fellows by JSPS (Grant Nos. 14J06592 and 15J00850).

References

1. M. Tabak *et al*., *Phys. Plasmas,* 1994, **1**, 1626−1634.
2. S. Fujioka *et al*., *Phys. Rev. E,* 2015, **91**, 063102.
3. D. J. Strozzi *et al*., *Phys. Plasmas,* 2012, **19**, 072711.
4. S. Fujioka *et al*., *Sci. Rep.,* 2013, **3**, 1170.
5. M. Bailly - Garndvaux *et al*., *arXiv*: 1608. 08101. 29 Aug 2016.
6. L. C. Jarrot *et al*., *Nature Phys.,* 2016, **12**, 499−504.
7. N. Miyanaga *et al*., *EDP Sciences, J. de Physique* IV, 2006, **133**, 81.
8. H. K. Chung, W. L. Morgan, Y. Ralchenko and R. W. Lee, *HEDP,* 2005, **1**, 3.

Invited

KINETIC SOLUTION FOR THE GENERATION OF MAGNETIC FIELDS VIA THE BIERMANN BATTERY

K.M. Schoeffler[1], **N.F. Loureiro**[2], and **L.O. Silva**[1]

[1] Instituto de Plasmas e Fusão Nuclear, Instituto Superior Técnico
Universidade de Lisboa, 1049-001 Lisboa, Portugal
[2] Plasma Science and Fusion Center, Massachusetts Institute of Technology, Cambridge MA
02139, USA

Abstract. Fully kinetic analytic calculations of an initially Maxwellian distribution with arbitrary density and temperature gradients exhibit the development of temperature anisotropies and magnetic field growth associated with the Biermann battery. The calculation, performed by taking a small order expansion of the ratio of the Debye length to the gradient scale, predicts anisotropies and magnetic fields as a function of space given an arbitrary temperature and density profile. These predictions are shown to qualitatively match the values measured from particle-in-cell simulations, where the development of the Weibel instability occurs at the same location and with a wavenumber aligned with the predicted temperature anisotropy.

In recent years, experiments with laser-target interactions create plasma with extremely strong magnetic fields (~ MGauss). With these conditions, and the unprecedented resolution that these experiments can now operate, we are able to probe physics that also occurs in astrophysical systems, in particular, the generation of these magnetic fields via the Biermann battery and the Weibel instability. Intense short pulse lasers are capable of creating plasmas that are so hot that the particles are essentially collisionless, and kinetic physics is essential.

We have developed an analytic solution to the kinetic evolution of a temperature and density gradient, which can be applied to such experiments and astrophysical systems. Besides confirming that in collisionless systems, the Biermann battery, which is caused by misaligned temperature and density gradients ($\nabla n \times \nabla T \neq 0$), grows at the same rate as predicted in fluid models, the solution shows that a temperature anisotropy is generated due to the temperature gradient growing at $A = (v_T\, t/L_T\,)^2$ where v_T is the thermal velocity and L_T is the temperature gradient length scale. This anisotropy is the driver of several instabilities including the Weibel instability, also shown numerically in [1, 2]. With the most general version of the solution, the direction and magnitude of these temperature anisotropies can be predicted for a general initial temperature and density distribution at early times, even in cases where there is an initial magnetic field.

Acknowledgements

This work was supported by the European Research Council (ERC-2010-AdG Grant No. 267841).

References

1. K.M. Schoeffler *et al*., *Phys. Rev. Lett.*, 2014, **112**, 175001.
2. K.M. Schoeffler *et al*., *Phys. Plasmas,* 2016, **23**, 056304.

Invited

COLLISIONLESS SUPER-ALFVENIC INTERACTION AND GENERATION OF LARGE AMPLITUDE PRE-SHOCK MAGNETOSONIC WAVE IN LASER PLASMA EXPERIMENT

I.F. Shaikhislamov, Yu.P. Zakharov, V.G. Posukh, A.V. Melekhov, and **A.G. Ponomarenko**

Institute of Laser Physics, Siberian Branch of the Russian Academy of Sciences
Novosibirsk, 630090, Russia, E-mail ildars@ngs.ru

Abstract. We report the experiment on generation of strong super-Alfvénic magnetosonic perturbation by laser-produced plasma expanding in magnetized background under conditions when the magnetic cavity size reaches the ion gyroradius. Detailed measurements of plasma density and velocity, electric and magnetic fields are presented which demonstrate strong magnetic compression at the front and cavity dynamics, laser plasma deceleration and formation, with record efficiency of energy transfer 25%, of strong non-linear magnetosonic wave propagating through background plasma.

Laboratory modeling of various processes occurring in space plasmas is an important way to study the basic physics. In 1970–1980 many laser plasma experiments were performed with the aim of modeling full-scale near-Earth space tests such as *AMPTE, CRRES, Argus, and Starfish*. This also led to the on-going attempts to create in laboratory *a collisionless shock wave* [1]. The results achieved at KI-1 laser facility at the Institute of Laser Physics remain one of the leading in this field [2]. Theoretical analysis of super-Alfvénic collisionless interaction based on Longmire model of displaced electrons [3] and Finite Larmor Coupling or Magnetic Laminar Mechanism shows that effectiveness of energy transfer from explosive plasma to magnetized background is determined by how large the size of realized magnetic cavity is in comparison to ion gyroradius [4]. It is predicted that collisionless shock wave can be generated only when cavity size is sufficiently larger than gyroradius – the aim which proved to be difficult to achieve in laser plasma experiments. In the present report we describe the experiment on generation of strong super-Alfvénic magnetosonic perturbation by laser-produced plasma expanding in magnetized background under conditions when the cavity size reaches the gyroradius value. To increase the effective number of laser-produced ions and the cavity size we use a quasi-directed flow produced by one-sided laser irradiation of a solid target as well as an optimized close to threshold mode of laser-plasma production. We present detailed measurements of plasma density and velocity, electric and magnetic fields which demonstrate strong magnetic compression at the front and cavity dynamics, laser plasma deceleration and formation, with record efficiency of energy transfer 25%, of strong perturbation propagating through background plasma. The observed edge of perturbation spatial structure as steep as ion inertia length, relative amplitude $B/B_0 \approx 2$ and propagation velocity $M_A \approx 2$ testify that this is a *non-linear magnetosonic wave* of nearly largest possible amplitude.

Acknowledgements

This work was performed under the research program of the Siberian Branch of the Russian Academy of Sciences (project II.10.1.4, 01201374303), and supported by the Russian Foundation for Basic Research (projects 16-52-14006).

References

1. R.P. Drake, *Phys. Plasmas*, 2000, **7**, 4690.
2. Yu.P. Zakharov *et al*., *Proceedings ESA*, 1986, **SP-251**, 37.
3. T.P. Wright, *Phys. Fluids*, 1971, **14**, 1905.
4. A.I. Golubev, A.A. Solov'ev, and V.A. Terekhin, *Prikl. Mekh. Tekh. Fiz*., 1978, **5**, 33.

Invited

LABORATORY INVESTIGATION OF LASER PLASMA EXPANSION ACROSS THE AMBIENT MAGNETIC FIELD

A. Soloviev[1], K. Burdonov[1], S.N. Chen[1,2], A. Eremeev[1], G. Revet[2], S. Pikuz[3], E. Filippov[3], M. Cerchez[4], T. Gangly[2], A. Sladkov[1], A. Korzhimanov[1], V. Ginzburg[1], E. Khazanov[1], A. Kochetkov[1], A. Kuzmin[1], I. Shaykin[1], A. Shaykin[1], I. Yakovlev[1], M. Starodubtsev[1], and **J. Fuchs[1,2]**

[1] Institute of Applied Physics, Russian Academy of Science, Nizhny Novgorod, Russia
[2] LULI, CNRS UMLR7605, Ecole Polytechnique, Palaiseau, France
[3] Joint Institute for High Temperatures, Russian Academy of Science, Moscow, Russia
[4] HHU, Dusseldorf, Germany

Abstract. We present the results of laboratory and numerical studies of magneto-hydrodynamic interaction of high-velocity streams of dense, highly-conductive plasma with an ambient magnetic field. Such processes take place in numerous astrophysical systems, as accreting compact stars, hot Jupiters etc. The main attention has been paid to the processes developing when the plasma flow expands across the ambient magnetic field. It has been shown that in the region where the pressure of the magnetic field is of the order of the gas dynamic pressure, a Rayleigh–Taylor instability modifies the flow's dynamics forming narrow tongs of supersonic plasma flows penetrating deeply into the magnetic field.

We present recent experiments, performed at PEARL laser facility (Institute of Applied Physics), aimed at investigating the dynamic of plasma flows expending into the ambient magnetic field. The main attention has been paid to the case when the plasma flow penetrates across the magnetic field. Such geometry of the experiment is related to laboratory modeling of accretion of matter into compact stars and, especially, to the processes developing at the inner edge of the accretion disks in the region where the pressure of the magnetic field of the star is of the order of the dynamic pressure of the accreting plasma. Using two femtosecond interferometers, 2D snapshots of plasma flow expanding into the ambient magnetic field have been obtained in two geometries (perpendicular and parallel to the direction of the magnetic field lines) and in different times after the plasma flow formation. It has been found that the plasma flow exhibits strong Rayleigh–Taylor instability in the region where the pressure of the magnetic field is of the order of the plasma flow dynamic pressure. As a result of this instability, the plasma flow deeply penetrates into the magnetic field forming a narrow ('pancake-like') tongs of supersonic plasma streams (in practice, a thin plasma layer penetrates between the magnetic field lines). This result, confirmed also by numerical modeling, calls into question the generally accepted astrophysical model of matter accretion in form of 'accretion columns', when the matter falls onto the star from the inner edge of the accretion disc (which is formed at the magnetic/plasma dynamic pressures balance region) along the magnetic field lines to the polar regions of the star. On the contrary, the results of the present experiment make it possible to propose an alternative model for the fall of matter onto the equator of the star.

Invited

ION ACCELERATION FROM THE MODULATED ELECTRIC AND MAGNETIC FIELDS BY BUNDLED PICOSECOND LASER BEAMS

A. Yogo[1,2], M. Hata[1], A. Morace[1], N. Iwata[1], Y. Arikawa[1], T. Johzaki[3], S. Fujioka[1], Y. Sentoku[1], S. Tosaki[1], K. Koga[1], H. Nishimura[1], K. Mima[1,4], M. Nakai[1], R. Kodama[1], and H. Azechi[1]

[1] Institute of Laser Engineering, Osaka University, Suita, Osaka, Japan
[2] PRESTO, Japan Science and Technology Agency, Kawaguchi, Saitama, Japan
[3] Graduate School of Engineering, Hiroshima University, Higashi-Hiroshima, Japan
[4] The Graduate School for the Creation of New Photon Industries, Hamamatsu, Shizuoka, Japan

Abstract. We demonstrated the laser-ion acceleration by bundled picosecond laser beams experimentally. 50-MeV protons were achieved from a typical thin aluminum target with $1.2{\cdot}10^{19}$ Wcm^{-2} as a total laser intensity of four bundled beams. This result can be attributed to the interference effects, which appear in multiple laser beams focused on the target with a small angle to each other. The modulated laser fields induce localized electric and magnetic fields also on the rear side, which make a beneficial effect for enhancing the ion energy owing to the high absorption efficiency due to the modulation.

Ion acceleration with picosecond (ps) laser pulses involves several characteristic mechanisms never seen with sub-picosecond pulses. Recently, we found [1] that multi-ps laser pulses induce the temporal evolution of plasma electron temperature beyond the ponderomotive scaling and boost the ion acceleration via the target normal acceleration (TNSA). In this study, we discuss the bundling effect of ps laser beams on the ion acceleration in the relativistic regime.

We had performed the ion acceleration at LFEX [2] laser facility of Osaka University. Four laser beams (2×2) were bundled and simultaneously focused onto the foil target (10-μm-thick aluminum) along the normal axis of the target surface. The beams were linearly polarized in the vertical direction with an angle between the neighboring beams 5.7°. The total beam energy was 1 kJ (250 J for each), the intensity was $1.2{\cdot}10^{19}$ Wcm^{-2} ($3{\cdot}10^{18}$ Wcm^{-2} for each), and the pulse duration was 1.5 ps (FWHM). The accelerated ions were analyzed by a Thomson Parabola (TP) at the normal direction of the target rear surface. The spatial profile of the ions was recorded by a Radio-Chromic Film (RCF, MD-V3) located at the entrance of the TP, 1 m away from the target. The TP analysis reveals proton acceleration exceeding 50 MeV at the maximum, and protons with lower energy (~5 MeV) has turbulent-like structures on the RCF (Fig. 1). Since the bundled four beams focused on the same spot are interfered, producing modulations like filamentations, of which size is determined by the incident angle, viz, controllable. These modulated laser fields induce localized electric and magnetic fields also on the rear side, which then affect the TNSA acceleration and modify the angular distribution of ions. The bundled beams also make a beneficial effect for enhancing the ion energy owning to the high absorption efficiency due to the modulation. Detailed discussion of experimental results including particle-in-cell simulations will be in the presentation.

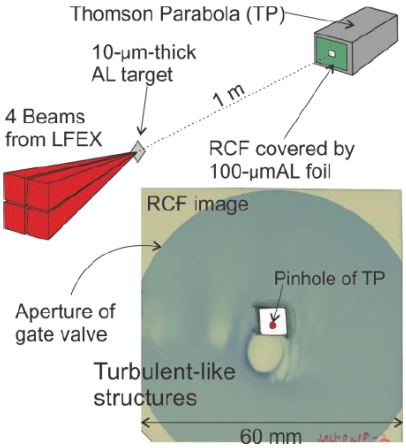

Fig. 1. Schematic of the experimental setup and the turbulent-like structure found on the ion spatial profile, which was measured simultaneously with the Thomson Parabola analyzer

Acknowledgements

This work was funded by the Grant-in-Aid for Scientific Research (Nos 25420911 and 26246043) of MEXT, A-STEP (No. AS2721002c), JST and PRESTO, JST. The authors thank the technical support staff of ILE for their assistance with the laser operation, target fabrication and plasma diagnostics. This work was supported by the Collaboration Research Program of the National Institute for Fusion Science (Nos NIFS15KUGK096, NIFS12KUGK057) and ILE, Osaka University (2015A1-32).

References

1. A. Yogo *et al.*, *Sci. Rep.*, 2017, **7**, 42451.
2. J. Kawanaka *et al.*, *J. Phys. Conf. Ser.*, 2008, **112**, 032006.

Invited

GENERATION AND APPLICATION OF A LASER DRIVEN MAGNETIC FIELD IN LAB-ASTROPHYSICS RESEARCHES

Zhe Zhang

Institute of Physics, Chinese Academy of Sciences, China

Abstract. Generation of a strong magnetic field by intense laser has been demonstrated. A hundreds to thousands Tesla level pulsed magnetic field can be produced. Besides the original design of a "capacitor-coil", many other types of coils have been tested with fs-ps short pulse laser. With such a strong magnetic field, laboratory researches of many astro-phenomena can be studied in a new regime and in a more controllable way.

Laboratory generation of strong magnetic fields opens new frontiers in plasma and beam physics, astro- and solar-physics, materials science, and atomic and molecular physics.

In 2013, a kilotesla laser driven magnetic field has been realized by a group in Osaka Univ. [1], and a 800 T magnetic field was reported on the LULI facility [2] by a "capacitor-coil" geometry. In SG-II facility in China, a new designed single open coil has been tested and a 200 T magnetic field is achieved [3]. The temporal and spatial distribution of the magnetic field is further controlled by the design of coil sharp. As an extension of this research, such laser driven magnetic field have been applied in magnetic reconnection experiment.

Reference

1. S. Fujioka, *et. al*., *Sci. Rep*., 2013, **3**, 1170.
2. J.J. Santos, *et. al*., *New J. Phys*., 2015, **17**, 083051.
3. B.J. Zhu, *et. al*., *Appl. Phys*., 2015, **107**, 261903.

Invited

LOW-BETA MAGNETIC RECONNECTION EXPERIMENTS DRIVEN BY INTENSE LASERS

J.Y. Zhong

Department of Astronomy, Beijing Normal University, Beijing, China
jyzhong@bnu.edu.cn

Abstract. The Sun is not so quiet as it looks. Solar flares, coronal mass ejections and solar wind strongly influence interplanetary and terrestrial space by virtue of shock waves, hard electromagnetic radiation and accelerated particles. It is very important to understand space weather and develop effective tools for space weather simulation and prediction to protect the performance and reliability of space borne and ground-based technological systems. It is believed that the coupling between the solar wind and the magnetosphere is mediated and controlled by the magnetic fields in the solar wind through the process of magnetic reconnection, which is considered to be an important mechanism of explosively transferring energy from magnetic fields to plasma flows and heat. In addition to (expensive) spacecraft, we show that the plasma reconnection process can also be studied by appropriately scaled lab experiments, in which large-scale space plasmas are scaled to (relatively low cost) small lab plasmas; these experiments also offer significant and flexible control over the conditions of reconnection.

One novel plasma device for magnetic reconnection is demonstrated by Shenguang II and Gekko XII lasers irradiating a double capacitor-coils target. Optical probing reveals a high velocity, accumulated plasma plume at the region of magnetic reconnection outflow. The background electron density and magnetic field are measured around 10^{18} cm^{-3} and 50–60 Tesla with Nomarski interferometry and Faraday effect, respectively. Compared with high beta magnetic reconnection experiments driven by Biermann battery effect, the present beta is much lower than one, which largely extends the parameter regime of laser driven magnetic reconnection and shows potential applications in astrophysical plasmas [1].

References

1. X.X. Pei, J.Y. Zhong, *et al*., *Physics of Plasmas*, 2016, **23**, 032125; doi: 10.1063/1.4944928.
2. J.Y. Zhong, *et al*., *Astrophys. J. Suppl. Ser*., 2016, **225**, 30.

INDEX OF AUTHORS

International Symposium

TOPICAL PROBLEMS OF NONLINEAR WAVE PHYSICS

Sponsors

The organization of NWP-2017 was supported by the Government of the Russian Federation under the program designed to support research projects implemented under the supervision of the world's leading scientists at Russian institutions of higher learning

Grant No. 14.Z50.31.0007

"Laboratory and numerical investigation of plasma phenomena in extreme astrophysical objects"

Leading scientist – Julien Fuchs

Grant No. 14.Z50.31.0033

"Novel approaches to investigation of climate processes and prediction of extreme events"

Leading scientist – Juergen Kurths

by the Russian Foundation for Basic Research

Grant No. 17-02-20327

by Russian and foreign companies producing optical and laser equipment

as well as by the European Physical Journal (EPJ)

AVESTA

femtosecond lasers and equipment

Amplifiers

MATEKO Ti:S Amplifier

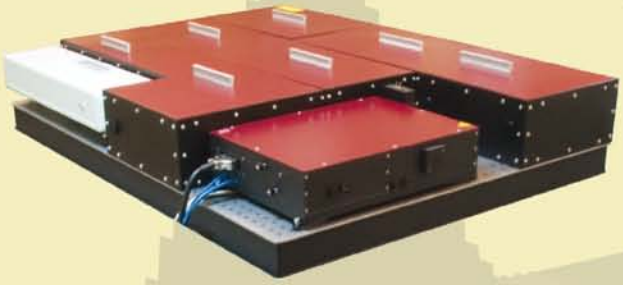

- Single-box design
- **Combined RA/MPA scheme** with a single pump
- **>10 mJ/pulse**
- Variable repetition rate
- **Contrast >10^4:1**
- <40 fs pulse duration
- Upgradeable up to TW level

TETA Yb Regenerative Amplifier

- 1030 / 515 / 343 / 248 nm possible outputs
- **>5 W average power** at 1030 nm
- **Industrial and scientific application**
- Compact single-box solution
- **More than 200 µJ/pulse at 1030 nm**
- <300 fs pulse duration
- High beam quality
- Excellent beam pointing and long term power stability

FREGAT Cr:Forsterite Regenerative Amplifier

- **Operating wavelength 1240 nm**
- Pulse duration: <120 fs
- Single-box design

Avesta Ltd., 11 Fizicheskaya Street
Troitsk, 142190, Moscow, Russia

Tel: +7 495 967-94-73; +7 495 851-00-78
Fax: +7 495 646-04-95

e-mail: fs@avesta.ru
www.avesta.ru

AVESTA

femtosecond lasers and equipment

REUS Ti:Sapphire Regenerative Amplifier

- Compact single-box rigid design
- **>2 mJ/pulse**
- Can be upgraded to higher energies
- <40 fs pulse duration
- **High beam quality**
- **Excellent beam pointing and long-term power stability**

AVET Ti:Sapphire TW Laser System

- Single-table design
- **Up to 10 TW commercial system**
- <45 fs pulse duration
- High beam quality
- Excellent beam pointing and power stability

Compulse Femtosecond Hollow Fiber Pulse Compressor

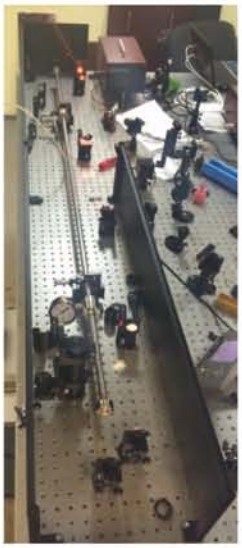

- Pulse duration down to <7 fs TL
- Up to 1:10 compression ratio
- Energy efficiency 50%
- Input pulse energy up to 1 mJ
- 800 and 1030 nm standard models

Avesta Ltd., 11 Fizicheskaya Street
Troitsk, 142190, Moscow, Russia

Tel: +7 495 967-94-73; +7 495 851-00-78
Fax: +7 495 646-04-95

e-mail: fs@avesta.ru
www.avesta.ru

INDUSTRIAL-GRADE ULTRAFAST LASERS TO ADVANCE YOUR RESEARCH

Whether you are working at 1 kHz or 1 MHz, Coherent femtosecond amplifiers operate at extraordinary levels of quality, accuracy, and repeatability. Our HALT designed, HASS verified scientific lasers deliver industrial-grade reliability.

Join the Industrial Revolution in Ultrafast Science

coherent.com/industrial-revolution

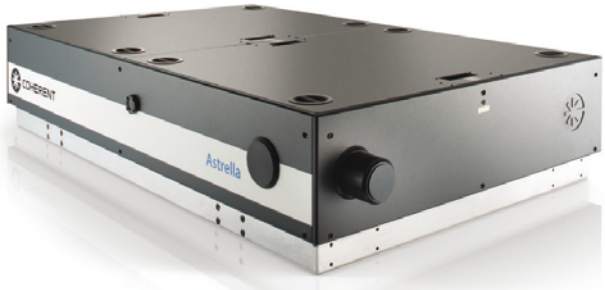

COHERENT®

Superior Reliability & Performance

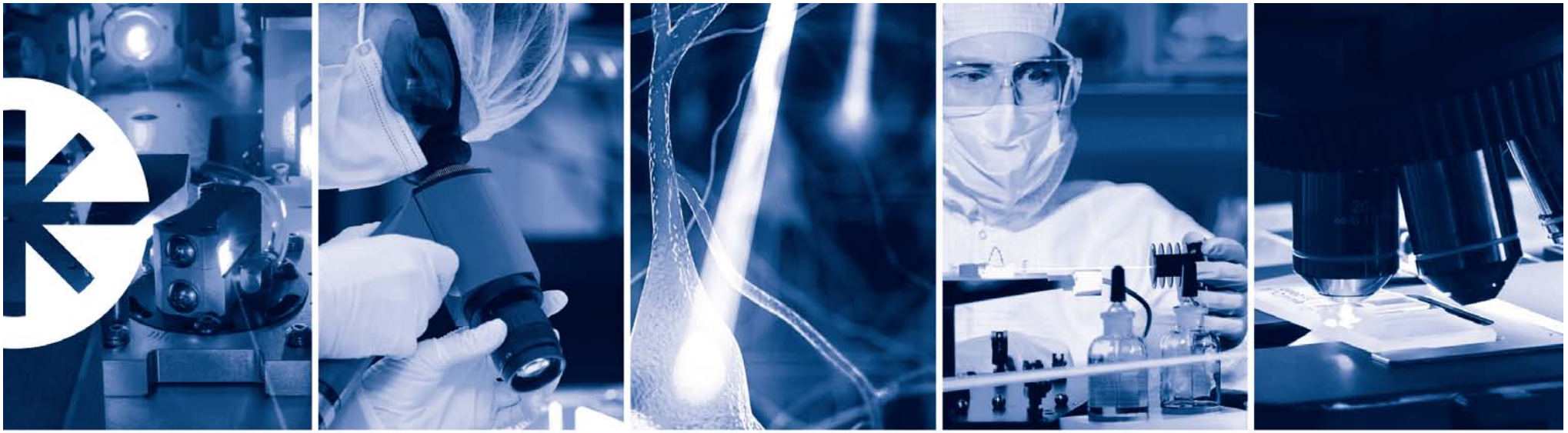

Lasers for Ultrafast Spectroscopy

Astrella, our one-box Ti:Sapphire amplifier, delivers industrial-grade reliability that allows you to focus on results, publication, and funding. Join the Industrial Revolution in Ultrafast Science to advance your research and reduce your cost of data.
coherent.com/industrial-revolution

COHERENT®
Superior Reliability & Performance

COHERENT

Обзор выпускаемых лазерных систем

Представитель компании Coherent
в России - **ООО «ЛазерТрэк»**

e-mail: lasertrack@lasertrack.ru
web-site: www.lasertrack.ru
Тел.: +7 (495) 775 38 63

Laser track

Устройства диагностики, контроля и измерения лазерного излучения

Непрерывные лазерные системы

Мощность

1 кВт

1 Вт

Квазинепрерывный лазер
355 и 532 нм
2 Вт – 24 Вт
Paladin

Ионные лазеры
УФ – ИК
100 мВт – 25 Вт
C. Systems & Sabre

FreD
ГВГ 244 нм

Твердотельный ГВГ-лазер
с диодной накачкой
266 нм, 200 мВт
Azure

Твердотельный лазер
с диодной накачкой
532 нм, 5 – 75 мВт
Compass 115M / 215M

ОПС-лазеры
355 – 1180 нм
10 мВт – 20 Вт
Tracer

8 Вт @ 532 нм

Verdi G
2 – 20 Вт @ 532 нм

Genesis CX SLM
250 мВт @ 355 нм

Genesis MX - Talpon
10 Вт @ 532 нм

OBIS LG
3 Вт @ 532 нм

Sapphire SF
200 мВт @ 561 нм

Диодные системы накачки
770 – 975 нм
20 Вт – 8 кВт

8 кВт @ 975 нм

100 Вт @ 800 нм

Волоконные лазеры
1100 нм
1 кВт

CO2-лазер
9.3, 9.6, 10.2, 10.6 мкм
20 – 100 Вт
C & Gem Series

Перестраиваемый
непрерывный Ti:S-лазер
700 – 1030 нм, 3.5 Вт

1 кГц одно-частотный
твердотельный лазер
с диодной накачкой
532 и 1064 нм, 20 мВт - 55 Вт
Mephisto MOPA

55 Вт @ 1064 нм

Mephisto

800 мВт @ 1319 нм

Prometheus

100 мВт @ 532 нм

Диодные модули
375 – 785 нм
1 – 200 мВт
OBIS LX & LS

150 мВт @ 488 нм

OBIS LX & LS

100 мВт @ 405 нм

Объединитель пучков Galaxy
8 волоконных входов

BioRay
50 мВт @ 450 нм

Лазеры с
несколькими выходами
375 - 830 нм
StingRay

200 мВт @ 830 нм

Ширина линии 9 мкм

200 300 400 700 800 900 1.000 10 мкм

Длина волны (нм)

Импульсно-периодические лазерные системы

Частота повторения
импульсов

МГц

500 кГц

100 кГц

1 кГц

Сверхбыстрые генераторы и ОПО
680 – 1080 нм
>3.5 Вт

140 фс @ 80 МГц

130 фс @ 76 МГц

340 - 1600 нм

505 - 4000 нм

10 фс @ 80 МГц

100 фс @ 80 МГц

Квазинепрерывные
пикосекундные лазеры
532 и 1064 нм, 5 и 10 Вт
Paladin

8 пс @ 80 МГц

Промышленные
пикосекундные лазеры
355, 532 и 1064 нм, 2 - 50 Вт

15 пс @ 1 МГц

Talisker 500, 1000 & HE
15 пс @ 1 МГц

15 пс @ 1 МГц

Talisker Ultra
15 пс @ 200 кГц

1.5 пс @ 80 кГц

Фемтосекундные
волоконные лазеры
1055 нм, 2 Вт

70 фс @ 70 МГц

Наносекундные
волоконные лазеры
355 нм, 23 Вт
Daytona

1 нс @ 525 кГц

Наносекундные твердотельные
лазеры с диодной накачкой
355, 532 и 1064 нм
30 мДж – 1 мДж
Helios

0.7 нс @ 50 кГц

Flare

2 нс @ 1 кГц

Лазеры с Q-модуляцией
266, 355, 532 и 1064 нм
0.5 – 45 Вт
Avia

60 нс @ 120 кГц

Matrix

30 нс @ 120 кГц

Evolution

250 нс @ 1 кГц

CO2-лазеры
9.1 – 10.8 мкм
100 – 1000 Вт
C-Series

0 – 100 кГц

E-Series

0 - 200 кГц

Сверхбыстрые усилители
800 нм
3 мкДж – 100 мДж

40 фс @ 250 кГц

40 фс @ 10 кГц

25 фс @ 10 кГц

240 нм – 20 мкм

40 фс @ 10 Гц

Промышленный усилитель
800 нм
6 мДж

35 фс @ 1 кГц

Эксимерные лазеры
157 – 308 нм
4 – 1200 Вт

ExciStar
5 нс @ 500 Гц

LEAP
22 нс @ 200 Гц

IndyStar
4 нс @ 2 кГц

LSX
24 нс @ 600 Гц

CompexPro
20 нс @ 100 Гц

VYPER
29 нс @ 600 Гц

фс пс нс мкс

Длительность импульса

«Laser components», Ltd

Laser components Ltd has leading positions among suppliers of optical and electronic components in Russia. The company supplies both standard catalog products and custom optical components for a wide range of wavelengths from 193 nm to 10 microns, from various optical materials.

Our products: windows, plates, filters, prisms, mirrors, lenses (with spherical and aspheric surfaces, including off-axis).

One of the important directions of the company's activity is the production of large-aperture optics according to customer's design: windows, mirrors, polarizers, diffraction gratings, phase plates, slabs of neodymium doped phosphate glass.

Also, the company offers a wide range of optomechanics and measuring equipment. Laser Components Ltd is the official distributor of European companies: Laserpoint (thermal sensors), Duma Optronics (laser beam profile meters), Lasertechnik (pyroelectronic detectors, THz detectors). One of the world's leading manufacturers of optical glass, the Chinese company CDGM Glass has granted Laser Components Ltd the right to exclusive sales of blanks of large sizes (up to 900 mm) of H-UK9L glass with high optical homogeneity (up to 2 ppm) and high volume threshold.

The main customers of the company are Rosteccorporation, ROSATOM Group and Roscosmos corporation.

Important advantages of the company are: many years of experience in the Russian market, an international team of professionals, the ability to control the quality of products at manufacturers, experience with purchasing procedures on electronic trading platforms (FL 223 and FL 44), as well as work on individual accounts within the framework of execution of state contracts (FL 159 and FL 275).

RESEARCH, DEVELOPMENT AND MANUFACTURING IN LITHUANIA

standa

OPTICAL TABLES
MOTION CONTROL
OPTICS & OPTO-MECHANICS
VACUUM COMPATIBLE POSITIONERS
DPSS LASERS & LIGHT MEASUREMENT

UP TO **Torr 10^{-8}** VACUUM

▶ ROTARY & TILT

▶ CUSTOM ENGINEERED

▶ LINEAR

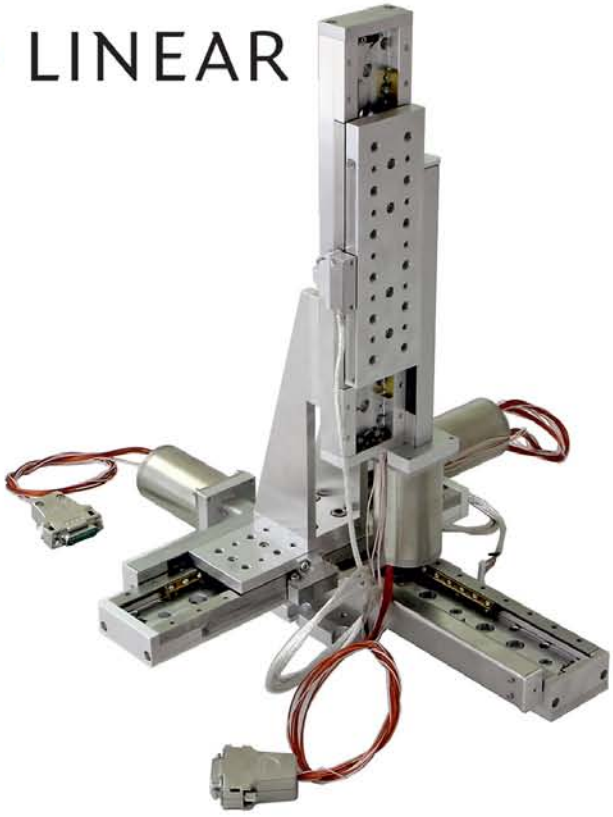

standa

OPTO-MECHANICAL EQUIPMENT

www.standa.LT E-mail: sales@standa.LT

Moscow University. View from the Moskva river

International Symposium

TOPICAL PROBLEMS OF NONLINEAR WAVE PHYSICS (NWP-2017)

Nizhny Novgorod, Russia
July 22 – July 28, 2017

MOSCOW was founded in 1147 by *Prince Yuri Dolgorukiy*. The historical heart of the capital is the ensemble of the Kremlin with the *Armory Chamber*, a treasury of Russian tsars. One can see murals by the world-famous painter *Andrei* Rublev in *the Annunciation Cathedral* of the Kremlin. *The Tsar Cannon* and *Tsar Bell* are unique masterpieces of the Old Russian foundry art.

Moscow, with its popluation of about 12 million people, is multifaced. Its iconic images include *the Red Square, the Spasskaya Tower* with its famous carillon, *St. Basil's Cathedral*, skyscrapers built in the 1930s, and many others. As you walk along *Tverskoy Boulevard, Stoleshnikov Lane, Great Nikitskaya Street*, and *Arbat*, you can feel the living breath of Moscow history.

The streets and lanes of *Zaryadye* and *Zamoskvorechye* have preserved ancient temples, strip malls, and merchant's estates. Moscow has more than a hundred museums. The *State Tretyakov Gallery* and *Pushkin Art Museum* are the richest art collections. The capital has more than thirty professional theaters, including *Bolshoy* with its celebrated Russian ballet.

The wonders of Moscow include Ostankino television tower and Moscow Metro. Moscow is one of the largest scientific centers with tens of universities, R&D institutions, and laboratories.

Panorama of the Moscow Kremlin from the Moskva river

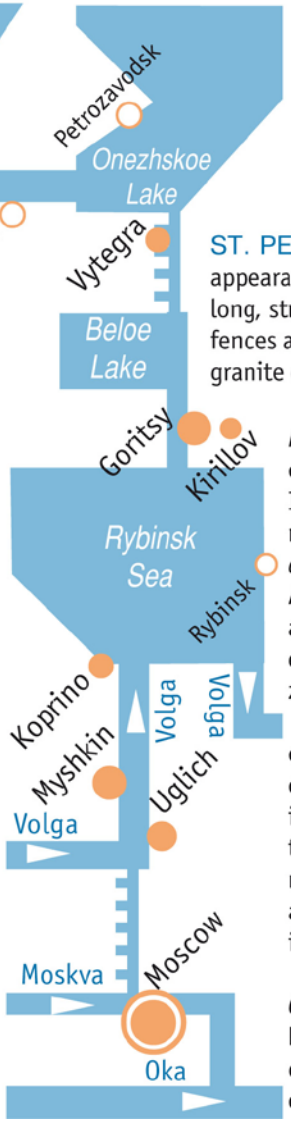

St. Petersburg. St.Anna Church on the bank of the Fontanka river nearby the Neva river

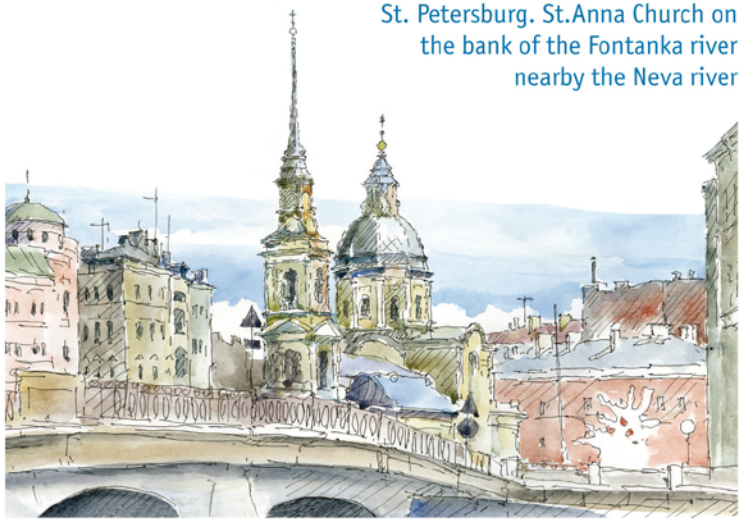

ST. PETERSBURG is one of the most beautiful cities in Europe. The majestic appearance of St. Petersburg is created by a variety of architectural details including long, straight boulevards, vast spaces, gardens and parks, decorative wrought-iron fences and sculptures. The Neva River itself, together with its many canals and their granite embankments and bridges, gives the city a unique and striking ambience.

The most famous of St. Petersburg's museums are *the Hermitage* and *the Russian Museum*. St. Petersburg has been known as the city of palaces. One of the earliest of these is the *Summer Palace*, a modest house built for Peter I in *the Summer Garden* (1710–1714). Much more imposing are the baroque residences of their associates, such as *the Kikin Hall* and *the Menshikov Palace* on the Neva Embankment designed by *Domenico Trezini* in 1710–1716. A residence adjacent to the Menshikov palace was redesigned for *Peter II* and now houses the state university. The most illustrious of imperial palaces is the baroque *Winter Palace* (1754–1762), a huge building with dazzlingly luxurious interiors, now housing *the Hermitage Museum*.

The largest church in the city is *St Isaac's Cathedral* (1818–1858), one of the biggest domed buildings in the world, constructed under supervision of *Auguste de Montferrand*. Another magnificent church in the Empire style is *the Kazan Cathedral* (1801–1811), situated in the Nevsky prospect. No tourist can miss *the Church of the Savior on Blood* (1883–1907), a gorgeous monument in the old Russian style which marks the spot of *Alexander II's* assassination. As *Peter the Great* forbade building onion domes, this church is exceptional in the city with its onion-shaped tower.

St Petersburg is surrounded by imperial residences: *Peterhof*, with *the Grand Peterhof Palace* and glorious fountain cascades; *Tsarskoe Selo* (Pushkin), with the baroque *Catherine Palace* and *the Alexander Palace* in classicist style; and *Pavlovsk*, which contains a domed palace of *Emperor Paul* and one of the largest English-style parks in Europe.

Uglich. Panorama from the Volga river

UGLICH the first records of which date back to 1148, is one of the most picturesque old Russian towns. The magnificent view from the Volga river includes an ensemble of 17th century churches, the Kremlin, trade rows, wooden houses. The most famous and dramatic event in the town's history took place at the end of the 16th century when *Tsarevich Dmitriy*, successor of the throne was allegedly murdered, which gave rise to the political crisis known as the Time of Troubles. In commemoration of Tsarevich Dmitriy a beautiful *church of St.Dmitry-on-Blood* was erected. The 17th-18th centuries was a time when wonderful architectural ensembles were constructed – *the monasteries of St. Alexius, Resurrection, Apparition of Christ*. By the middle of the 19th century the town was rebuilt according to the master-plan. Many buildings in the center of the town are preserved to the present day: the building of the Town Council, the fire tower, as well as some mansions.

Uglich. Dam and lock-gate

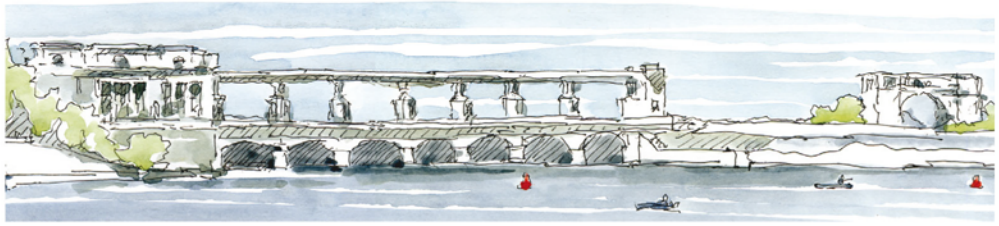

MYSHKIN. The site of the present-day Myshkin was inhabited already in the V-III centuries B.C. According to the reform of *Catherine II*, Myshkin got the status of town in 1777. Two cathedrals make the center of the town: *Nikolsky* and *Uspensky*, which was built in the first half of 19th century with the donations of Myshkin merchants.

But it is Mice that the town is famous for. It is the only town in the world that is named in the honor of Mouse.

Myshkin. Former public library

The world's only museum of Mouse boasts enormous collections of decorative mice. Thousands of tourists from all over the world visit the small mouse town every year to kneel before the great Mice.

Kirillo-Belozersky Monastery

KIRILLO-BELOZERSKY MONASTERY in the town of Kirillov on *Lake Siverskoye* is situated not far from GORITSY.

The monastery was founded by monk *Kirill Belozersky* at the end of the 14th century. The icons in *the Assumption Cathedral* date back to the 15th century, and the murals in the cathedral telling the story of the Virgin Mary's life, to the 17th century.

The Apocalypse murals in the porch that were painted at the same time are not less interesting. The magnificent ensemble of the monastery comprises *the Churches of Baptism of Our Saviour, of John the Baptist*, and of *the Archangel*, farmeries, fortress walls with high bartizans and two over-the-gate churches. The local museum has collections of manuscripts, ancient utensils, samples of wooden carving and traditional embroideries.

Goritsy. Panorama from the water

Located at the crossing of a waterway connecting central Russia with Lake Onega and a road connecting St. Petersburg with Arkhangelsk, VYTEGRA was once an important transit point for cargo. The idea to build a canal connecting the drainage basins of the Neva and the Volga rivers was already discussed by *Peter the Great*, but the canal, formerly the *Mariinsky System*, was only built in 1810.

In the 20th century, it was reconstructed and renamed *the Volga–Baltic Waterway*. The remains of *the Mariinsky System*, a few dwelling houses of the 19th century, *the Presentation Church* and *B440 Foxtrot-class submarine* are the main sites of interest in Vytegra.

Valaam Monastery. Transfiguration Cathedral

VALAAM ARCHIPELAGO is staggeringly beautiful due to the fantastic maze of its coves, lakes, and rocks. The ancient *Valaam Monastery* is situated here; it was first mentioned in chronicles in the 10th century.

The Monastery was completely self-sufficient and monks produced all the necessary products themselves while working at small factories, sawmills and farms, constructing buildings. At the beginning of the 20th century the Valaam Monastery became one of the wealthiest Russian Monasteries, comprising a kind of a small state with 13 smaller monasteries under control.

During *the Second World War* the Archipelago was under control of Finland and returned back to the USSR in 1944. Since that time the Monastery was closed until 1989. Now it is functioning again. The monastery, hermits' huts, and chapels built in the Russian-Byzantine style are architectural masterpieces.

Vytegra. Submarine-museum

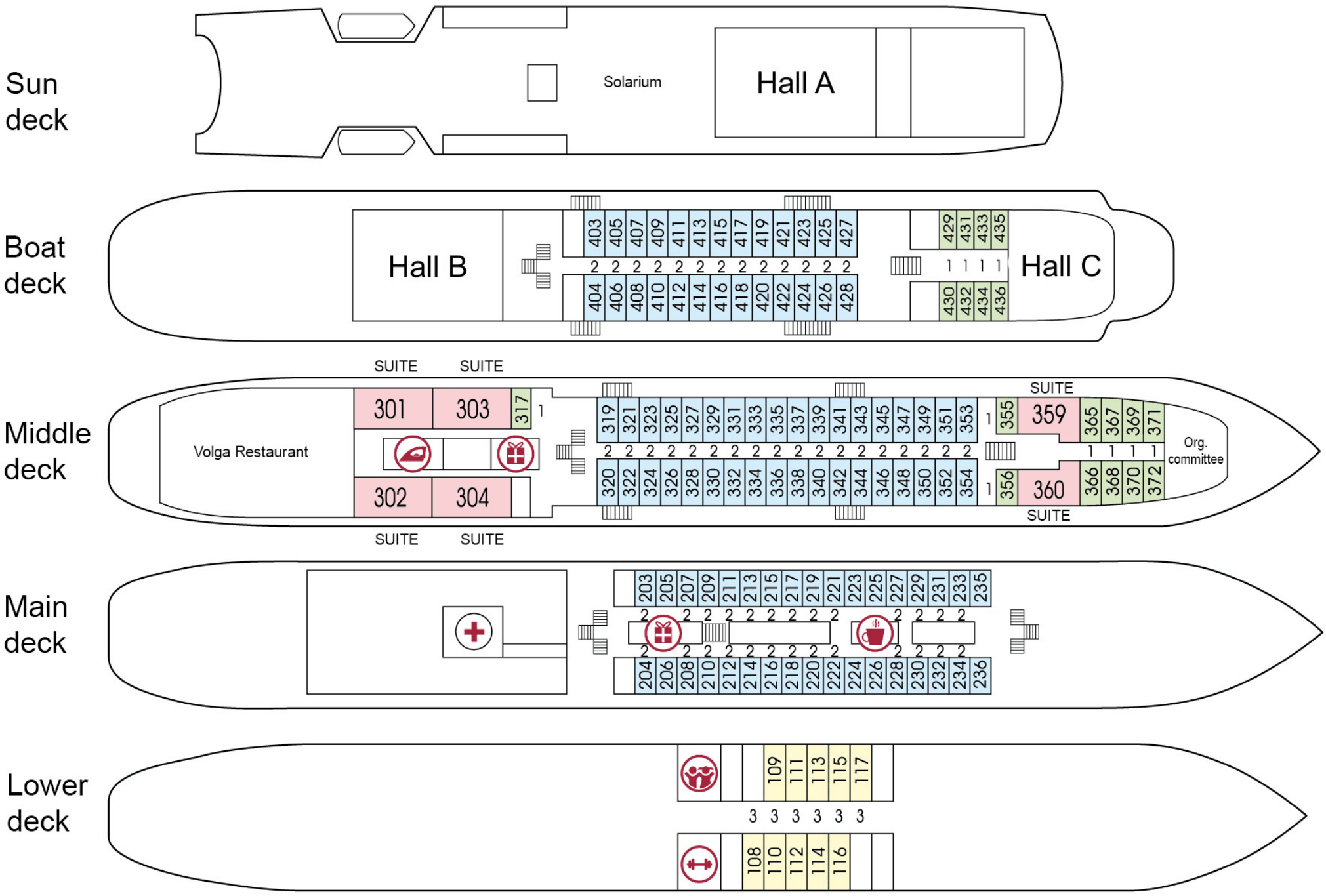
Sun deck
Solarium
Hall A
Boat deck
Hall B
Hall C
403 405 407 409 411 413 415 417 419 421 423 425 427
404 406 408 410 412 414 416 418 420 422 424 426 428
429 431 433 435
430 432 434 436
Middle deck
SUITE SUITE
301 303 317
302 304
SUITE SUITE
Volga Restaurant
319 321 323 325 327 329 331 333 335 337 339 341 343 345 347 349 351 353
320 322 324 326 328 330 332 334 336 338 340 342 344 346 348 350 352 354
SUITE
355 359 365 367 369 371
356 360 366 368 370 372
SUITE
Org. committee
Main deck
203 205 207 209 211 213 215 217 219 221 223 225 227 229 231 233 235
204 206 208 210 212 214 216 218 220 222 224 226 228 230 232 234 236
Lower deck
109 111 113 115 117
108 110 112 114 116

International Symposium

TOPICAL PROBLEMS OF NONLINEAR WAVE PHYSICS

NWP-2017

PROCEEDINGS